The Role of Perilipin 5 (PLIN5) in Muscle Metabolism

Ruzaidi Azli Mohd Mokhtar

Bachelor of Agriculture

Master of Science

A thesis submitted for the degree of Doctor of Philosophy at

Monash University in 2016

Department of Physiology

School of Biomedical Sciences

Faculty of Medicine, Nursing and Health Sciences

Copyright notice

Abstract

The perilipin (PLIN) family of proteins reside on, or near, intracellular lipid droplets and play a major role in the regulation of lipid metabolism in most tissues. PLIN5 is highly expressed in tissues that have a high capacity for fatty acid metabolism, especially skeletal muscle. However, there is very limited knowledge about the function of PLIN5 in skeletal muscle. Therefore, the aims of this thesis were to delineate the role of PLIN5 on substrate metabolism in muscle. Accordingly, we generated whole-body $Plin5^{-/-}$ mice to determine PLIN5's involvement in lipid metabolism and insulin action in chapter 2. Loss of PLIN5 had no effect on body weight, feeding or adiposity but increased whole-body carbohydrate oxidation. $Plin5^{-/-}$ mice developed skeletal muscle insulin resistance, which was associated with increased intramyocellular triglyceride lipolysis and ceramide accumulation. Liver insulin sensitivity was improved in $Plin5^{-/-}$ mice, indicating tissue-specific effects of PLIN5 on insulin action. Thus, we conclude that PLIN5 plays a critical role in coordinating skeletal muscle triacylglycerol metabolism, which impacts sphingolipid metabolism, and is requisite for the maintenance of skeletal muscle insulin action.

In chapter 3, we successfully generated mice with muscle-specific ablation of PLIN5 ($Plin5^{MKO}$) in order to investigate the effects of muscle-specific PLIN5 deletion on energy homeostasis, muscle metabolism and glucose tolerance *in vivo*. There was an increase in whole-body fatty acid oxidation and reciprocal decrease in carbohydrate oxidation in $Plin5^{MKO}$ mice. Intriguingly, fatty acid and glucose oxidation were not different between genotypes when assessed in skeletal muscle *ex vivo*. The mismatch between the *in vivo* and *ex vivo* studies of fatty acid oxidation indicate that PLIN5 deletion in skeletal muscle may alter endocrine signaling to modulate whole body metabolism. In mice fed a HFD, glucose tolerance was markedly enhanced in $Plin5^{MKO}$ compared with control (lox/lox) mice and this was associated with increased glucose clearance without changes in endogenous glucose production. We proposed that this may be caused by an increase in non-insulin stimulated glucose clearance.

Lastly, we studied the role of PLIN5 in the regulation of skeletal muscle substrate metabolism during acute exercise. We also assessed whether PLIN5 is required for the metabolic adaptations and enhancement in exercise tolerance following endurance exercise training. Using $Plin5^{MKO}$

mice, we showed that PLIN5 is dispensable for normal substrate metabolism during exercise as reflected by levels of blood metabolites and rates of glycogen and triglyceride depletion that were indistinguishable from lox/lox mice. $Plin5^{MKO}$ mice exhibited a functional impairment in their response to endurance exercise training as reflected by reduced maximal running capacity and reduced time to fatigue during prolonged submaximal exercise. The reduction in exercise performance was not accompanied by alterations in carbohydrate and fatty acid metabolism during submaximal exercise. Similarly, mitochondrial capacity and mitochondrial function was not different between lox/lox and $Plin5^{MKO}$ mice. Thus, PLIN5 is dispensable for normal substrate metabolism during exercise and is not required to promote mitochondrial biogenesis or enhance the cellular adaptations to endurance-exercise training. Together, the work in this thesis extends our understanding of the important role of PLIN5 in skeletal muscle metabolism.

Publications during enrolment

<u>Mohktar RAM</u>, Montgomery MK, Murphy RM, Watt MJ. Perilipin 5 is dispensable for normal substrate metabolism and in the adaptation of skeletal muscle to exercise training. Am J Physiol Endocrinol Metab. 2016 *In press*

Mason RR, **<u>Mokhtar R</u>**, Matzaris M, Selathurai A, Kowalski GM, Mokbel N, et al. PLIN5 deletion remodels intracellular lipid composition and causes insulin resistance in muscle. Mol Metab. 2014;3(6):652–63.

General declaration

I hereby declare that this thesis contains no material which has been accepted for the award of any other degree or diploma at any university or equivalent institution and that, to the best of my knowledge and belief, this thesis contains no material previously published or written by another person, except where due reference is made in the text of the thesis.

This thesis includes 2 original papers published in peer reviewed journals and 1 unpublished publication. The core theme of the thesis is the role of perilipin 5 in regulating substrate metabolism in muscle. The ideas, development and writing up of all the papers in the thesis were the principal responsibility of myself, the student, working within the Department of Physiology under the supervision of Professor Matthew Watt and Dr. Clinton Bruce.

The inclusion of co-authors reflects the fact that the work came from active collaboration between researchers and acknowledges input into team-based research.

In the case of Chapter 2 and 4 my contribution to the work involved the following:

Thesis chapter	Publication title	Publication status*	Nature and extent of candidate's contribution
2	PLIN5 deletion remodels intracellular lipid composition and causes insulin resistance in muscle	Published in Molecular Metabolism	Designed or had input into the design of some of experiments. Performed the some of experiments and data analysis. Wrote and edited the manuscript.
4	Perilipin 5 is dispensable for normal substrate metabolism and in the adaptation of skeletal muscle to exercise training	Published in American Journal of Physiology - Endocrinology and Metabolism	Designed or had input into the design of all experiments. Performed all experiments and data analysis. Wrote and edited the manuscript.

I have renumbered sections of submitted or published papers in order to generate a consistent presentation within the thesis.
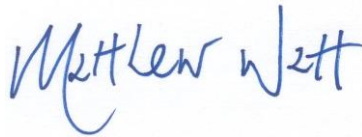
Student signature: **Date: 08/09/2016**

The undersigned hereby certify that the above declaration correctly reflects the nature and extent of the student's and co-authors' contributions to this work. In instances where I am not the responsible author I have consulted with the responsible author to agree on the respective contributions of the authors.

Main Supervisor signature: **Date: 09/09/2016**

Acknowledgements

There are many people I wish to thank for their involvement in the completion of this PhD thesis, as their guidance, knowledge and support have proven invaluable in this journey.

First and foremost, I would like to express my sincere gratitude to my main supervisor, Professor Matthew Watt for his continuous support of my study and related research, for his patience, motivation, and immense knowledge throughout the last 4 years. His guidance helped me a lot, especially during the writing of this thesis. I could not have imagined having a better supervisor for my PhD and I consider myself extremely lucky to have him as my supervisor. Without his guidance and help, this thesis would not have been possible.

To my co-supervisor Dr. Clinton Bruce, thank you for your valuable insights and support that you have provided over the last 4 years. Thank you for giving me an access to your laboratory and research facilities because without your support, it would not be possible for me to finish my PhD work.

My sincere thanks also go to Dr. Nancy Mokbel, from the Garvan Institute of Medical Research for teaching me the isolation method for primary myoblast. I would also like to express my gratitude to Dr. Robyn Murphy, from La Trobe University for helping me develop a technique to measure the respiration of muscle fibre using SeaHorse analyzer. The experience of working together with both of them will never be forgotten.

I also wish to express my gratitude to all members of the Watt lab (past and present) especially Dr. Jennifer Lo, Dr. Ruth Meex and Maria Matzaris, for their guidance and knowledge, whether directly or indirectly. I know that I could not have achieved so much alone and really appreciated each and every minute they spent in the lab with me.

Of course, I must also thank the many people outside of the laboratory and academic setting within the Department of Physiology for their support. Special thanks to the Ministry of Higher Education Malaysia and Universiti Malaysia Sabah for providing me with a scholarship for my

Abbreviations

2DG	2-deoxyglucose
ACS	Acyl-CoA synthetases
ADP	Adenosine diphosphate
AMP	Adenosine monophoshate
AMPK	5'AMP-activated protein kinase
ANOVA	Analysis of variance
ASM	Acid soluble metabolite
ATGL	Adipose triglyceride lipase
ATP	Adenosine triphosphate
BAT	Brown adipose tissue
BCA	Bicinchoninic acid assay
BSA	Bovine serum albumin
CaMK	Ca^{2+}dependent calmodulin kinase
CGI-58	Comparative gene 58
CPT	Carnitine palmitoyl transferase
CS	Citrate synthase
DAG	Diacylglycerol
DEXA	Dual energy X-ray absorptiometry
DGAT	Diacylglycerol acyl transferase
DMEM	Dulbecco's Modified Eagle Medium
DNA	Deoxyribonucleic acid
EDL	Extensor digitorum longus
EDTA	Ethylenediaminetetraacetic acid
EGP	Endogenous glucose production
ELISA	Enzyme-linked immunosorbent assay
ER	Endoplasmic reticulum
ERK	Extracellular signal-regulated kinase
FABP	Fatty acid binding protein
FAT	Fatty acid translocase

FATP	Fatty acid transport proteins
FBS	Fetal bovine serum
FCCP	Carbonyl cyanide-*4*-(trifluoromethoxy)phenylhydrazone
FFA	Free fatty acid
FGF	Fibroblast growth factor
G0S2	G0/G1 switch gene 2
GC–MS	Gas chromatography mass spectrometry
GDR	Glucose disposal rate
GIR	Glucose infusion rate
GLUT	Glucose transporter
HDL	High density lipoprotein
HFD	High fat diet
HSL	Hormone sensitive lipase
IMCL	Intramyocellular lipid
IMTG	Intramyocellular triacylglycerol
IPITT	Intraperitoneal insulin tolerance test
IRS	Insulin receptor substrate
KHB	Krebs-Henseleit buffer
LCFA-CoA	Long chain fatty acid CoA
LD	Lipid droplet
LPL	Lipoprotein lipase
MAG	Monoacylglycerol
MCK	Muscle creatine kinase
MGL	Monoacylglycerol lipase
OCR	Oxygen consumption rate
OGTT	Oral glucose tolerance test
ORO	Oil red O
PBS	Phosphate buffered saline
PCR	Polymerase chain reaction
PGC	Peroxisome proliferator-activated receptor gamma coactivator
PKA	Protein kinase A

PKC	Protein kinase C
PLIN	Perilipin
PPAR	Peroxisome proliferator-activated receptor
RER	Respiratory exchange ratio
RIPA	Radio-Immunoprecipitation Assay
RNA	Ribonucleic acid
SDS	Sodium dodecyl sulphate
SEM	Standard error of the mean
T2D	Type 2 diabetes
TAG	Triacylglycerol
TBARS	Thiobarbituric acid reactive substances
TEM	Transmission electron microscopy
TG	Triglyceride
VLDL	Very low density lipoprotein
WAT	White adipose tissue
β-HAD	ß-hydroxyacyl CoA dehydrogenase

Tables of Contents

CHAPTER 1

Literature Review

1.1 Introduction

Obesity is defined as an excess of body fat (>32% of body mass in females and >25% in males), which is stored as triglycerides in adipose tissue. Obesity prevalence has increased at an alarming rate in recent years, becoming a worldwide health problem, with incalculable social costs. In Australia, more than half of the adult population is obese or overweight and the economic cost of obesity is estimated to be more than $21 billion annually (1). Obesity is associated with many other life-threatening complications including non-alcoholic fatty liver disease, cardiovascular disease, certain cancers and type 2 diabetes mellitus (T2D) (2). Strikingly, about 90% of individuals with T2D are classified as overweight or obese (3), suggesting that factors associated with being obese cause T2D development (4,5).

Insulin resistance is the key etiological factor linking obesity to T2D. Insulin resistance is defined as an inability of cells to respond to the normal actions of the hormone insulin and is functionally characterised by the inability of insulin to inhibit glucose output from the liver and to promote glucose uptake in fat and muscle, resulting in elevated blood glucose levels. The factors leading to insulin resistance are complex and varied and one theory, the 'lipotoxicity' theory, suggests that increases in lipolysis from an expanded adipose tissue mass leads to raised levels of plasma free fatty acids (FFA), which in turn leads to an increased delivery of FFA to peripheral tissues such as liver and muscle, ectopic lipid deposition and the induction of insulin resistance through the activation of several stress signalling and proinflammatory pathways (6–8). While increased delivery of FFA may be important in driving this process, it is becoming increasingly evident that impaired lipid metabolism within the liver and skeletal muscle also play an important role in the pathogenesis of insulin resistance.

Perilipin 5 (PLIN5) was the most recent protein to be identified from the PLIN protein family, and was originally named *OXPAT* due to its abundant expression in highly oxidative tissues such as liver, brown adipose tissue and skeletal and cardiac muscle (9). PLIN5 shares homology with the critical adipocyte regulatory protein PLIN1, and appears to control fatty acid fluxes in the heart, skeletal muscle and liver by modulating several processes including fatty acid oxidation and storage. Cell biology studies demonstrate that PLIN5 is intimately involved with lipid trafficking and metabolism at the surface of lipid droplets (10–14), which are intracellular

2

organelles with a primary role in storing neutral lipids including triglycerides and sterol lipids (15–17). While cell biology studies have proved to be informative, there remains a lack of information on the role of, and requirement for, PLIN5 in regulating substrate metabolism in whole animals, and in particular, the role of PLIN5 in regulating skeletal muscle metabolism. These observations provide the basis to study the role of PLIN5 in energy homeostasis and substrate metabolism in health and metabolic disease.

1.2   Introduction to Lipid Metabolism

1.2.1   Fatty acid metabolism- from adipose to muscle

Fatty acids serve a multitude of processes in all organisms that include providing energy for adenosine triphosphate (ATP) production, acting as a component of bulk energy storage depots (e.g. triglycerides in lipid droplets), participating in cell signalling by direct effects (e.g. PPAR signalling) and by producing the backbone to molecules (e.g. steroid hormones), and providing structural components of cell membranes (e.g. phospholipids). Fatty acids are mainly stored in adipose tissues in discrete anatomical locations, with some storage occurring in non-adipose tissues. Adipose tissue mass varies greatly in humans with most individuals storing in the range of 15-30% of total body weight (18). To be more specific, it is estimated that the average non-obese male (~70 kg) stores between 9 and 15 kg (equating to an energy store of 80,000 to 140,000 kcal) of triglycerides (TGs) in adipose tissue (19). The vast majority of adipose tissue is composed from triacylglycerol (glycerol + 3 fatty acids; TAG) and is thereby the major fuel store that is used to maintain energy production both at rest and during energetic stresses such as low intensities exercise, cold exposure and fasting.

Lipids are typically transported from adipocytes to other tissues as free fatty acids (FFAs) bound to albumin, or derived from TAG in chylomicrons or very low density lipoproteins (VLDLs) in the plasma, where the fatty acids are released by lipoprotein lipase (LPL) before their cellular uptake (20). The mobilisation of lipids from adipose tissue to the target site of oxidation inside the mitochondria of other cells, including skeletal muscle, is a complex process and involves numerous steps (18). An overview of these processes is shown in Fig. 1-1 and is expanded upon in later sections. In short, fatty acids are transported into cells by passive diffusion or protein-mediated transfer. The fatty acid is activated to fatty acyl-CoA by acyl-CoA synthetases (ACS)

3

and can then undergo a multitude of fates, which is heavily influenced by the energy requirements of the cell. From a metabolic viewpoint, and at a most basic level, the fatty acyl-CoA would likely be transported to the endoplasmic reticulum where enzymes of the Kennedy pathway direct fatty acids to storage as triglyceride during states of low energy demand. In contrast, when energy demand is high, the fatty acyl-CoA is directed to the mitochondria where it is transported into the matrix by the carnitine palmitoyl transferase complex for eventual ß-oxidation and energy production.

1.2.2   Lipid droplets and fatty acid metabolism

Although adipose tissue is the major site for TAG storage in the body, almost all cell types have the capability to store fatty acids as TAG within specialised intracellular organelles called lipid droplets (LDs) (21–23). LDs store hydrophobic lipids including TAG, diacylglycerol (DAG), retinyl esters, cholesterol esters, free cholesterol and ceramides within a monolayer of phospholipids and LD-associated proteins (22,24–27) (Fig. 1-2), and these lipids can be used as substrates for the formation of intracellular membranes or energy production in the form of ATP. LDs are found in different sizes ranging from 2 µm in muscle cells to 100 µm in adipocytes (28) and are highly mobile structures that are transported along microtubules (29). Due to its dynamic structure, LDs are continuously being synthesized and degraded in the cells and interact with other organelles such as the endoplasmic reticulum (site of TG synthesis) and the mitochondria (site of fatty acid oxidation) (30,31) (Fig. 1-3). Owing to this complex regulation, the primary function of LDs is to act as a hub for fatty acid trafficking within cells. Most importantly, LDs serve to protect the cell by sequestering lipids into a protective environment and preventing the excessive accumulation of lipid intermediates such as ceramide, diglyceride and sphingolipids, which cause so-called 'lipotoxic' outcomes such as ER stress, activation of pro-inflammatory signalling, insulin resistance and apoptotic cell death.

It is now well documented that LDs are coated with a large number of proteins, which serve roles in lipid metabolism, cell signaling, vesicle trafficking, and energy homeostasis (32). Studies of the LD proteome have reported more than 300 different proteins on the surface of the LD (33,34) (Fig. 1-2). Not surprisingly, several of these proteins are involved in triglyceride synthesis (diacylglycerol acyl transferase; DGAT2) and breakdown (adipose triglyceride lipase; ATGL),

and vesicle trafficking (Rab proteins) (35–38), but the majority of the protein functions remain to be determined. The LD protein coat is highly heterogeneous and varies according to the tissue type and subcellular location; therefore, it has been suggested that LD function is mediated by the proteins co-located in it phospholipid monolayer.

The discovery of the protein perilipin 1 (PLIN1) as a scaffold protein on adipocyte LDs provided a major conceptual shift in the understanding of lipid droplet biology (39,40). Since these early studies, four other proteins that have now been classified as part of the PLIN super-family (PLIN1-5, for nomenclature, Section 1.6). The grouping of these proteins was based on a 100 amino acid region of high sequence homology near their N-terminus (41). Each PLIN protein has unique tissue distribution, subcellular location and lipid binding properties, indicative of divergent cellular functions (9,42) and are outlined in detail in Section 1.6.
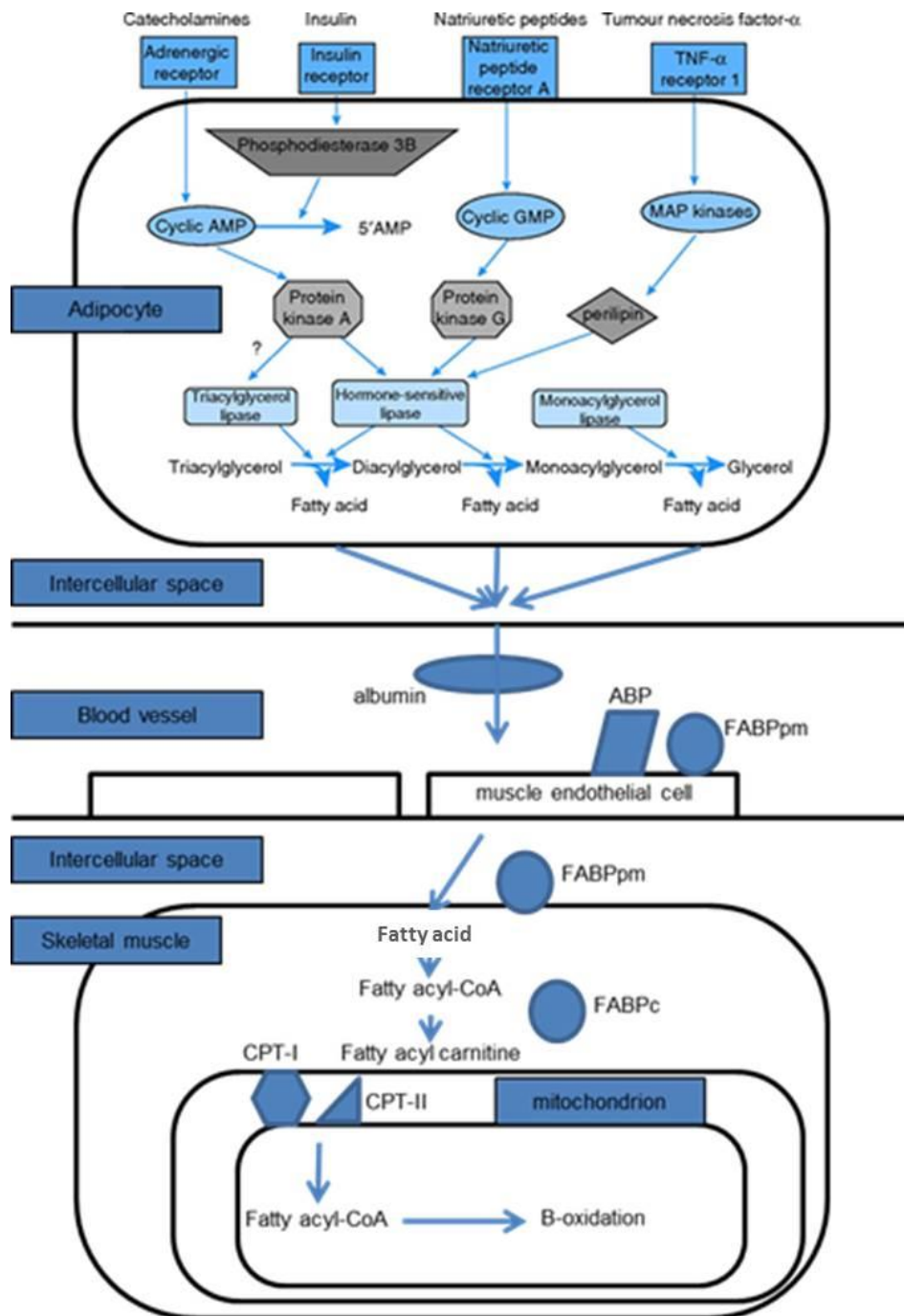
Fig 1-1. *Fatty-acid mobilisation in the adipocyte and transportation to the mitochondrial cytosol in the skeletal muscle for ß-oxidation.* AMP, adenosine monophosphate; GMP, guanosine monophosphate; ABP, albumin binding protein; FABPpm, plasma membrane fatty-acid binding protein; FABPc, cytoplasmic fatty-acid binding protein; CoA, coenzyme A; CPT-I, carnitine–palmitoyl transferase-I; CPT-II, carnitine–palmitoyl transferase II (Adapted from Lange, 2004) (18).
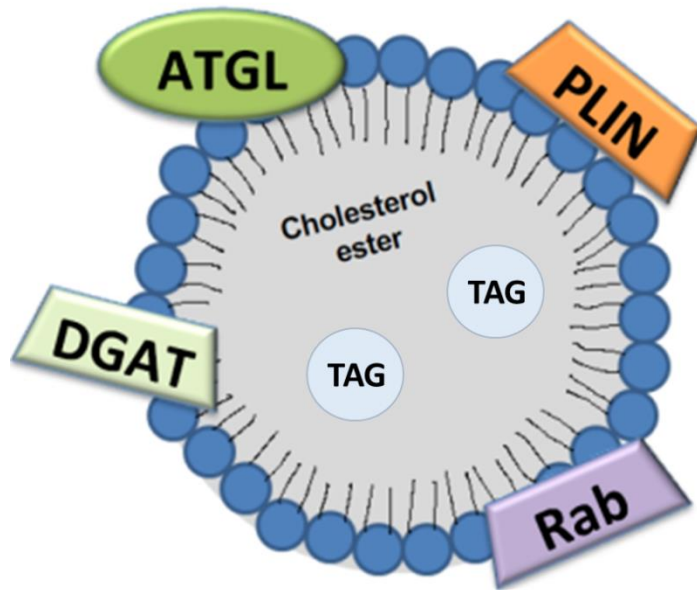
Fig 1-2. *Structure of a lipid droplet. showing the phospholipid monolayer surrounding the neutral lipid core containing TAGs and cholesterol esters.* The surface of the lipid droplet is coated with a variety of proteins (ATGL: adipose triglyceride lipase; DGAT: diglyceride acyltransferase, Rab:, PLINs: perilipins, etc) (Adapted from Farese and Walter, 2009) (43).
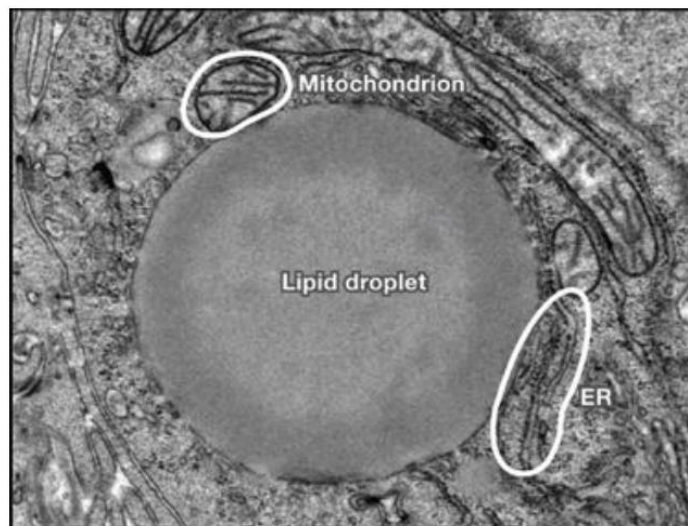
Fig 1-3. *Electron micrograph showing a lipid droplet in a cultured hepatoma cell. The phospholipid monolayer surrounding the LD is visible, as is the close association with mitochondria and endoplasmic reticulum membranes (Adapted from Walter and RV Farese 2009)* (44).

1.3   Lipid Metabolism in Skeletal Muscle

1.3.1   Fatty acid uptake, transporters and binding proteins

Once located in the interstitial space of muscle, FFA uptake can occur through passive diffusion or via protein-mediated mechanisms using transporters such as fatty acid translocase (FAT/CD36), fatty acid binding protein (FABPpm) and fatty acid transport proteins (FATP1-6) (45,46). FATP1 and FATP4 are the most abundant transport protein in muscle (47). As the exact mechanism of transmembrane translocation of fatty acids is still not clear, different models have been proposed for fatty acid uptake into muscle (Fig. 1-4).

In cultured human myotubes, FATP1 and CD36 are normally located in the cytosol and plasma membrane, respectively (48), and increases in fatty acid transport are typically associated with an increased number of transporters at the plasma membrane, rather than an increase in total transporter expression *per se* (49,50). In this regard, skeletal muscle CD36 and FATP1, but not FABPpm, are regulated by translocation from an intracellular location to the plasma membrane by insulin (51–54), while FABPpm and CD36 translocate during muscle contraction (45,49) through an incompletely described mechanism (49). Recent studies report that FABPpm coimmunoprecipitates with CD36, indicating a direct interaction between these two proteins (55). It is currently unclear how this interaction impacts fatty acid transport.

Upon entry to the myocyte, fatty acids either bind with cytoplasmic fatty acid binding protein (FABPc) or may be activated by ACS to become long chain fatty acid CoA (LCFA-CoA) (56). These LCFA-CoAs may be esterified to TAG for storage in LDs, incorporated into phospholipids for use in cellular membranes, metabolised to lipid second messengers such as eicosanoids, oxidized in the mitochondria for energy (ATP) production or alter gene expression.
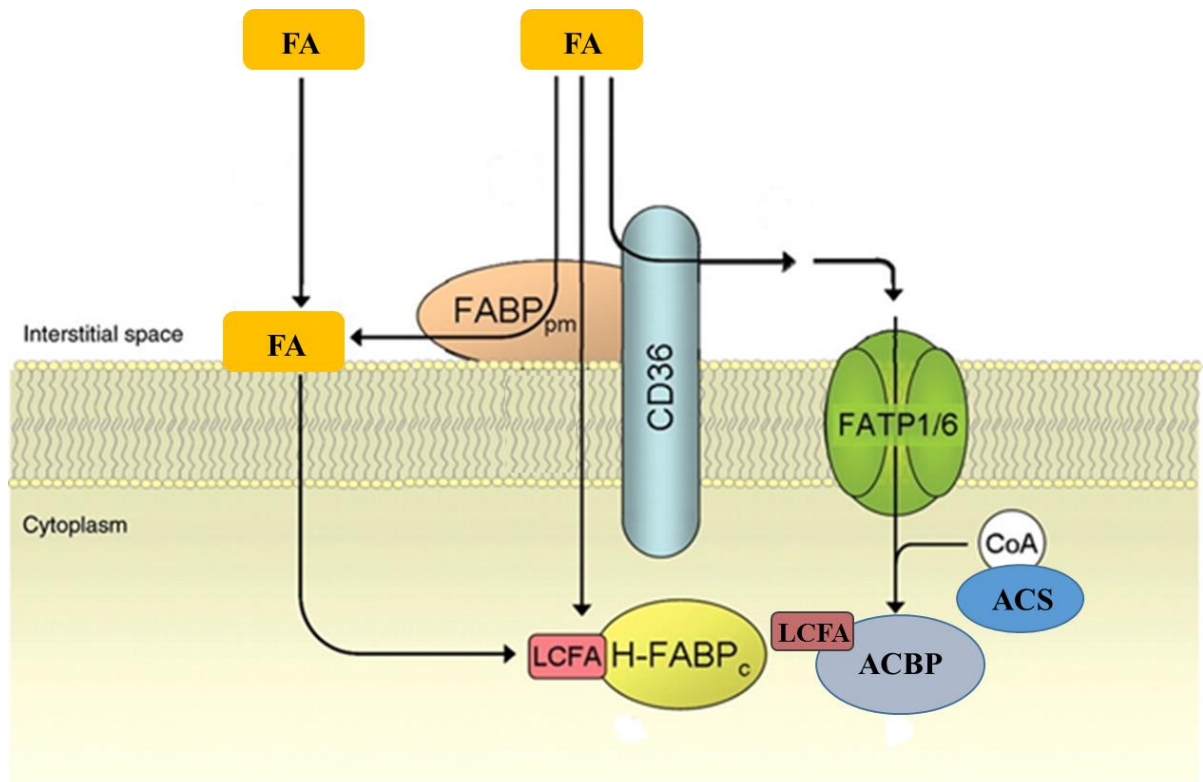
Fig 1-4. *Fatty acid cell uptake. Fatty acid may be taken up by the cell via passive diffusion or via fatty acid translocase (CD36/FAT), fatty acid binding protein (FABPpm) and fatty acid transport proteins (FATP1-6).* FATP1 and CD36 translocate to the plasma membrane in response to insulin, and both CD36 and FABPpm translocate in response to contraction. Once the fatty acids enter the cell they are transported to their destination by FABPc or may be activated by acyl-CoA synthetase (ACS) to form long-chain FA– CoA (LCFA-CoA). LCFA-CoA can then be transported by acyl-CoA binding protein (ACBP) (Adapted from Scwenk et al., 2008) (57).

1.3.2 Lipid droplets

Skeletal muscle contains several small LDs that are predominantly located in the subsarcolemmal region or in-between the myofibrils and in close proximity to mitochondria and sarcoplasmic reticulum (31,58,59). This is clearly shown in transmission electron microscopy (TEM) images (Fig. 1-5). It is likely that the close contact of LDs with mitochondria has an important role in energy metabolism by facilitating the efficient transfer of fatty acids from the LD for oxidation in the mitochondria, particularly during exercise (58). Endurance exercise training increases the LD-mitochondria contact, indicating that this might be an important adaptive strategy for efficient fatty acid oxidation (58). The proteins controlling this process are currently unknown, and to date, there are a few studies have directly examined the skeletal muscle LD proteome.

Radiotracer studies estimate that approximately 50 - 60 % of the circulating fatty acids that enter the myocytes are first stored as TAG in LDs (60–63) which is variously described as intramyocellular lipid (IMCL) or intramyocellular triacylglycerol (IMTG). The amount of IMTG stored in skeletal muscle varies and is dependent upon dietary status, age, sex, training status (64) and the muscle fibre type (65). With respect to the latter, muscle fibres can be classified by their oxidative phosphorylation ability and contractile properties. Type I fibres have high oxidative capabilities due to high numbers of mitochondria and have high amounts of IMTG; while type II fibres are less oxidative, exhibit higher glycolytic potential and store less IMTG (66).

There are, however, several proteins that are validated LD-associated proteins in skeletal muscle and these include FSP27 (CIDEC) (67), FIT1 (68) and FIT2 (69), and spastin (70). FSP27 is found to stimulate LD fusion and growth by lipid exchange and transfer at LD contact sites (71,72). FIT1 is thought to directly bind with TAGs and help the lipid partitioning into LD (68), while FIT2 was show to be a potential regulator of energy metabolism in skeletal muscle (69). In addition, FIT2 overexpression was found to increase skeletal muscle lipid storage and enhance energy expenditure (69). Spastin, a microtubule-severing protein, was recently shown to localise to LDs and is reported to increase LD numbers in skeletal muscle (70). There are many putative LD coat proteins identified by mass spectrometry analysis in the LD fraction of skeletal muscle

(33), but very little is known about the role of these proteins, especially in the regulation of intramyocellular lipid metabolism.
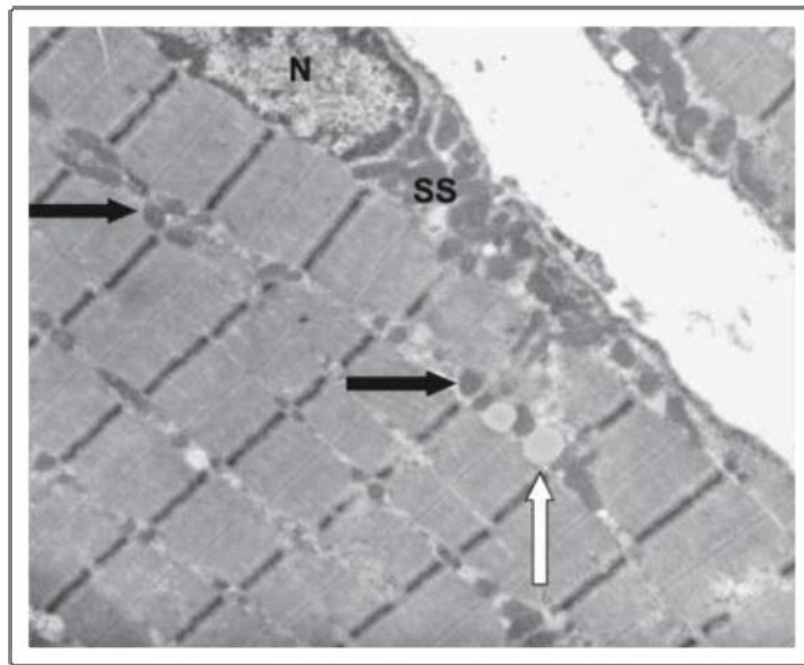
Fig 1-5. *Transmission electron micrograph (TEM) of human skeletal muscle.* Image from a type IIX or IIA fiber (note the thin Z-line), with the light arrow indicating an intramyocellular lipid droplet and dark arrows indicating mitochondrial fragments in cross section (Adapted from Tarnopolsky et al. 2007) (58).

1.3.3   IMTG Lipolysis

Lipolysis involves the sequential cleavage of fatty acids from a TAG molecule to produce free fatty acids. Lipolysis occurs at the interface of the phospholipid membrane surrounding the LD and the cytosol and is dependent on the actions of three lipases that sequentially cleave a fatty acid from the glycerol backbone (Fig. 1-6). In adipose tissue, lipolysis is initially catalysed by ATGL, which converts TAG to DAG (73). However, the role of ATGL in skeletal muscle is not yet well understood. ATGL overexpression was reported to enhance fatty acid release and oxidation, and reduce TAG content in human primary myotubes (74) and in mice *in vivo* (75). In agreement, ATGL knockout mice demonstrate reduced TAG lipolysis leading to IMTG accumulation (76), thereby underlining the importance of ATGL to the liberation of fatty acid stored in intramyocellular LDs.

In adipose tissue, ATGL activity is enhanced upon binding with its co-activator, comparative gene 58 (CGI-58) (77), and reduced by G(0)/G(1) switch gene 2 (G0S2) (78,79) (Fig. 1-6). ATGL activity is also increased by protein kinase A (PKA)-mediated phosphorylation (80). CGI-58 and G0S2 are both expressed in skeletal muscle (21,77,78,81). The importance of CGI-58 to ATGL activation in skeletal muscle is demonstrated in individuals who have a mutation of the CGI-58 gene and have increased IMTG content in their muscle (77), while mice with muscle-specific deletion of CGI-58 stored more TG in their muscles (82). However, Mason et al. demonstrated that ATGL and CGI-58 co-localisation following exercise was not changed when compared to rest (83). In addition, they also demonstrated that ATGL Ser[404] phosphorylation did not change after 90 min of exercise compared to rest, suggesting that unlike in adipose tissue, ATGL phosphorylation may not be an important regulator of skeletal muscle lipolysis (84). The role of G0S2 in inhibiting ATGL activity is well studied in murine and human adipose tissue (78,79); however, the role of G0S2 in muscle is currently unknown.

Hormone-sensitive lipase (HSL) is the lipase responsible for hydrolyzing DAG to monoacylglycerol (MAG), and it also possesses TAG lipase activity (73,85). HSL demonstrates the greatest affinity for DAG and appears to be required for complete TAG hydrolysis since HSL-null mice demonstrate DAG accumulation in skeletal muscle (86). HSL resides in the cytosol under resting conditions and is translocated to the lipid droplet during times of

heightened requirement for lipolysis (25). Early studies using an anti-HSL antibody to block HSL action in skeletal muscle lysates demonstrated that TG hydrolase activity was reduced by 40% and 95% in resting and exercise samples, indicating that the hydrolase activity of HSL accounts for ~60% of total neutral hydrolase activity at rest, whereas during exercise increased HSL accounts for almost all of the total lipase activity (87). While this indicates the importance of HSL activation in the lipolytic process, studies in the muscle of ATGL null mice also indicate an important role for this protein (88–90) and further studies are required to delineate the precise contribution of this lipase. In general, HSL activation is a hormonal- and contraction-mediated process. Firstly, adrenaline concentrations are increased during exercise which activates β-adrenergic receptors leading to PKA stimulation and serine phosphorylation (Ser^{563} and Ser^{660}) of HSL (91). Upon phosphorylation, cytosolic HSL is redistributed to LDs, a process which appears to be crucial for complete hydrolase activity of HSL (14,25), and has been shown to occur in isolated rat soleus muscle in response to adrenaline and electrically-stimulated muscle contraction (25). However, it is not known whether HSL translocation to LDs occurs in response to dynamic exercise in either rodent or human skeletal muscle.

In the final step of lipolysis, monoacylglycerol lipase (MGL) degrades MAG to generate a free fatty acid and glycerol molecule (92). MGL is a key enzyme in the hydrolysis of the endocannabinoid 2-arachidonoylglycerol (2-AG) (93,94) and also converts MAGs to FFA and glycerol. MGL-knockout mice have increased MAG in adipose tissue, liver and brain and this is associated with a down-regulation of FFA and glycerol release from white adipose tissue (WAT) (95). Thus, it appears likely that MGL might also be indispensable for the breakdown of MAG in other tissues including skeletal muscle. MGL ablation may also play a role in protection from diet-induced insulin-resistance (95,96); however, the physiological role of MGL in skeletal muscle lipolysis remains to be determined.

The lipases were historically thought to have free access to their substrates, which are stored in LDs. However, the discovery of PLIN1 as a scaffold protein that dictates access of proteins to the surface of LDs in adipose tissue altered the view of lipolytic control. Other homologous proteins of the PLIN family exist in skeletal muscle and appear to perform similar functions (see section 1.6).

Lipolysis is stimulated by several hormones, such as epinephrine and norepinephrine, through activation of ß-adrenergic receptors located on the sarcolemmal membrane (97,98). ß-adrenergic agonists activate adenylate cyclase (AC), the enzyme that converts ATP to cyclic-adenosine monophospate (cAMP). An increase in cAMP stimulates cAMP dependent PKA, the main kinase responsible for the activation of lipases and proteins involved in lipolysis (97,98). Other than the ß-adrenergic pathway, extracellular signal-regulated kinase (ERK)/ mitogen activated protein (MAP) kinase 3 and Ca^{2+}dependent calmodulin kinase (CaMK), which are activated by skeletal muscle contraction through the release of calcium ions (Ca^{2+}), have also been suggested to regulate muscle lipolysis (99) by phosphorylation and activation of HSL. ERK is suggested to increase lipolysis, while CaMK reduces the lipolytic rate. AMP-dependent protein kinase (AMPK) is a energy-sensing enzyme and its activity is increased during exercise as a consequences of increased levels of AMP. The role of AMPK in skeletal muscle lipolysis is controversial with reports that it decreases lipolysis, increases lipolysis or has no effect (84,87,91). A summary of this data can be seen in Figure 1-7.
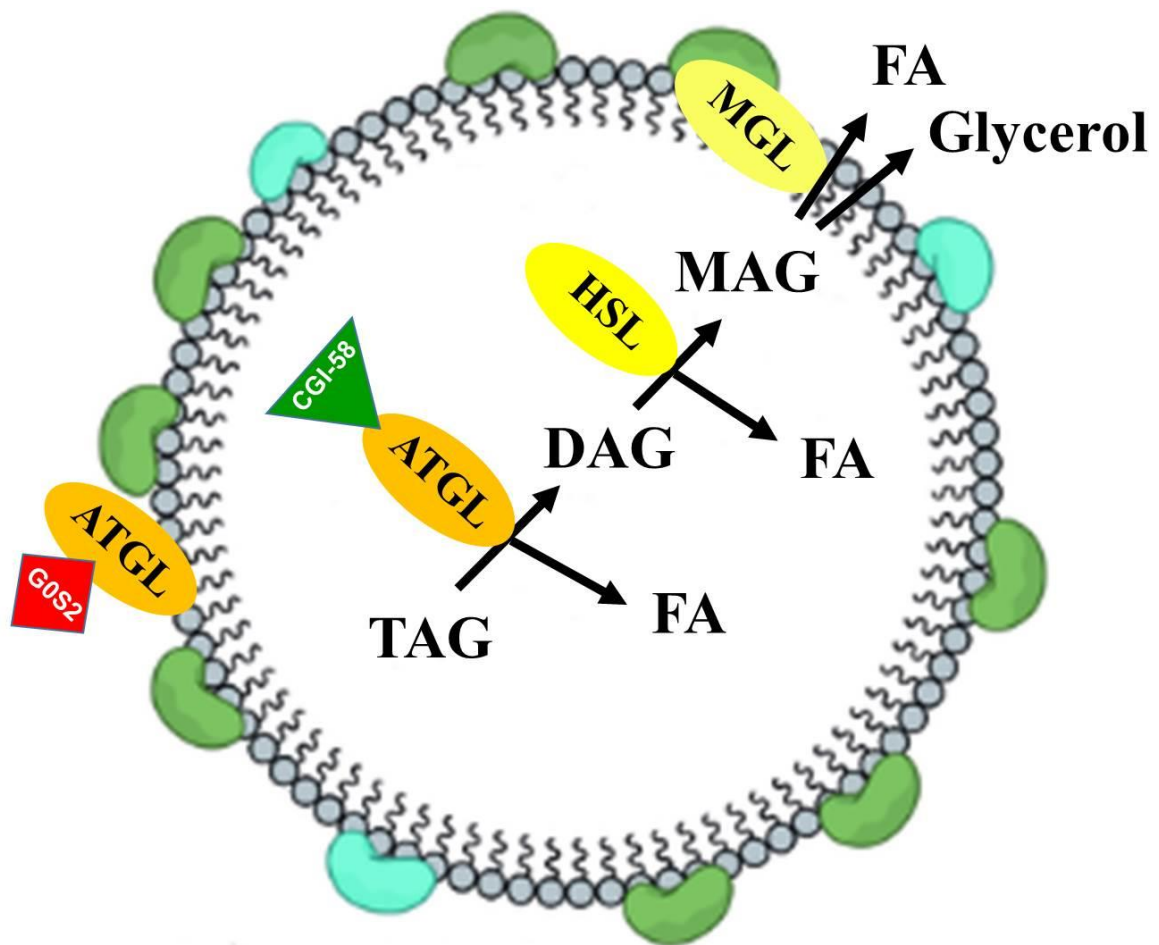
Fig 1-6. *Sequential hydrolysis of TAG by ATGL, HSL, and MGL, resulting in the release of three fatty acids and a glycerol.* For full hydrolytic activity, ATGL interacts with its coactivator protein CGI-58, whereas G0S2 will inhibit the lipolytic activity of ATGL. TAG=triacylglycerol; DAG=diacylglycerol, MAG=monoacylglycerol; ATGL= adipose triglyceride lipase; HSL= hormone sensitive lipase; MGL monoglyceride lipase) (Adapted from Lass et al. 2011) (97).
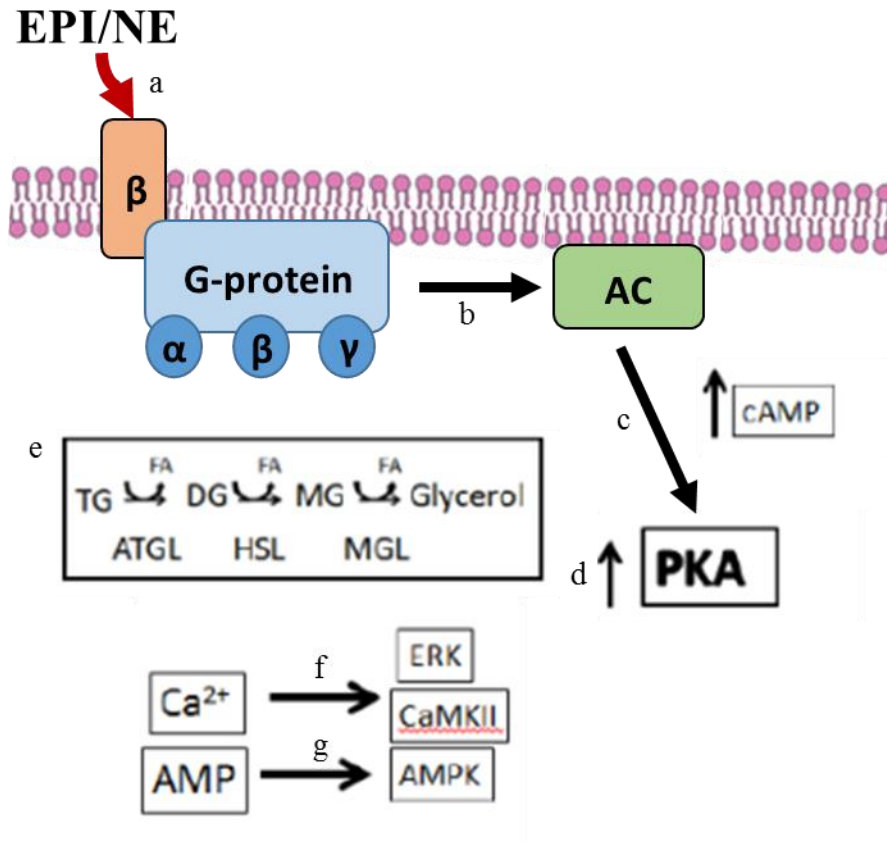
Fig 1-7. *Kinases and hormones regulate lipolysis in skeletal muscle.* Lipolysis in skeletal muscle can occur with **(a)** ß-adrenergic stimulation activating G-proteins by epinephrine and norepinephrine, which result in **(b)** activation of adenylate cyclase converting ATP into cyclic-AMP. **(c)** cyclic AMP activates **(d)** cyclic-AMP dependent protein kinase A (PKA), **(e)** that phosphorylates ATGL, and HSL to increase triglyceride breakdown. Besides the ß-adrenergic pathway, lipolysis can be stimulated through muscle contraction, where **(f)** calcium is released from the sarcoplasmic reticulum and works as a second messenger to activate extracellular related kinase (ERK) and calcium calmodulin kinase II (CaMKII), which in turn regulate HSL activity. At higher intensity of contractions, intracellular AMP levels will rise and **(g)** act as a second messenger that will activate AMP activated protein kinase (AMPK), which can also alter the rate of lipolysis. EPI/NE; epinephrine/norepinephrine, AC; adenylate cyclase, TG; triglyceride, DG; diglyceride, MG; monoglyceride, FA; fatty acid, ATGL; adipose triglyceride lipase, HSL; hormone sensitive lipase, MGL; monoglyceride lipase. (Adapted from Macpherson & Peters, 2015) (100).

1.3.4 Fatty acid entry to mitochondria

Fatty acids derived from the circulation or intramyocellular TAG hydrolysis are transported to the mitochondria where they are sequentially degraded to produce reducing equivalents for ATP production. The transport of fatty acids across the double bilayer membrane of the mitochondria is a highly regulated process (101) (Fig. 1-8). Briefly, fatty acyl-CoA is converted into an acyl-carnitine by the enzyme carnitine palmitoyl transferase 1 (CPT I) to facilitate its passage through the outer mitochondrial membrane. After passing the outer membrane, the acyl-carnitine is shuttled between the inner and outer membrane by antiport translocase. The acyl-carnitine is then passed through the inner membrane and converted back into an acyl-CoA molecule by carnitine palmitoyl transferase 2 (CPT II) once its enter the mitochondrial matrix (22,102,103).

Fig 1-8. *Schematic representation of the fatty acids enter the mitochondrion for β-oxidation.* CPT I, carnitine palmitoyl transferase 1; CPT II, carnitine palmitoyl transferase 2. (Adapted from Kiens, 2006) (103).

1.4   Lipid Metabolism and Exercise

Lipids and carbohydrates are the main energy substrates during exercise. Several studies using stable isotope methodologies have reported the relationship between exercise intensity and duration and substrate metabolism (104,105). Van Loon *et al.* showed that muscle utilization of circulating glucose increases progressively up to n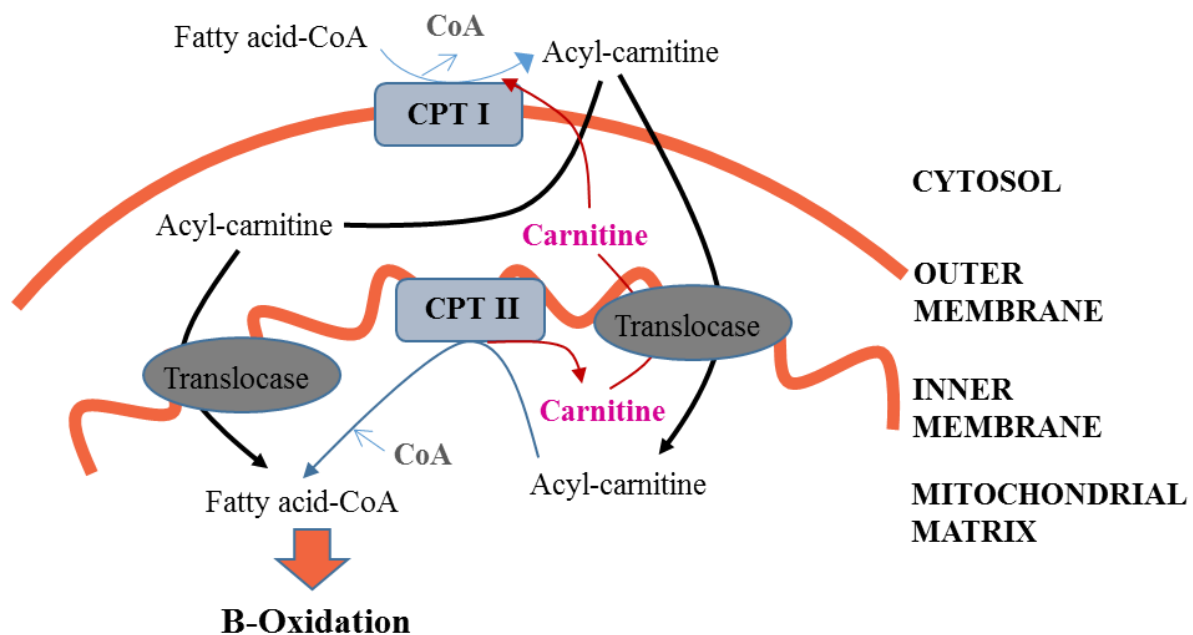ear-maximal intensities, whereas utilization of circulating FFAs declines modestly as the exercise intensity is increased (Fig. 1-9), suggesting that the majority of energy at high exercise intensities is provided by muscle glycogen (106). In another study, the energy contribution from fatty acid oxidation *i.e.* plasma and IMTG-derived fatty acids was progressively increased during prolonged moderate intensity exercise (>60 min) (Fig. 1-10), together with declining proportion of energy derived from both muscle glycogen and plasma glucose (105).

Fatty acids are the main energy source in the major organs of the body and provide essential energy substrates particularly at rest and during moderate intensity exercise. At rest, the lipolysis rate in adipose tissue typically provides FFA at a rate in excess of the amount required for oxidation (107), resulting in increase plasma FFA levels and re-esterification of FFAs into peripheral tissues. Early studies using indirect calorimetry measures together with the infusion of a ^{13}C labelled tracer to predict the contribution of the IMTG pool to total fat oxidation during an acute exercise bout (64,105,106,108,109) demonstrated that the rate of non-plasma fatty acid oxidation (i.e. IMTG and lipoprotein-derived TG) is at the highest during exercise between 40 and 65% VO_2 max, and accounts for ~30-50% of total fat oxidation (105,110). This result is further supported by Alsted *et al.*, which showed IMCL content was decreased by 77% following 20 min of *ex vivo* contractions with an obvious reduction in LD size and number (111). In addition, van Loon (2004) reported that net IMTG breakdown is significantly increased in response to moderate-intensity exercise, therefore providing additional evidence that the IMTG pool contributes to total fat oxidation during exercise in human (112). Together, these data demonstrate that the fatty acids release from adipose tissue lipolysis and IMTG lipolysis are important sources of energy during exercise.

Aside from a direct role in metabolism, fatty acids may provide important signals that lead to adaptations in skeletal muscle. For example, a single exercise session can induce the channeling

of fatty acids toward neutral TAG storage during post-exercise period (113) and stimulate gene expression of multiple genes involved in TAG synthesis and LD assembly and mobilisation in skeletal muscle (114). Others have also suggested that endurance exercise can induce an increase in type I muscle fiber numbers (115–117), and that the fatty acid-sensitive peroxisome proliferator-activated receptor δ (PPARδ) and PPARδ coactivator 1α (PGC-1α) are suspected to be involved in mediating these positive adaptions in the skeletal muscle in response to exercise (118–125). Interestingly, there are several studies reported that individuals who regularly exercise (i.e. athletes) have higher IMTG levels and oxidative capacity, and are more insulin sensitive compared to untrained individuals (19,115,126) and that exercise training increases IMTG levels and improves insulin resistance (58,116,117,127,128). Paradoxically, an increase in skeletal muscle lipid accumulation is also associated with insulin resistance (129). This phenomenon is known as the "athlete's paradox" and it is suggested that regular exercise increases IMTG pool turnover, which then leads to protection from accumulation of 'lipotoxic' intermediates associated with insulin resistance. (115,130,131).
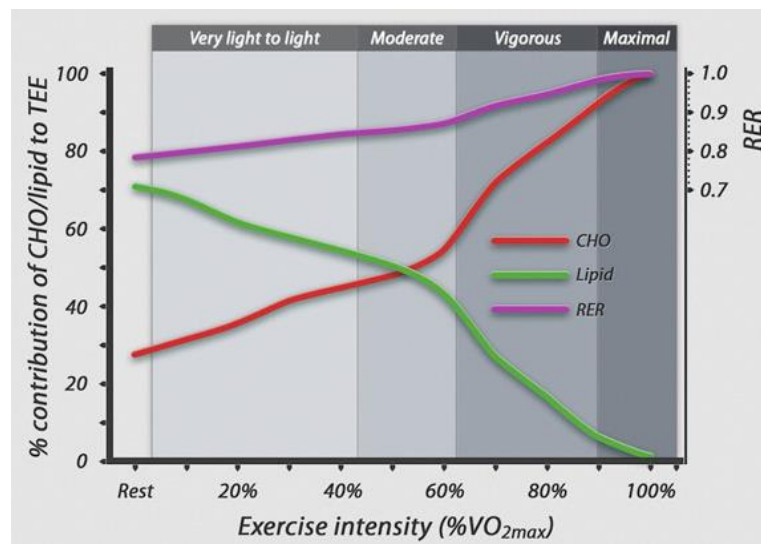
Fig 1-9. *Substrate contribution to exercise of increasing intensity.* Carbohydrate oxidation rate and relative contribution to energy provision progressively increases as the exercise intensity increases, The contribution of lipid oxidation to energy provision decreases proportionally with increasing exercise intensity, as reflected by a steady rise in respiratory exchange ratio (RER) (66).
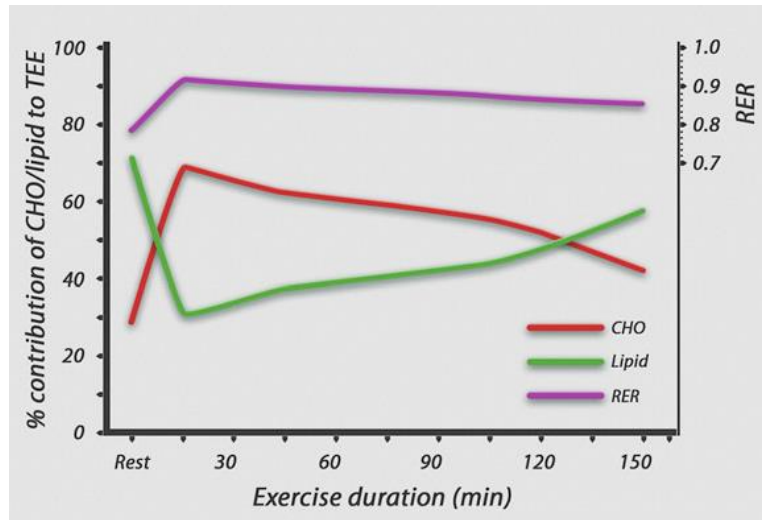
Fig 1-10. *Substrate contribution to energy expenditure during prolonged moderate-intensity exercise (65% VO₂max).* An initial rise in the RER occurs at the onset of exercise, reflecting the increase in relative contribution of carbohydrate to energy provision compared to resting metabolism. Thereafter, a small but steady decline in the RER is observed with extended duration of exercise, reflecting the declining relative contribution of carbohydrate and increasing contribution of lipids to energy provision (66).

1.5   Lipid Metabolism and Insulin Resistance

The close links between obesity and T2D indicates that an oversupply of lipids, or defects in lipid metabolism, are causative for insulin resistance. It is documented that plasma fatty acid concentrations are increased in obese individuals, which is mainly the result of increased fatty acid release associated with the expansion in fat mass (132). Early studies using C57BL/6J mice fed a high-fat diet (HFD) showed the mice have an increased in body weight gain, a stable hyperglycemia and a progressive increased of hyperinsulinemia, indicating a progressive worsening of insulin resistance (133,134). Others showed that systemic lipid infusion in mice can led to increases in basal hepatic glucose production and marked insulin resistance, revealed by impaired suppression of liver glucose production and reduced peripheral glucose disposal during hyperinsulinemic-euglycemic clamps (135,136). Several transgenic mouse models also demonstrate a clear link between defect of fatty acid metabolism and impaired insulin action (137–139).

The functional imbalance between IMTG storage, lipolysis and fatty acid oxidation also may result in the accumulation of fatty acid metabolites. Metabolites such as DAGs, LCFA-CoAs and ceramides have been reported to negatively impact and interfere the insulin signalling cascade. DAG, is an intermediate in both IMTG synthesis and hydrolysis, is increased many models of obesity-induced insulin resistance (140,141). Furthermore, the saturation of DAG is usually higher in sedentary lean and obese individuals compared with athletes (142,143), although this is not always the case (115). Nevertheless, on balance, DAG accumulation is an important predictor of insulin resistance and it is thought to induce insulin resistance by activating specific protein kinase C (PKC) isoforms which inhibits insulin signalling at the insulin receptor substrate (IRS) proteins (Fig. 1-11) This was first shown by Yu *et al.* that demonstrated enhanced PKC-θ activation with concomitant reduction of tyrosine phosphorylation and increased of serine phosphorylation of IRS-1 in response to a lipid infusion in humans (144). Many studies have since established the predominant site of serine phosphorylation by novel PKCs and other stress kinases which include ser307, ser636/639, and ser1101 (145,146). Given that serine phosphorylation of IRS-1 generally inhibits IRS1 tyrosine phosphorylation and subsequent downstream activation of PI3-K and Akt/PKB, it is postulated that insulin-stimulated glucose transporter 4 (GLUT4) translocation is consequently reduced (Fig. 1-11).

Ceramide accumulation is also reported to occur in obese individuals and T2D patients compared with lean controls (147–149). Its content is higher in type I fibres compared to type II fibres in healthy lean individuals (150) and obese subjects with or without T2D (151). The ceramide fatty acid saturation is most likely more important rather than total ceramide content itself, as it seems to be increased in obese individuals compared to lean (147,149). Bergman et al. (2016) reported increased content of muscle C18:0 ceramide, dihydroceramide and glucosylceramide species are in obesity and in insulin resistance individuals (152). Thus, higher fatty acid saturation appears to be an important factor in the mechanism by which ceramide accumulation leads to skeletal muscle insulin resistance (Fig. 1-11). Taken together, further studies are still required to elucidate the exact role of lipid metabolite species in the development of skeletal muscle insulin resistance.

Insulin resistance and T2D are also reported to associate with a reduction in mitochondrial function that is postulated to cause ectopic fat accumulation in muscle and other tissues (153). Studies in elderly (154) and young (155) individuals revealed that higher levels of TGs in muscle and liver is significantly associated with insulin resistance and compromised mitochondrial function. It is suggested that a reduction in the number of muscle mitochondria, which may be caused by a decrease in the expression of nuclear-encoded genes that control mitochondrial biogenesis, such as PGC-1α (156) and PGC-1β (157), can induce the accumulation of intramyocellular fat in the insulin-resistant individuals. In addition, the activation of PGC-1α has also been reported to be related with the improvement of mitochondrial function and insulin sensitivity in animal and human studies (158,159). Thus, it is likely that defects in mitochondrial function can lead to the development of insulin resistance, which possibly caused by the elevation of intracellular fatty acid metabolites that disrupt insulin signalling, especially in the muscle and liver. However, not all studies provide conclusive support for the theory that mitochondrial dysfunction is associated with insulin resistance. For example, Choi et al. have reported that PGC-1α overexpressing mice have enhanced mitochondrial function but have a defect in insulin action as evidenced by decreased insulin-stimulated muscle glucose uptake (160). This is supported by other studies which have reported that muscle mitochondrial function was not altered in obese and T2D individuals when compared with controls (161–164). This

shows that mitochondrial dysfunction is not a really a requisite factor of insulin resistance in all circumstances.
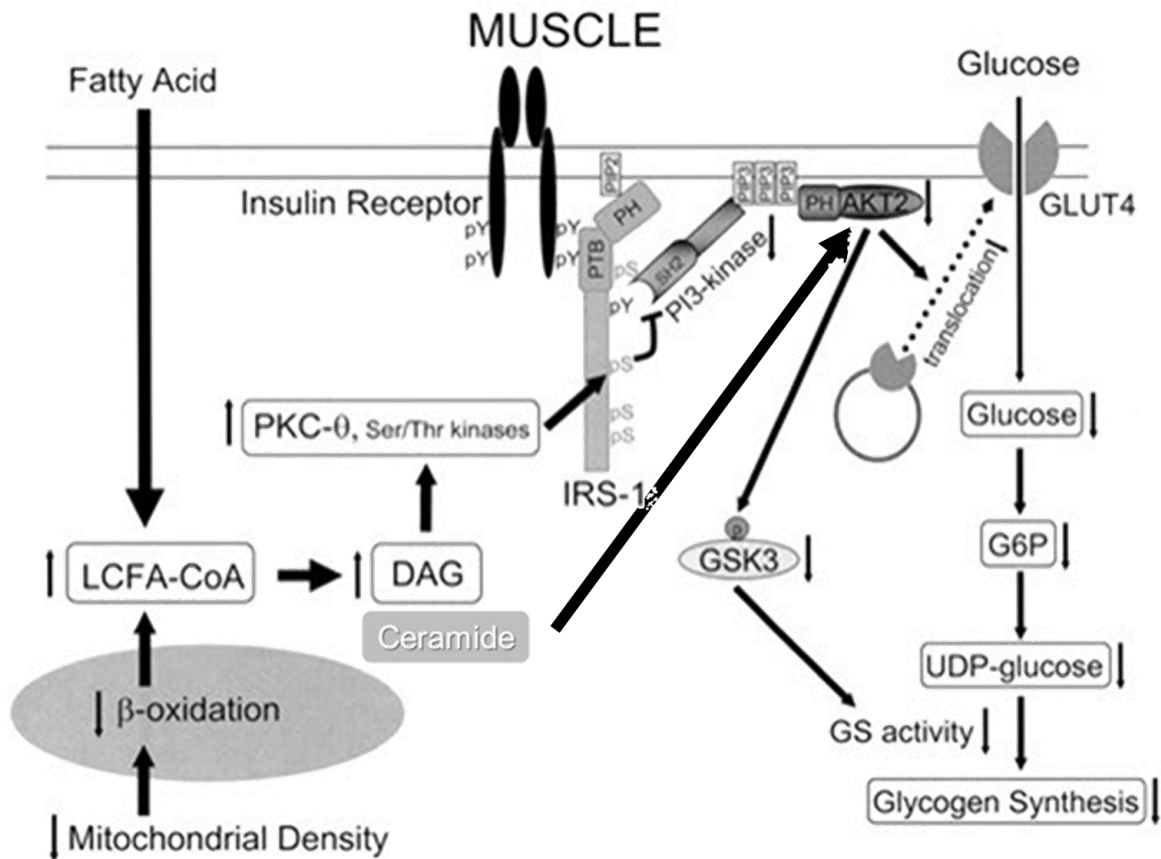
Fig 1-11. *Lipid-induced insulin resistance in skeletal muscle*. Increases in intramyocellular fatty acyl CoAs and diacylglycerol/ceramide due to increased delivery from plasma and/or reduced β-oxidation due to mitochondrial dysfunction activate serine/threonine kinases such as protein kinase C (PKC-θ rodents, PKC-β and -δ humans) in skeletal muscle. The activated kinases phosphorylate serine residues on IRS-1 and inhibit insulin-induced PI 3-kinase activity, resulting in reduced insulin-stimulated AKT2 activity. Lowered AKT2 activity fails to activate GLUT4 translocation, and other downstream AKT2-dependent events, and consequently insulin-induced glucose uptake is reduced (165).

1.6   The Perilipin Family

As previously mentioned, intracellular LDs contain a large number of proteins co-located within the phospholipid monolayer (33) surrounding the LD (166). PLIN1 was the first identified lipid droplet-associated protein (38,39) and since then four other PLIN proteins have been identified. The PLIN protein family are identified by the specific amino acid region called the PAT domain found on PLIN1-3 and PLIN5, in addition to a specific 11-mer repeat region found on all PLIN proteins (Fig. 1-12). Each PLIN protein has been known by several names (167) but are now known by the PLIN1-5 nomenclature after the 2007 Federation of American Societies for Experimental Biology (FASEB) Conference on Lipid Droplets: Metabolic Consequences of the Storage of Neutral Lipids in Vermont, USA (167). Each PLIN possesses a unique tissue (Fig. 1-13) and intracellular distribution, indicating that specificity in their regulation of LD metabolism (Table 1-1).
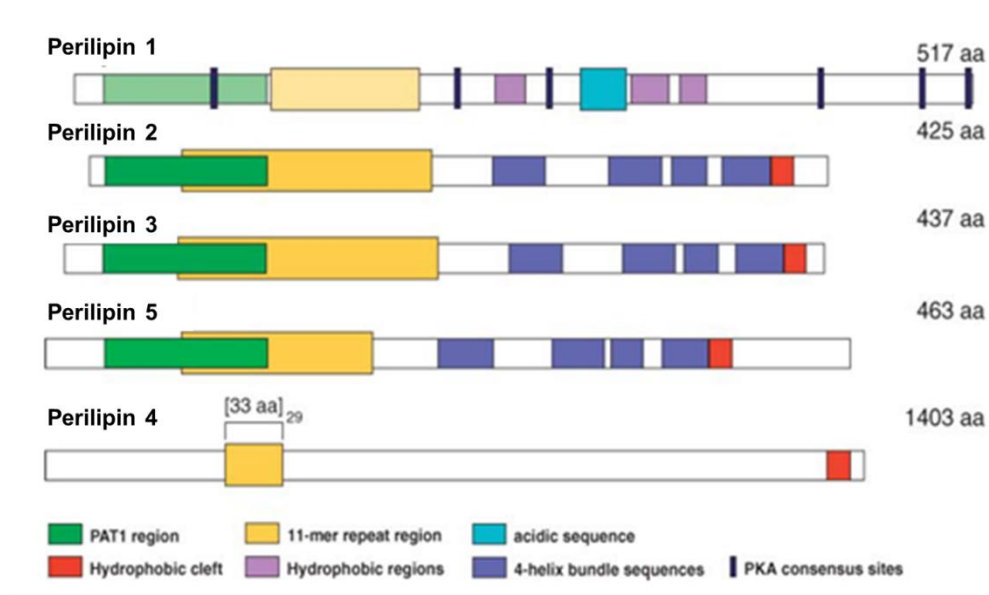
Fig 1-12. *Schematic diagram of the structural features of perilipin family proteins. Modified from Brasaemle (2007).*
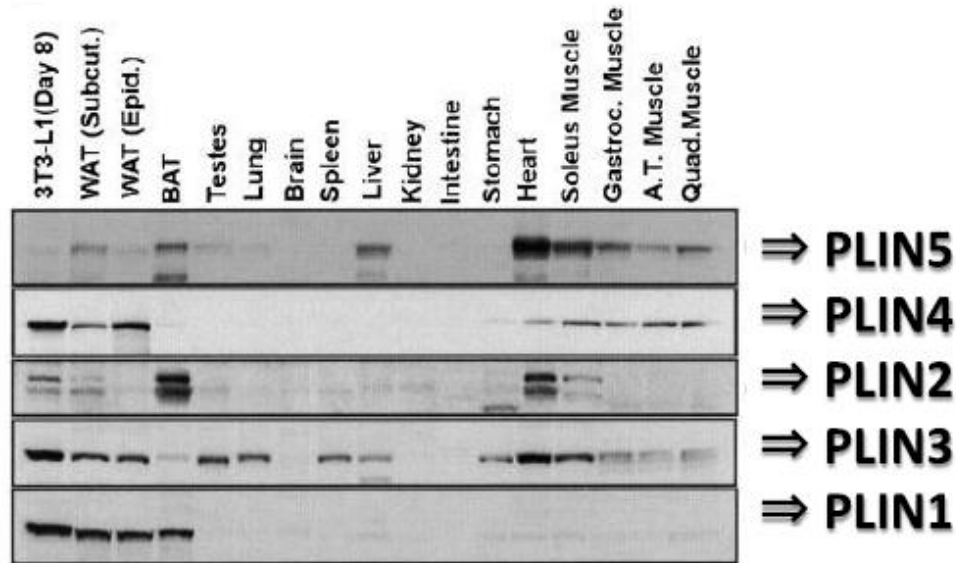
Fig 1-13. *PLIN family protein expression in 3T3-L1 adipocytes and mouse tissues (adapted from Wolins et al. 2006).*

Name	Other names	Molecular mass (kDa)	Cellular location	Chromosome location	Tissue distribution
Perilipin 1	Peri	~62	Membrane bound	15q26	Adipocytes, steroidogenic
Perilipin 2	Adipophilin, Adipose differentiation-related protein, ADPH, ADRP, ADFP	~50	Membrane bound	9p22.1	Ubiquitous
Perilipin 3	Tail-Interacting Protein of 47 kDa, TIP47, PP17, M6PRBP1	47	Cytosol	19p13.3	Ubiquitous
Perilipin 4	S3-12, K1AA1881	150	Cytosol	19p13.3	WAT, skeletal and cardiac muscle
Perilipin 5	Myocardial Lipid Droplet Protein, Lipid Storage Droplet Protein 5, MLDP, OXPAT/PAT-1, LSDP5	~50	Cytosol	19p13.3	Oxidative tissue (skeletal, cardiac muscle)

Table 1-1. *Summary of perilipin family proteins.*

1.6.1   Perilipin 1 (PLIN1)

PLIN1 is the most well-characterised PLIN protein and is mainly expressed in adipose tissue and steroidogenic cells (168). Although PLIN1 mRNA expression has been detected at low levels in skeletal muscle, it is suggested that is due to contamination by adipocytes existing between the muscle fibres (169). In adipose tissue, PLIN1 is a major regulator of lipid storage and hydrolysis in LDs. PLIN1 plays an important role in regulating the activation of ATGL and HSL driving lipolysis in adipose tissue (38). Overexpression of PLIN1 in 3T3-L1 adipocytes showed a massive reduction in lipolytic activity and a significant increase in TGs level, indicating that PLIN1 plays a role in limiting the access of lipases to LDs and protecting the TG storage (170). Under basal conditions, PLIN1 was found to bind with CGI-58, the co-activator for ATGL, on the LD surface and this is thought to inhibit the lipolytic activity of the ATGL (38,170,171). PLIN 1 is also thought to coat the LDs and prevent the access of HSL in the cytosol to the LDs and therefore protect the lipid core from the lipolytic activity of HSL (172–174). PKA-mediated phosphorylation in specific serine residues of PLIN 1 causes the release of CGI-58, which then caused the activation of ATGL (21,76). Phosphorylation of PLIN1 also leads to the activation of HSL, which allows access of HSL to LD. Both proteins need to be phosphorylated by PKA in order for HSL to interact with PLIN1 and stimulate lipolysis (14,172,175)

PLIN1 function was further confirmed using PLIN1 knockout mice that demonstrated a substantial increase in basal lipolysis, a 75% reduction in adipose tissue mass, and protection against diet-induced obesity (176,177). In addition, HSL-stimulated lipolysis in isolated adipocytes was reduced (176), indicating that PLIN1 not only involves in regulation of lipase activity under basal conditions, but also play a roles in recruitment and activation of lipases under activated lipolytic conditions. In support, PKA was found to phosphorylate PLIN1 on serine residues causing the translocation of HSL to PLIN1- coated LDs (178). Therefore, PLIN1 phosphorylation appears to facilitate HSL access to the stored TAG. Interestingly, adipose-specific overexpression of PLIN1 (aP2-PLIN1) mice also demonstrated a lower body weight compare to its control when fed either a low or high fat diet due to upregulation of oxidative genes in brown adipose tissue (BAT) (179). As brown fat is known to regulate obesity susceptibility in mice (180), increased in the oxidative capacity of BAT in this animal model can be used as a prediction to decrease susceptibility to diet-induced obesity.

PLIN1 is expressed in human adipose tissue and its role in the progression of metabolic disease remains unclear as researchers cannot determine a causative link between PLIN1 level and obesity/T2D in humans. The results in human studies are inconsistent with some reported decreased (181–183) of PLIN1 expression in obese subjects while the other reported vice versa (184).

1.6.2 *Perilipin 2 (PLIN2)*

PLIN2 (adipose differentiated related protein, ADRP or adipophilin) was the second PLIN to be discovered, and is expressed in most tissues, with the highest expression in the liver (185). PLIN2 protein plays an important role in LD formation and fatty acid storage (186,187). At first, PLIN2 protein was thought to be involved in LD synthesis as PLIN2 was found to exist during early adipocyte differentiation and was localises to LD surfaces (187). Later, Wolins et al. showed that PLIN2 translocated to the LD surfaces with addition of fatty acids in fully differentiated adipocytes (188). Many studies have since demonstrated that PLIN2 protein expression is increased with the enhancement in LD formation (189–191), indicating the involvement of PLIN2 in LD growth. PLIN2 protein is also found to be responsible for increased fatty acid uptake and TAG accumulation in cells (192) including fibroblasts (193), HEK 293 cells (194), hepatic stellate cells (195) and COS-7 cells (192). In addition, PLIN2 is found to interact with DGAT2 (196), supporting the role of PLIN2 in LD synthesis and growth. PLIN2 function appears to be similar to PLIN1 where it may limit the access of ATGL to the stored TAG, thereby reducing the rate of TAG turnover (194,197) through binding with CG1-58 (198).

There were no dramatic effects on adipocyte differentiation or lipolysis or marked changes in the metabolic phenotype in global PLIN2 knockout mice compared to littermate control mice (199). However, there is a significant reduction in TG content and LD number in the liver of PLIN2 knockout mice (199,200), and resistance to diet-induced hepatosteatosis. PLIN2 overexpression in skeletal muscle leads to IMTG accumulation and increased ceramide levels (201), which paradoxically coincided improve skeletal muscle insulin sensitivity (201). Therefore, it can be postulated that PLIN2 is important for lipid storage in skeletal muscle by increasing TAG storage into LDs and thereby protecting against lipotoxicity-associated insulin resistance.

PLIN2 muscle protein expression was reported to be lower in T2D patients compared to healthy individuals (202). However, PLIN2 content is higher in skeletal muscle from individuals that are insulin resistant and have undergone therapeutic weight loss or metformin treatment to increase muscle insulin sensitivity (203). This indicates that PLIN2 might be responsible for the reduction of lipid toxicity in skeletal muscle by enhancing the lipid synthesis or oxidation. Another work using human skeletal muscle revealed that PLIN2 content in skeletal muscle is unaffected after a single bout of endurance exercise (204). Interestingly, they found that PLIN2-associated LDs were significantly reduced while PLIN2 that's not associated with LDs were unchanged, suggesting an important role of PLIN2 in exercise induced lipolysis (204). Notably, only about two-thirds of LDs in skeletal muscle contain PLIN2 (166), indicating the likelihood of other PLIN proteins in regulating the remaining LD pool.

1.6.3   Perilipin 3 (PLIN3)

PLIN3 was first discovered as an effector protein for mannose-6- phosphate receptor trafficking and initially was known as tail interacting protein of 47 kDa (TIP-47) (186,205,206). As this protein was found to have relationship with LDs and shared 43% gene sequence homology to PLIN2 (207), it was later renamed PLIN3. PLIN3 was the first 'exchangeable' LD protein identified (207), with a possible role of trafficking proteins and/or lipids within the cytosol (208). PLIN3 is predominately located in the cytosol (endosomes, golgi, mitochondria) and is sometimes bound to LDs (206,209,210). PLIN3 can move from the cytosol to LDs in response to lipid loading (188,207), and is therefore implicated as a fat storage protein.

Overexpression of PLIN3 in macrophages increased TAG levels (211). This finding is supported by the other studies, showing that PLIN3 knockdown caused the decreased TAG content (211–213). The knockdown of PLIN2 also found to cause the translocation of PLIN3 to the LD surface (211), suggesting that PLIN3 might compensate for the loss of PLIN2 on the LD and help to maintain the normal LD function. Furthermore, knock-down of PLIN3 in PLIN2-null fibroblasts reduces the number of LDs (213), and it is therefore suggested that PLIN3 may also protect against lipolysis and promote TAG storage. The study of PLIN3 function *in vivo* is limited. Reduction of PLIN3 expression via antisense oligonucleotide treatment caused a reduction in

hepatic steatosis, improved glucose tolerance and enhanced insulin-mediated glucose disposal in peripheral tissues (214). Thus, these findings suggested that PLIN3 might be a potential target for the treatment of nonalcoholic fatty liver and other related metabolic disorders.

PLIN3 is expressed in skeletal muscle (10,215); however, few studies have elucidated its role in this tissue. PLIN3 expression in skeletal muscle has been shown to be higher in women compared to men and it does not increase after training (215). In contrast, Louche *et al*. (2013) showed that PLIN3 protein content is upregulated after training exercise in obese subjects (216). PLIN3 also has been found to coimmunoprecipitate with ATGL and CGI-58 in skeletal muscle, and these relationships were maintained even after electrical stimulated contraction (217). In addition, PLIN3 also has been demonstrated to be phosphorylated in skeletal muscle (218); however, the role of PLIN3 phosphorylation in the regulation of substrate metabolism remains to be established.

1.6.4   *Perilipin 4 (PLIN4)*

PLIN4, previously called S3-12, was the fourth member of PLIN family and was initially identified in adipocytes (219) and then later in skeletal and cardiac muscle (220). It is heavily expressed in white and brown adipose tissue (188). PLIN4 does not share a strong homology with the other PLIN proteins with a protein mass of ~160 kDa that is almost three times bigger than the other PLIN proteins (220). A very small number of studies have investigated its function; it can translocate to newly formed LDs during lipid loading in adipocytes (220) and is thereby thought to play an important role in the biogenesis of nascent LDs.

Global PLIN4 deletion in mice does not alter body weight or total adiposity, although there is a reduction in cardiac TAG accumulation (221) under low and high-fat feeding. Interestingly, the deletion of PLIN4 also results in PLIN5 down-regulation, indicating strong associations between these two LD proteins. PLIN4 protein was found to be increased in skeletal muscle of mice fed with HFD (23), while this does not occur in humans (215). The precise role of PLIN4 in non-adipose tissue, especially skeletal muscle, remains to be determined.

1.7   Perilipin 5

1.7.1   *The cell biology of PLIN5*

PLIN5 was the last of the PLIN family members to be discovered and was described by three independent groups in 2006-2007. It was originally known by three different names: lipid droplet storage protein 5 (LSDP5), OXPAT, and myocardial lipid droplet protein (MLDP) (10,11,222). PLIN5 is mainly expressed in highly oxidative tissues including skeletal muscle, heart, liver, and brown adipose tissue (10). PLIN5 expression is highest in muscle fibres with a high capacity for fatty acid oxidation (Type I > Type 2a > Type 2b), which corresponds to fibre types that also have the highest IMTG content (9,223). PLIN5 is highly homologous (~55%) with the other PLIN proteins, such as PLIN2 and PLIN3, and is transcriptionally regulated by PPARα in muscle and liver, and by PPARγ in WAT, where it is lowly expressed (10,11,222). Similar to PLIN3, PLIN5 is mainly found at the LD surface as well as in the cytosol and mitochondria (10,11,222). As lipolysis occurs on the surface of LDs, it is possible that PLIN5 is translocated to the LD surface in circumstances that promote lipolysis, such as muscle contraction. However, MacPherson et al. showed that PLIN5 is not recruited to LDs with contraction in isolated skeletal muscle (100).

While the expression of PLIN5 in skeletal muscle has been well described, understanding of its role in the control of intramyocellular lipid trafficking, substrate utilization and insulin action is still inconclusive. Studies in cultured cells (other than skeletal muscle) demonstrate that PLIN5 appears to be important for the accumulation of TAG, since forced expression of PLIN5 in Chinese hamster ovary (CHO) cells (11) or COS-7 cells (10) promotes fatty acid uptake and increases TAG concentration. These observations suggest that PLIN5 may either promote TAG synthesis and / or decrease TAG lipolysis. In agreement, PLIN5-null mice demonstrate reduced TAG concentrations in the heart compared to wild-type controls (224), which was due to an increase in lipolysis in cardiomyocytes. Interestingly, PKA-stimulation of alpha mouse liver 12 (AML12) cells that overexpress PLIN5 promotes TAG hydrolysis, which in turn provided an increase in the availability of FAs for β-oxidation (225). Collectively, these studies suggest that PLIN5 is a major regulator of intracellular TAG turnover by inhibiting TAG hydrolysis under basal state conditions and facilitating lipolysis under PKA-stimulated conditions. This relationship is explained by PLIN5 interactions with key lipolytic proteins. Studies employing

multiple techniques, such as Anisotropy Forster Resonance Energy Transfer (AFRET), co-immunoprecipitation, [^{32}P]orthophosphate radiolabeling, and measurement of lipolysis, have shown that PLIN5 can bind either CGI-58 or ATGL (but not both simultaneously) under basal conditions (Fig. 1-14), which reduces the binding of ATGL to CGI-58, preventing the co-activator induced increase in ATGL TAG hydrolase activity, and therefore limiting lipolysis (12,13). Phosphorylation of PLIN5 under PKA-stimulating conditions caused the release of ATGL and CGI-58 from PLIN5 to facilitate their interaction and enhance TAG hydrolysis (12,13) (Fig. 1-14).

Aside from its role in TAG metabolism, it has been postulated that PLIN5 plays a role in mitochondrial metabolism. PLIN5 has been found to localize to mitochondria in smooth and skeletal muscle (226) and it is proposed to promote the interaction of the LD and mitochondria (225,226), which may help in channelling the fatty acids from LD lipolysis towards the mitochondria for β- oxidation (10,225–227). This is supported by studies reporting increased PLIN5 mRNA and protein content in liver and heart in response to conditions that increase fatty acid oxidation, such as fasting (10,11,222). In addition, PLIN5 expression was remarkably higher in endurance-trained athletes compared to sedentary controls (114,115), and increases in response to endurance and interval training (215,228). In addition, Peters *et al.* demonstrated that there is a strong relationship between PLIN5 expression and the improvement of oxidative capacity with endurance exercise training (215).

The role of PLIN5 in skeletal muscle metabolism is less clear. Mild overexpression of PLIN5 via deoxyribonucleic acid (DNA) electrotransfer into the glycolytic muscle of rats increased TAG accumulation (226), which is consistent with the general consensus that PLIN5 plays an important role in LD accumulation (9,11,222). Although PLIN5 increased TAG accumulation, this appeared to have no effect on skeletal muscle insulin action (227). Bosma *et al*. have also shown that PLIN5 may also localise to the mitochondria, therefore given the role of PLIN5 in controlling TAG hydrolysis, it is suggested that this PLIN protein channels fatty acid released by lipolysis into the mitochondria for β-oxidation (226). Interestingly, Mason *et al*. showed that PLIN5 was significantly colocated with mitochondria and LDs, but PLIN5-mitochondrial co-localization and PLIN5-LD co-localization remained unchanged during moderate-intensity

exercise (83), questioning a dynamic role of PLIN5 in mitochondrial-LD interactions. While these short-term overexpression models have provided useful insights into PLIN5 function in muscle, the physiological significance of PLIN5 deletion on skeletal muscle and systemic metabolic control remains unresolved.
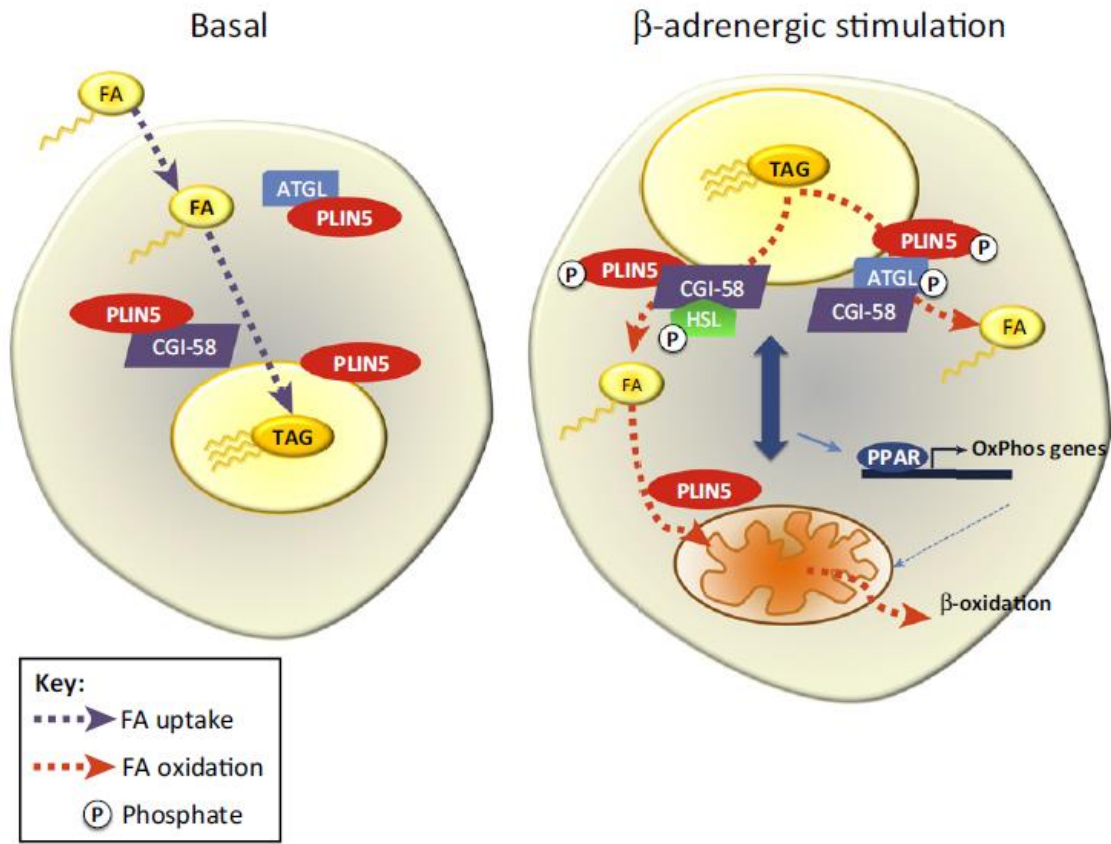
Fig 1-14. *Proposed mechanism of PLIN5 protein in regulation of fatty acid metabolism in skeletal muscle based on evidence from cell-based studies.* Under basal conditions, PLIN5 is suggested to be involved in fatty acid metabolism by; 1) independently binds to ATGL and its coactivator CGI-58 to prevent their interaction and thereby reduce lipolysis and 2) facilitates sequestering of fatty acid into LDs to prevent excessive fatty acid oxidation. While under β-adrenergic stimulation, PLIN5 is proposing to enhance the lipase interaction on the LD surface and also directing fatty acids to the mitochondria for β-oxidation. The released of fatty acids can also activate a PPAR α or δ transcription program (OxPhos genes) that increases the oxidative capacity of cells. PLIN5 may be required for maintaining close LD–mitochondrial contact (denoted by blue arrow). (229).

1.7.2   Plin5 and in vivo physiology

The establishment of whole-body *Plin5* null (*Plin5*^{-/-}) and *Plin5* overexpression mice have provided further opportunity to researchers to study PLIN5 function in non-adipose tissue, especially heart, skeletal muscle and liver (224,230). Kuromoto *et al.* studied cardiac function of *Plin5*^{-/-} mice and demonstrated that *Plin5* ablation causes an increase in ATGL lipase activity and lipolysis, fatty acid oxidation and oxidative stress (224). They also reported an aging related decline in heart function in the *Plin5* null mice, most probably as a consequence of oxidative stress in these mice (224). In agreement, Pollak *et al.* showed that a reduction in ATGL- and HSL-mediated lipolysis led to decreased fatty acid oxidation in mice with cardiac-specific overexpression of PLIN5 (CM-PLIN5) (231). Furthermore, these CM-PLIN5 mice also demonstrated cardiac steatosis, increased heart weight, left ventricular hypertrophy, and mild cardiac dysfunction (231,232). Thus, PLIN5 is needed to maintain normal lipid homeostasis and function in the heart.

Wang *et al.* have developed another *Plin5* null mouse line and focussed their studies on lipid metabolism in liver (230). They showed that *Plin5* deletion caused a reduction of hepatic lipid content and smaller-sized LDs, which was likely due to the elevated intrahepatic lipolysis and fatty acid oxidation. The *Plin5* null mice also displayed hepatic injury as demonstrated by liver function abnormality, activation of endoplasmic reticulum (ER) stress signalling and increased lipid peroxidation, especially in mice fed a high-fat diet (230). Therefore, these findings support the hypothesis that PLIN5 is required to prevent FFA accumulation, lipotoxicity, and liver damage. Others have shown that PLIN5 is required to regulate ß-cell lipid metabolism and insulin secretion in a cAMP-dependent manner, thereby implicating PLIN5 in the regulation of postprandial insulin secretion (233). No study to date has examined the role of PLIN5 deletion on skeletal muscle substrate metabolism *in vivo*, and this will be a primary focus of this thesis.

1.8   PLIN5 and Exercise

1.8.1   PLIN5 and acute exercise

The role of PLIN5 in regulating substrate metabolism during contraction or exercise training is unresolved. Previous studies have reported that PLIN5 is not recruited towards LDs with contraction in isolated muscle (234). Furthermore, they also identified that PLIN5 associates with ATGL, CGI-58 and HSL at rest in rodent skeletal muscle, while the degree of PLIN5 phosphorylation does not change following tetanic contractions (217,218). In agreement, Mason et al. reported that the PLIN5-ATGL and PLIN5-CGI-58 interactions were not impacted by 60 min of moderate intensity exercise in human vastus lateralis muscle (83). It is possible that these studies lacked the sensitivity to detect small changes in protein association and further work examining protein localization and associations are warranted. Therefore, it is known that PLIN5 is phosphorylated by PKA, however, the critical residues and functional relevance remains unresolved. Shepherd and colleagues reported that LDs containing PLIN5 were preferentially used over LDs that did not containing PLIN5 after sprint interval and endurance training (228). Just how PLIN5 is involved in the regulation of substrates metabolism during exercise is yet to be determined.

1.8.2   PLIN5 and endurance exercise training

Endurance exercise training induces a plethora of structural and functional changes in skeletal muscle including an increase in mitochondrial content and oxidative capacity (235,236) and an increase in LD storage (19,115,126,143). These training adaptations are known to improve the muscles ability to use stored triglycerides more efficiently. PLIN5 has been speculated to act as regulator or break in the process of fatty acid release to the mitochondria during lipolysis in cardiac and skeletal muscle. Therefore, increased expression of PLIN5 in endurance trained individual (115) is thought to cause the increase in IMCL storage. Many studies have showed a very close relationship between muscle oxidative capacity and PLIN5 content following endurance training, suggesting that PLIN5 is involved in the regulation of fatty acid oxidation in muscle (10,215). Intriguingly, a recent study demonstrated that PLIN5 protein content is increased in isolated mitochondria after a 30 min *in vivo* contraction compared to mitochondria isolated during rest state (237), suggesting that PLIN5 protein may play a role in mitochondria

during muscle contraction, possibly by enhancing LD-mitochondria coupling during contraction-induced lipolysis.

1.9   PLIN5 and Metabolic Disease

Dysfunctional lipid metabolism is a feature of obesity and T2D and contributes to the accumulation of lipids in most tissues examined, including the liver and skeletal muscle which are the key insulin sensitive tissues involved in glycemic control (238). As mentioned previously, lipid accumulation is caused by the elevation of plasma FFA availability and fatty acid uptake, and will eventually overwhelm capacity for fatty acid oxidation leading to ectopic lipid accumulation. As PLIN5 is involved with TAG metabolism and possibly the oxidative disposal of fatty acids (12,13,20,114,227), it can be interpreted that this protein also be important in regulating insulin action. However, the role of PLIN5 in development of metabolic diseases remains understudied.

PLIN5 expression is increased in the skeletal muscle and liver of mice fed a HFD compared with mice fed a low-fat diet (23,221,230,239,240). In contrast to this common finding in mice, studies in humans are equivocal, with the majority of studies reporting no impact of obesity or T2D on PLIN5 expression in skeletal muscle (169,215,223,241,242). Thus, whether PLIN5 is involved in the pathogenesis of metabolic disease remains undetermined.

1.10 Summary and Research Aims

In summary, PLIN5 regulates lipid metabolism in highly oxidative tissues by interacting with other key proteins involved in TAG metabolism. The general consensus from the cell biology studies and *in vivo* studies in transgenic mice is that PLIN5 is important in suppressing TAG lipolysis in non-adipose tissues under basal state conditions, and may promote lipolysis during ß-adrenergic stimulation. PLIN5 is also postulated to be part of the adaptive response to exercise training and may facilitate the efficient transfer of fatty acids released from lipolysis to mitochondria for β-oxidation by promoting the interaction of LDs to the mitochondria. This may impact energy homeostasis in both health and metabolic disease. To date, little is known about the function of PLIN5 in skeletal muscle, especially in regards to metabolic control in states of energy oversupply (i.e. obesity) and during energetic stress (i.e. exercise). Therefore, this thesis seeks to delineate the roles of PLIN5 in regulating substrate metabolism in skeletal muscle by creating unique *in vivo* and *in vitro* models combined with detailed metabolic assessment.

Specifically, the aims of this research are:

1. To understand the effect of whole-body PLIN5 deletion on lipid and glucose metabolism, and in turn, the regulation of insulin action.
2. To determine the effects of muscle-specific PLIN5 deletion on energy homeostasis, muscle metabolism and glucose tolerance *in vivo*.
3. To examine the role of PLIN5 in the regulation of skeletal muscle substrate metabolism during acute exercise.
4. To determine whether PLIN5 is required for the molecular and metabolic adaptations and enhancement in exercise tolerance following endurance exercise training.

Declaration for Thesis Chapter 2

Monash University

Declaration by candidate

In the case of Chapter 2, the nature and extent of my contribution to the work was the following:

Nature of contribution	Extent of contribution (%)
Experimental design, performed the most of experiments and data analysis, wrote and edited the manuscript. Most of data presented in this chapter were published in Molecular Metabolism journal (Volume 3, No. 6, 652-663). My contribution in this manuscript was the figure 2.14, 2.15, 2.17 and 2.30 with slightly additional changes for this chapter. I directly contributed to data collection and analysis for figure 2-9, 2-20 and 2-29 and also contributed to the draft of the manuscript. Figure 2-31 was not in the manuscript and it is additional data that was not published elsewhere. Additional and detail in methodology also were added to improve the flow of this chapter.	40

The following co-authors contributed to the work. If co-authors are students at Monash University, the extent of their contribution in percentage terms must be stated:

Name	Nature of contribution	Extent of contribution (%) for student co-authors only
Rachael Mason	Experimental design, performed the most of experiments and data analysis, wrote and edited the manuscript	50
Maria Matzaris	Assisted with experimental work	NA
Arathy Selathurai	Assisted with experimental work	NA

Greg Kowalski	Assisted with experimental work	NA
Nancy Mokbel	Assisted with experimental work	NA
Clinton Bruce	Assisted with experimental work and provided intellectual input	NA
Matthew Watt	Assisted with experimental design and work, provided intellectual input and editing of manuscript	NA

The undersigned hereby certify that the above declaration correctly reflects the nature and extent of the candidate's and co-authors' contributions to this work*.

Candidate's Signature		**Date** 09/09/2016

Main Supervisor's Signature		**Date** 09/09/2016

CHAPTER 2

PLIN5 deletion remodels intracellular lipid composition and causes insulin resistance in muscle

2.1   Introduction

The close association between the growing epidemics of obesity and T2D continues to fuel interest in understanding how alterations in lipid metabolism contribute to the development of insulin resistance. An excess of fatty acids beyond the cells energy requirements results in the accumulation of TG within LDs, and the deposition of lipids in tissues other than adipose tissue is a feature of obesity and T2D. Skeletal muscle serves as an important site for glucose disposal after a meal (243) and it has been known for many years that the accumulation of IMTG predicts insulin resistance in muscle, independent of adiposity (244–247). However, the association is not clear cut because highly trained endurance athletes store as much TAG in their muscles as patients with T2D, yet display remarkable insulin sensitivity (126). Thus, the matching of fatty acid flux from the lipid droplet with mitochondrial demand for fatty acid substrate may be an important regulatory process to avoid defects in insulin action.

Both skeletal and cardiac muscle store significant amounts of TAG within intracellular LDs, which are located in close proximity to the mitochondria and ER (248). Intracellular TAG is an important energy substrate in skeletal (64) and cardiac muscle (249) and TAG turnover is relatively high in muscles (62,249), which ensures a continuous substrate supply to buffer changes in systemic FFA levels. However, an oversupply of fatty acids, beyond the energetic needs of the myocyte, eventually causes insulin resistance via a diverse range of mechanisms including the accumulation of lipid metabolites, maladaptive proinflammatory signalling and alterations in membrane physical properties (250). In this context, an inability to mobilize fatty acids from TAG (251,252) and/or increase TAG breakdown in skeletal muscle (74), without an increase in energy demand, can result in excessive intracellular lipid accumulation and insulin resistance.

The understanding of LD biology and the regulation of intracellular lipid fluxes have expanded in recent years with the discovery of PLIN family members (186). PLIN1 was first discovered as a LD-associated protein in white adipocytes and is a critical regulator of lipid metabolism (38,176), and more recently PLIN2 and PLIN5 have been shown to play major roles in liver and cardiac metabolism, respectively (224,253–255). While PLIN5 is highly expressed in skeletal muscle (10), its role in the control of IMCL trafficking, substrate utilization and insulin action is

not well understood. Mild overexpression of PLIN5 via DNA electrotransfer into the glycolytic muscle of rats increased TAG accumulation (226), which is consistent with the general consensus that PLIN5 plays an important role in LD accumulation (10,11,222). While PLIN5 increased TAG accumulation, this appeared to have no effect on skeletal muscle insulin action (227). Intriguingly, and perhaps paradoxically, the same authors have shown that PLIN5 may also localize to the mitochondria, suggesting that PLIN5 might direct fatty acids from the LD to the mitochondria for oxidation (226). While these short-term overexpression models have provided useful insights into PLIN5 function in muscle, the physiological significance of PLIN5 deletion on skeletal muscle and systemic metabolic control remains unresolved.

2.2   Aims

To understand the effect of whole body PLIN5 deletion on lipid and glucose metabolism, and in turn, in regulating insulin action.

2.3   Materials and Methods

The following section describes materials and methods used for chapter 2. Additional or variation of material and methods used in other chapters will be contained within their respective sections.

2.3.1   Generation of PLIN5 null mice and mouse breeding

A targeted vector containing *Plin5* (NM_001013706.2; Fig. 2-1) interrupted in exon 5, 6, 7 was generated by the trans-NIH Knock-Out Mouse Project (KOMP) and obtained from the KOMP Repository (Project ID CSD40589, ES clone EPD0301_4_E04). Blastocysts were collected from the mating of Balb/c mice. Cells were microinjected into the blastocyl cavity and injected blastocysts were transferred to the uteri of pseudopregnant CD1 female mice. To test for germline transmission, male chimeras were bred to C57BL/6N wild type female mice. Mice were confirmed to contain the PLIN5 disrupted allele by Southern blot analysis of KpnI digested genomic tail DNA. Genomic DNA was used for PCR. Mice were backcrossed onto a C57Bl/6 background for 2 generations. All studies were approved by the Monash University Animal Ethics Committee (SOBSA-2007-79, MARP-2013-050).
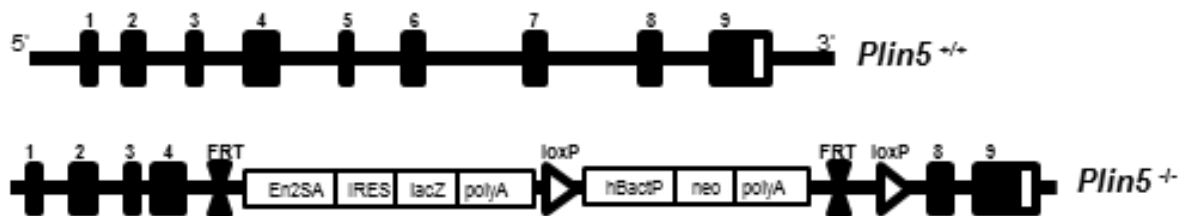
Fig 2-1. *Targeting vector used for the generation of Plin5$^{-/-}$ mice.*

2.3.2 Mice

Heterozygous mice were mated, with male *Plin5$^{-/-}$* and *Plin5$^{+/+}$* littermates used for experiments. Mice were maintained at 22°C on a 12:12-h light-dark cycle. Mice were fed a standard chow diet (4.8% total fat, 20% protein, 59.4% total carbohydrates, 14 MJ/kg digestible energy, 12% total energy from lipids; Specialty Feeds, WA, Australia) and had free access to water. All experiments were performed in 4 h fasted mice commencing at 1100 h unless otherwise stated.

2.3.3 Assessment of whole body metabolism, body composition and physical activity

Whole body metabolism was measured in metabolic cages (Columbus Instruments, Columbus, OH). Mice were housed individually for 48 h for assessment of oxygen uptake, carbon dioxide production and physical activity. Whole body fat and lean mass were measured by Dual Energy X-ray absorptiometry (Lunar Pixi #51042, PIXImus, WI, USA). Mice underwent a familiarisation protocol that consisted of progressively increasing the intensity and duration of the treadmill running (Eco 3/6 treadmill, Columbus Instruments, Columbud, OH) before experimental testing (Table 2-1). To determine maximal running speed, mice ran at 10 m/min on a 5% grade for 2 min and the speed was increased by 2 m/min until exhaustion.

	Monday	Tuesday	Wednesday	Thursday	Friday
Week 1	Day -7 Stand on treadmill for 10min	Day -6 • Stand for 5min 5 min at 7m/min	Day -5 • 5 min at 10m/min • 4 min at 13m/min 1 min at 17m/min	Day -4 Rest	Day -3 • 5 min at 10m/min • 4 min at 13m/min 1 min at 17m/min
Week 2	Day 0 Max run speed • Start: 10m/min • Inc. every 2 min by 2m/min until fatigue Increasing velocity	Day 1 Rest	Day 2 Rest	Day 3 Endurance test • Start at 16m/min until fatigue Steady velocity	Day 4 Rest

Table 2-1. *Outline of treadmill familiarisation and exercise testing of mice.*

2.3.4 Rates of whole-body substrate oxidation

Absolute rates of carbohydrate and lipid oxidation were calculated using the following equation (256):

Carbohydrate oxidation (g/min) = 4.585 VCO_2 – 3.2255 VO_2

Lipid oxidation (g/min) = 1.7012 VO_2 – 1.694 VCO_2

2.3.5 *Fatty acid metabolism ex vivo*

Mice were fasted for 3 h and anaesthetised with 5% isoflurane in an induction chamber and maintained sedation with 2% isoflurane in oxygen by a face mask (8323001, Univentor, Malta). Deep sedation was assessed by testing reflexes (pinch test of paw). The soleus muscle was excised from tendon to tendon and placed in a glass vial and pre-incubated with 1 ml of warmed, pregassed (95% O_2 / 5% CO_2), modified Kreb-Henseleit buffer (4.5% NaCl, 5.75% KCl, 6.1% $CaCl_2$, 10.55% KH_2PO_4, 19.1% $MgSO_4$, 1.3% $NaHCO_3$) supplemented with 5 mM glucose, 2% bovine serum albumin (BSA, Bovogen, VIC, Australia) and 0.5 mM oleate (CLM-460- 0, Novachem, VIC, Australia). The buffer was then exchanged with Kreb buffer with added [1-^{14}C] oleate (0.5 µCi/ml, Perkin Elmer, MA, USA) with or without 20 mM forskolin (F3917, Sigma-Aldrich) for 2 h in the buffer with a 0.5 ml collection tube inside a 1.7 ml collection tube containing 1 M sodium hydroxide (NaOH, used to trap released CO_2). After 2 h the soleus muscle was removed, washed in ice-cold PBS, the tendons were removed, and the muscle weighed and snap frozen in liquid nitrogen. One ml perchloric acid was added to each vial and was quickly closed so that any ^{14}C labelled CO_2 remaining in the incubation buffer was released and captured by the NaOH. Vials when incubated for 90 min on an orbital rocker after which the 0.5 ml inner collection tube containing the NaOH was gently removed and placed in a scintillation tube with 2 mL scintillation fluid and ^{14}C was determined on a scintillation counter (LS 6500, Beckman Coulter, USA).

The soleus muscle was homogenised (PRO Scientific, Oxford, CT) in 2:1 v:v chloroform: methanol plus 600 µL phosphate buffered saline (PBS). Samples were spun at 1000 g for 10 min. The upper aqueous phase was removed to a scintillation tube and scintillation fluid added to measure ^{14}C contained in acid soluble metabolites (ASMs). This represents fatty acids that are

partially oxidised and the sum of ^{14}C ASMs and $^{14}CO_2$ equals total fatty acid oxidation. The lower organic phase was removed into a clean 12 x 75 mm glass tube and dried down under nitrogen before being resuspended in 50 µl of 2:1 v:v chloroform: methanol containing a small amount of TAG and DAG. The lipid mixture was applied to a glass thin layer chromatography plate (Analtech, DE, USA) using a Hamilton syringe (1700, NV, USA). The plate was exposed to a solvent system (Heptane: Isopropylether: Acetic acid (60:40:3)) in a glass tank. Once the plate was resolved, the TG and DG bands were identified under ultraviolet light and scraped into scintillation tubes to measure ^{14}C fatty acid incorporation into TAG and DAG (LS 6500, Beckman Coulter, USA). Fatty acid uptake was determined as the sum of $[1\text{-}^{14}C]$ oleate oxidation to $^{14}CO_2$ and incorporation of $[1\text{-}^{14}C]$ oleic acid into TAG and DAG in the muscles.

2.3.6 Tissue lipids

TAG were extracted from mixed quadriceps skeletal muscle using the method of Folch et al. (1957), with some minor modifications (257). Briefly, lipids were Folch extracted by homogenising tissue with 1.8 ml of chloroform:methanol (2:1). Samples were incubated at room temperature for 30 min before adding 600 µL of PBS. After centrifugation for 10 min at 1000 g, the lower phase was collected and evaporated under a stream of nitrogen and the resulting lipid reconstituted in 100% ethanol and TAG content determined using the TG-GPO-PAP reagent (04657594190, Roche Diagnostics, Basel, Switzerland) and a standard curve (0-2.5 mg/ml).

DAG and ceramide contents were determined by an $[^{32}P]$ ATP-linked enzymatic method as previously described (258). Briefly, tissue was homogenised with 1.8 ml of chloroform/methanol/PBS (1:2:0.8) with 0.2% SDS before room temperature incubation for 1 h. Additional 0.5 mL chloroform and 1% perchloric acid was added and centrifuged for 10 min at 1000 rpm. The upper phase was aspirated, and 0.9 mL of organic phase transferred into a new tube and dried under a stream of nitrogen at 40°C.

The octylglucoside/cardiolipin mix (7.5 mg cardiolipin, 75 mg octylglucoside and 1ml 1 mM diethylenetriamine-pentaacetic acid (DETAPAC, pH7.0) was added to the reaction buffer (200mM Imidazole, 200mM NaCl, 50mM $MgCl_2$, 4 mM EDTA) was mixed with DAG kinase (D3065, Sigm-Aldrich), 20 mM ATP, 20 mM DTT (dissolved in DETAPAC) and ^{32}P-ATP

(Perkin Elmer) and added the dried lipid. The samples were incubated at room temperature for 2-3 h. 1% perchloric acid is added and samples vortexed before centrifugation at 100 rpm for 10 min. The lower phase was removed and dried under nitrogen at 40°C before being resuspended in chloroform/methanol (2:1).

The lipid mixture was applied to a silica gel 60 thin layer chromatography plate (Analtech, DE, USA) using a Hamilton syringe (1700, NV, USA). The plate was exposed to a solvent system (chloroform/acetone/methanol/acetic acid/water, 50:20:15:10:5). Plates were developed under autoradiograph film for 12 h at room temperature and DAG and ceramide bands were identified. Corresponding bands were scraped into scintillation vial with scintillation fluid and counted for ^{32}P (LS 6500, Beckman Coulter, USA). Lipidomics was performed on cell lysates as described (259).

2.3.7 Glucose tolerance tests

Mice were intraperitoneally injected with D-glucose (2 g/kg mass). Tail blood was collected and blood glucose was determined using a glucometer (Accu-chek, Roche, Mannheim, Germany). Plasma insulin was determined by an in-house ELISA. All samples were run as duplicates and were within the range of the standard curve (0 – 10 ng/ml).

2.3.8 Hyperinsulinemic-euglycemic clamp studies

Mice were anaesthetized and a catheter was inserted into the jugular vein as previously described (260). Following five days recovery, mice were fasted for 4 h prior to beginning the clamp. Mice were conscious but restrained for the duration of the procedure. Blood glucose was equilibrated with a 90 min continuous infusion of [3-^{3}H]-glucose (0.05 µCi/min). Hyperinsulinemic-euglycemic clamp commenced with the increase of [3-^{3}H]-glucose tracer to 2 µCi/min and insulin infusion (4 mU/kg/min). Exogenous glucose (25% w/v) was infused to maintain basal blood glucose levels, which averaged 8.1 ± 0.3 mM. Tail blood samples were collected and blood glucose was measured every 5 min. After 120 min, a 10 µCi bolus of 2-deoxy-d-[1-^{14}C] glucose (2-[^{14}C] DG; Perkin Elmer) was administered to assess tissue-specific glucose uptake ($R_g{}'$). At the conclusion of the clamp, mice were anaesthetized with an intravenous injection of

sodium pentobarbitone (100 mg/kg iv) and tissues rapidly dissected and snap frozen in liquid nitrogen for analysis of 2-[^{14}C] DG uptake.

For the determination of plasma [3-^{3}H]glucose and 2-[^{14}C]DG concentrations, 10 µl plasma and 10 µl saline were added to a 1.5 mL tube, and was deproteinised with 100 µl zinc sulphate (ZnSO$_4$, 0.3 N, Z2876, Sigma-Aldrich) and 100 µl barium hydroxide (BaOH$_2$, 0.3 N, B4059, Sigma-Aldrich), centrifuged for 1 min at 16, 000 g. 100 µl of supernatant was removed into a scintillation tube and dried at 37°C to remove ^{3}H$_2$O, then resuspended with 1 ml water and counted in scintillation fluid (Ultima Gold; Packard, Meridien, CT) on dual channels for separation of ^{3}H and ^{14}C (LS 6500, Beckman Coulter, USA). The plasma concentration of ^{3}H$_2$O was determined by the difference between ^{3}H counts without and with drying.

The rate of glucose appearance (endogenous R$_a$) and disappearance (R$_d$) were determined using steady-state equations. Endogenous glucose production during the clamp was calculated by subtracting the glucose infusion rate (GIR) from R$_d$. The insulin-stimulated component of the total R$_d$ (IS-Rd) is equal to clamp R$_d$ minus the basal glucose turnover rate.

For estimating insulin-stimulated glucose uptake in individual tissues, 2-deoxy-D-[1-^{14}C] glucose (2-[^{14}C] DG; Perkin Elmer) was administered as a bolus (10 µCi) at 120 min after the start of clamps. Because 2-deoxyglucose is glucose analog that is phosphorylated but not metabolised, insulin-stimulated glucose uptake in individual tissues can be estimated by determining the tissue content of 2-deoxyglucose-6-phosphate. Accumulation of [^{14}C]-2DG was determined in an aqueous extract of tissue after homogenization. Free and phosphorylated [^{14}C]-2DG were separated by ion exchange chromatography on Dowex l-X8 columns (acetate form). The area under the tracer disappearance curve of [^{14}C]-2DG, together with the radioactivity for the phosphorylated [^{14}C]-2DG from individual tissues, were used to calculate the glucose metabolic index (Rg′).

2.3.9 Blood biochemistry

Whole blood was collected into EDTA tubes then centrifuged for 3 min at 8,000 x *g*. Plasma free fatty acids and triacylglycerol were determined by enzymatic colorimetric assays (Wako Chemicals, Wako, VA, USA). High density lipoproteins (HDL) and very (VLDL) and low density lipoproteins (LDL) were assessed by ELISA (Ab65390, Abcam, Cambridge, UK). Plasma insulin was determined by an in-house ELISA. Plasma β-hydroxybutyrate was analyzed by a colorimetric assay (700190, Cayman Chemicals, Ann Arbor, MI, USA).

2.3.10 Immunohistochemistry

Tissues (mixed quadriceps muscle and heart) were rapidly frozen in melting isopentane after being coated in OCT Tissue-Tek (Sakura Finetek, The Netherlands). Serial 10 μm sections were cut at -20°C on to SuperFrost Ultra Plus glass slides. Slides were fixed in Bouin's solution with 0.1% Trition X-100 (Sigma-Aldrich) for 30 min. Sections were stained for lipid droplets with freshly made, filtered oil red O (Sigma-Aldrich) made in 60% triethylphosphate (Sigma-Aldrich). β-galactosidase expression was identified using commercial reagents (MIR 2600, Mirus Bio, Madison, WI). Sections were blocked in PBS with 1% BSA for 1 h then incubated overnight with PLIN5 antibody (Cat. no. GP31, Progen Biotechnik, Germany, ~0.02mg/ml) while mitochondrial staining was performed using the mitochondrial antibody directed against the oxidative phosphorylation complexes I–V (Total OXPHOS Cat. no. ab110413, Abcam, Cambridge, UK). Images were captured using a Zeiss microscope (Zeiss, Oberkochen, Germany) with an AxioCam MR camera using DAPI UV (340-380nm), FITC (465-495nm) and Red (568nm) excitation filters. An average of 5 fibres per section, with 4 sections per mouse was analysed. For negative controls, primary antibodies were substituted for concentration matched guinea pig serum for PLIN5 (Antibodies Australia), or OXPHOS cocktail pre-absorbed 4:1 overnight with mouse IgG_1 and IgG_{2a} (Dako, Denmark). Immunohistochemistry images were analyzed for colocalization with ImageJ (NIH) by using Manders' colocalisation coefficient, M2, which provides a fraction of the colocalizing objects in the images. For colocalisation analysis, single negative controls were performed to assess autofluorescence in the corresponding channel. Electron microscopy was performed as described previously (261).

2.3.11 qRT-PCR

Total RNA was extracted from ~ 30 mg mixed quadriceps skeletal muscle using Qiazol extraction reagent (Qiagen, Germany). Briefly, 1 ml Qiazol lysis reagent per 100 mg tissue was homogenised, before being incubated at room temperature for five minutes. Chloroform, 0.2 ml per 1 ml Qiazol was added and shaken vigorously for 15 sec. Sample were centrifuged at 12, 000 g for 15 min at 4°C. The upper aqueous phase was removed into a clean tube and 0.5 ml isopropanol per 1 ml Qiazol and shaken vigorously. Samples were incubated for 10 min at room temperature, then centrifuged at 12, 000 g for 10 min at 4°C. Supernatant was removed and the RNA pellet cleaned with 75% ethanol and left to dry completely before being redissolved in RNase free water. The RNA concentration was assessed using the Nanodrop 1000 Spectrophotometer (Thermo Fisher Scientific, MA, USA). Reverse transcription of 1 μg mRNA was performed (iScript cDNA Synthesis Kit, Bio- Rad Laboratories, Hercules, CA) and gene products were determined by real-time quantitative RT-PCR (Realplex Mastercycler, Eppendorf) using the TaqMan Universal PCR Master Mix (4304437, Life Technologies) and TaqMan Gene Expression Assays (Table 2.2). 18S rRNA (MP212372) was used as a loading control. The RT-PCR protocols consisted of 2 min at 50°C, 10 min at 95°C, then 40 cycles of 15 sec at 95°C, 60 sec at 60°C. The relative quantification was calculated using the ΔΔCt method, normalising values to wild type littermates.

Gene name	Primer Number from Applied Biosystems
Plin2	Mm00475794_m1
Plin3	Mm00482206_m1
Plin4	Mm00491061_m1
Pnpla2	Mm00503040_m1
Abhd5	Mm00470731_m1
Lipe	Mm00495359_m1
Cd36	Mm01135198_m1
Dgat1	Mm00515643_m1
Cpt1b	Mm00487191_g1
Mcad	Mm00431611_m1
Pdk4	Mm01166879_m1
Acox	Mm00443579_m1
ATP synthase	Mm00558162_m1
Nrf1	Mm00447996_m1
Ppargc1a	Mm00447180_m1
Tfam	Mm00447485_m1
Ucp2	Mm00495907_g1
Pepck	Mm01247058_m1
G6pc	Mm00839363_m1
TNFa	Mm00443258_m1
IL-6	Mm00446191_m1
Asah1	Mm00480021_m1
SPT1	Mm00839568_m1
SPT2	Mm00448871_m1
Smpd1	Mm00488318_m1
Smpd2	Mm01188195_g1

Table 2-2. *qRT-PCR primers*

2.3.12 *Immunoblot analysis*

Mixed quadriceps muscle were lysed in Radio-Immunoprecipitation Assay (RIPA) buffer containing (65 mM Tris, 150 mM NaCl, 1 M dithiothreitol, 1% NP40, 0.5% sodium deoxycholate, 0.1% sodium dodecyl sulphate (SDS), 10% glycerol) with 10x protease inhibitors (Complete Protease Inhibitor Cocktail, Roche, Basel, Switzerland) and 25x phosphatase inhibitors (PhosSTOP Phosphatase Inhibitor Cocktail, Roche, Basel, Switzerland). Lysates were solubilised in Laemmli sample buffer and boiled for 5 min then resolved on Stain-free Bio-rad Mini-PROTEAN® TGXTM gels (Bio-Rad Laboratories, NSW, Australia) and activated for 1 min after SDS–electrophoresis, transferred to polyvinylidene difluoride membranes using the trans-blot turbo transfer system. Stain-free blot images were collected after transfer using the ChemiDoc MP and ImageLab software for protein loading controls (Version 4.1, Bio-rad Laboratories, NSW, Australia) and membranes were then blocked in 2.5% skim milk or bovine serum albumin (BSA). Membranes were incubated with primary antibody at 4°C overnight. Membranes were probed with commercial antibodies (Table 2.3).

Membranes were washed, incubated with the corresponding horseradish peroxidase- conjugated secondary antibodies: anti-Rabbit (NA934OV, GE Healthcare, UK), anti- Guinea Pig (43R-ID039HRP, Fitzgerald, MA, USA) and anti-Mouse (NA931, GE Healthcare, UK) and the immunoreactive proteins were subsequently detected by enhanced chemiluminescence (32106, Pierce, Rockford, IL or CPS3500, Sigma- Aldrich) and quantified by densitometry using ImageLab software (Version 4.1, Bio-rad Laboratories, NSW, Australia).

Antibody	Catalogue number	Company
pJNK	9251	Cell Signalling, Danvers, MA
NF-κB IKBα	9242	Cell Signalling, Danvers, MA
β-Tubulin	T0198	Sigma-Aldrich, St. Louis, MO
PLIN2	SC-32888	Santa Cruz, Dallas, TX
PLIN3	NB110-40764	Novus, Littleton, CO
PLIN4	GP-34	Progen, Heidleberg, Germany
xBP1	SC-7160	Santa Cruz, Dallas, TX
p-PERK	SC-32577	Santa Cruz, Dallas, TX
p-EIF2α	SC-101670	Santa Cruz, Dallas, TX
GADD	SC-8327	Santa Cruz, Dallas, TX

Table 2-3. *Antibodies used for immunoblot analyses.*

2.3.13 Measurement of Thiobarbituric acid reactive substances (TBARS)

TBARS was measured in mixed quadriceps muscle lysates by using a colorimetric assay for the formation of malondialdehyde (10009055, Cayman Chemicals, Ann Arbor, MI, USA) as an indicator of oxidative stress.

2.3.14 In vitro phosphorylation

Recombinant HA-tagged murine PLIN5 was phosphorylated by cAMP-dependent PKA as described (80) and the location of the HA-PLIN5 was confirmed by immunoblot.

2.3.15 Isolation of primary myoblast

Primary myoblasts were isolated using an explant culture method (262). Briefly, primary myoblasts were isolated from the *vastus lateralis* muscles of mice. First, the muscles were removed, trimmed of excess connective tissue and fat, and rinsed in PBS containing 1% penicillin/streptomycin antibiotic mixture. The muscles were transferred into 10 cm petri dish and a few drops of plating medium consisted of Dulbecco's modified Eagle's minimal essential medium (DMEM) and Ham's F-12 Nutrient Mix supplemented 40% Fetal Bovine Serum (FBS) and 10% AmnioMAX-II complete medium.. The muscle was minced into small fragments (1-3 mm^3) using a sterile razor blade. The fragments were then transferred onto the surface of collagen/matrigel (0.17mg/ml collagen and 1/50 dilution of matrigel in 1:1 DMEM and Ham's F-12 Nutrient Mix) pre-coated 6 cm petri dish. One ml of plating medium was gently added to the tissues to ensure the medium covered the tissue and the tissue fragments were maintained at 37°C in a humid air atmosphere containing 5% CO_2. After 48 h, the tissue fragments were overlayed with 2 ml plating medium and maintained at 37°C, 5% CO_2 for 2-5 days, until outgrowth was visible from the explants. Thereafter, the plating medium was aspirated and the explants washed with PBS. The solution was discarded and 2 ml of trypsin solution was added and left for three minutes to detach the adherent cells. The trypsin solution was neutralized using 3 ml DMEM/F12 growth medium. The cell suspension was transferred to collagen/matrigel pre-coated flask containing 8 ml of growth medium and the flasks were kept in the humidified incubator. Once confluent the myoblasts were passaged once more before further analysis.

2.3.16 Cell culture

Myoblasts were differentiated to myotubes by switching to 3% horse serum medium and were left to differentiate for 5 days prior to experiments. Fatty acid metabolism (radiometric methodology) was assessed as described in section 2.3.4.

2.3.17 Mitochondrial metabolism

Cellular bioenergetics profile of primary myoblast with and without PLIN5 knockdown was assessed using a Seahorse XFe24 Flux Analyzer (Seahorse Bioscience). Briefly, cells were seeded in Seahorse XF24 plates treated with CELL-TAK (BD Bioscience). Three replicate oxygen consumption rate (OCR) measurements were obtained at baseline and following injection of oligomycin (2 μM), carbonylcyanide-ptrifluoromethoxyphenylhydrazone (FCCP, 3 μM, Sigma) and antimycin A plus rotenone (3 μM, Sigma). The value of the basal respiration, mitochondrial proton leak, maximal respiration, and non-mitochondrial respiration was determined as described in the Seahorse Operator's Manual. Data were normalized for protein concentration by lysing samples after each experiment.

2.3.18 Statistics

Data are expressed as means ± SEM. Statistical analysis was performed by one-way or two-way analysis of variance (ANOVA) with repeated measures, and specific differences were located using a Bonferroni post hoc test. Unpaired t-tests were used where appropriate (GraphPad Prism Version 5.02). Statistical significance was set *a priori* at $P \leq 0.05$.

2.4   Results

2.4.1   *Generation of PLIN5 deficient mice*

Interbreeding of heterozygous mice for the Plin5 null allele yielded mice that were homozygous for each of the two alleles. The absence of the Plin5 allele was confirmed by Southern blotting (Fig. 2-2) and the absence of PLIN5 mRNA was confirmed by PCR (Fig. 2-3). The absence of PLIN5 protein was confirmed with immunohistochemistry of skeletal muscle (Fig. 2-4). A secondary confirmation was the presence of the lacZ in the hearts of $Plin5^{-/-}$ mice, as detected by β-galactosidase staining (Fig. 2-4). TAG content was reduced by 52% in the hearts of $Plin5^{-/-}$ mice (Fig. 2-5) and coincided with a marked reduction of LDs stained by ORO (Fig. 2-6). This is consistent with the prominent reduction in cardiac lipid content reported in another line of $Plin5^{-/-}$ mice (224). There was no such reduction in TAG content in the liver or mixed skeletal muscle (Fig. 2-6). Interestingly, TAG content was lower in red quadriceps (oxidative) muscle and tended (122%, P<0.08) to be higher in white quadriceps (glycolytic) muscle of $Plin5^{-/-}$ compared with $Plin5^{+/+}$ mice (Fig.2-6). This may reflect the greater capacity of oxidative fibers to oxidize TG-derived fatty acids compared with glycolytic fibers (263). While the deletion of one *Plin* gene can induce compensatory increases in the other *Plin* genes (221,224), the expression of *Plin* 2, 3 and 4 were not altered in $Plin5^{-/-}$ mice (Fig. 2-7), nor were there changes in the expression of prominent lipases or co-activator proteins associated with TAG lipolysis (Fig. 2-7 and 2-8). *Plin*1 was not detected in skeletal muscle.
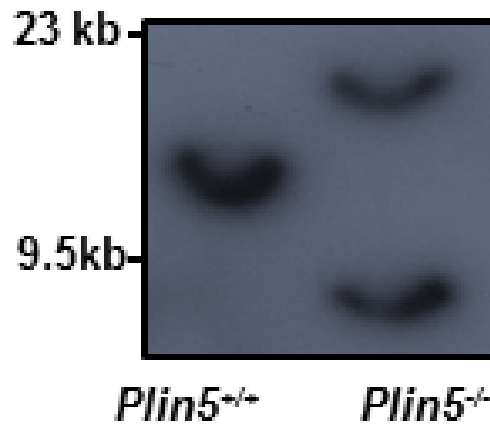
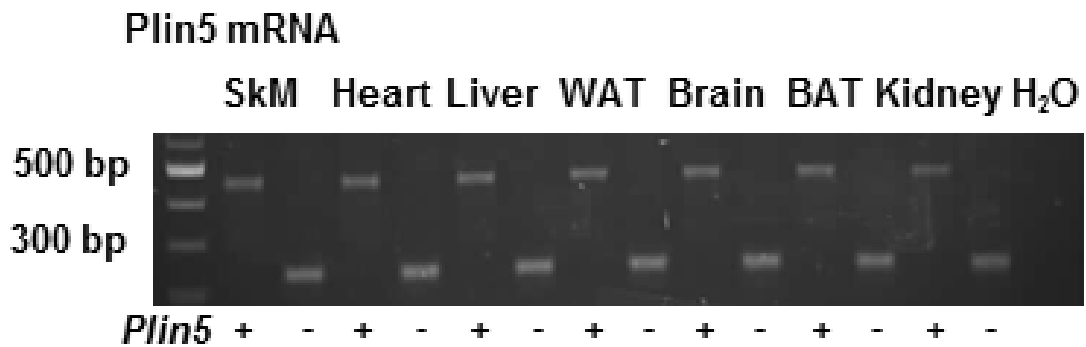**Fig 2-2.** *Confirmation of Plin5 disruption by Southern blotting of genomic tail DNA.*

Fig 2-3. *RT-PCR of RNA from Plin5$^{+/+}$ and Plin5$^{-/-}$ mice. SkM, skeletal muscle, WAT, white adipose tissue, BAT, brown adipose tissue. Upper band (Plin5$^{+/+}$) 466 bp; lower band (Plin5$^{-/-}$) 254 bp.*
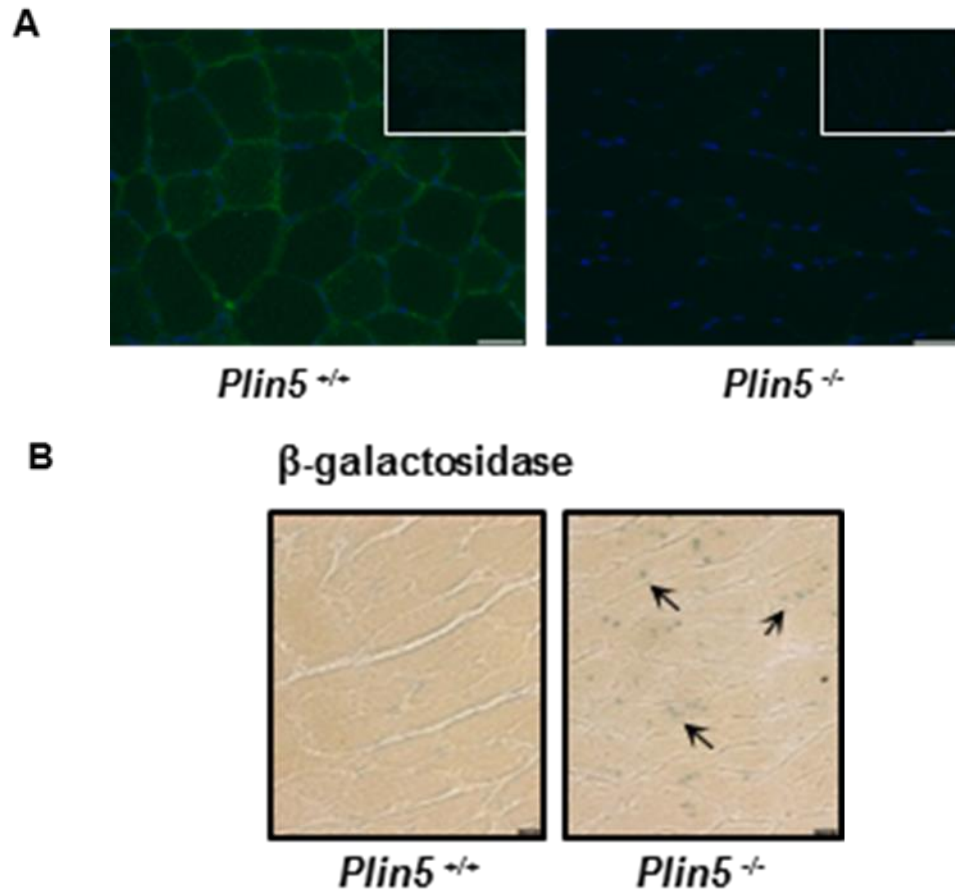
Fig 2-4. (A) *Representative images of mixed quadriceps muscle sections stained with PLIN5 antibody from Plin5$^{+/+}$ and Plin5$^{-/-}$ mice, with concentration matched serum controls in inset. Scale bar = 50 μm. (B) Confirmation of lacZ expression in Plin5$^{-/-}$ hearts through β-galactosidase staining. Arrows pointing to regions of staining. Scale bar = 10 μm.*
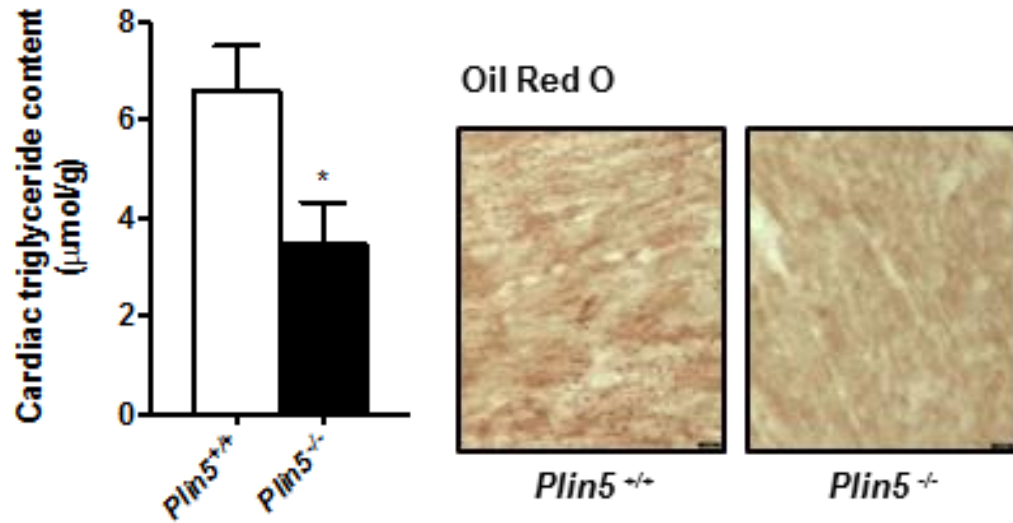
Fig 2-5. *Left: Cardiac triacylglycerol content ($\male$, n=13 Plin5$^{+/+}$, n=15 Plin5$^{-/-}$, Age= 12-17 weeks). *P<0.05 vs Plin5$^{+/+}$ mice. Right: Representative image of lipid droplet staining with ORO in heart. Scale bar = 10 μm.*
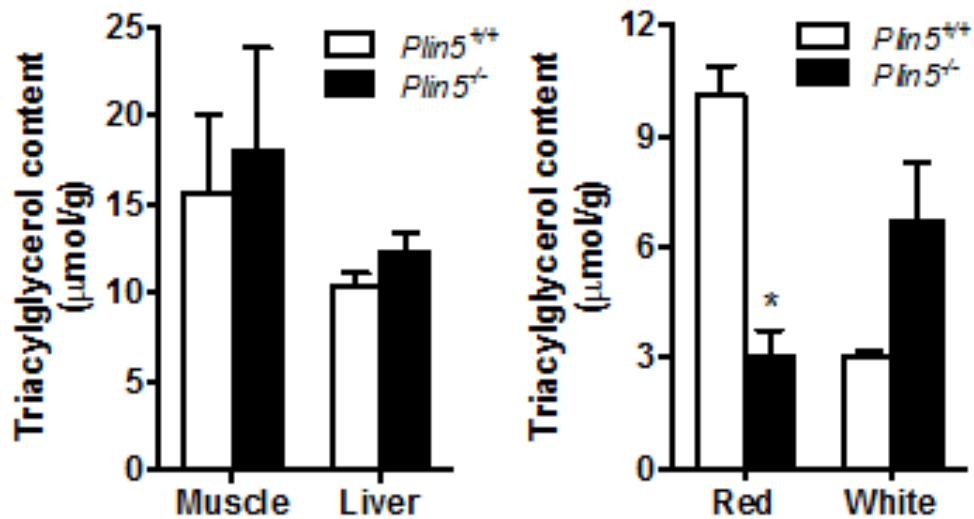

Fig 2-6. *Left: Skeletal muscle (mixed quadriceps) and liver triacylglycerol content ($\male$, n=13 Plin5$^{+/+}$, n=15 Plin5$^{-/-}$, Age= 12-17 weeks). Right: Triacylglycerol content in red and white portions of the quadriceps ($\male$, n=4 Plin5$^{+/+}$, n=4 Plin5$^{-/-}$, Age= 12-17 weeks). *P<0.05 vs Plin5$^{+/+}$ mice.*
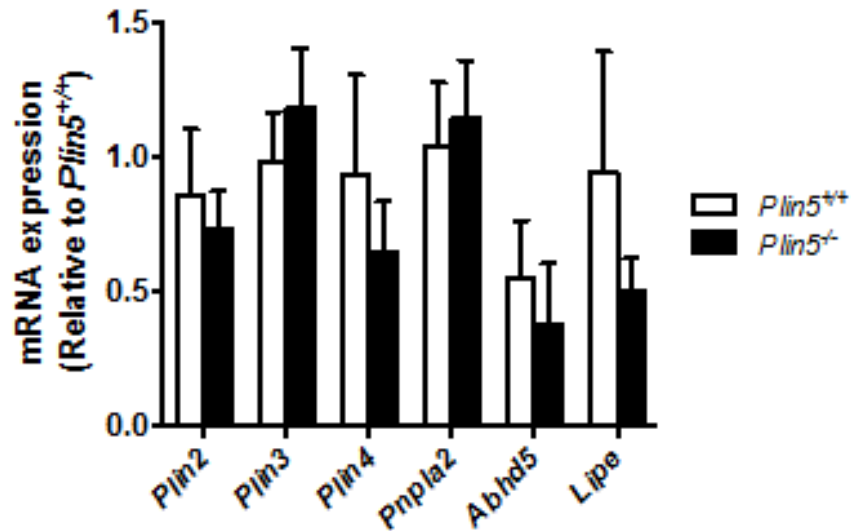
Fig 2-7. *Skeletal muscle expression of PLIN genes Plin2, Plin3 and Plin4 and of lipase and lipase coactivator genes Pnp1a2, Abhd5 and Lipe ($\male$, n= 4-5 Plin5$^{+/+}$, n= 6-7 Plin5$^{-/-}$).*
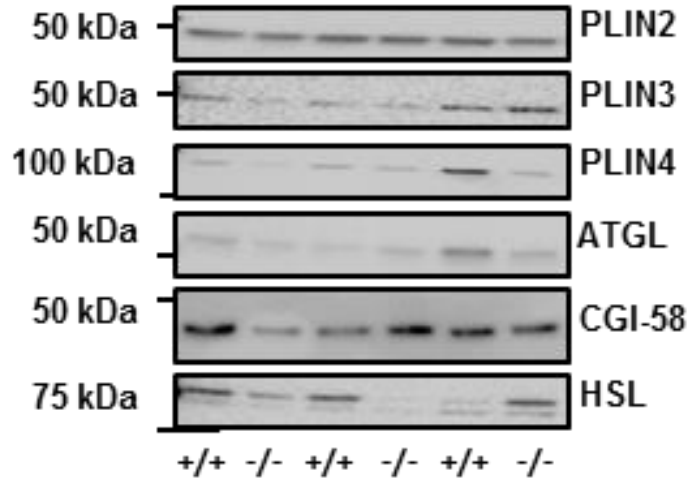

Fig 2-8. *Contents of PLIN proteins and lipases in skeletal muscle ($\male$, n= 3 Plin5$^{+/+}$, n= 3 Plin5$^{-/-}$). Representative blots from a total of n=6 for each genotype. Densitometry showed no significant difference between genotypes for any protein assessed.*

2.4.2 Whole body fatty acid oxidation is decreased in the absence of PLIN5

$Plin5^{+/+}$ and $Plin5^{-/-}$ mice had similar body weights during development (Fig. 2-9A) and DEXA examination revealed no difference in lean and fat mass (Fig. 2-9B). This was supported by post mortem examination showing no difference in epididymal fat, heart and liver mass, indicating that the absence of PLIN5 had no effect on adiposity and gross morphology (Table 1). Neither food intake (Fig. 2-10A) nor energy expenditure (VO_2) was different between genotypes (Fig. 2-10B). However, the RER was increased in $Plin5^{-/-}$ mice (Fig. 2-10C), demonstrating an ~11% decrease in whole-body fatty acid oxidation and a reciprocal increase in carbohydrate oxidation. These changes cannot be attributed to increased physical activity (Fig. 2-10D). Fasting muscle and liver glycogen (Fig. 2-11), plasma glucose and insulin concentrations were not different between groups; neither were plasma FFAs, TAGs and HDL or VLDL/LDL cholesterol levels (Table 2-3). Plasma ß-hydroxybutyrate, a marker of liver fatty acid oxidation, was not altered by genotype (Table 2-4).

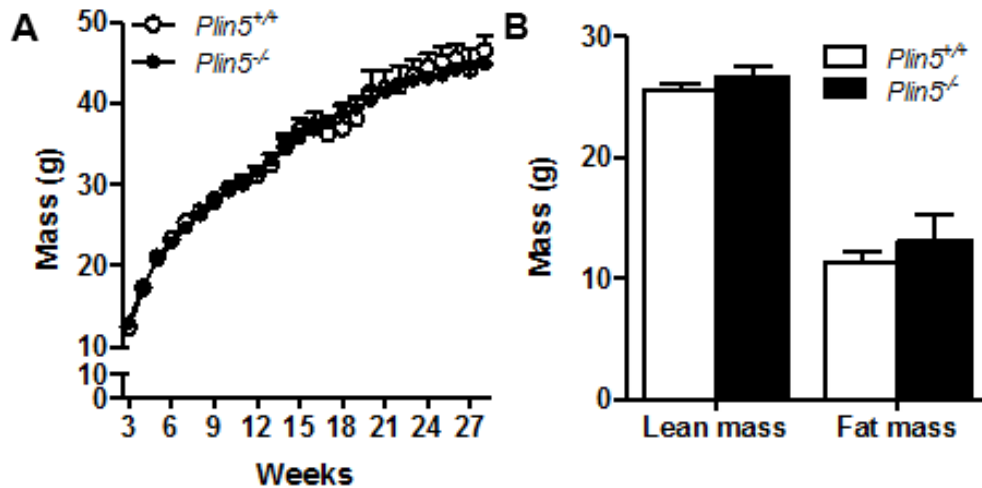

Fig 2-9. *Plin5 deletion does not alter growth and adiposity (A) Body mass (♂, n=6-16 Plin5$^{+/+}$, n=10-16 Plin5$^{-/-}$). (B) Lean mass and fat mass assessed by DEXA (♂, n=10 Plin5$^{+/+}$, n=6 Plin5$^{-/-}$, age=14-16 weeks).*
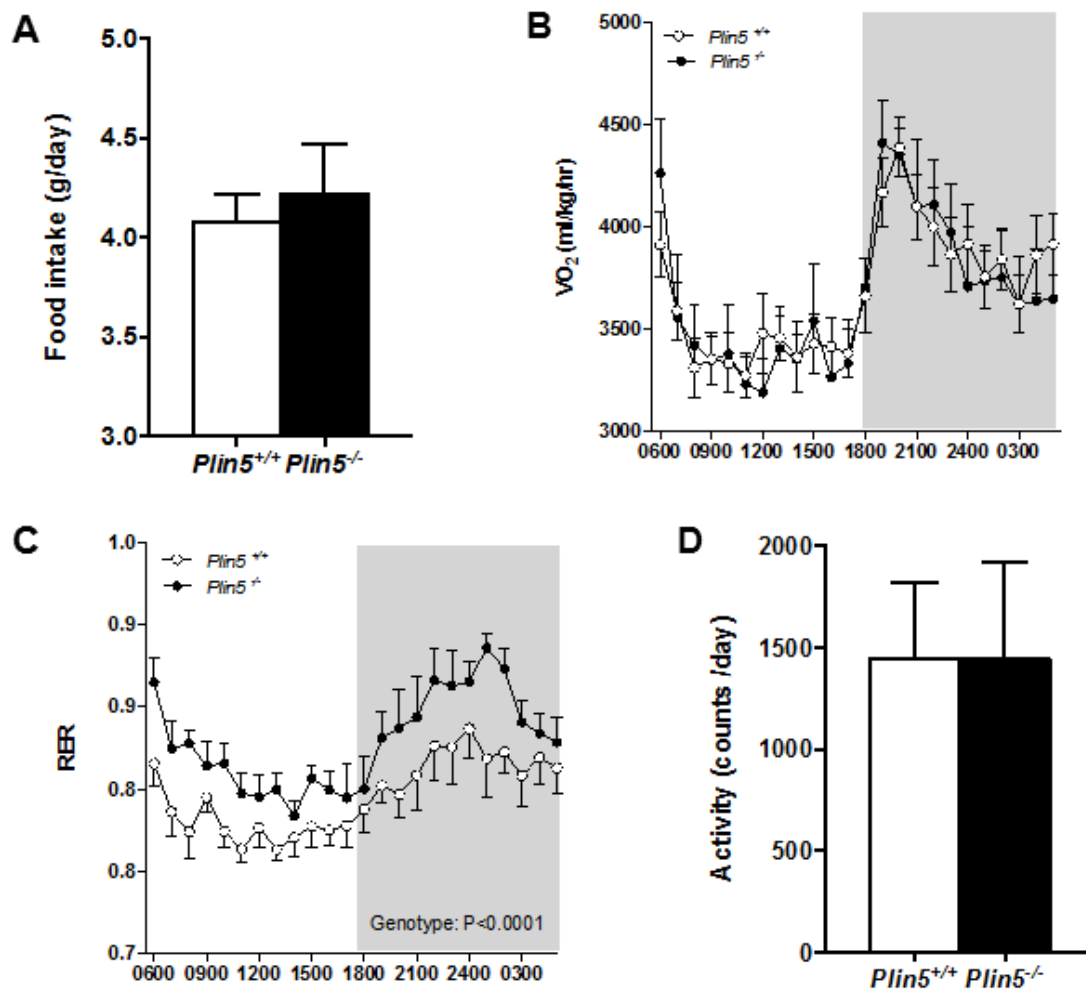
Fig 2-10. *Plin5 deletion does not alter energy expenditure but does impact substrate partitioning. (A) Food intake ($\male$, n=5 Plin5$^{+/+}$, n=5 Plin5$^{-/-}$, age=14-16 weeks), (B) Oxygen consumption (VO$_2$), (C) respiratory exchange ratio (RER) ($\male$, n=10 Plin5$^{+/+}$, n=6 Plin5$^{-/-}$, age=14-16 weeks) and (D) Total daily activity ($\male$, n=9 Plin5$^{+/+}$, n=5 Plin5$^{-/-}$, age=14-16 weeks) were assessed by indirect calorimetry.*
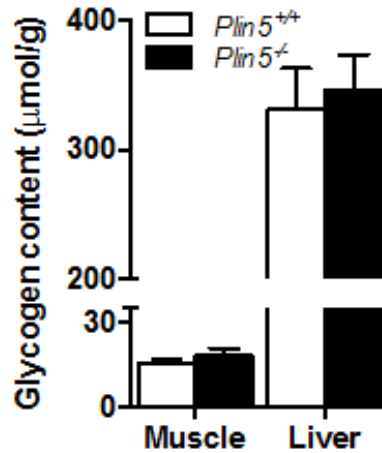
Fig 2-11. *Muscle (n=7 Plin5^{+/+}, n=8 Plin5^{-/-}) and liver (n=8 Plin5^{+/+}, n=9 Plin5^{-/-}) glycogen content in 4 h fasted mice (♂, age=14-16 weeks).*

	Plin5^{+/+}	Plin5^{-/-}	P value
Heart mass (mg)	135.5 ± 4.9	138.8 ± 5.6	0.66
Liver mass (g)	1.3 ± 0.1	1.2 ± 0.1	0.82
Epidydimal fat mass (g)	0.78 ± 0.1	0.77 ± 0.1	0.98
Blood glucose (mmol/l)	8.6 ± 0.3	8.9 ± 0.3	0.57
Plasma insulin (pmol/l)	133 ± 34	140 ± 12	0.86
Plasma FFA (mmol/l)	0.66 ± 0.07	0.72 ± 0.06	0.56
Plasma TG (mmol/l)	1.03 ± 0.17	1.28 ± 0.12	0.24
Plasma HDL (mmol/l)	0.98 ± 0.02	1.00 ± 0.04	0.69
Plasma VLDL/LDL (mmol/l)	0.24 ± 0.02	0.26 ± 0.03	0.59
Plasma ß-hydroxybutyrate (µmol/l)	133 ± 17	135 ± 26	0.95

Table 2-4. *Tissue weights and blood chemistry in Plin5^{-/-} and Plin5^{+/+} mice fed a low-fat diet. Tissue masses were from mice aged 14-16 weeks. Heart (♂, n=17 Plin5^{+/+}, n=18 Plin5^{-/-}), liver (♂, n=5 Plin5^{+/+}, n=3 Plin5^{-/-}) and epididymal fat pad (♂, n=17 Plin5^{+/+}, n=18 Plin5^{-/-}). All mice were fasted for 4 h before blood sampling. n=8 for each genotype. Data are mean ± SEM.*

2.4.3 Effects of PLIN5 deletion on skeletal muscle substrate metabolism

Based on the high abundance of PLIN5 in skeletal muscle (10) and the quantitative importance of skeletal muscle in regulating whole-body substrate metabolism (264), we next examined the effects of PLIN5 deletion on skeletal muscle fatty acid metabolism in isolated *soleus* muscle. Total fatty acid uptake, fatty acid oxidation and the incorporation of fatty acids into TAG and DAG were not different between the two genotypes (Fig. 2-12A-D). ß-adrenergic activation of PKA is a major regulator of TG metabolism in adipocytes and most likely oxidative skeletal muscle (263,265,266), although PKA action in muscle requires further confirmation. We first performed *in vitro* kinase assays to demonstrate that PLIN5 is a substrate for PKA (Fig. 2.13), then we examined fatty acid metabolism in response to forskolin, an activator of cAMP/PKA signaling. Forskolin reduced fatty acid uptake, oxidation and storage; however, these effects were not impacted by *Plin5* deletion. Thus, PLIN5 deletion does not affect the uptake, oxidation or esterification of extracellular-derived fatty acids in muscle under basal and PKA-stimulated conditions. Further studies in isolated *soleus* muscle revealed no difference in glucose oxidation between $Plin5^{+/+}$ and $Plin5^{-/-}$ mice (104 ± 5 vs. 105 ± 5 nmol/mg tissue/h, respectively. P=0.92, n=8 per genotype).

PLIN5 interacts with ATGL to inhibit spontaneous and ß-adrenergic stimulated lipolysis (12), suggesting that PLIN5 is more likely to regulate fatty acid flux from endogenous TAG stored in LDs rather than modulate the oxidation of extracellular-derived fatty acids (12,224). We performed pulse-chase experiments on primary myotubes generated from the skeletal muscle of wild-type and $Plin5^{-/-}$ mice to evaluate TAG metabolism. Plin5 mRNA expression was retained in myotubes generated from $Plin5^{+/+}$ mice and was absent in $Plin5^{-/-}$ myotubes (Fig. 2.14). Intracellular TAG was pre-labelled with [1-^{14}C] oleate for 4 h, then incubated in medium without radiolabeled fatty acids for 4 h, with or without isoproterenol. The oxidation of TAG-derived fatty acids was increased in $Plin5^{-/-}$ myotubes (genotype effect, P=0.009, Fig. 2-15A) and this coincided with increased depletion of the ^{14}C labelled TAG in $Plin5^{-/-}$ myotubes (genotype effect, P=0.02, Fig. 2-15B). Hence, PLIN5 deletion causes degradation of TAG in skeletal muscle. Consistent with this notion, 24 h fasted wild-type mice stored significant amounts of lipid in their skeletal muscle whereas the skeletal muscle of $Plin5^{-/-}$ mice were devoid of marked lipid staining

(Fig. 2-16), indicating increased intramyocelluar lipolysis and demonstrating an inability to expand the intramyocellular TAG pool.
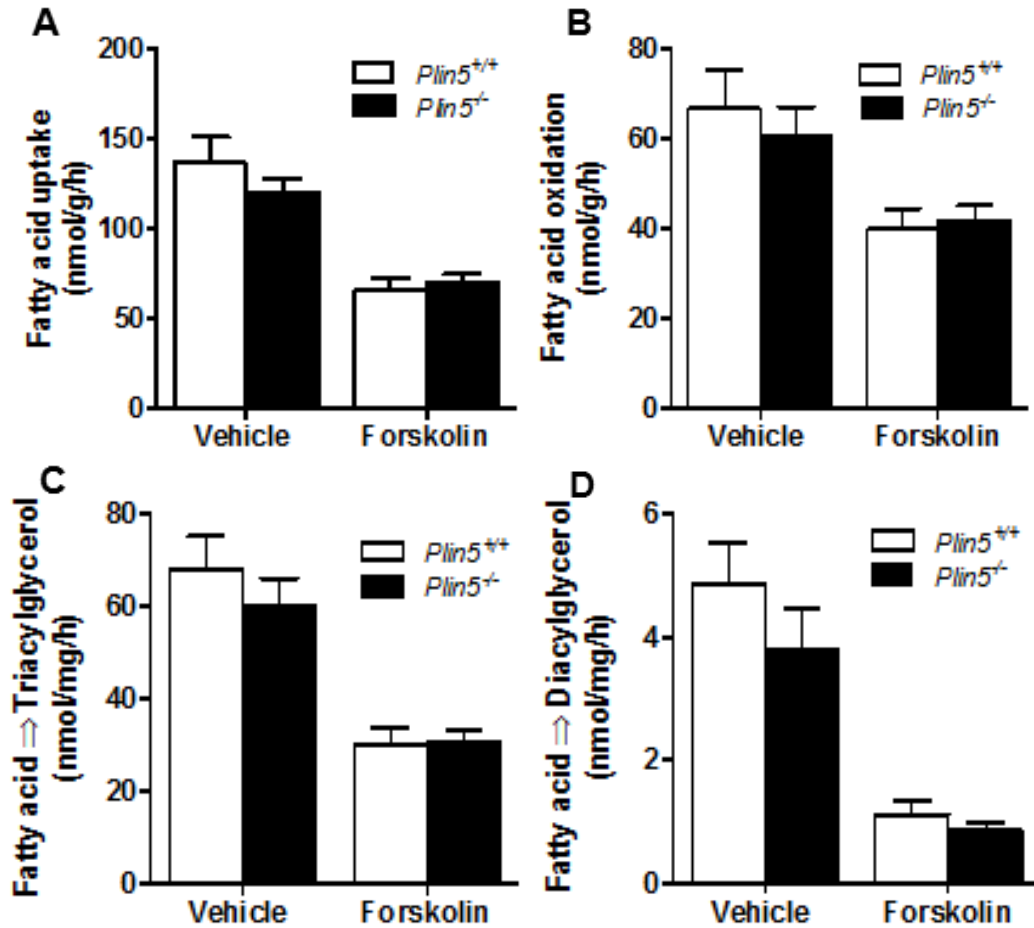

Fig 2-12. *Fatty acid metabolism was examined in isolated soleus muscle. (A) Fatty acid uptake, (B) fatty acid oxidation, (C) fatty acid incorporation into triacylglycerol (TAG) and (D) fatty acid incorporation into diacylglycerol (♂, Vehicle: n=12-16 Plin5^{+/+}, n=15-18 Plin5^{-/-}; Forskolin, n=7-12 Plin5^{+/+}, n=9-12 Plin5^{-/-}, age=14-16 weeks).*

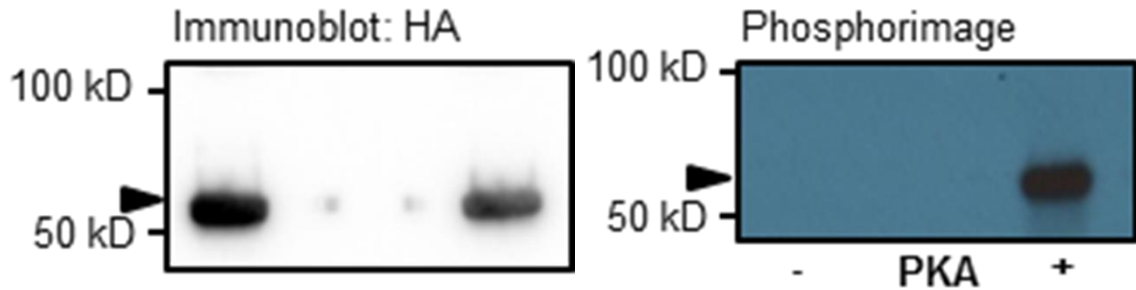**Fig 2-13.** *Recombinant murine PLIN5 was phosphorylated by cAMP-dependent protein kinase (PKA) catalytic subunit in kinase assay buffer containing [γ-32P]ATP. The protein mixture was separated by SDS-PAGE and PLIN5 identified by immunoblotting against HA (left band). The* ^{32}*P-labeled PLIN5 was detected by phosphorimaging (right band). Arrow denotes PLIN5. Representative of 2 independent experiments.*
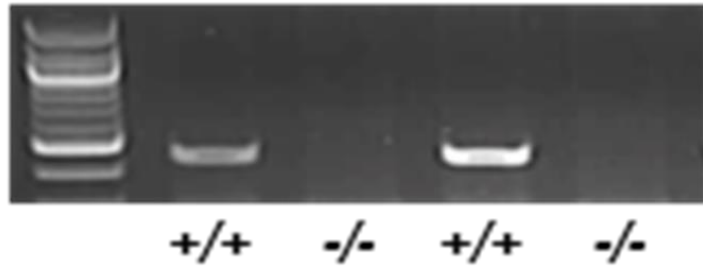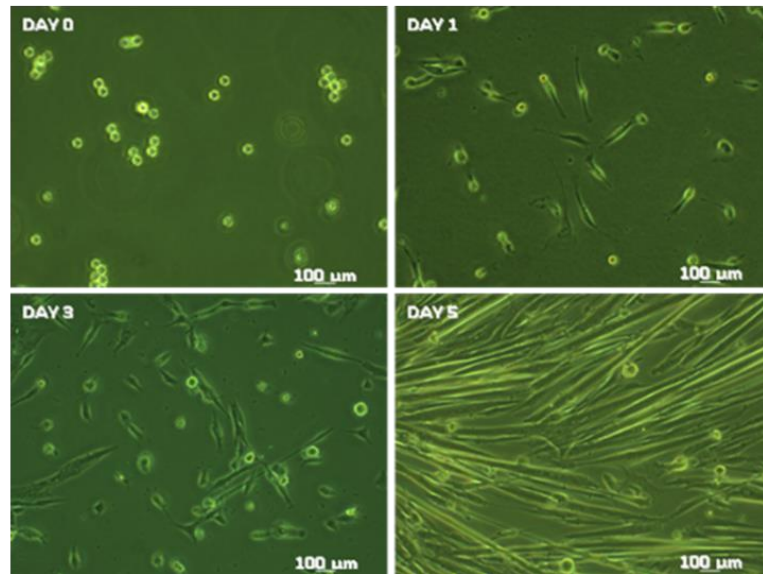
Fig 2-14. *(A)Plin5 mRNA expression in primary myotubes isolated from Plin5$^{-/-}$ and Plin5$^{+/+}$ mice. (B) Light microscopy demonstrating the growth of satellite cells from day 0, 1, 3 and 5 (fully differentiated myotubes) in culture.*
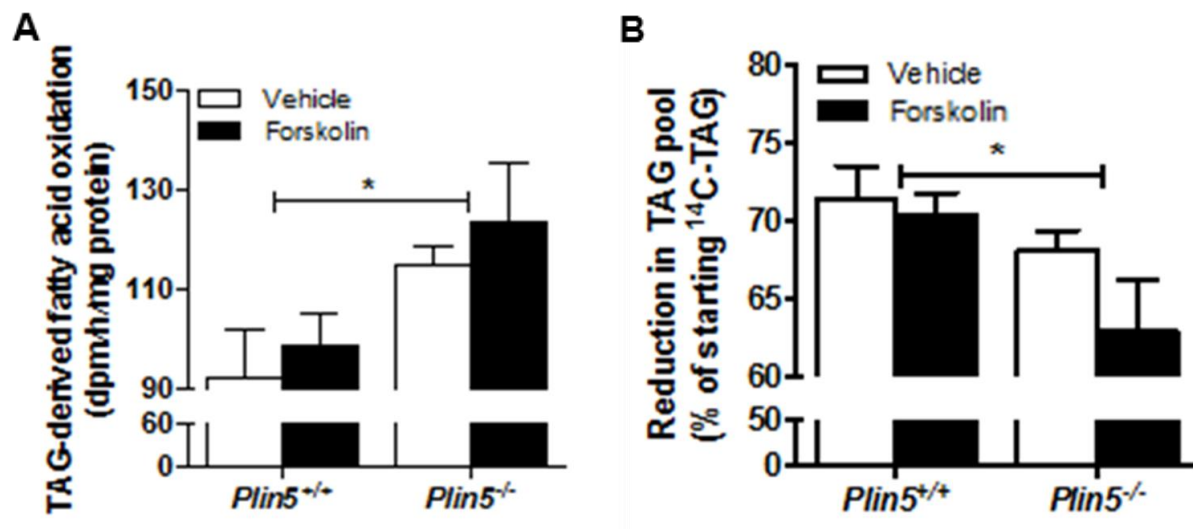
Fig 2-15. *(A) Oxidation of triacylglycerol-derived fatty acids in myotubes and (B) the percentage reduction of the radiolabelled TAG lipid pool (n=8 for each group from 2 independent donor mice and two independent experiments). *main effect for genotype, P<0.05.*
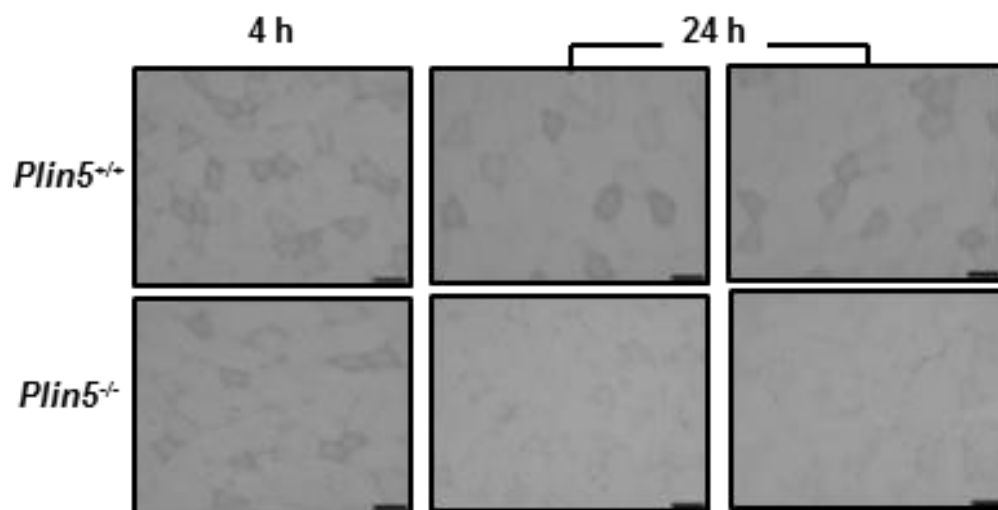
Fig 2-16. *Representative image of lipid droplets stained with oil red O in mixed quadriceps muscle of Plin5⁻/⁻ and Plin5⁺/⁺ mice following a 4 h and 24 h fast. Scale bar = 50 μm. Images representative of n=5 independent animals for each genotype.*

2.4.4 *Mitochondrial function is normal in the skeletal muscle of Plin5$^{-/-}$ mice*

Intramyocellular lipid droplet biology and mitochondrial biogenesis/ metabolism are linked through shared molecular signals (114) and increasing intramyocellular TAG flux is proposed to enhance mitochondrial biogenesis, most likely via PPAR mediated transcriptional reprogramming (88,267). We first assessed mitochondrial function in primary myotubes. Oxygen consumption rate was not different under basal or maximally stimulated conditions in *Plin5$^{-/-}$* vs. wild-type myotubes (Fig. 2-17). In line with these *in vitro* observations, markers of mitochondrial content and function were conserved in skeletal muscle *in vivo*. The expression of genes related to fatty acid uptake and storage (*Cd36*, *Dgat1*), fatty acid oxidation (*Cpt1b*, *Mcad*, *Pdk4*) and oxidative phosphorylation (*Acox, ATP synthase, Nrf1, Ppargc1a, Tfam, UCP2*) were similar in the mixed quadriceps muscle between genotypes (Fig. 2-18). In support of these observations, the maximal activities of the mitochondrial enzymes citrate synthase (CS) and ß-hydroxyacyl CoA dehydrogenase (β-HAD) were not affected in *Plin5$^{-/-}$* mice (Fig. 2-19) and the maximal running capacity of *Plin5$^{-/-}$* mice was not different from *Plin5$^{+/+}$* littermates during the graded exercise test (Fig. 2-20). Others have suggested that PLIN5 regulates intracellular lipid fluxes by physically recruiting mitochondria to the LD surface (225). We detected no difference in the mitochondria to LD contact within skeletal muscle of *Plin5$^{-/-}$* and *Plin5$^{+/+}$* mice using confocal microscopy (Fig. 2-21). Electron microscopy images supported these findings (Fig. 2-22). While the assessment of LD and mitochondria interactions is difficult to assess quantitatively, due to the limitations of resolution with confocal microscopy and the small field of view and qualitative nature of the EM data, this imaging nevertheless supports the conclusions drawn from the mRNA, protein and protein activity data.
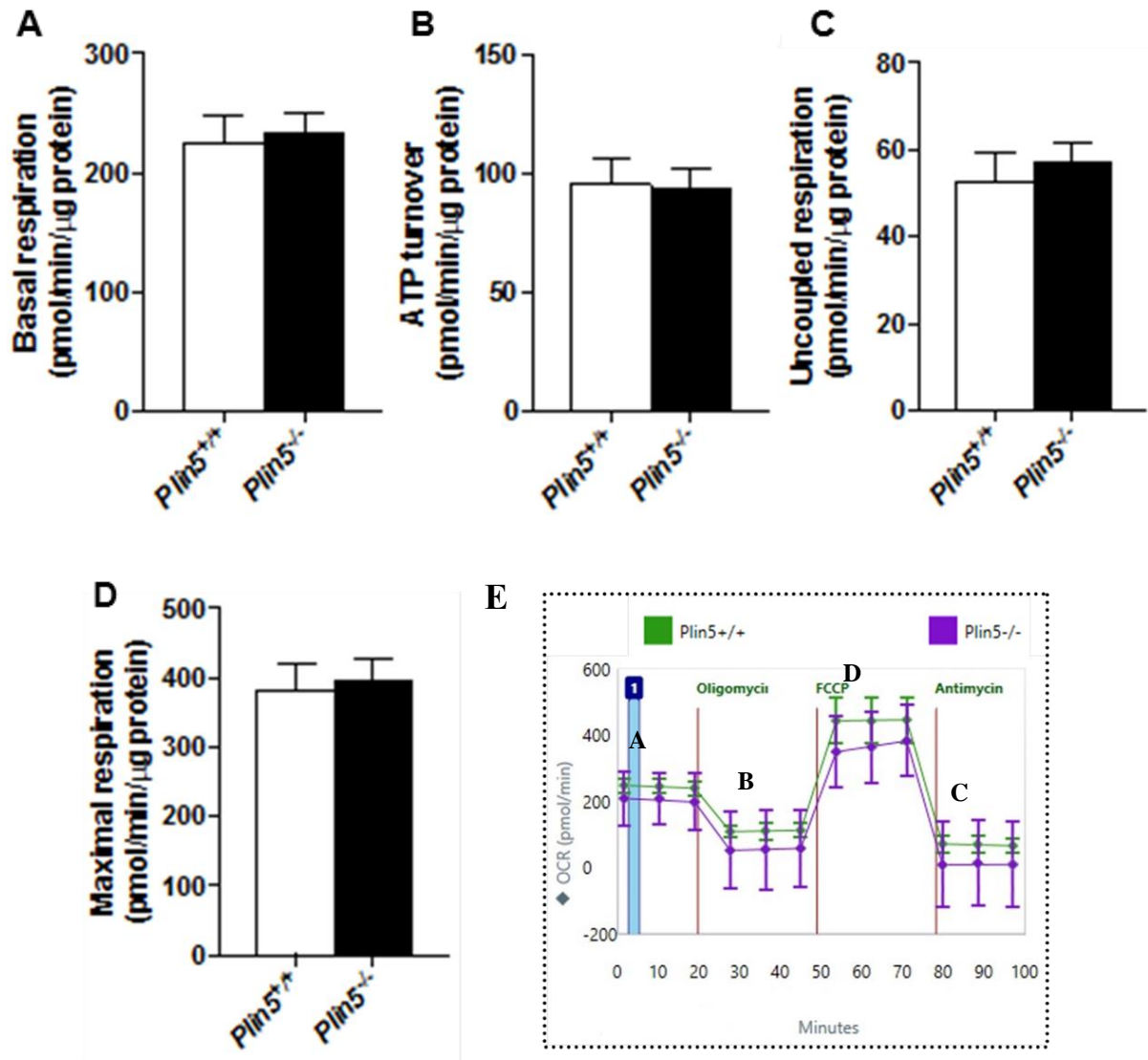
Fig 2-17. *Measures of mitochondrial capacity in Plin5$^{-/-}$ vs. Plin5$^{+/+}$ myotubes: (A) basal mitochondrial oxygen consumption rate, (B) ATP turnover, (C) uncoupled respiration and (D) maximal respiration (n=10 for each group obtained from three independent donor mice and three independent experiments). (E) Seahorse XF raw data trace showing the effect of different compounds on OCR in Plin5$^{-/-}$ vs. Plin5$^{+/+}$ myotubes. The cells are metabolically perturbed by the addition of three different compounds in succession, to obtain different parameters of mitochondrial function. The value in the graphs (A-D) above was calculated from the each parameter in this stress test graph.*
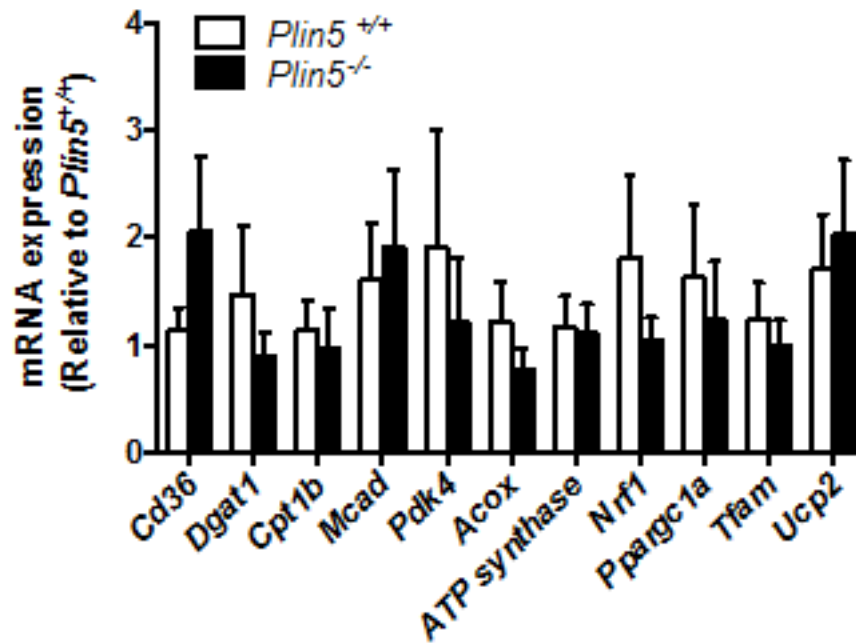
Fig 2-18. *Expression of fatty acid uptake, storage, and oxidation genes and oxidative phosphorylation genes ($\male$, n=4-6 Plin5$^{+/+}$, n=5-7 Plin5$^{-/-}$).*
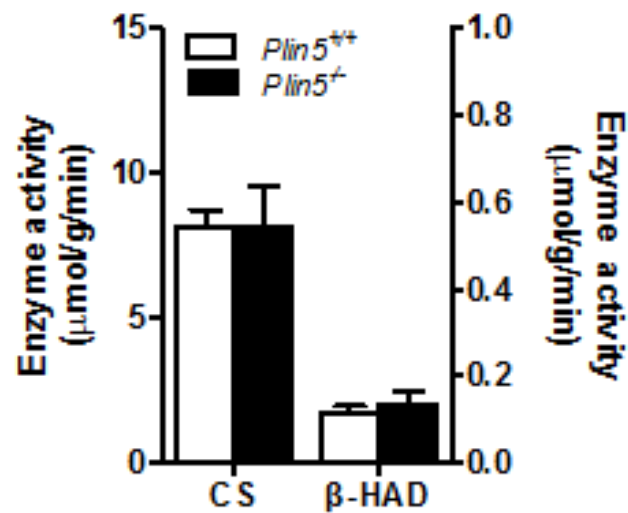
Fig 2-19. *Skeletal muscle citrate synthase and ß-hydroxyacyl CoA dehydrogenase (ß-HAD) maximal enzyme activity ($\male$, n=8 Plin5$^{+/+}$, n=8 Plin5$^{-/-}$).*
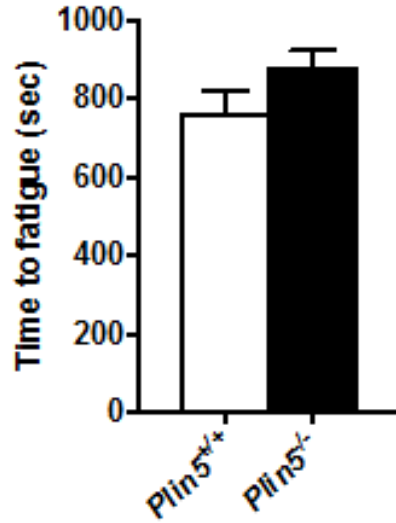
Fig 2-20. *Maximal running capacity assessed on a treadmill ($\male$, n=7 Plin5$^{+/+}$, n=12 Plin5$^{-/-}$). The exercise intensity was increased every minute until mice reached exhaustion.*
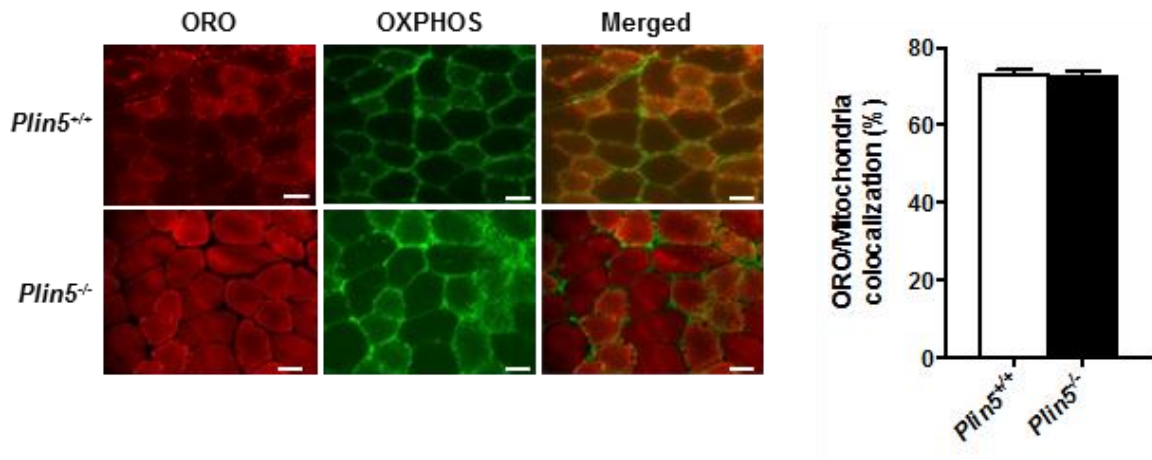
Fig 2-21. *Confocal images (left) showing oil red O (lipid, red), OXPHOS (mitochondria, green) staining and the merged images in mixed quadriceps muscle. Scale bar = 50 μm. The mitochondria/oil Red O colocation was not different between genotypes ($\male$, n=3 Plin5$^{+/+}$, n=3 Plin5$^{-/-}$. 9 independent sections were counted per animal with an average total of 27 ± 2 fibers per animal).*
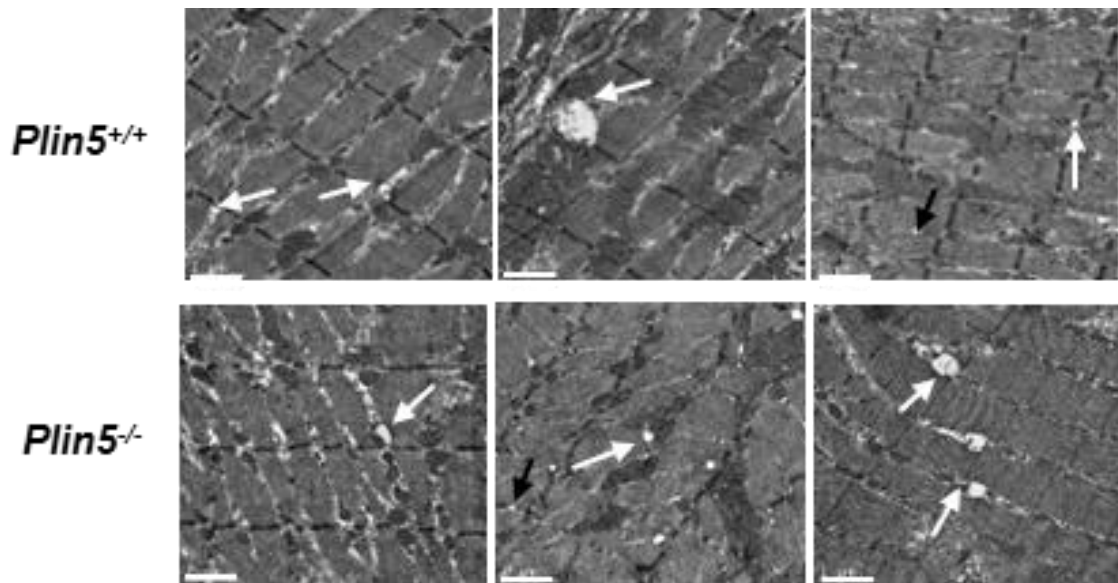
Fig 2-22. *Electron microscopy imaging of mixed quadriceps muscle. The white arrows highlight lipid droplets and mitochondria in contact, black arrows highlight lipid droplets not in contact with mitochondria. Scale bar = 1 μm.*

2.4.5 Glucose tolerance is improved in PLIN5 deficient mice

Skeletal muscle TAG accumulation is associated with insulin resistance (245,268) yet, paradoxically; decreasing intramyocellular TAG turnover can improve insulin action (89,90,269). Therefore, we next asked whether *Plin5* deletion would impact glucose tolerance and insulin action. Glucose tolerance was improved in *Plin5*$^{-/-}$ mice compared to wild-type mice as indicated by an attenuated blood glucose excursion after glucose administration (Fig. 2-23A). Plasma insulin increased (P=0.07, main effect) mildly after glucose administration and was not different between genotypes (P=0.26) (Fig. 2-23B). This suggests improved glucose effectiveness or enhanced insulin sensitivity in *Plin5*$^{-/-}$ mice.
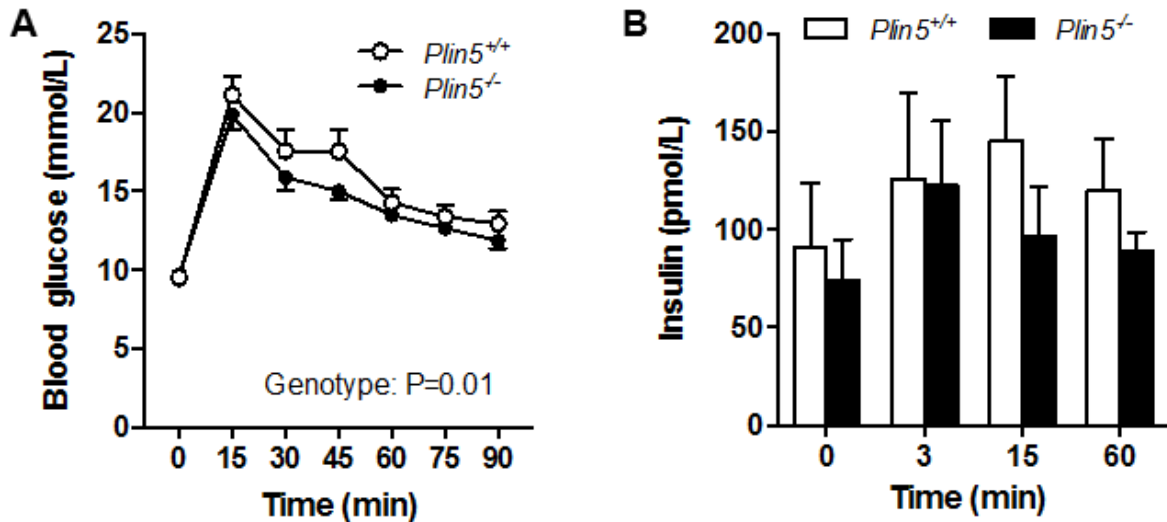
Fig 2-23. *(A) Glucose tolerance of Plin5*$^{-/-}$ *mice and Plin5*$^{+/+}$ *littermates (♂, n=23 Plin5*$^{+/+}$, *n=22 Plin5*$^{-/-}$, *age=10-17 weeks). (B) Plasma insulin in response to glucose tolerance test (♂, n=10 Plin5*$^{+/+}$, *n=7 Plin5*$^{-/-}$, *age=10-17 weeks).*

2.4.6 PLIN5 deletion exerts tissue-specific effects on insulin action

To assess whole body and tissue-specific insulin action, we performed hyperinsulinemic euglycemic clamps on *Plin5*^{-/-} and wild-type mice. Mice were clamped at 8.1 ± 0.3 mM glucose, 398 ± 38 pM insulin (no differences between genotypes) and steady-state GIR was achieved in both groups (Fig. 2-24). The glucose infusion rate required to maintain euglycemia was 15% lower in the *Plin5*^{-/-} mice (P=0.08), indicating a strong trend towards impaired whole-body insulin action (Fig 2-24). Hepatic glucose production was 41% lower (P=0.08) in *Plin5*^{-/-} vs. wild-type mice during the clamp (Fig. 2-25A), which was associated with reduced expression of the gluconeogenic genes *G6pc* and *Pepck* in livers from *Plin5*^{-/-} mice (Fig. 2-25B), suggestive of enhanced hepatic insulin sensitivity. The glucose disposal rate (GDR) during the clamp was reduced by 22% in *Plin5*^{-/-} mice (Fig. 2-26) and this was associated with reduced 2-deoxyglucose uptake into mixed skeletal muscle (34%, P=0.08, Fig. 2-27) and reduced muscle glycogen content after the clamp (Fig. 2-28). Glucose uptake into the heart (Fig. 2-27*)* was not different between genotypes and glucose uptake was reduced in white adipose tissue of *Plin5*^{-/-} mice (40%, Fig. 2-27), although this is a quantitatively small contribution to systemic glucose disposal. Taken together, these data show that *Plin5*^{-/-} mice become insulin resistant due to reduced insulin-stimulated glucose disposal in skeletal muscle and adipose tissue, but maintain insulin sensitivity in the liver.
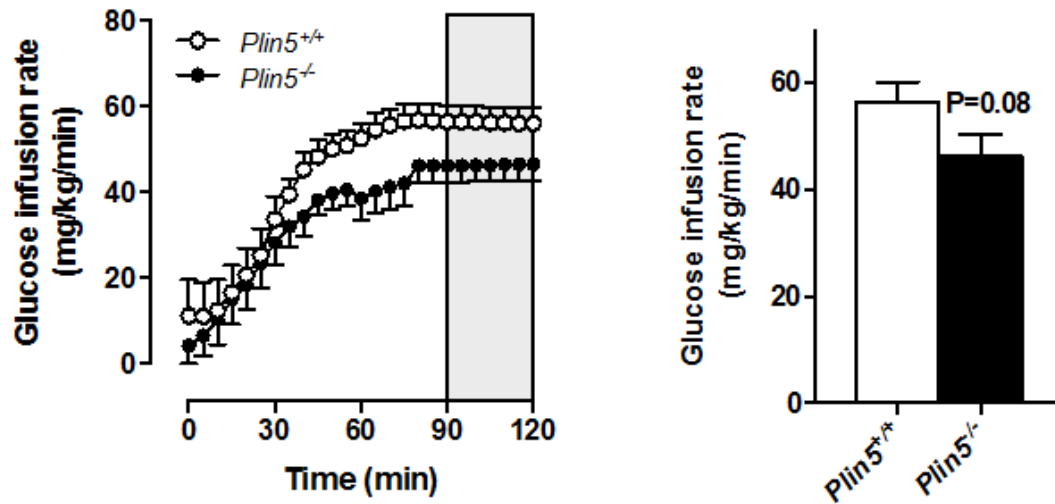
Fig 2-24. *Glucose infusion rate during the hyperinsulinemic euglycemic clamp with the steady-state period highlighted in grey shading (left). Right figure shows an average glucose infusion rate during steady state (♂, n=10 Plin5$^{+/+}$, n=12 Plin5$^{-/-}$, age= 13-16 weeks).*
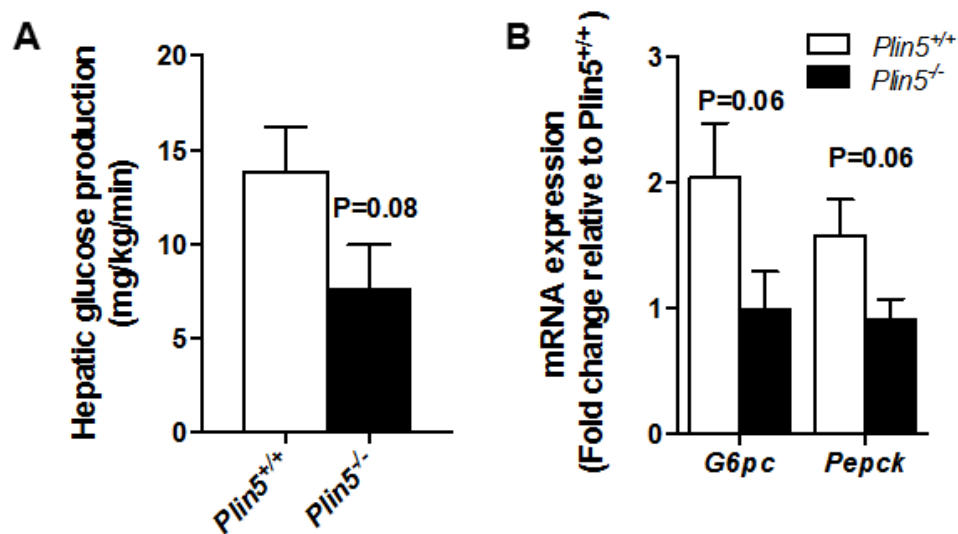
Fig 2-25. *(A) Hepatic glucose production during hyperinsulinemic euglycemic (♂, n=10 Plin5$^{+/+}$, n=12 Plin5$^{-/-}$, age= 13-16 weeks) and (B) expression of gluconeogenic genes G6pc and Pepck (♂, n=9 Plin5$^{+/+}$, n=10 Plin5$^{-/-}$, age= 13-16 weeks).*
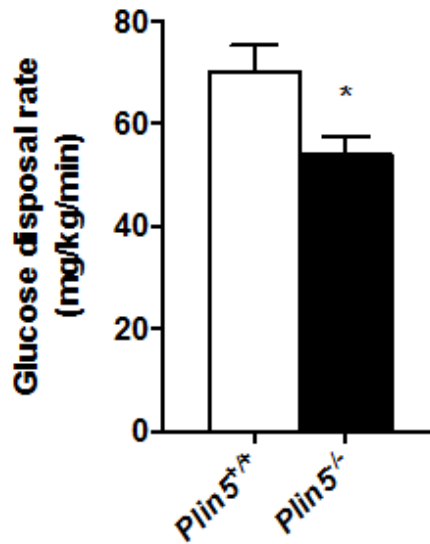
Fig 2-26. *Glucose disposal rate during the hyperinsulinemic euglycemic clamp (♂, n=10 Plin5^{+/+}, n=12 Plin5^{-/-}, age= 13-16 weeks). *P<0.05 vs Plin5^{+/+}.*
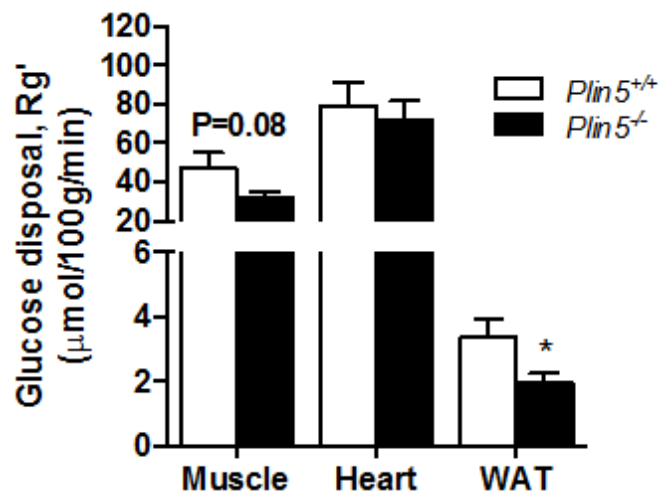
Fig 2-27. *Uptake of 2-deoxyglucose by skeletal muscle, heart and epididymal white adipose tissue (WAT) (♂, n=7 Plin5^{+/+}, n=8 Plin5^{-/-}, age= 13-16 weeks). *P<0.05 vs Plin5^{+/+}.*
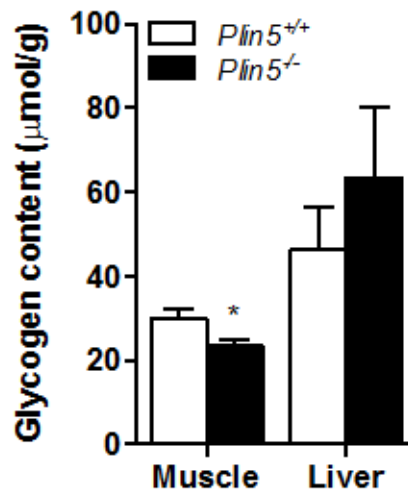
Fig 2-28. *Muscle (n=9 Plin5$^{+/+}$, n=9 Plin5$^{-/-}$) and liver (n=8 Plin5$^{+/+}$, n=8 Plin5$^{-/-}$) glycogen content following hyperinsulinemic euglycemic clamp (♂, age=13-16 weeks). *P<0.05 vs. Plin5$^{+/+}$.*

2.4.7 Evidence of altered lipid partitioning but not ER stress, inflammation or oxidative stress in the skeletal muscle of PLIN5$^{-/-}$ mice

Ceramide and DAG are widely acknowledged as key drivers of insulin resistance (250). Ceramide was increased by 53% in the skeletal muscle of *Plin5*$^{-/-}$ compared with *Plin5*$^{+/+}$ mice, whereas DAG was not different (Fig. 2-29). Lipidomic analysis of cultured myotubes supported this observation: ceramide (Figure 2-30A&B), dihydro- and hexosyl-ceramides and sphingomyelin (Fig. 2-30B) were increased in *Plin5*$^{-/-}$ myotubes, whereas other lipid types such as phospholipids and sterols were mostly unchanged (Fig. 2-30C). The increase in sphingolipids was associated with an increase in the gene expression of key enzymes involved in ceramide synthesis including serine palmitoyltransferase 2 and sphingomyelin phosphodiesterase 2 (Fig 2-31). There was no evidence for inflammation (JNK phosphorylation, degradation of IKBα, TNFα and IL-6 mRNA expression), ER stress (phosphorylated GADD34 and PERK) or oxidative stress (thiobarbituric acid reactive substances) in the skeletal muscle of *Plin5*$^{-/-}$ mice compared with wild-type mice (data not shown).
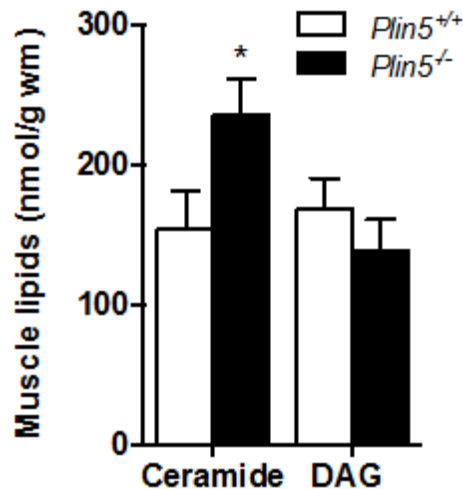
Fig 2-29. *Ceramide and diacylglycerol content in skeletal muscle (♂, n=8 Plin5*$^{+/+}$*, n=8 Plin5*$^{-/-}$*, age= 13-16 weeks). *P<0.05 vs Plin5*$^{+/+}$*.*
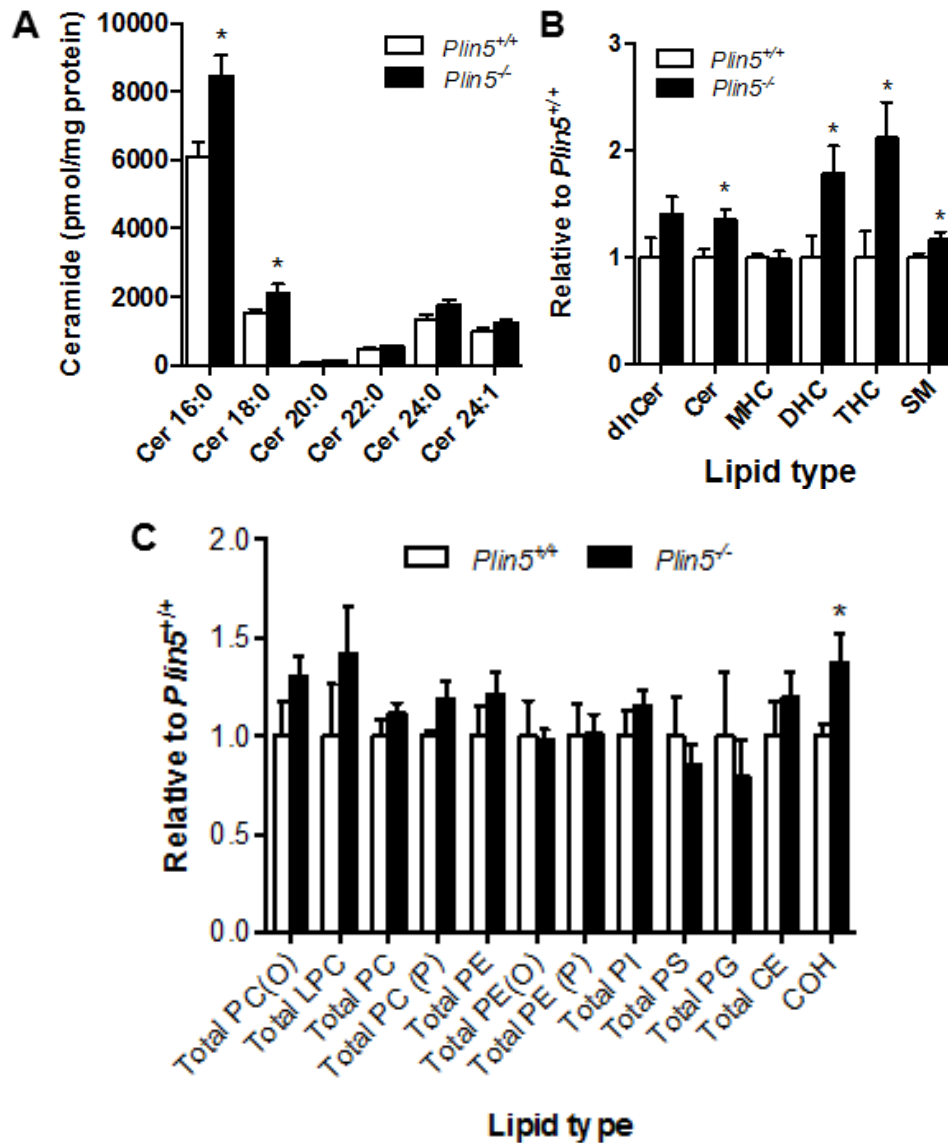
Fig 2-30. *(A) Ceramide species in Plin5$^{-/-}$ vs. Plin5$^{+/+}$ myotubes (n=6 for each group) *P<0.05 vs. Plin5$^{+/+}$. (B) Sphingolipids in Plin5$^{-/-}$ vs. Plin5$^{+/+}$ myotubes (n=6 for each group) *P<0.05 vs. Plin5$^{+/+}$. dhCer, dihydroceramide; Cer, ceramide; MHC, monohexosylceramide; DHC, dihexosylceramide; THC, trihexosylceramide; SM, sphingomyelin. (C) Lipids were assessed by electrospray ionization-tandem mass spectrometry in Plin5$^{-/-}$ vs. Plin5$^{+/+}$ myotubes (n=6 for each group). Alkylphosphatidylcholine (PC(O)), lysophosphatidylcholine (LPC), phosphatidylcholine (PC), alkenylphosphatidylcholine (PC(P)), phosphatidylethanolamine (PE), alkylphosphatidylethanolamine (PE(O)), alkenylphosphatidylethanolamine (plasmalogen) (PE(P)), phosphatidylinositol (PI), phosphatidylserine (PS), phosphatidylglycerol (PG), cholesterol ester (CE) and cholesterol (COH). *P<0.05 vs. Plin5$^{+/+}$*
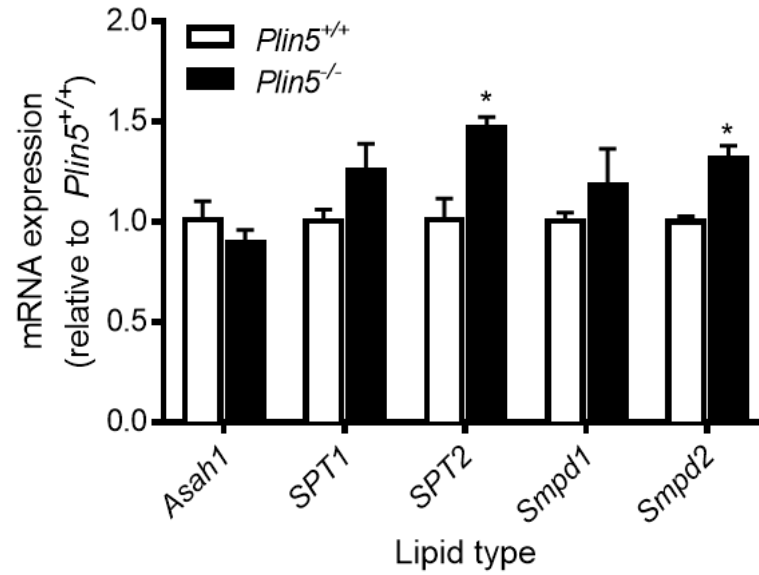
Fig 2-31. *mRNA expression of key enzymes involved in sphingolipid metabolism in Plin5^{-/-} vs. Plin5^{+/+} myotubes. (n=4 for each group) *P<0.05 vs. Plin5^{+/+}.*

2.5   Discussion

Lipid metabolism and insulin action are intimately linked (270) and LDs stored within tissues are critical for controlling intracellular lipid flux (271). In this regard, the highly conserved PLIN family of proteins reside on the surface of LDs and are important for LD formation, lipolytic regulation during times of energetic demand and protection against lipotoxicity when cells are exposed to an excess of fatty acids. PLIN5 is unique among this family because it is highly expressed in oxidative, glucoregulatory tissues such as skeletal muscle (10), is localized to multiple intracellular locations including the LD, ER, mitochondria and the cytosol (272) and may regulate a dynamic interaction between the LD and mitochondria that is proposed to be relevant to the etiology and treatment of insulin resistance (114,225). Uncertainty surrounds the metabolic roles of PLIN5 (discussed below), partly because most cell systems used to date poorly reflect the metabolic requirements of the major oxidative tissues *in vivo*. To address this question, we generated *Plin5^{-/-}* mice and examined lipid metabolism and insulin action in skeletal muscle, a major site for fatty acid and glucose disposal.

The controversy surrounding PLIN5's involvement in metabolism arises from the apparently conflicting observations in immortalized cell lines that PLIN5 promotes both fatty acid oxidation and storage (10) and either increases or decreases lipolysis (11–13,273). The prevailing views with respect to lipolysis are: (1) ATGL and CGI-58 interact separately with PLIN5 on lipid droplets to facilitate their interaction and drive lipolysis (13,273); or (2) PLIN5 and CGI-58 independently recruit ATGL to LDs with opposite effects, CGI-58-ATGL interactions drive lipolysis while PLIN5 binding to ATGL inhibits lipolysis (11,12). In the current study, we show that PLIN5 does not influence fatty acid transport into myotubes, fatty acid oxidation or fatty acid esterification into glycerolipids. However, PLIN5 ablation increases intramyocellular lipolysis and invokes a remarkable decrease in muscle LD content in fasted, but not fed mice. Hence, our data agree with the interpretation that PLIN5 provides a critical barrier function on LDs to prevent excessive lipolysis. These novel findings in skeletal muscle mostly agree with the previously described role of PLIN5 in the heart. *Plin5* ablation reduced LD size, which was due to increased ATGL-mediated TAG lipolysis and, independently, an increased capacity for fatty acid oxidation in cardiomyocytes (224). On the other hand, cardiac-specific overexpression of PLIN5 inhibits ATGL-mediated lipolysis resulting in increased LD size, myocardial steatosis,

mild impairments in oxidative metabolism and modest cardiac dysfunction (231,255). Together, these studies support the view that PLIN5 is a highly abundant protein in muscle that is required to repress intramyocellular lipolysis. This effect is most prominent during prolonged nutrient deprivation, where fatty acid substrate from both intramyocellular and adipose tissue TAG is enhanced. Hence, PLIN5 may protect myocytes from unnecessary depletion of intramyocellular fuels and/or control intracellular fatty acid flux to prevent lipotoxic outcomes.

Mitochondrial dysfunction in skeletal muscle is proposed to contribute to reduced fatty acid oxidation, lipid deposition and the development of insulin resistance in obese individuals (274). Indeed, such observations have provided the impetus for developing therapeutics aimed at enhancing mitochondrial function and fatty acid oxidation to treat obesity (e.g. acetyl CoA carboxylase inhibitors, AMPK activators). While this rationale is probably oversimplified (275), emerging evidence indicates that increasing fatty acid flux from lipid droplets can induce mitochondrial biogenesis, most likely via a PPAR-mediated program, and in turn improve cell function (88,114,267,276). While we demonstrated that fatty acid oxidation from intramyocellular lipid was increased with Plin5 deletion, mitochondrial content and function were not enhanced in either isolated myotubes or intact skeletal muscle; exogenous fatty acid and glucose oxidation were not enhanced *in vitro* and whole-body fatty acid oxidation was actually reduced by ~11% in *Plin5*^{-/-} mice. The brain and skeletal muscle account for ~45% of the daily energy expenditure (277), therefore in the absence of increased glucose oxidation in these tissues, other tissues are most likely accounting for the decrease in systemic fatty acid oxidation and reciprocal increase in glucose oxidation. While the effects of PLIN5 overexpression in skeletal muscle are equivocal (226,227), overexpression of PLIN5 in cardiac muscle reduces intracellular lipolysis and is associated with reduced mRNA contents of oxidative phosphorylation proteins, decreased mitochondrial enzyme activities and mildly impaired mitochondrial respiration (231,255). Aside from tissue specific actions, the reasons for this apparent discrepancy are unclear. It is possible that the increase in intramyocellular lipolysis with *Plin5* deletion was insufficient to drive a PPAR transcriptional program. This possibility is supported by the similarity in PGC1α mRNA and PGC1α target genes between *Plin5*^{-/-} and control mice shown here, and further supported by a recent report in muscle-specific ATGL null and overexpressing mice showing a dissociation of intramyocellular lipolysis, mitochondrial

biogenesis and fatty acid oxidation (75). Alternatively, PLIN5 may modulate the cells molecular program via direct transcription/co-activator functions, which may be functionally redundant in $Plin5^{-/-}$ mice.

While intramyocellular TG accumulation is linked to insulin resistance (244,245), emerging data now link the etiology of insulin resistance to the uncoupling of intramyocellular lipolysis from the cellular demand for fatty acids (74,147). In this context, we proposed that the increase in muscle lipolysis combined with no additional demand for fatty acid substrate would reduce insulin sensitivity in $Plin5^{-/-}$ mice. Indeed, our results show that $Plin5^{-/-}$ mice have reduced skeletal muscle insulin sensitivity, as demonstrated during hyperinsulinemic euglycemic clamps. This was associated with ceramide accumulation, which is a negative regulator of insulin signal transduction (270). Other complex ceramides and sphingomyelin were increased, while phospholipids, sterol lipids and DAG were unchanged with $Plin5$ deletion. Hence, fatty acids derived from accelerated intracellular lipolysis appear to be preferentially directed into sphingolipids, which in turn cause insulin resistance. The expressions of several enzymes involved in ceramide production were also increased, indicating upregulation of enzyme capacity to facilitate the increase in substrate flux. This interpretation is consistent with a recent human study demonstrating the inverse: increased PLIN5 content, decreased muscle ceramide (not DAG) and improved insulin sensitivity in the skeletal muscle of endurance trained compared with obese men (115). The reduction in skeletal muscle insulin sensitivity in $Plin5^{-/-}$ mice is unlikely to be due to impaired blood flow and insulin delivery, secondary to impaired cardiac function, because impairments in the cardiac function of $Plin5^{-/-}$ mice is not apparent until 30-38 weeks of age (224), and we assessed insulin sensitivity in mice aged 16 weeks when cardiac function is normal.

In contrast to muscle, both hepatic glucose production and the insulin sensitive gluconeogenic gene expression were lower in $Plin5^{-/-}$ mice during the insulin clamp conditions, suggestive of improved hepatic insulin sensitivity. Moreover, $Plin5^{-/-}$ mice have normal fasting glucose and insulin and improved glucose tolerance compared with wild-type mice following glucose administration. This highlights the important role of liver in maintaining glycemia under basal and post-prandial conditions (i.e. GTT) (278,279) and suggests that the improved hepatic insulin

action compensates for the reduced peripheral insulin sensitivity in *Plin5*^{-/-} mice. It is important to note that progressive declines in muscle insulin sensitivity have no impact on glucose tolerance in C57Bl/6 mice (260) and that glucose effectiveness is quantitatively more important than insulin sensitivity in the determination of glucose tolerance (280). The contribution of glucose effectiveness over insulin sensitivity is more pronounced with intraperitoneal glucose administration, which bypasses the gut and precludes an incretin effect, thus resulting in minimal insulin secretion. Hence, our glucose tolerance and insulin clamp data are concordant. The uncoupling of muscle and liver insulin sensitivity is not without precedence either; *Plin1*^{-/-} mice present with a very similar phenotype (176), although the factors governing these responses in each genotype are unlikely to be conserved given the unique tissue expression patterns of PLIN1 (adipose) and PLIN5 (muscle, liver). Understanding the cell-specific mechanisms that mediate the dichotomy in insulin action is beyond the scope of these studies and future work will address this intriguing question.

Taken together, our studies show that PLIN5 suppresses skeletal muscle lipolysis, particularly during prolonged nutrient deprivation, does not influence mitochondrial reprogramming and is required for the maintenance of insulin sensitivity in skeletal muscle by preventing ceramide production. Others have shown that PLIN5 expression is increased by PPARα agonists, fasting, fatty acids and endurance exercise training (10,11,114,222); situations characterised by increased lipid flux in skeletal muscle. Hence, our data support the hypothesis that PLIN5 is required to match lipolysis of intramyocellular TAG to metabolic demands, which helps to maintain insulin sensitivity in skeletal muscle.

CHAPTER 3

Altered lipid metabolism and glucose homeostasis in
***Plin5* muscle-specific knockout mice.**

3.1   Introduction

PLIN5 is a lipid-droplet associated protein that is highly expressed in tissues where fatty acid serves as a prominent metabolic substrate, such as liver, skeletal muscle and heart, and PLIN5 is known to regulate lipid metabolism in most tissues. Early studies in cultured cells (i.e. CHO, COS-7, AML-12 cells) showed that PLIN5 remodelled intracellular lipid metabolism, with evidence that PLIN5 over expression increased FFA uptake and FFA oxidation (10) and decreased intracellular triglyceride hydrolysis (11,12), which resulted in TG accumulation (10,11). Later studies by Kuramoto et al. (224) demonstrated that cardiomyocytes isolated from PLIN5$^{-/-}$ mice had increased fatty acid oxidation and reduced TG concentrations in the heart, which was attributable to PLIN5 restricting lipase access to TG located in intracellular LDs. Similar observations have been made in isolated hepatocytes where ectopic PLIN5 expression enhanced TG storage by inhibiting lipolysis and fatty acid ß-oxidation, without effecting *de novo* lipogenesis (230,281,282). Therefore, these data suggest that PLIN5 suppresses TG lipolysis and TG-derived FFA oxidation to protect cells from lipotoxic stress.

In our previous study examining whole-body *Plin5*$^{-/-}$ mice (283), we showed that PLIN5 ablation leads to increases in intramyocellular TG lipolysis, which in turn resulted in the accumulation of ceramide in muscle. This was associated with insulin resistance in skeletal muscle and WAT, yet insulin sensitization in the liver. These tissue-specific responses are difficult to reconcile and it is possible that PLIN5 deletion could alter inter-tissue communication to impact muscle insulin action. Evidence for this possibility comes from recent studies in mice over expressing PLIN5 in skeletal muscle. These mice undergo transcriptional reprogramming resulting in a 80-fold increase in fibroblast growth factor (FGF)-21 in skeletal muscle and a 2-fold increase in serum FGF-21 that was associated with protection against high-fat diet induced insulin resistance (284).

Therefore, the aim of this study was to investigate the cell autonomous effects of *Plin5* deletion in skeletal muscle using *in vivo* models. To do this, we generated mice with muscle-specific *Plin5* deletion and examined whether these mice exhibited impaired lipid and glucose metabolism, and altered insulin action when fed a standard diet or HFD.

3.2   Aims

To determine the effects of muscle specific PLIN5 deletion on energy homeostasis, muscle metabolism and glucose tolerance *in vivo*.

3.3   Materials and Methods

The following section describes materials and methods used for chapter 3. Additional or variation of material and methods used in other chapters will be contained within their respective sections.

3.3.1   Mouse generation

All procedures were approved by the Monash University Animal Ethics Committee (MARP/2013/050) and conformed to National Health and Medical Research Council of Australia guidelines regarding care and use of experimental animals. A targeted vector containing Plin5 (NM_001013706.2) interrupted in exon 5, 6 and 7 was generated by the trans-NIH Knock-Out Mouse Project (KOMP) and obtained from the KOMP Repository (Project ID CSD40589, ES clone EPD0301_4_E04). The targeting vector is composed of an FRT site followed by lacZ sequence and a loxP site. The first loxP site is followed by neomycin under the control of β-actin promoter / neomycin phosphotransferase gene / SV40 polyA promoter, a second FRT site and a second loxP site. A third loxP site is inserted downstream of the targeted exons (Fig. 3-1). ES cells positive for bilateral homologous recombination were introduced into mouse blastocysts to generate chimeric mice (Monash Gene Targeting). Mice were bred with mice expressing Flp recombinase to remove the neomycin resistance cassette and to verify germline transmission. These mice were bred with mice overexpressing Cre recombinase under the control of the murine muscle creatine kinase (MCK) promoter (MCK-Cre mice) to create mice with muscle-specific ablation of *Plin5* (Plin5$^{lox.lox}$.Cre$^{+/-}$, denoted herein as *Plin5^{MKO}* mice) and wild-type littlermates (i.e. Plin5$^{lox.lox}$.Cre$^{-/-}$ mice, denoted herein as lox/lox) (285). The breeding strategy is shown in Fig. 3-1. Mice were confirmed to contain the PLIN5 disrupted allele by PCR of genomic DNA (Fig. 3-2).
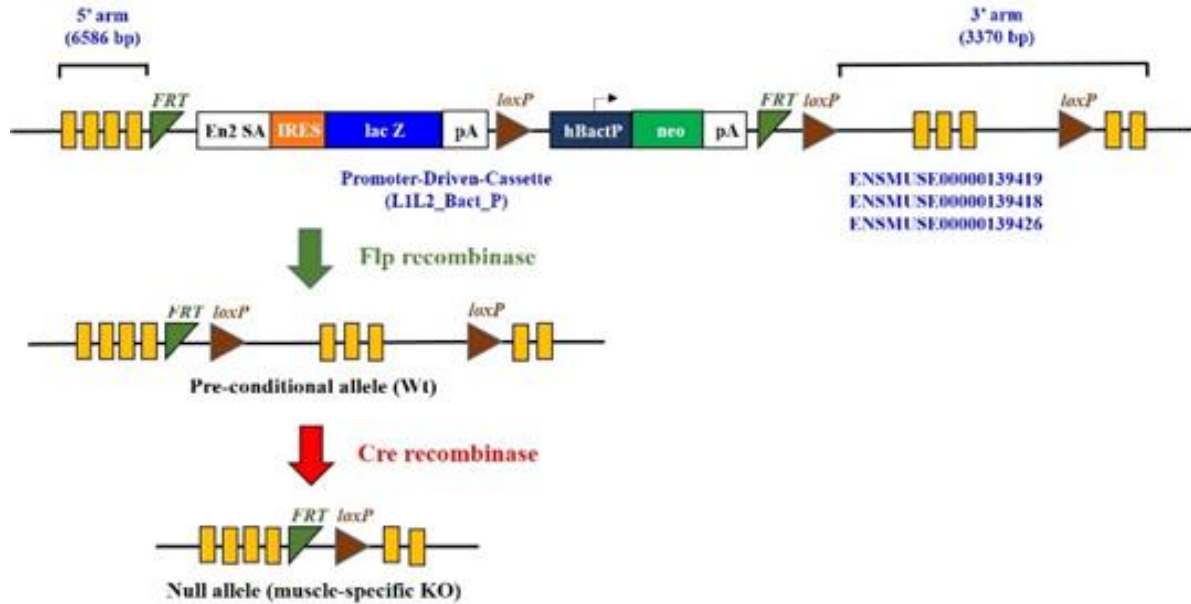
Figure 3-1. *Diagram of the promoter-driven cassette and breeding strategy employed to generate muscle-specific Plin5 knock-out (Plin5^{MKO}) mice.*

1. Plin5$^{lox.lox}$.Cre$^{+/-}$ = *Plin5^{MKO}*
2. Plin5$^{+/+}$.Cre$^{-/-}$ = control
3. Plin5$^{+/+}$.Cre$^{+/-}$ = control
4. Plin5$^{lox.lox}$.Cre$^{-/-}$ = lox/lox

Figure 3-2. *PCR of tail genomic DNA of mice generated by crossing mice expressing Flp recombinase with mice overexpressing Cre recombinase. Mice number 1 (Plin5$^{lox.lox}$.Cre$^{+/-}$) denoted herein as Plin5^{MKO} mice and mice number 4 were chosen as control littlermates (lox/lox, i.e. Plin5$^{lox.lox}$.Cre$^{-/-}$ mice).*

3.3.2 Experimental design

Mice were housed at 22°C on a 12:12-h light dark cycle. Mice were fed regular rodent chow (5% calories from fat, Specialty Feeds, WA, Australia) until 6 weeks of age. The food was changed to a high-fat diet (HFD; 43% calories from fat, Specialty Feeds) for some mice and all mice had free access to water. Experiments were performed in mice aged 18 weeks of age unless otherwise stated. Mice were fasted for 4 h (0700-1100 h) before all experiments, which commenced at 1100 h unless otherwise stated.

3.3.3 Assessment of whole body metabolism

Whole body metabolism was measured in metabolic cages (Columbus Instruments, Columbus, OH). Mice were housed individually for 48 h for assessment of food and water intake, oxygen uptake, carbon dioxide production and physical activity.

3.3.4 Fatty acid metabolism ex vivo

Mice were anaesthetized with isoflurane and kept under sedation while the soleus muscle was excised. Fatty acid metabolism was assessed by radiometric methods as described in section 2.3.4.

3.3.5 Glucose metabolism ex vivo
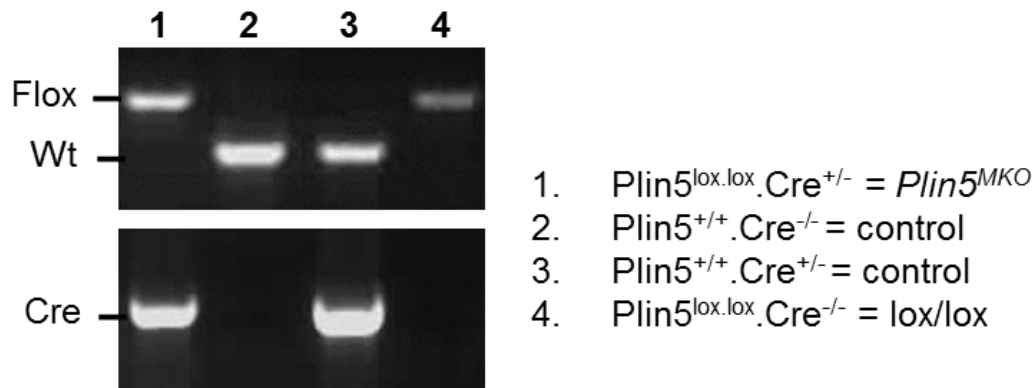
Glucose metabolism was assessed by radiometric methods. Briefly, the extensor digitorum longus (EDL) muscle was isolated from anaethetised mice by excising from tendon to tendon and was quickly placed in plastic scintillation vials containing 0.5 ml of gassed (O_2:CO_2 – 95:5%) Krebs-Hanseleit bicarbonate (KHB) buffer with 0.1% fat-free BSA, 8 mM mannitol and 200 mM pyruvate. Muscles were incubated for 20 min and the buffer was removed and new pre-incubation buffer containing 0.5 ml of gassed (O_2:CO_2 – 95:5%) KHB buffer with 0.1% fat-free BSA, 8 mM mannitol and 10 mM glucose was added and incubated for 10 min. After pre-incubation, the muscles were transferred to a second set of vials with 0.5 ml of KHB buffer containing either [³H] 2-Deoxy-D-glucose (1 µCi/ml) and cold deoxyglucose (10 µM) for the determination of glucose uptake. Glucose uptake was assessed in the absence or presence of 10 nM insulin using contralateral muscles from the same mouse.

3.3.6 Oral glucose tolerance tests (OGTT)

Mice were administered with D-glucose (2 g/kg mass) by oral gavage needle. The oral gavage needle used was a straight 22 g needle, 25 mm in length with a 1.25 mm ball diameter. Tail blood was collected and blood glucose was determined using a glucometer (Accu-chek, Roche, Mannheim, Germany) at the times indicated. Plasma insulin was determined by ELISA (Cat. No. EZRMI-13K, Merck Millipore, Billerica, MA, USA).

3.3.7 Intraperitoneal insulin tolerance test (IPITT).

Animals received a single intraperitoneal injection with insulin (1 U/kg; Novo-Nordisk, Bagsværd, Denmark), and blood glucose was determined using a glucometer (Accu-chek, Roche, Mannheim, Germany) before and at 15, 30, 45, 60 and 90 min post-injection.

3.3.8 Stable isotope labeled OGTT

An OGTT using stable isotope labeled glucose was performed to determine glucose metabolism in high-fat fed mice as described previously (286). This method allows for the simultaneous assessment of the glucose disposal and endogenous glucose production (EGP) under dynamic conditions that closely reflect the postprandial state. Briefly, mice received an oral gavage of stable isotope labeled glucose ($[6,6]$-^{2}H glucose, 2 g/kg mass, Cambridge Isotope Laboratories, MA, USA). Blood glucose was measured with a glucose meter (Accu-Check, Roche, NSW, Australia) prior to and at 15, 30, 60 and 120 min following gavage. Blood (~10 µL) was collected from the tail tip prior to and at 15 and 60 min following glucose gavage. Samples were spun in a centrifuge (4 °C, 8,000 x g, 5 min) and plasma was used to perform mass isotopomer analysis of plasma glucose via gas chromatography–mass spectrometry (GC–MS).

Samples were deproteinized by adding 50 µL of ice cold methanol to 2.5 µL of plasma. After thorough mixing the sample was centrifuged (4°C, 8,000 x g, 10 min) and the supernatant was dried and methoximated by the addition of 20 µL methoxyamine HCl in pyridine (20mg/ml, Supelco, Sigma-Aldrich, St. Louis, USA). After incubation at 90°C for 1 h methoximated glucose was converted to the TMS derivative by the addition of 20 µL N,O-bis(trimethylsilyl) trifluoroacetamide (BSTFA) + 1% trimethylchlorosilane (TMCS) (Thermo Fisher Scientific, Waltham, USA). Samples were analysed using a 7890A gas chromatography (GC) system and a

5975C mass selective detector (MSD) (Agilent Technologies, Santa Clara, USA) in electron ionization (EI) mode using helium as a carrier. The GC was equipped with a DB5 capillary column with a 10 m inert duraguard (J&W Scientific, 30 m, 250 µm inner diameter, 0.25 µm film thickness). The injector insert and GC-MS transfer line temperatures were 270 and 250 °C, respectively. The oven temperature gradient was set to: 100 °C (2 min); 100°C to 320°C at 25 °C/min; 320 °C for 2 min. Sample (1 µL) was injected with the inlet set to split mode (10:1). The isotopomers of the glucose MOX-TMS derivative were identified and quantitated by selected ion monitoring (SIM) for ions m/z 319 (M0) to 321 (M2). The mass isotopomer abundances were determined using Mass Hunter Workstation (Agilent Technologies, Santa Clara, USA). Correction for natural abundance (background enrichment) was performed by running unlabelled basal (pre-gavage) plasma samples and also using standards of known 6,6-^{2}H glucose enrichment (12.5%, 25%, 50%, 75% and 100%). The true fractional abundance (mole % excess) of the M0 (endogenous glucose), and M2 (6,6-^{2}H glucose) isotopomers were multiplied by the blood glucose concentration at each corresponding time point of the OGTT to calculate the absolute concentrations of load (labelled) and endogenous (unlabelled) glucose.

3.3.9   Quantitative RT-PCR.

RNA was extracted from tissues using QIAzol lysis reagent (Qiagen, Doncaster, Victoria, Australia). RNA quantity was determined at 260 nm (NanoDrop p2000 Spectrometer, Biolab, Clayton, Australia), reverse transcribed (iScript cDNA Synthesis Kit, Bio- Rad Laboratories, Hercules, CA), and gene products were determined by real-time quantitative RT-PCR (ep realplex Mastercycler, Eppendorf, Hamburg, Germany) using SYBR Green PCR Master Mix (Brilliant II SYBR® Green QPCR Master Mix, Agilent Technologies, Santa Clara, CA, USA) for *Plin5* and TaqMan Universal PCR Master Mix (AmpliTaq Gold® DNA Polymerase, Applied Biosystems, Scoresby, VIC, Australia) for all other genes. The primers used for SYBR Green based real time PCR are: *Plin5* For 5'-GTGACTACCTGTGCCCTGGAC-3', *Plin5* Rev 5'-TGATGGCTGCTGCAGGAAG-3' and for the housekeeping gene, *18S* For 5'-ATCGGGGATTGCAATTATTC-3', *18S* Rev 5'-TGTACAAAGGGCAGGGACTT-3'.The primers used for Taqman probe-based assays are listed in Table 3-1. *18S* was used as a reference gene and did not vary between groups. The mRNA levels were determined by a comparative C_T method.

Gene name	Primer Number from Applied Biosystems
Plin2	Mm00475794_m1
Plin3	Mm00482206_m1
Plin4	Mm00491061_m1
Pnpla2	Mm00503040_m1
Abhd5	Mm00470731_m1
Lipe	Mm00495359_m1
G0s2	Mm00484537_g1

Table 3-1. *qRT-PCR primers*

3.3.10 Immunoblot analysis

Antibodies were obtained from the following sources: PLIN5 (Cat. No. GP31, Progen Biotechnik, GmbH, Heidelberg, Germany) and α-actin (Cat. No. ab3280, Abcam, Cambridge, UK). Conventional immunoblotting procedures were used to detect the target proteins. Mixed quadriceps muscle and heart were homogenized in 100 mM TRIS buffer (pH 7.4) using a tissue lyser (TissueLyser LT, Qiagen, Doncaster, Victoria, Australia). Tissue lysates were cleared by centrifugation at 13,400 g for 10 min and the protein concentration was determined by bicinchoninic acid (BCA) assay (Pierce Kit; Progen Industries, Darra, QLD, Australia). Equal amounts of protein were separated on 4-15% gradient stain free gel (Bio-Rad Laboratories, NSW, Australia) and the proteins were transferred (Trans-Blot Turbo Transfer System, Bio-Rad Laboratories, CA, USA) to polyvinylidene difluoride membranes. The membranes were blocked for 60 min in PBS containing 5% BSA and 5% milk and then probed with primary antibodies (diluted in PBS containing 0.5% BSA and 0.5% milk) overnight. After washing with PBS, membranes were incubated for 1 h with appropriate secondary antibodies (diluted in PBS containing 0.5% BSA and 0.5% milk). Finally, after three 10 min washes in PBS, proteins were visualized by ImageLab software Version 4.1 (ChemiDoc MP) and density quantified using Image Lab software (version 4.1).

3.3.11 Statistical analysis

Data are presented as mean ± SEM. Statistical analysis was performed by one-way or two-way analysis of variance (ANOVA) with repeated measures, and specific differences were located using a Bonferroni post hoc test. Unpaired t-tests were used where appropriate (GraphPad Prism Version 6). Statistical significance was set a priori at $P<0.05$.

3.4 Results

3.4.1 Validation of model

Plin5 mRNA expression was reduced by 70% in skeletal muscle and was completely ablated in the heart of *Plin5^{MKO}* compared with lox/lox mice (Fig. 3-3). PLIN5 protein content was undetectable in both skeletal muscle and the heart of *Plin5^{MKO}* mice (Fig. 3-4). Muscle-specific ablation of *Plin5* was evidenced by similar *Plin5* mRNA expression in other tissues, including the liver and adipose tissue (Fig. 3-3). *Plin5* ablation did not affect the mRNA expression of other PLIN family members (i.e. *Plin2*, *3*, *4*) or regulators of TG metabolism (i.e. *Abdh5*, *G0S2, Lipe*, *Pnpla2*) in muscle or heart (Fig. 3-5 & 3-6).
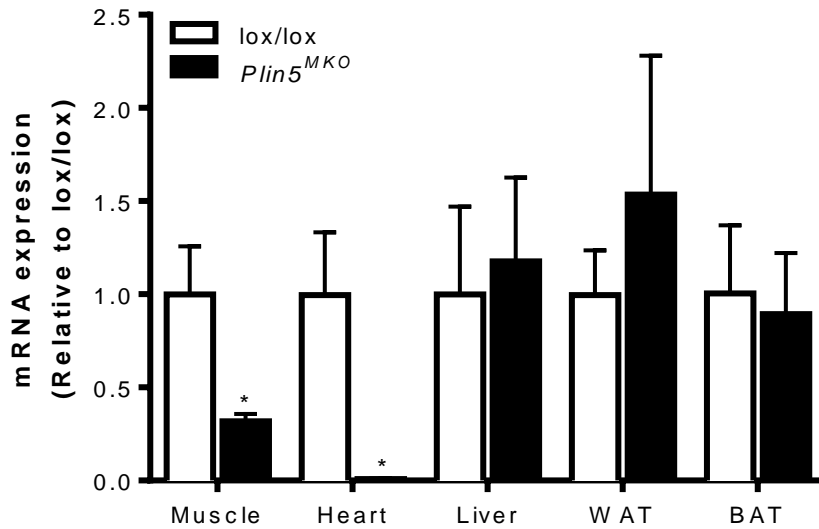
Fig 3-3. *qRT-PCR demonstrating Plin5 mRNA in tissues of lox/lox and Plin5^{MKO} mice. n=12 per genotype for skeletal muscle, n=3 per genotype for other tissues. Values are means ± SEM. *P<0.05 vs lox/lox.*
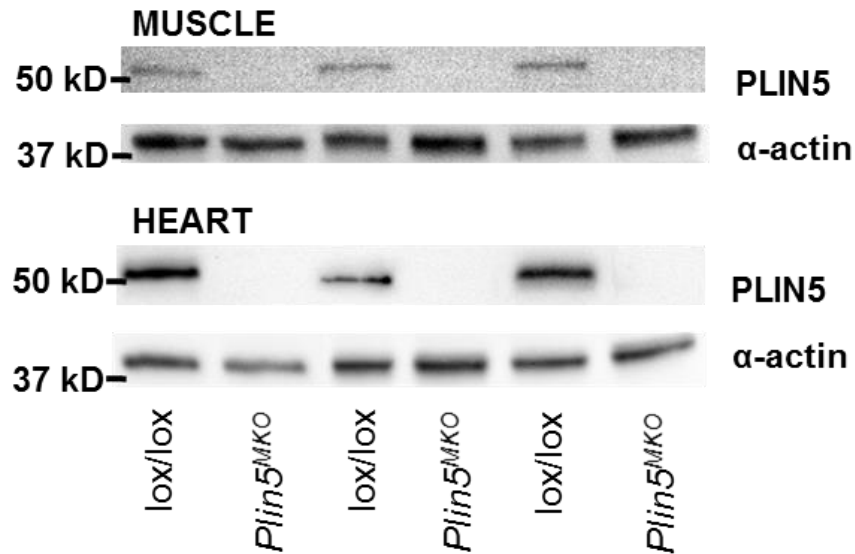
Fig 3-4. *Immunoblot confirming the absence of PLIN5 in the skeletal muscle and heart of Plin5^{MKO} mice.*
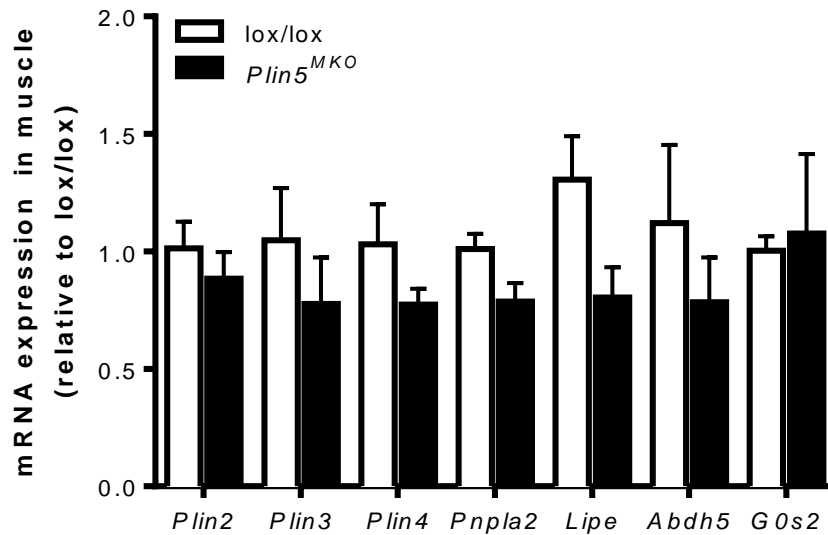
Fig 3-5. *qRT-PCR showing the relative mRNA content of perilipin family members and lipolytic regulators in skeletal muscle. n=3 per genotype for Plin2, Plin3, Plin4, Abdh5, G0s2; n=6 per genotype for Pnpla2 and Lipe. Values are means ± SEM.*
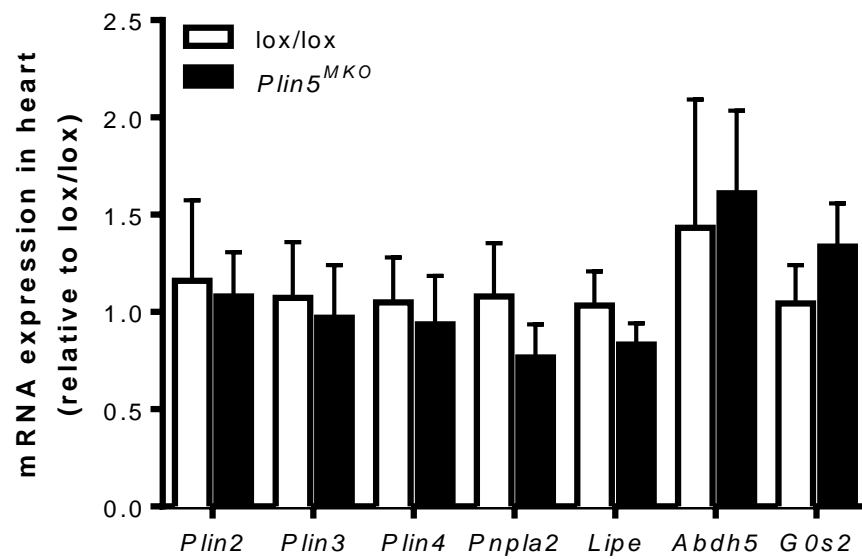
Fig 3-6. *qRT-PCR showing the relative mRNA content of perilipin family members and lipolytic regulators in the heart. n=3 per genotype for each gene. Values are means ± SEM.*

3.4.2 Metabolism in Plin5^{MKO} mice fed a chow diet

Plin$^{lox/lox}$.Cre$^{-/-}$ mice were chosen as the lox/lox littermates in this study because the growth and glucose tolerance of these mice was the same as other control groups (*Plin5$^{+/+}$.Cre$^{+/-}$* and *Plin5$^{+/+}$.Cre$^{-/-}$*, Fig. 3-7A & B). Body mass of lox/lox and *Plin5^{MKO}* mice were not different from birth through to 18 weeks of age (Fig. 3-8). Consistent with this notion, food intake (Fig. 3-9), water intake (Fig. 3-10), oxygen consumption (representing energy expenditure, Fig. 3-11) and daily physical activity (Fig. 3-12) were not different between genotypes. The respiratory exchange ratio (RER) was reduced in *Plin5^{MKO}* compared with lox/lox mice, demonstrating an increase in whole-body fatty acid oxidation in *Plin5^{MKO}* mice (Fig. 3-13). Skeletal muscle is a major energy consuming tissue (264), and we reasoned that increases in muscle fatty acid oxidation were driving this whole-body response. Examination of isolated soleus muscle demonstrated no significant differences in fatty acid uptake, fatty acid oxidation and fatty acid incorporation into intramyocellular TG and DG between genotypes (Fig. 3-14). While we previously reported that whole-body Plin5 deletion results in mild improvements in glucose tolerance in mice(283), there was no significant difference in glucose tolerance between lox/lox and *Plin5^{MKO}* mice (Fig. 3-15). Together, these data demonstrate that *Plin5* ablation in the muscle results in increased whole-body fatty acid oxidation but that this is not due to increased skeletal muscle fatty acid oxidation. Aside from this, there is no prominent change in energy metabolism, body mass regulation or glucose tolerance in *Plin5^{MKO}* mice.
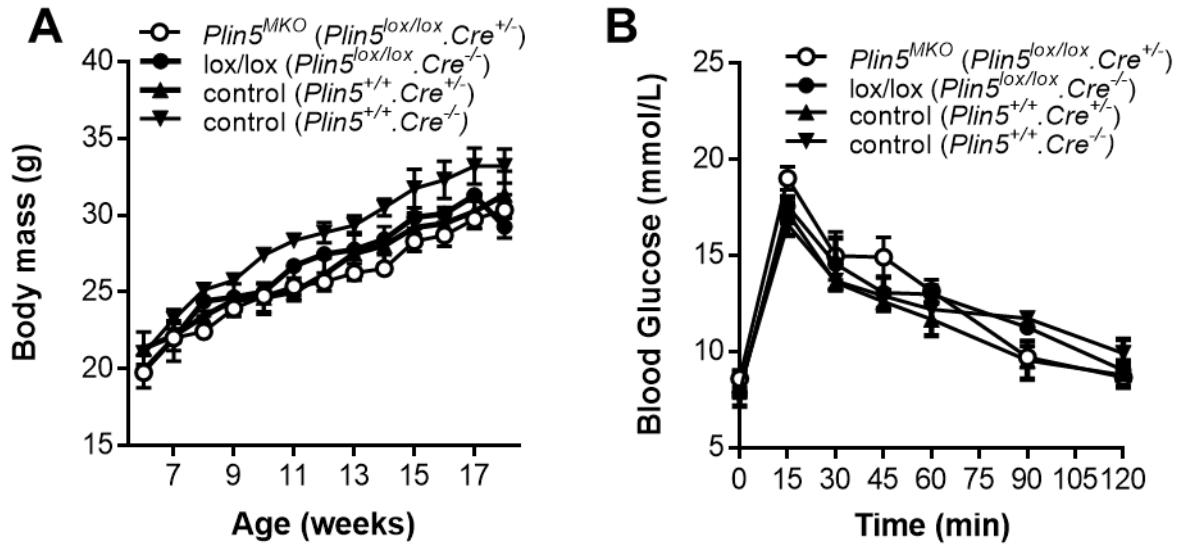
Fig 3-7. *Comparison in (A) growth and (B) glucose tolerance between Plin5^{MKO}, lox/lox and other 2 control mice. Values are means ± SEM.*

Fig 3-8. *Body mass of wild-type (lox/lox) and muscle-specific Plin5 knock-out (Plin5^{MKO}) mice (n = 14 lox/lox, n = 9 Plin5^{MKO}) fed with chow diet.*
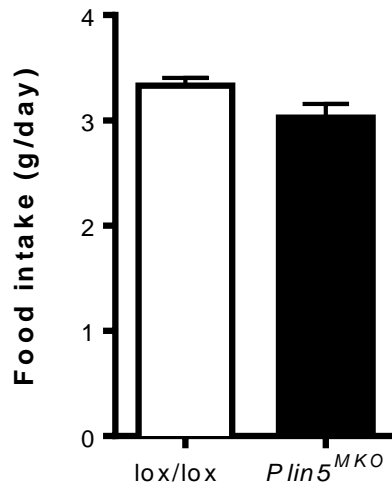
Fig 3-9. *Food intake measurements of chow-fed mice (n = 10 lox/lox, n = 9 Plin5^{MKO}, Age = 14-15 weeks)*
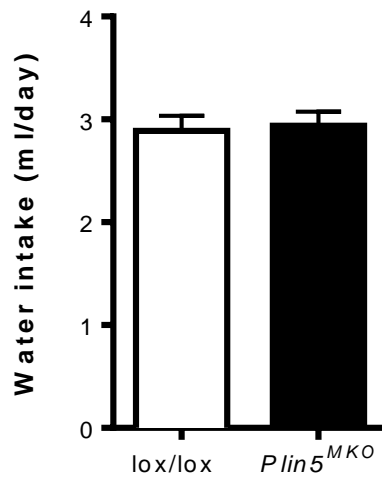
Fig 3-10. *Water intake measurements of chow-fed mice (n = 10 lox/lox, n = 9 Plin5^{MKO}, Age = 14-15 weeks)*
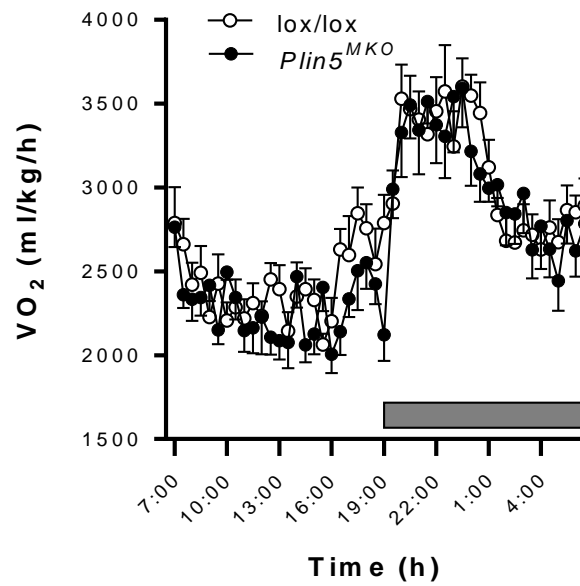
Fig 3-11. *Oxygen consumption (VO₂) was assessed by indirect calorimetry in mice (n = 10 lox/lox, n = 6 Plin5^MKO, Age = 14-15 weeks) fed with chow diet. Shaded area represents dark phase.*
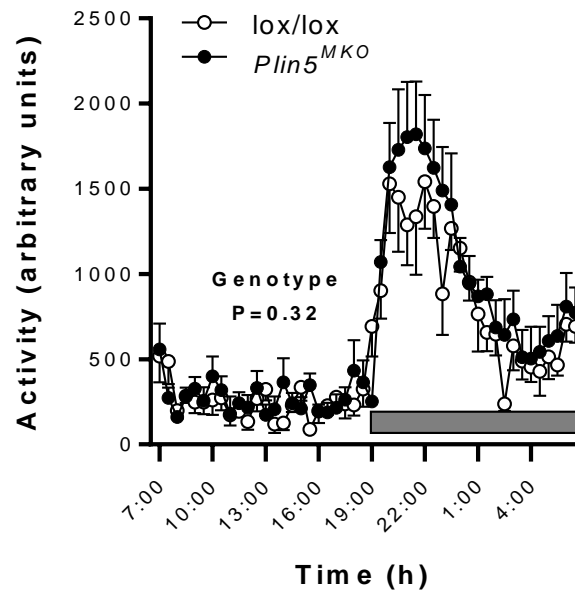
Fig 3-12. *Activity was assessed by indirect calorimetry in mice (n = 10 lox/lox, n = 6 Plin5^{MKO}, Age = 14-15 weeks) fed with chow diet. Shaded area represents dark phase.*
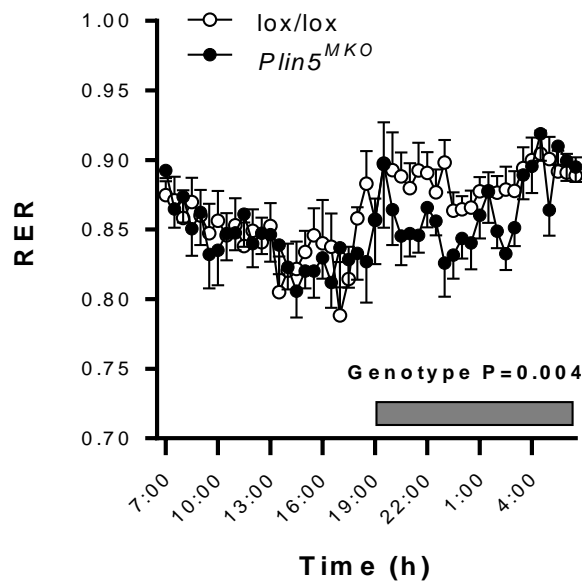
Fig 3-13. *Respiratory exchange rate (RER) was assessed by indirect calorimetry in mice (n = 10 lox/lox, n = 6 Plin5^{MKO}, Age = 14-15 weeks) fed with chow diet. Shaded area represents dark phase.*
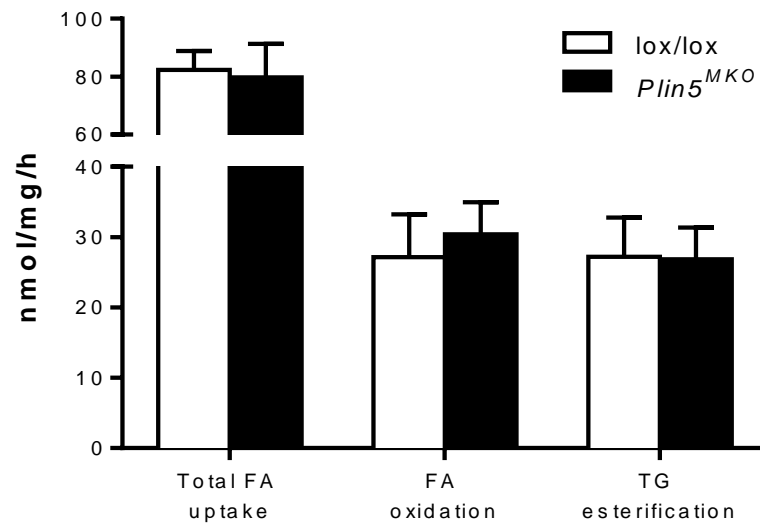
Fig 3-14. *Fatty acid metabolism (fatty acid uptake, fatty acid oxidation and triglyceride esterification) in isolated soleus muscle of chow-fed mice (n = 4 lox/lox, n = 6 Plin5[MKO], Age = 18 weeks)*
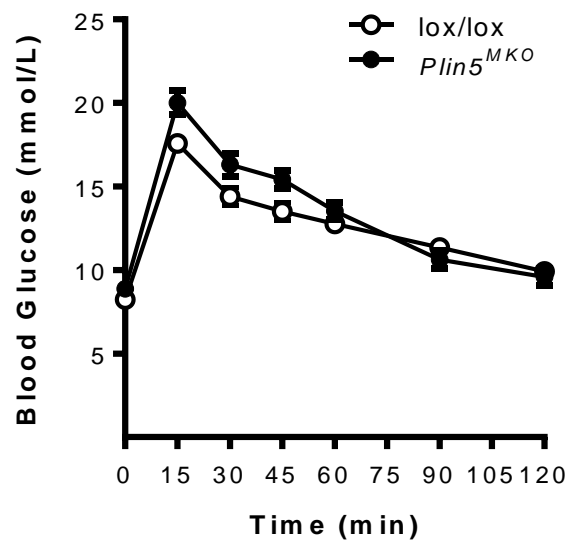
Fig 3-15. *Glucose tolerance test carried out in chow-fed mice (n = 14 lox/lox, n = 16 Plin5[MKO], Age = 12-13 weeks).*

3.4.3 Metabolism in Plin5^{MKO} mice fed a high-fat diet

Because PLIN5 is an important regulator of lipid metabolism (10,224,283), we reasoned that the potential effects of *Plin5* deletion would only become evident when mice were challenged with a lipid stress. Accordingly, lox/lox and *Plin5*^{MKO} mice were fed a diet containing 43% energy from fat for 12 weeks and glucose and lipid metabolism were assessed. The body mass of lox/lox and *Plin5*^{MKO} mice was similar at the commencement of high-fat feeding (i.e. at 6 weeks of age). Body mass gain was greater in lox/lox compared with *Plin5*^{MKO} mice such that lox/lox mice were 11% heavier than *Plin5*^{MKO} mice after 12 weeks of high-fat feeding (Fig. 3-16). Interestingly, there was no change between genotypes in epididymal adipose tissue, heart, liver, kidney or quadriceps skeletal muscle mass when tissues were examined post mortem (Fig. 3-17). Food and water intake was not different between genotypes (Fig. 3-18 & 3-19). Oxygen consumption was not significantly different between genotypes (Fig. 3-20), although it is notable that oxygen consumption was about 9% greater in *Plin5*^{MKO} mice compared with lox/lox mice during the dark phase. Daily physical activity was similarly unaffected by muscle-specific *Plin5* deletion (Fig. 3-21). The RER was markedly decreased in *Plin5*^{MKO} mice, which coincides with a 14% increase in fatty acid oxidation in *Plin5*^{MKO} compared with lox/lox mice (Fig. 3-22). Similar to our observation in chow-fed mice, fatty acid metabolism in isolated soleus muscle was not different between genotypes, with the exception of fatty acid storage into TG, which was decreased in *Plin5*^{MKO} compared with lox/lox mice (Fig. 3-23). Thus, aside from a subtle decrease in body mass, the prominent change in phenotype in *Plin5*^{MKO} is the increase in whole-body FA oxidation, which cannot be accounted for by changes in muscle FA oxidation.
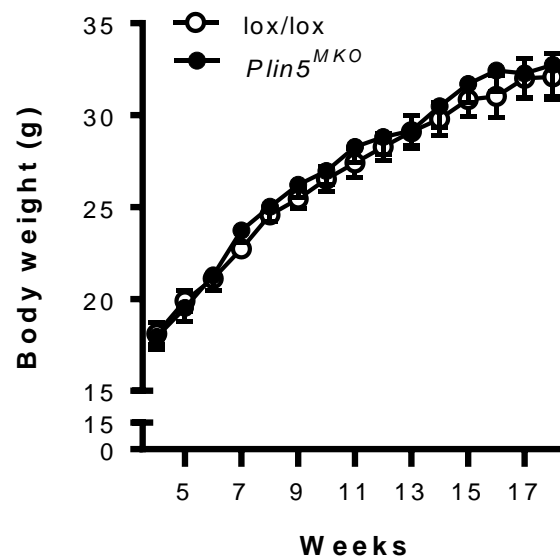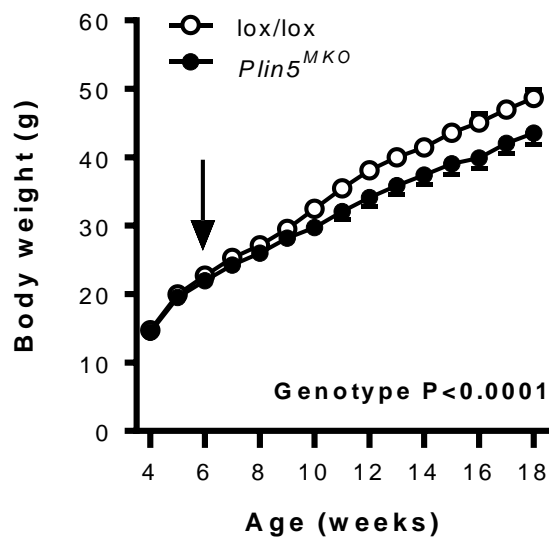
Fig 3-16. *Body mass of control (lox/lox) and muscle-specific Plin5 knock-out (Plin5^{MKO}) mice (n = 16 lox/lox, n = 14 Plin5^{MKO}) fed with high-fat diet.*
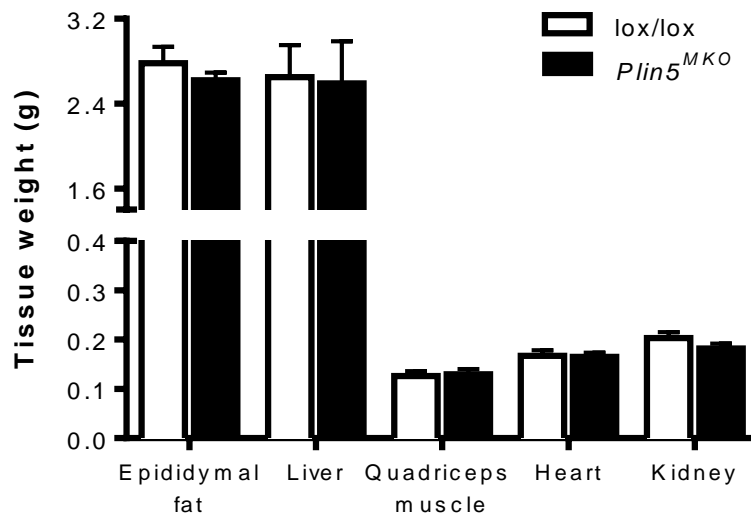

Fig 3-17. *Individual tissue mass analysis in mice (n = 7 lox/lox, n = 5 Plin5^{MKO}, Age = 18 weeks) fed with high-fat diet.*
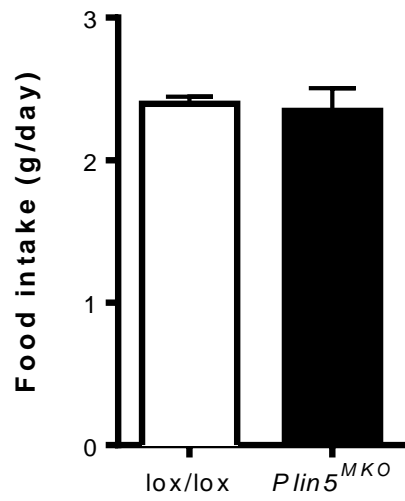
Fig 3-18. *Food intake measurements of high-fat fed mice (n = 5 lox/lox, n = 5 Plin5^{MKO}, Age = 14-15 weeks).*
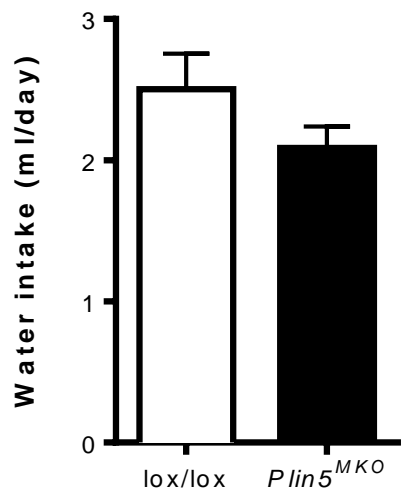
Fig 3-19. *Water intake measurements of high-fat fed mice (n = 5 lox/lox, n = 5 Plin5^{MKO}, Age = 14-15 weeks).*
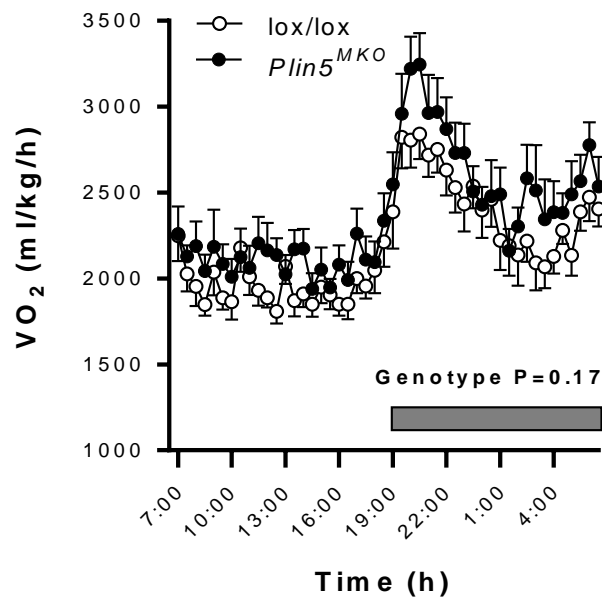
Fig 3-20. *Oxygen consumption (VO$_2$) was assessed by indirect calorimetry in mice (n = 10 lox/lox, n = 8 Plin5^{MKO}, Age = 14-15 weeks) fed with high-fat diet. Shaded area represents dark phase.*
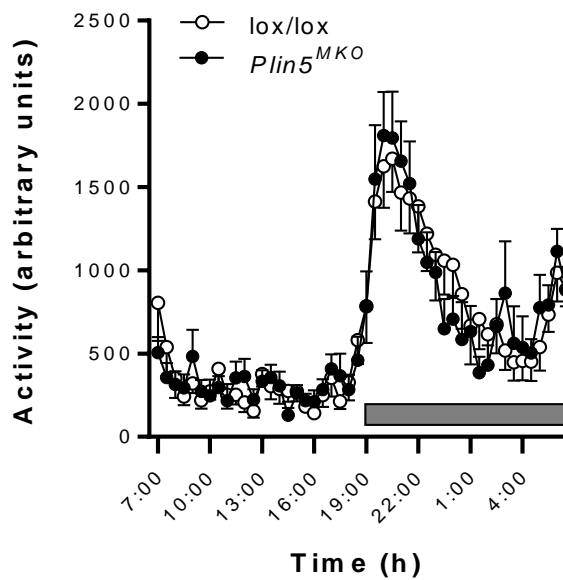

Fig 3-21. *Activity was assessed by indirect calorimetry in mice (n = 10 lox/lox, n = 8 Plin5^{MKO}, Age = 14-15 weeks) fed with high-fat diet. Shaded area represents dark phase.*
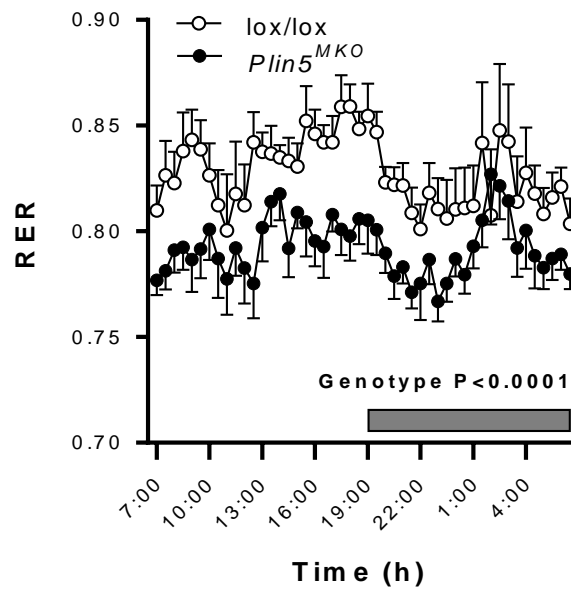
Fig 3-22. *Respiratory exchange ratio (RER) was assessed by indirect calorimetry in mice (n = 10 lox/lox, n = 8 Plin5^{MKO}, Age = 14-15 weeks) fed with high-fat diet. Shaded area represents dark phase.*
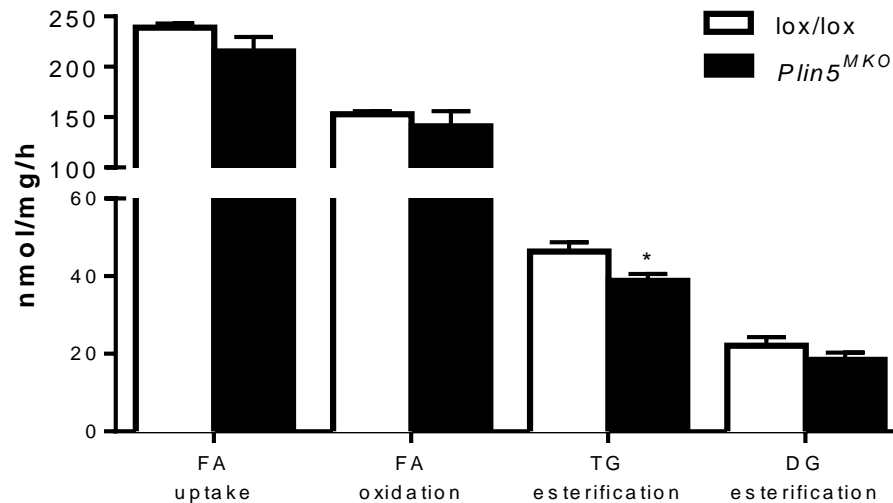
Fig 3-23. *Fatty acid metabolism (fatty acid uptake, fatty acid oxidation, triglyceride and diglyceride esterification) in isolated soleus muscle of high-fat fed mice (n = 6 lox/lox, n = 6 Plin5^{MKO}, Age = 18 weeks). *P<0.05 vs lox/lox.*

3.4.4 Glucose tolerance and insulin action in Plin5^MKO mice fed a high-fat diet

Glucose tolerance was markedly enhanced in *Plin5^MKO* mice compared with lox/lox littermates (Fig. 3-24) and this was not due to differences in plasma insulin before or after glucose administration (Fig. 3-25). We repeated these experiments using stable glucose isotopes (i.e. [6,6]-^{2}H glucose) to determine whether the improvements in glucose tolerance were due to changes in EGP or clearance of the exogenous glucose. EGP was not different between genotypes during the GTT (Fig. 3-26) whereas the clearance of exogenous glucose was increased in *Plin5^MKO* compared with lox/lox mice (Fig. 3-27). The improvement in glucose clearance in *Plin5^MKO* mice was not accompanied by enhanced whole-body insulin action as determined during insulin tolerance tests (Fig. 3-28). Similarly, insulin-stimulated glucose uptake into isolated EDL muscle was not different between genotypes (Fig. 3-29). Together, these data indicate that the marked improvement in glucose tolerance observed with muscle *Plin5* deletion is not attributable to hepatic actions, changes in plasma insulin or muscle-specific insulin action.
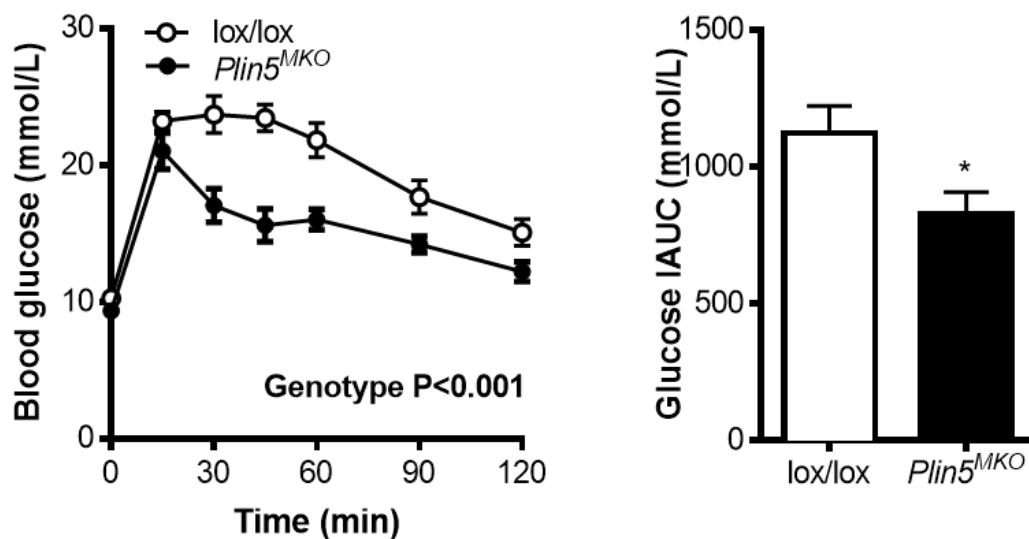
Fig 3-24. *Glucose concentrations and incremental area under the curve (iAUC) responses to an oral glucose tolerance test in wild-type (lox/lox) and muscle-specific Plin5 knock-out (Plin5^MKO) mice (n = 10 lox/lox, n = 8 Plin5^MKO, Age = 12-13 weeks) fed with high-fat diet. *P<0.05 vs lox/lox.*
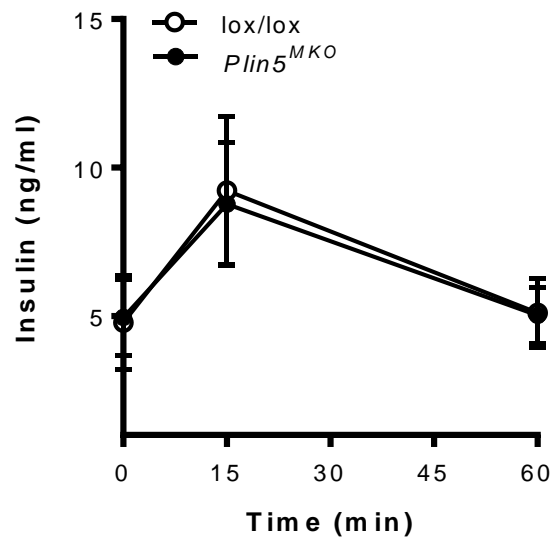
Fig 3-25. *Plasma insulin level responses to an oral glucose tolerance test in wild-type (lox/lox)
and muscle-specific Plin5 knock-out (Plin5^{MKO}) mice (n = 10 lox/lox, n = 8 Plin5^{MKO}, Age = 12-
13 weeks) fed with high-fat diet.*
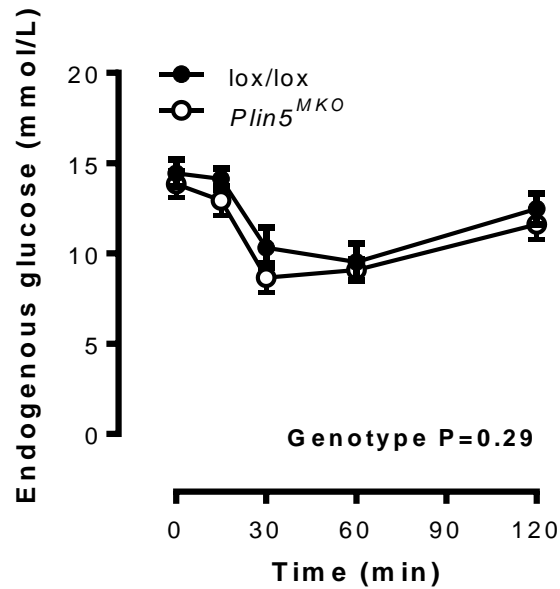
Fig 3-26. *Change in endogenous glucose production (EGP) during OGTT of high-fat fed mice (n
= 10 lox/lox, n = 11 Plin5^{MKO}, Age = 15-16 weeks).*
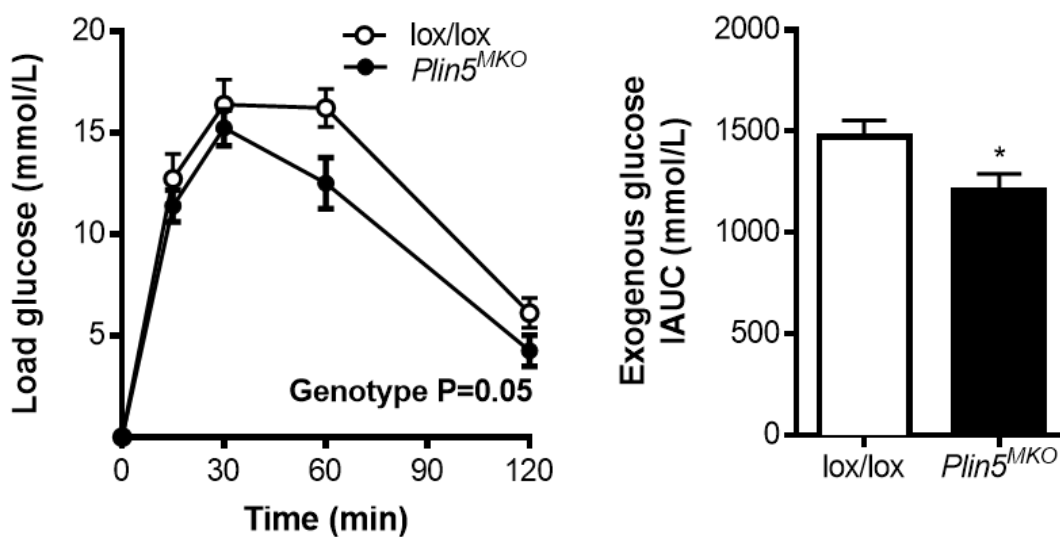
Fig 3-27. *Change in exogenous glucose during OGTT of high-fat fed mice (n = 10 lox/lox, n = 11 Plin5^{MKO}, Age = 15-16 weeks). *P<0.05 vs lox/lox.*
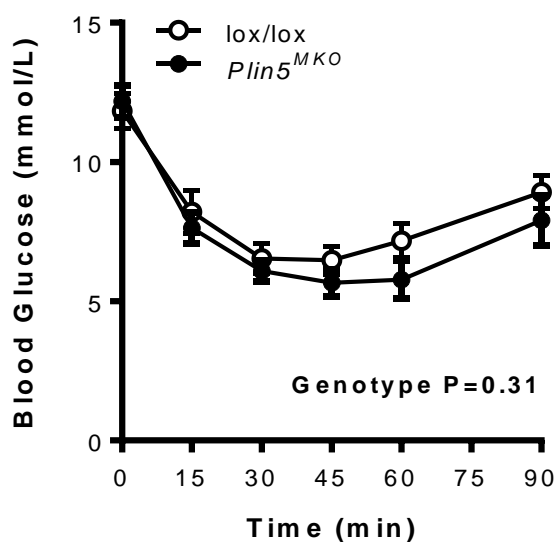
Fig 3-28. *Intraperitoneal insulin tolerance test of high-fat fed mice (n = 13 lox/lox, n = 11 Plin5^{MKO}, Age = 13-14 weeks).*
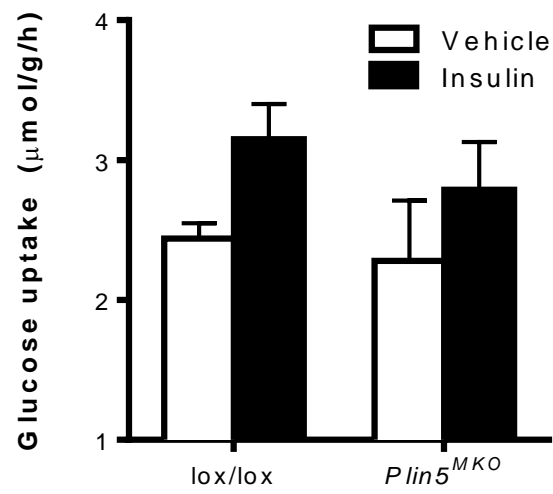
Fig 3-29. *Isolated EDL glucose uptake of high-fat fed mice (n = 3 lox/lox, n = 3 Plin5^{MKO}, Age =*

18 weeks).

3.5   Discussion

PLIN5 is an important regulator of lipid metabolism in oxidative tissues such as skeletal muscle, heart and liver (10,11,222,224,230,231,283) and dysregulation of PLIN5 function has been implicated in the pathogenesis of insulin resistance and obesity-related co-morbidities (224,230,283). In the present study, we created muscle-specific *Plin5* knockout mice to determine the importance of PLIN5 in modulating skeletal muscle lipid metabolism and glycemic control.

It is well documented that the expression of muscle creatine kinase (MCK) is highly restricted to skeletal muscle and heart (287). In this study, we demonstrated that expression of Cre recombinase using the MCK promoter in the *Plin5$^{lox/lox}$* mice mediated recombination and subsequent inactivation of loxP containing *Plin5* gene with ~70% efficiency in skeletal muscle and almost 100% in heart.   The presence of residual *Plin5* gene in the skeletal muscle of *Plin5^{MKO}* mice was not unexpected and is likely due to *Plin5* expression in non-myocyte cell types such as endothelial cells and fibroblasts (288). It is also possible that there was incomplete recombination of the *Plin5* gene due to incomplete deletion of *neo* gene (289); however, this is unlikely because we were unable to detect PLIN5 protein in skeletal muscle in these mice. Thus, we were successful in generating mice with muscle-specific ablation of PLIN5.

PLIN5 is clearly important in the regulation of lipid metabolism and previous studies examining PLIN5 function using whole-body *Plin5$^{-/-}$* mice and indirect calorimetry reported a mild decrease (283) or no change (224) in whole-body fat oxidation. Given that skeletal muscle accounts for ~30% of whole-body energy expenditure (290), we hypothesized that muscle-specific PLIN5 ablation would increase whole-body carbohydrate oxidation. In contrast, *Plin5^{MKO}* mice exhibited a reduction in the RER compared to their lox/lox littermates, demonstrating an increase in whole-body fatty acid oxidation and a concomitant decrease in carbohydrate oxidation. Moreover, this effect was more pronounced in *Plin5^{MKO}* mice fed a HFD, where whole-body fatty acid oxidation was 14% higher than in lox/lox mice. Intriguingly, the increase in fatty acid oxidation *in vivo* was not evident when individual soleus muscles were dissected and studied *ex vivo*. This suggests that the increased fatty acid oxidation measured *in vivo* might be caused by a circulating factor that was eliminated when the muscle was isolated for *ex vivo* study. Such

regulation was evident in mice with muscle-specific overexpression of PLIN5, which resulted in marked increases in FGF-21, increased energy expenditure and metabolic benefits to muscle and liver (284). Disparities between *in vivo* and *in vitro* metabolic outputs have been reported elsewhere. For example, Kienesberger et al. demonstrated that ATGL$^{-/-}$ null mice exhibit whole body and muscle insulin sensitivity when assessed *in vivo*, but reported no change in insulin sensitivity compared with wild-type littermates when assessed *ex vivo* (89). Such regulation highlights the important of integrating cell autonomous signals (i.e. within muscle) with systemic factors to regulate homeostatic systems (291). Alternatively, the increase in whole-body fatty acid oxidation may not be mediated by changes in skeletal muscle fatty acid oxidation, but rather, by other tissues such as the heart, where PLIN5 was also deleted. Although about 70% of the hearts energetic requirements are met by fatty acid β-oxidation (292), the overall contribution of the heart to whole-body substrate oxidation is only 5-10% (264). Therefore, it is unlikely that the increased whole-body fatty acid oxidation in *Plin5^{MKO}* mice *in vivo* is solely mediated by changes in substrate turnover in heart. Further investigation in other tissues (such as BAT and liver) is required to delineate the exact mechanisms at play.

It is well established that *Plin5* gene expression and protein content are increased in the muscle and liver of mice fed a HFD (23,221,230,239,240), perhaps indicating that PLIN5 is increased to prevent lipotoxic stress in these tissues. Consistent with this notion, overexpression of PLIN5 in type II muscle demonstrates a potential protective function on detrimental metabolic consequences induced by high fat feeding, as indicated by lower inflammatory markers in liver and higher expression of browning factors in WAT (284). Furthermore, PLIN5 overexpression in mice fed a HFD were protected against impairments in insulin action despite increased, lipid accumulation in the muscle and liver compared with control littermates (227,293). Our previous studies in whole body *Plin5$^{-/-}$* mice fed a high-fat diet demonstrated no effect of PLIN5 deletion on skeletal muscle insulin action, but marked improvements in glucose tolerance (283). We were unable to ascribe a beneficial role of PLIN5 deletion to skeletal muscle glucose metabolism in this previous study, owing to the potential for glycemic control by other tissues and the possibility of tissue crosstalk in mice with global PLIN5 deletion. Hence, we sought to determine whether PLIN5 is required to protect skeletal muscle from defects in glycemic control induced by high-fat feeding. Here, we show that *Plin5^{MKO}* mice exhibited normal glycemic control when

fed a standard low-fat 'chow' diet. On the other hand, mice fed a HFD were almost completely protected from HFD-induced glucose intolerance, which was due to an increase in exogenous glucose clearance by peripheral tissues and not to changes in EGP (i.e. liver or kidney). Although we previously reported that there was a reduction in muscle glucose uptake during hyperinsulinemic-euglycemic clamp (Chapter 2), we cannot see any changes in insulin-stimulated glucose uptake in isolated EDL muscles *ex vivo*. This may be due to differences in the protocol of insulin stimulation (*in vivo* vs. *ex vivo*) as discussed above. In addition, the absence of detectable changes in whole-body insulin action suggests that non-insulin stimulated glucose clearance is increased in *Plin5^{MKO}* mice (294). Understanding the mechanistic basis for this observation will be the focus of future investigations.

The *Plin5^{MKO}* mice also showed a mild attenuation in weight gain compared to their lox/lox littermates when fed a HFD, although we observed no pronounced difference in the mass of lean tissues and adipose tissue assessed post mortem. The small change in body mass was associated with a subtle increase in whole-body energy expenditure in the *Plin5^{MKO}* mice, although this did not reach statistical significance. Notably, there was no change in food and water intake. While fatty acid oxidation was increased in the *Plin5^{MKO}* mice and others have speculated that an increase in whole-body fatty acid oxidation can drive a 'lean phenotype' (295,296), this is simplistic and the basic laws of bioenergetics do not support the interpretation. Indeed, previous data in ACC2$^{-/-}$ mice shows that increasing fatty acid oxidation does not increase energy expenditure or body mass gain (275), highlighting that negative energy balance is requisite for weight loss. Thus, we conclude that the mild increase in energy expenditure, irrespective of changes in substrate partitioning, is most likely responsible for the subtle reduction in weight gain in the *Plin5^{MKO}* mice. The significance of this finding is especially intriguing given that PLIN5 over expression in skeletal muscle results in similar phenotypic traits; that is, increased energy expenditure and resistance to weight gain (284). Just how deletion and over expression of the same protein induce the same responses is presently unresolved.

In conclusion, the results of this study shows that skeletal muscle PLIN5 deletion enhances whole-body fatty acid oxidation and protects against disturbances of glucose homeostasis in the setting of high-fat feeding. The mismatch between the *in vivo* and *ex vivo* studies of fatty acid

oxidation indicate that PLIN5 ablation may alter endocrine signalling to modulate whole body metabolism. Further studies are required to fully understand how PLIN5 ablation alters metabolism in muscle.

Declaration for Thesis Chapter 4

Monash University

Declaration by candidate

In the case of Chapter 4, the nature and extent of my contribution to the work was the following:

Nature of contribution	Extent of contribution (%)
Experimental design, performed tissue collection, biochemical analysis and immunohistochemistry, performed data analysis, wrote and edited the manuscript	85

The following co-authors contributed to the work. If co-authors are students at Monash University, the extent of their contribution in percentage terms must be stated:

Name	Nature of contribution	Extent of contribution (%) for student co-authors only
Magda Montgomery	Assisted with experimental work and editing of manuscript	NA
Robyn Murphy	Assisted with experimental design and work	NA
Matthew Watt	Assisted with experimental design and work, provided intellectual input and editing of manuscript	NA

The undersigned hereby certify that the above declaration correctly reflects the nature and extent of the candidate's and co-authors' contributions to this work*.

Candidate's Signature		Date 09/09/2016

Main Supervisor's Signature	_Matthew Watt_	Date 09/09/2016

CHAPTER 4

Perilipin 5 is dispensable for normal substrate metabolism and in the adaptation of skeletal muscle to exercise training

4.1　Introduction

Cytosolic lipid droplets store vast quantities of TGs and are thereby important energy depots in most tissues, including high energy consuming tissues such as the liver, heart and skeletal muscle. LDs are a central reservoir for fatty acid trafficking, and at least in skeletal muscle, most of the fatty acids that enter the myocyte are first stored as TG within the LD before being hydrolyzed and released into the cytoplasm for oxidation or incorporation into other lipid pools (60,61,297). Such regulation serves the major purposes of supplying fatty acid substrate to match the energetic demands of the tissue and to provide a reservoir for lipid storage, which protects the myocyte from lipotoxic stress and cell death under conditions of excessive lipid flux.

LDs are coated by a multitude of proteins (298) that work in a coordinated manner to regulate cellular processes including protein degradation, membrane trafficking, cholesterol homeostasis, and most prominently, lipid storage and mobilization (98,299). Pioneering work over the last decade has identified the key proteins involved in regulating lipolysis, including the critical lipase adipose triglyceride lipase (ATGL) (73), the ATGL co-activator comparative gene identification-58 (CGI-58) (77) and the ATGL suppressor G0/G1 Switch 2 (G0S2) (78). The perilipin (PLIN) family of proteins are also localized to the LD and are thought to be key regulators of lipid metabolism by coordinating the trafficking and the reversible interactions of the major lipolytic proteins. PLIN5 is highly expressed in oxidative tissues such as skeletal muscle and heart (10) and regulates lipid metabolism, particularly during fasting (224,283). PLIN5 interacts with ATGL and CGI-58 to suppress TG breakdown (12,13,300), which limits the production of bioactive lipid metabolites and cellular stress signals, and thereby prevents tissue dysfunction including age-associated declines in heart function (224), muscle insulin resistance (235) liver injury (230) and pancreatic ß-cell function (233).

Aside from its role in TG metabolism, PLIN5 is postulated to be involved in the adaptive response to exercise training. PLIN5 protein content is increased in response to both acute exercise and chronic training (229), and cross-sectional studies report marked upregulation of PLIN5 in endurance-trained athletes compared with sedentary individuals (114). In addition, PLIN5 is localized to the mitochondria (83,226) and appears to remodel the spatial relationship between LDs and the mitochondria, and thereby facilitate enhanced contact between these

organelles (61,301). Together, these adaptive responses would be predicted to enhance mitochondrial capacity and facilitate efficient fatty acid oxidation. Arguing against this interpretation is the converse findings that PLIN5 muscle-specific overexpression (284) or whole-body *Plin5* deletion (224,283) does not impact skeletal muscle mitochondrial capacity and function, or exercise tolerance compared with wild-type mice. A limitation of these latter studies, however, is that mice were examined in the sedentary state and the importance of PLIN5 in facilitating an adaptive response may only become apparent in the context of exercise training, which presents a major metabolic challenge and generates a complex array of molecular signals to drive mitochondrial adaptation and improved exercise performance (302).

4.2　Aims

The overarching aim of this study was to examine the role of PLIN5 in exercise metabolism and adaptation to exercise training. The specific aims of this study were:

(1) To examine the role of PLIN5 in the regulation of skeletal muscle substrate metabolism during acute exercise

(2) To determine whether PLIN5 is required for the molecular and metabolic adaptations and enhancement in exercise tolerance following endurance exercise training.

4.3　Materials and Methods

The following section describes materials and methods used for chapter 4. Additional or variation of material and methods used in other chapters will be contained within their respective sections.

4.3.1　Mouse generation

The procedures were approved by the Monash University Animal Ethics Committee. Male lox/lox and *Plin5^{MKO}* litter mates were used for all experiments. All procedures of mouse generation were explained in Chapter 3 section 3.3.1.

4.3.2   Experimental design

Mice were housed at 22 °C on a 12:12-h light dark cycle. Mice were fed regular rodent chow (5% total fat, 60% carbohydrate and 20% protein, Specialty Feeds, WA, Australia) and had free access to water. Mice were fasted for 4 h before all experiments.

4.3.2.1   Acute exercise study

Mice were subjected to a 3-day familiarization protocol that consisted of progressively increasing the intensity and duration of treadmill running on an enclosed treadmill (Modular Treadmill 0184-003L, Columbus Instruments, Columbus, OH) before experimental testing. The experimental trial consisted of running at 10 m/min (5% grade) for 40 min in an enclosed treadmill attached to an Oxymax open-circuit calorimeter (Columbus Instruments, 7560 Oxymax Equal Flow Sixteen Chamber System). Expired gases were collected continuously and oxygen uptake (VO_2) and carbon dioxide production (VCO_2) were calculated. RER was calculated as VCO_2/VO_2. At the conclusion of the experiment, mice were rapidly removed from the enclosed treadmill and killed by cervical dislocation. Trunk blood was collected into tubes containing EDTA and tissues were dissected and frozen in liquid nitrogen within 3 min.

4.3.2.2   Exercise training study

Mice were subjected to the 3-day familiarization protocol described above (Eco 3/6 treadmill; Columbus Instruments, Columbus, OH) before experimental testing. To determine maximal running velocity, mice ran at 10 m/min at a 5% grade for 2 min. The treadmill velocity was increased by 2 m/min every 2 min until fatigue. This was defined as spending ≥10 s at the base of the treadmill despite manual encouragement. Two days later, endurance capacity was assessed by running mice at 16 m/min at a 5% grade until they reached fatigue. The exercise tolerance experiments were performed by an investigator who was blinded to the genotype of the mice. All mice undertook six weeks of endurance exercise training on a treadmill as described previously (90). Maximal running velocity and endurance capacity were again assessed in the last week of training, with 24 h recovery between tests. Forty-eight h after the last training session, mice ran on the treadmill at 16 m/min for 60 min (5% grade) before tissues were collected as described for the acute exercise study. The relative exercise intensity attained in the pre- and post-training metabolic trials was similar, equating to ~53% and ~45% workload maximum, respectively.

4.3.3 Assessment of cellular respiration

After euthanasia, *extensor digitorum longus (EDL)* muscles were harvested from 16-week-old male mice. Single muscle fibers were mechanically isolated from the muscle as previously described (301) and placed in collagen/matrigel pre-coated Seahorse XF24 cell culture V7 microplates (Seahorse Bioscience, Billerica, MA). The muscle fibers were placed in an incubator at 37 °C for 60 min in culture media before experiments. All experiments were performed using an XF24 Extracellular Flux Analyzer (Seahorse Bioscience) according to previously described methods with slight modifications (303). After calibration of the XF24 Extracellular Flux Analyzer, the microplate containing the lox/lox and *Plin5^{MKO}* muscle fibers (in bindles of 5-10) were placed in the analyzer. Basal oxygen consumption rate (OCR; pmol/min) was determined in prewarmed Seahorse XF assay medium (Seahorse Bioscience, Billerica, MA) at ~37 °C (pH 7.4) supplemented with 25 mM glucose and 1 mM pyruvate. Seahorse injection ports were loaded with malate, glutamate and succinate at a final concentration 5.0, 1.0 and 5.0 mM, respectively. It was then followed by the addition of adenosine diphospate (ADP) at final concentration of 5.0 mM to stimulate maximal respiration. The SeaHorse XF24 Extracellular Analyzer was run using 8 min cyclic protocol commands (mix for 3 min, stand for 2 min and measure for 3 min) in triplicate as previously described (235). OCR rates were normalized to NADH:ubiquinone oxidoreductase subunit A9 (FA9) protein content in muscle, as a marker of mitochondrial abundance, which was determined by immunoblot analysis.

4.3.4 Tissue metabolites

Tissues were extracted in chloroform:methanol (2:1 vol/vol) and the phases separated with 4 mM MgCl$_2$ as previously described (64). Quadriceps muscle and heart TG content was determined using a colorimetric assay kit (Triglycerides GPO-PAP, Roche Diagnostics). Tissue glycogen content was determined as glucose residues after hydrolysis of the muscle sample in 1M HCl at 100 °C for 2 hours and expressed per wet weight tissue (304).

4.3.5 Blood metabolites

Plasma was separated by centrifugation at 3000 x *g* for 10 min at 4 °C. Plasma glucose was measured with a glucometer (Accu-Check, Roche, NSW, Australia). Plasma FFA was measured spectrophotometrically by an enzymatic colorimetric assay (NEFA C Kit;Wako Chemicals, Richmond, VA, USA). Plasma TG levels were determined biochemically from plasma using a colorimetric assay kit (Triglycerides GPOPAP; Roche Diagnostics, Indianapolis, IN). Commercial kits were used for the assessment of β-hydroxybutyrate and lactate (Sigma-Aldrich, St. Louis, MO, USA). Plasma glycerol content was determined spectrophotometrically employing a colorimetric enzymatic assay (Free Glycerol Reagent, Sigma-Aldrich, St. Louis, MO, USA) and quantified against a glycerol standard.

4.3.6 MtDNA

Total DNA was isolated from quadriceps muscle and heart tissue using a conventional phenol-chloroform method. The DNA pellet was resuspended in distilled water and the isolated DNA was then used to determine the ratio between mtDNA and nuclear DNA (nDNA) content by real-time PCR. The mtDNA (represented by *Cox1*) and nDNA (represented by *Cytc*) contents were determined by real-time RT PCR (ep realplex Mastercycler, Eppendorf, Hamburg, Germany) using SYBR Green PCR Master Mix (Brilliant II SYBR® Green QPCR Master Mix, *Agilent Technologies*, Santa Clara, CA, USA). The sequences used to amplify a fragment of COXI were For 5′-TGCAACCCTACACGGAGGTAATA-3′, Rev 5′-ATGTATCGTGAAGCACGATGTCA-3′ and to amplify a fragment of Cyt c were For 5′-TGCCCAGTGCCACACTGT-3′, Rev 5′-CTGTCTTCCGCCCGAACA-3′. The obtained cycle threshold (Ct) values reflecting the initial content of the specific transcript in the samples were converted to an arbitrary amount by using standard curves obtained from serial dilution of a pooled sample made from all samples. The DNA results are presented as mtDNA normalized to nDNA content (mtDNA/nDNA).

4.3.7 Immunoblot analysis

Antibodies were obtained from the following sources: OXPHOS (Cat. No. MS604, MitoSciences, Eugene, OR, USA). Immunoblot analysis was performed as described previously in Chapter 2 section 2.3.12. Stain-free images were collected after transfer for loading control (ChemiDoc MP and ImageLab software Version 4.1, Biorad Laboratories, NSW, Australia).

4.3.8 Enzyme activity assays

Citrate synthase (CS) activity was determined using established methods expressed per wet weight tissue (304). Briefly, the activity was measured in a reaction mixture containing 100 mmol/l Tris-HCl, 1 mmol/l $MgCl_2$, 1 mmol/l EDTA, 0.2 mmol/l dithio-bis(2-nitrobenzoic acid), 0.3 mmol/l acetyl CoA, and 0.5 mmol/l oxaloacetate (omitted for control), pH 8.2. The rate of change in absorbance was monitored at 412 nm.

4.3.9 Statistical analysis

Statistical analysis was performed using unpaired Student's t-tests or two-way analysis of variance (ANOVA) where appropriate. Individual means were compared using a Bonferroni post hoc analysis when required. Statistical significance was set *a priori* at $P \leq 0.05$. Data are reported as means ± SEM.

4.4   Results

4.4.1   Exercise tolerance in Plin5^MKO mice

Plin5^MKO mice exhibited normal growth (Fig. 4-1) and their body composition was not different from control (lox/lox) mice at 10 weeks of age (Fig. 4-2). To determine whether *Plin5* deletion in muscles impacts exercise capacity, mice underwent two exercise tolerance tests, an incremental test to volitional exhaustion (i.e. similar to VO_2 max test) and an endurance-running test performed at a pre-determined sub-maximal workload. Exercise performance in both tests was not different between *Plin5^MKO* and lox/lox mice (Fig. 4-3 & 4-4).
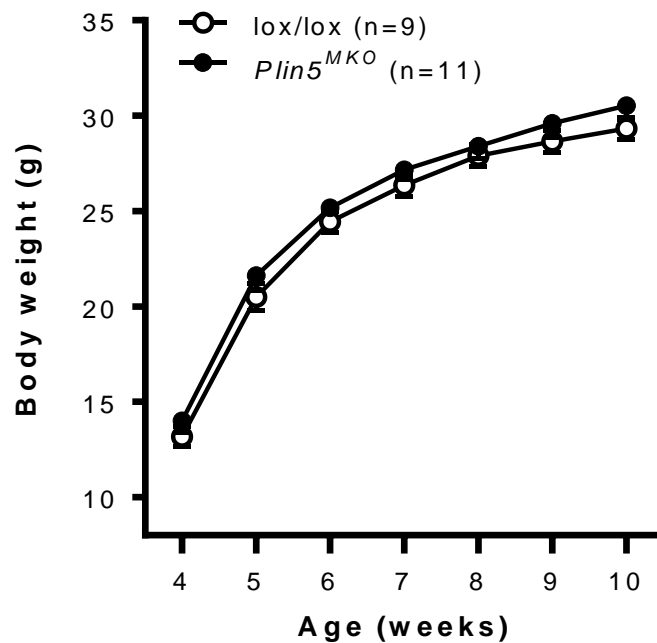
Fig 4-1. *Body mass of control (lox/lox) and muscle-specific Plin5 knock-out (Plin5^MKO) mice.*
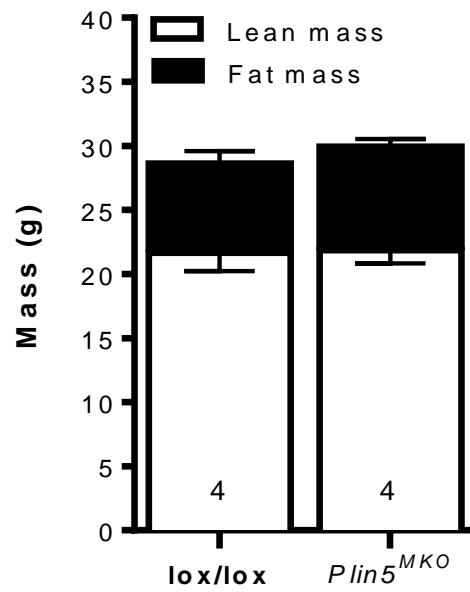
Fig 4-2. *Lean and fat mass was determined in 10 week old mice by DEXA analysis. Values are means ± SEM. The numbers in the respective columns denotes n for each experiment.*
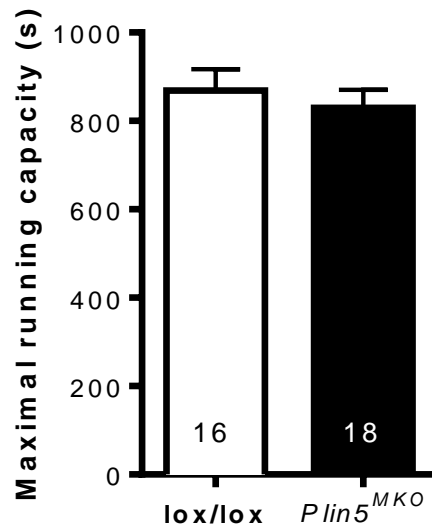
Fig 4-3. *Maximal running capacity as determined by an incremental running test to volitional exhaustion. Values are means ± SEM. The numbers in the respective columns denotes n for each experiment.*
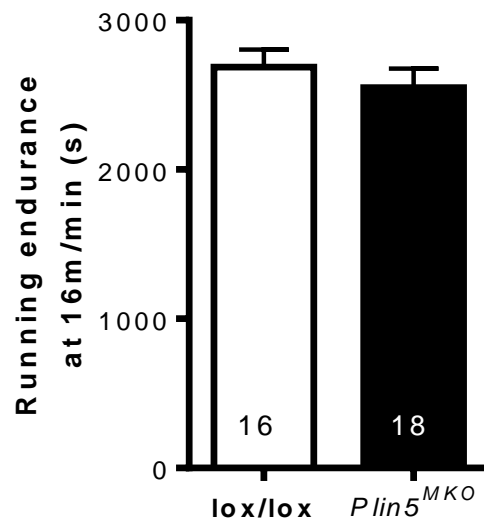
Fig 4-4. *Running endurance capacity as determined by time to volitional exhaustion when running at a constant submaximal workload. Values are means ± SEM. The numbers in the respective columns denotes n for each experiment.*

4.4.2 Metabolism in Plin5^{MKO} mice during moderate intensity exercise

In light of previous studies demonstrating an important role for PLIN5 in modulating muscle TG metabolism (235,236) and the reciprocal relationship between carbohydrate and fatty acid oxidation, we next assessed whole-body substrate metabolism and tissue metabolites before and after acute, moderate intensity exercise. Oxygen uptake was not different between *Plin5^{MKO}* mice compared with lox/lox mice (previously shown in Fig. 3-11). The RER was increased from rest during exercise in both groups, and there was no effect of *Plin5* deletion on RER (genotype, P = 0.17), indicating no change in whole body substrate partitioning at rest or during exercise (Fig. 4-5). Skeletal muscle TG content was not different between genotypes before exercise and was decreased after exercise in both lox/lox and *Plin5^{MKO}* mice (Fig. 4-6). The decrease in skeletal muscle TG was not different between genotypes. Heart TG content was reduced by 40% in *Plin5^{MKO}* compared with lox/lox mice, and similar to the exercise-induced changes in skeletal muscle, the heart TG content was significantly reduced in both genotypes after exercise (Fig. 4-7). The pre-exercise glycogen content was not different in skeletal muscle, heart or liver (Fig. 4-8, 4-9 & 4-10), and while exercise reduced glycogen content in these tissues, there was no difference between lox/lox and *Plin5^{MKO}* mice (Fig. 4-6). We also assessed plasma glucose, plasma TGs, plasma FFA and plasma ß-hydroxybutyrate and these were not significantly different between genotypes before or after acute exercise (Table 4-1). Similarly, plasma lactate was not different between genotypes after exercise (Table 4-1). Together, these data indicate that PLIN5 deletion in muscle and heart has limited effects on substrate metabolism during acute sub-maximal exercise in sedentary mice.
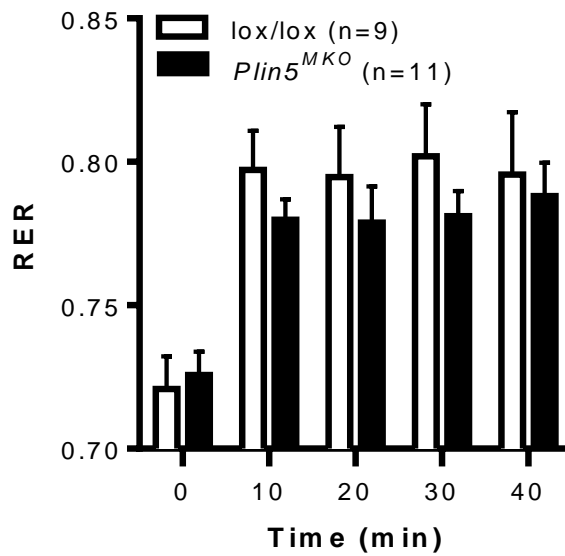
Fig. 4-5. *The respiratory exchange ratio (RER) was assessed at rest and during exercise in untrained mice.*
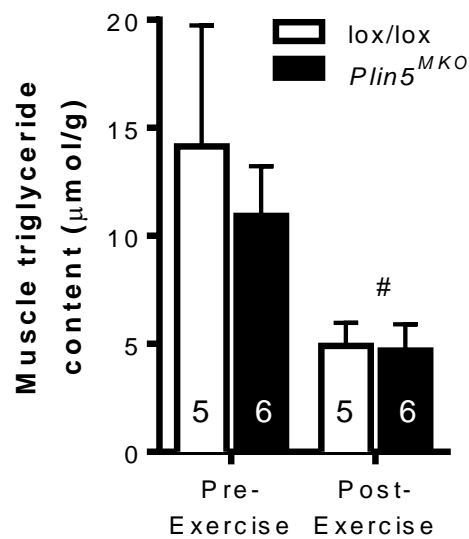
Fig 4-6. *Muscle triglyceride content before and after exercise in untrained mice. Mice remained in their cages (denoted as Pre-Exercise) or completed 40 min of treadmill running at 10 m/min (5% grade) (denoted as Post-Exercise). Values are means ± SEM. #P<0.05, main effect for exercise. The numbers in the respective columns denotes n for each experiment.*
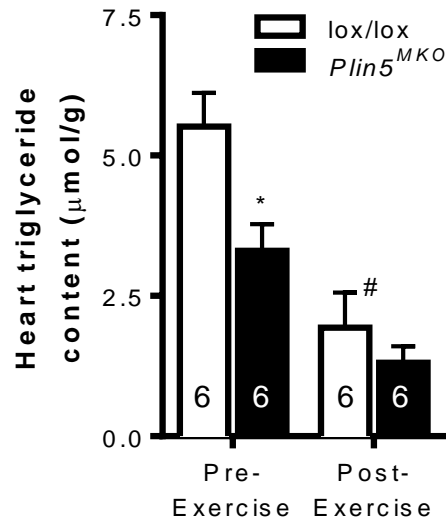
Fig 4-7. *Heart triglyceride content before and after exercise in untrained mice. Values are means ± SEM. *P<0.05, main effect for genotype. #P<0.05, main effect for exercise. The numbers in the respective columns denotes n for each experiment.*

Fig 4-8. *Muscle glycogen content before and after exercise in untrained mice. Values are means ± SEM. #P<0.05, main effect for exercise. The numbers in the respective columns denotes n for each experiment.*

Fig 4-9. *Heart glycogen content before and after exercise in untrained mice. Values are means ± SEM. #P<0.05, main effect for exercise. The numbers in the respective columns denotes n for each experiment.*

Fig 4-10. *Liver glycogen content before and after exercise in untrained mice. Values are means ± SEM. #P<0.05, main effect for exercise. The numbers in the respective columns denotes n for each experiment.*

Sedentary mice				
Variable	**lox/lox**		*Plin5^{MKO}*	
	Pre	Post	Pre	Post
Blood glucose (mM)	9.3 ± 1.0 (9)	11.1 ± 1.3 (9)	9.4 ± 0.7 (11)	11.4 ± 1.5 (11)
Plasma FFA (mM)	1.04 ± 0.06 (9)	0.86 ± 0.13 (9)	0.98 ± 0.05 (11)	0.80 ± 0.09 (11)
Plasma triglycerides (mM)	0.25 ± 0.03 (9)	0.25 ± 0.02 (9)	0.29 ± 0.04 (11)	0.26 ± 0.02 (11)
Plasma ß-hydroxybutyrate (μM)	50 ± 10 (9)	102 ± 6 (9)	44 ± 6 (7)	90 ± 6 (11)
Plasma lactate (mM)	ND	2.5 ± 0.2 (8)	ND	2.5 ± 0.2 (11)

Table 4-1. *Effects of muscle-specific Plin5 deletion on plasma metabolites before and after submaximal running in untrained mice. FFA, free fatty acid. ND, not determined. Values are means ± SEM. n for each measurement is denoted in parenthesis.*

4.4.3 Exercise training study

It has been suggested that PLIN5 may be important for the molecular adaptations to exercise training (83,305). Accordingly, we investigated exercise performance, mitochondrial content and function and substrate metabolism in $Plin5^{MKO}$ and lox/lox mice after six weeks of endurance exercise training. Body mass increased over the duration of the exercise-training period (P<0.0001, main effect time) and there was no differences between lox/lox and $Plin5^{MKO}$ mice (Fig. 4-11). Consistent with these findings, terminal tissue masses (lean and fat) were not different between genotypes (Fig. 4-12). The integrated functional adaptation to exercise training was examined by assessing exercise capacity in mice. Endurance exercise training increased maximal running velocity and endurance running capacity in lox/lox mice by 61% and 310%, respectively, and by 36% and 288% in $Plin5^{MKO}$ mice. Thus, $Plin5^{MKO}$ mice exhibited impaired exercise performance compared with lox/lox mice, with a 20% reduction in the time to exhaustion during an incremental run to fatigue (Fig. 4-13) and a 15% reduction in running time to exhaustion at a set submaximal workload (Fig. 4-14).
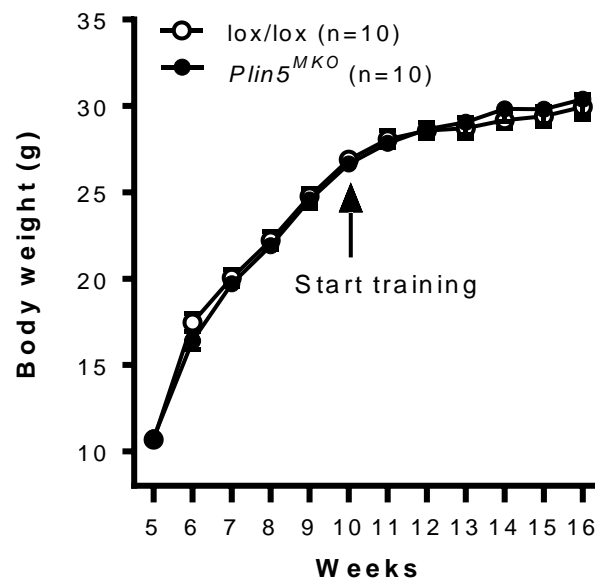
Fig. 4-11. *Body mass of lox/lox and Plin5^{MKO} mice. Mice underwent 6 weeks endurance exercise-training program at aged 10 weeks.*
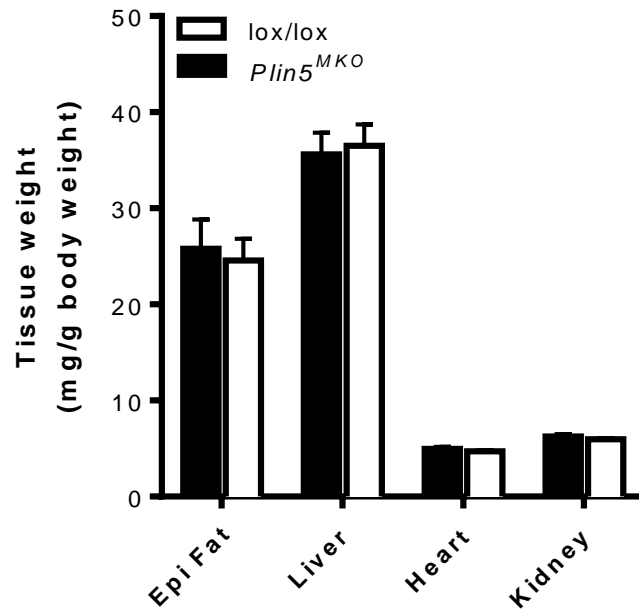
Fig 4-12. *Tissues from 18 week old mice were dissected and weighed. All mice underwent 6 weeks endurance exercise-training program at aged 10 weeks. Epididymal fat; n=10 for lox/lox, n=10 for Plin5^{MKO}. For all other tissues; n=4 for lox/lox, n=4 for Plin5^{MKO}.*
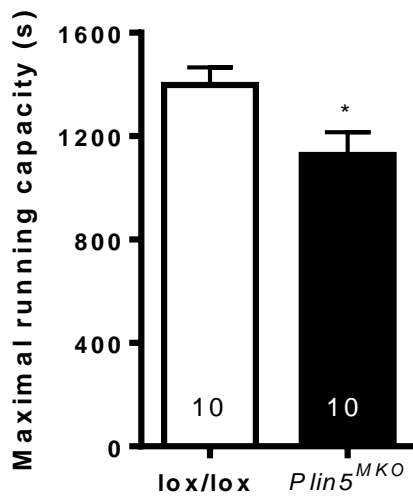
Fig 4-13. *Maximal running capacity as determined by an incremental running test to volitional exhaustion in exercise trained mice. Values are means ± SEM. *P<0.05, main effect for genotype. The numbers in the respective columns denotes n for each experiment.*
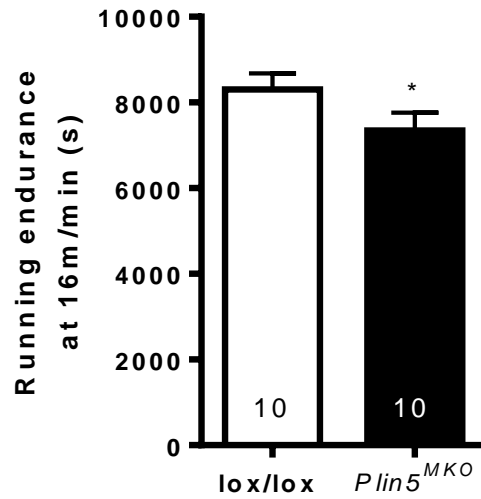
Fig 4-14. *Running endurance capacity as determined by time to volitional exhaustion when running at a constant submaximal workload in exercise trained mice. Values are means ± SEM. $^{*}P<0.05$, main effect for genotype. The numbers in the respective columns denotes n for each experiment.*

We next tested whether the reduced exercise capacity in $Plin5^{MKO}$ mice was associated with alterations in substrate metabolism. Neither skeletal muscle, heart nor liver glycogen content was different between genotypes at the onset of exercise (Fig. 4-15, 4-16 & 4-17). Glycogen content was decreased in all tissues after exercise ($P<0.05$, main effect for time) and there was no difference between genotypes for glycogen content in any tissue assessed after exercise (Fig. 4-15, 4-16 & 4-17). Skeletal muscle TG content was not different between lox/lox and $Plin5^{MKO}$ mice at rest and tended ($P=0.06$, main effect for time) to be increased in both genotypes at the cessation of exercise (Fig. 4-18). Heart TG content was decreased by 60% in $Plin5^{MKO}$ mice compared with lox/lox mice ($P<0.05$, main effect for genotype) and was not significantly altered after an acute exercise bout (Fig. 4-19). Plasma glucose, FFA, TGs, glycerol and lactate was not different between genotypes at rest or at the cessation of exercise (Table 4-2). Interestingly, ß-hydroxybutyrate was lower in $Plin5^{MKO}$ mice compared with lox/lox mice (Table 4-2). Overall, these data demonstrate that substrate metabolism during moderate intensity exercise is similar in lox/lox and $Plin5^{MKO}$ mice after the completion of an exercise training program.
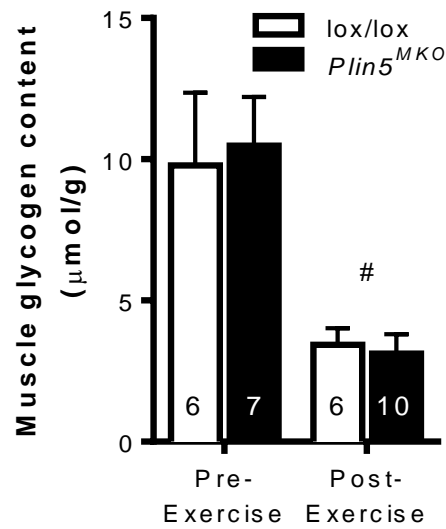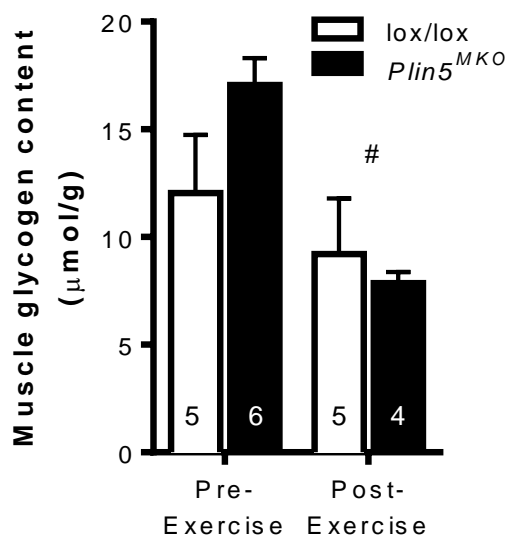

Fig 4-15. *Muscle glycogen content before and after exercise in exercise trained mice. Values are means ± SEM. [#]P<0.05, main effect for exercise. The numbers in the respective columns denotes n for each experiment.*
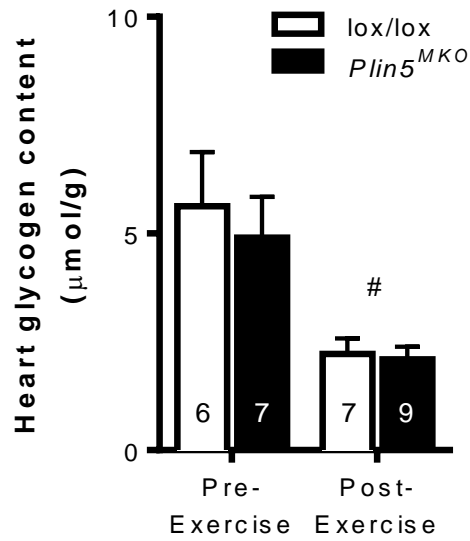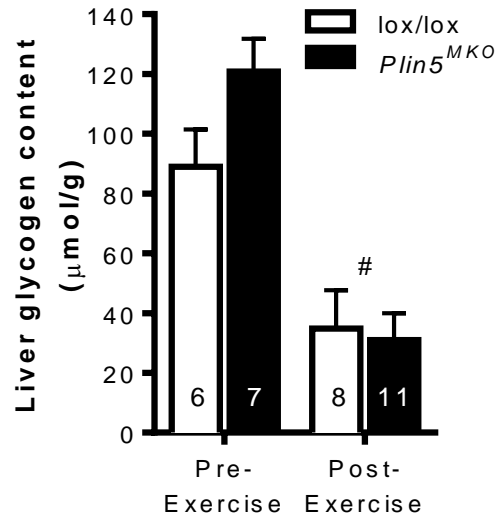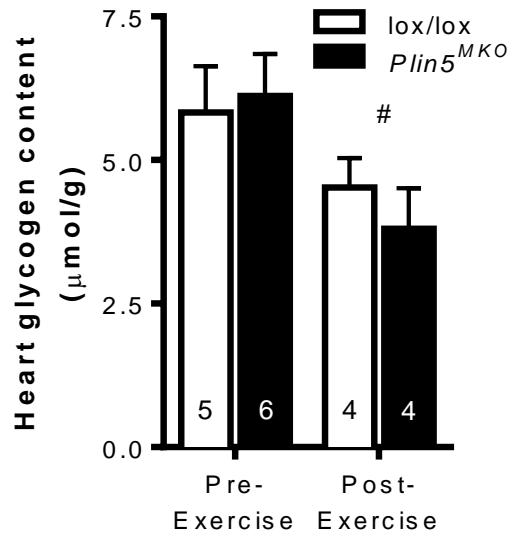
Fig 4-16. *Heart glycogen content before and after exercise in exercise trained mice. Values are means ± SEM. $^{\#}P<0.05$, main effect for exercise. The numbers in the respective columns denotes n for each experiment.*
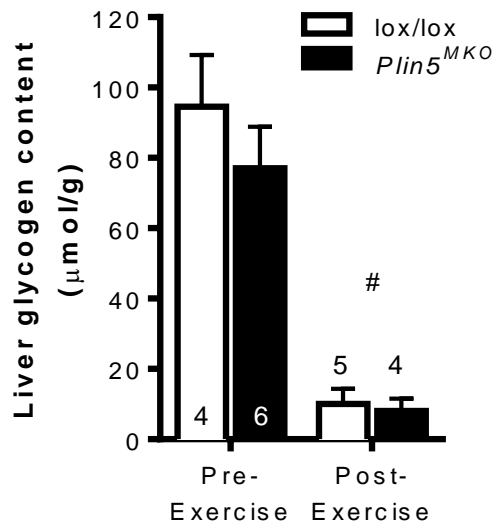
Fig 4-17. *Liver glycogen content before and after exercise in exercise trained mice. Values are means ± SEM. $^{\#}P<0.05$, main effect for exercise. The numbers in the respective columns denotes n for each experiment.*
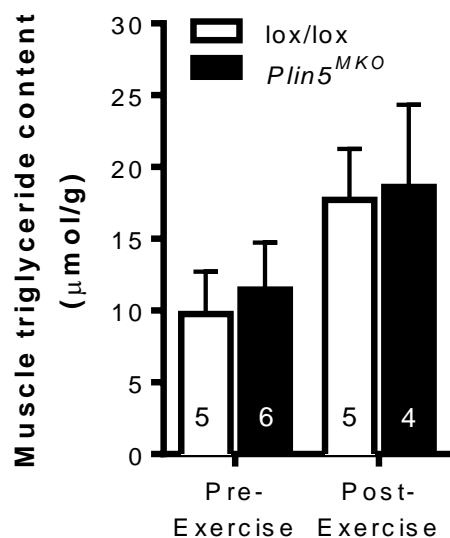
Fig 4-18. *Muscle triglyceride content before and after exercise in exercise trained mice. Values are means ± SEM. The numbers in the respective columns denotes n for each experiment.*
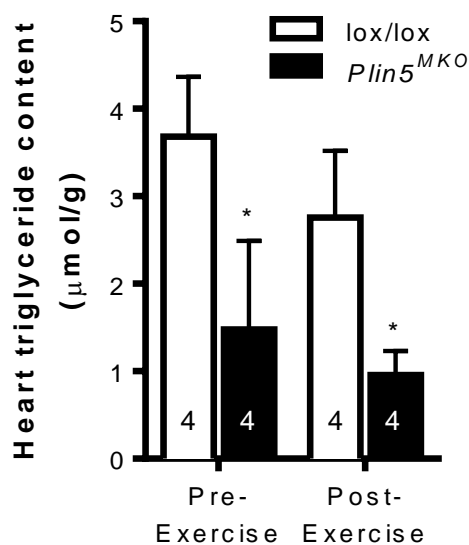
Fig 4-19. *Heart triglyceride content before and after exercise in exercise trained mice. Values are means ± SEM. $^*P<0.05$, main effect for genotype. The numbers in the respective columns denotes n for each experiment.*

Exercise trained mice				
Variable	**lox/lox**		**_Plin5_^{MKO}**	
	Pre	Post	Pre	Post
Blood glucose (mM)	12.7 ± 0.3 (5)	13.7 ± 1.4 (5)	13.2 ± 0.5 (6)	11.8 ± 0.6 (4)
Plasma FFA (mM)	0.74 ± 0.09 (5)	1.28 ± 0.13 (5)	0.76 ± 0.06 (6)	1.34 ± 0.05 (4)
Plasma triglycerides (mM)	0.60 ± 0.07 (5)	0.90 ± 0.14 (5)	0.63 ± 0.10 (6)	0.69 ± 0.09 (4)
Plasma ß-hydroxybutyrate (µM)	94 ± 44 (3)	218 ± 41 (5)	29 ± 10 (6)[*]	123 ± 19 (4)[*]
Plasma lactate (mM)	2.3 ± 0.1 (5)	2.7 ± 0.1 (5)	2.2 ± 0.1 (6)	2.6 ± 0.1 (4)
Plasma glycerol (µM)	0.36 ± 0.09 (5)	0.64 ± 0.13 (3)	0.22 ± 0.04 (6)	0.50 ± 0.06 (4)

Table 4-2. *Effects of muscle-specific Plin5 deletion on plasma metabolites before and after submaximal running in exercise trained mice. Values are means ± SEM. n for each measurement is denoted in parenthesis.* *P<0.05, main effect for genotype.*

Mitochondrial content and function are closely linked with exercise capacity (306), therefore we hypothesised that the impaired exercise performance in the exercise trained $Plin5^{MKO}$ mice (Fig. 4-13 & 4-14) was due to attenuation of the exercise induced mitochondrial adaptation. Mitochondrial DNA (2-fold) and citrate synthase activity (1.5-fold) was increased in trained lox/lox and $Plin5^{MKO}$ mice compared with untrained mice, demonstrating the effectiveness of the training program to enhance skeletal muscle respiratory capacity (data not shown). Markers of mitochondrial content / capacity including the levels of several mitochondrial respiratory chain proteins (Fig. 4-20), mitochondrial DNA (Fig. 4-21) and maximal citrate synthase activity (Fig. 4-22) were not different between $Plin5^{MKO}$ and lox/lox mice in either the skeletal muscle or heart. To test the functional capacity of the skeletal muscle, we performed assessment of oxygen consumption rate in skeletal muscle fiber bundles isolated from the EDL of lox/lox and $Plin5^{MKO}$ mice under basal and malate/glutamate/succinate/ADP stimulated conditions. Basal respiration was not different between genotypes (Fig. 4-23). Addition of malate/glutamate/succinate/ADP increased the oxygen consumption rate by ~9-fold and there was no difference between lox/lox and $Plin5^{MKO}$ mice. Collectively, these data demonstrate that $Plin5$ ablation in muscle does not impact mitochondrial content or function in response to exercise training.
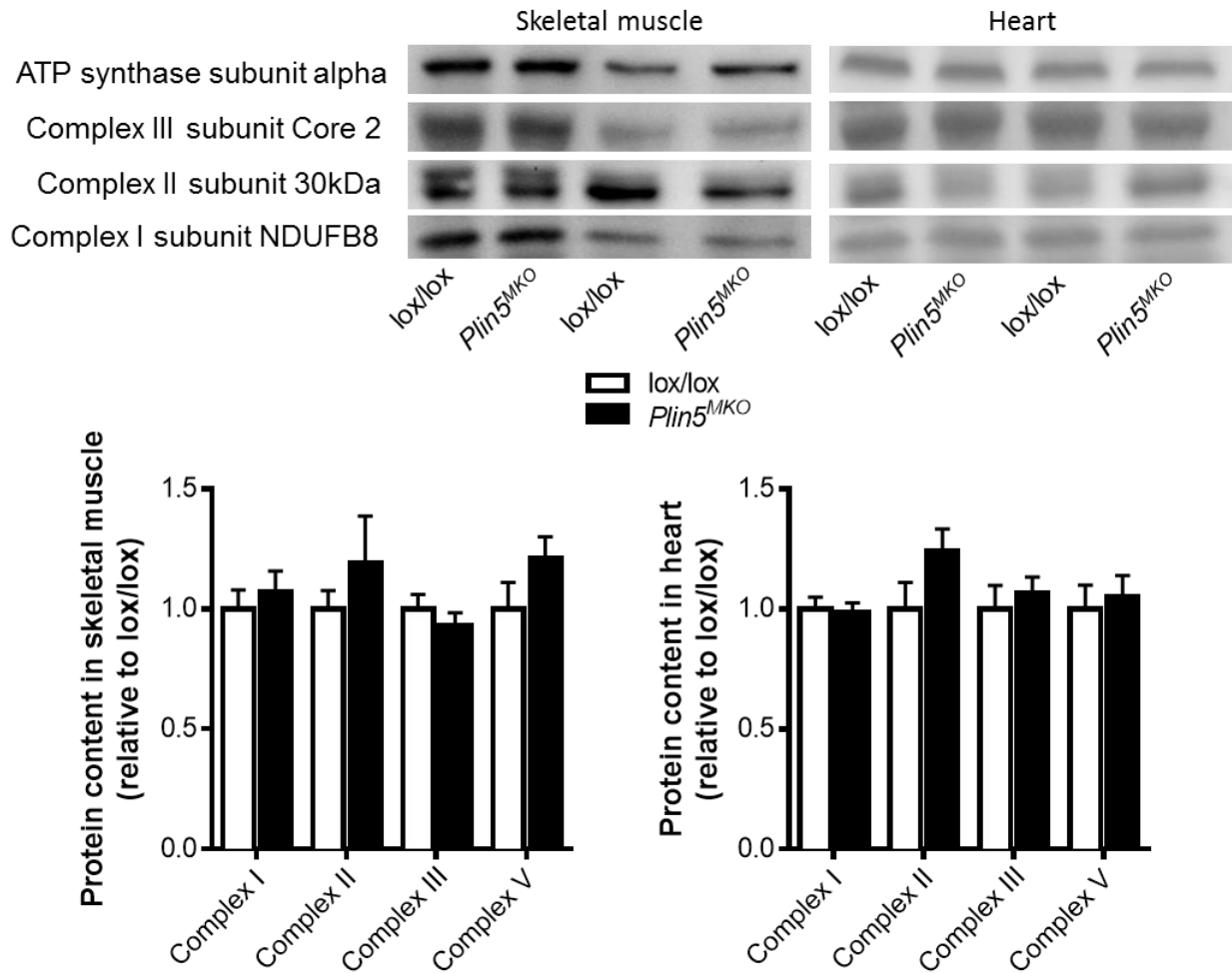
Fig. 4-20. *Immunoblots showing mitochondrial protein complexes in muscle and heart. Quantification of the immunoblot density expressed relative to total protein loading (stain-free gel- image not shown). n=4 for lox/lox, n=4 for Plin5^{MKO}.*
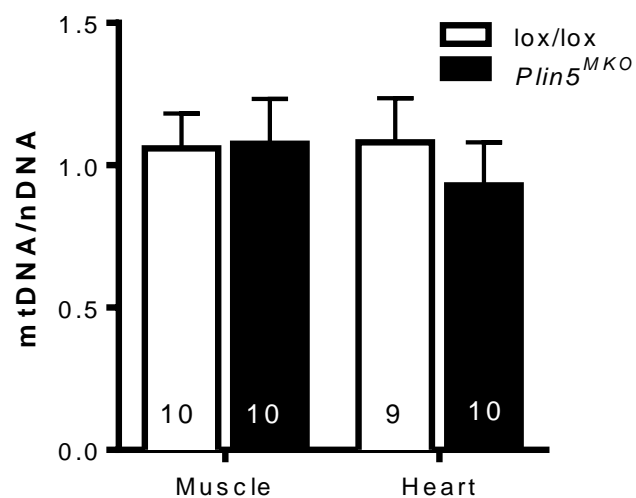
Fig. 4-21. *Mitochondrial DNA (mtDNA) in muscle and heart. Values are means ± SEM. The numbers in the respective columns denotes n for each experiment.*
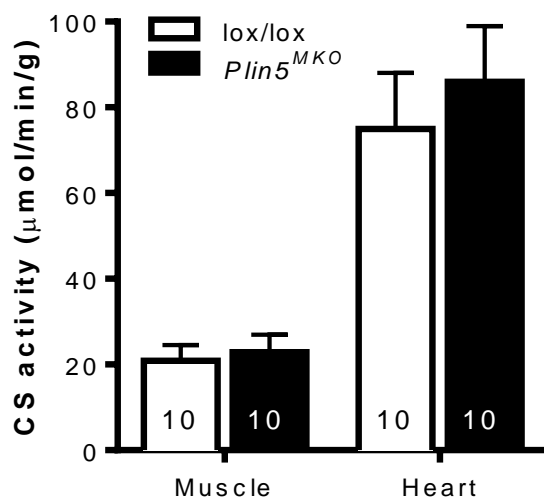
Fig 4-22. *Maximal citrate synthase activity determined in the muscle and heart. Values are means ± SEM. The numbers in the respective columns denotes n for each experiment.*
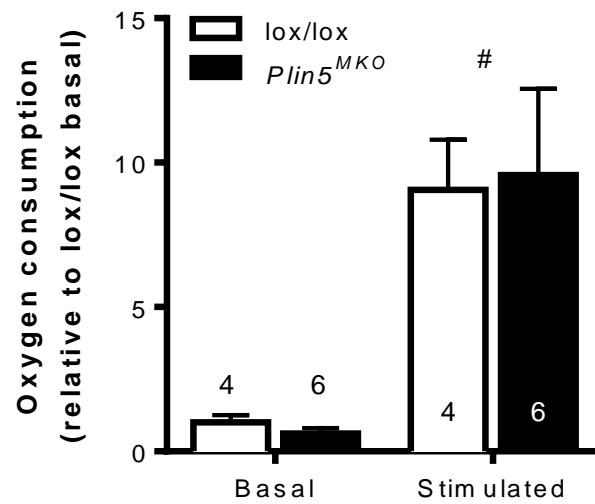
Fig. 4-23. *Determination of O$_2$ consumption in isolated fibers from the extensor digitorum longus (EDL) muscle. Muscle fibers were incubated under basal state and stimulated conditions of respiration. Values are means ± SEM. [#]P<0.05, main effect for stimulation. The numbers in the respective columns denotes n for each experiment.*

4.5   Discussion

Previous studies have shown that PLIN5 regulates cellular lipid balance in highly oxidative tissues such as the heart and skeletal muscle by interacting with the lipolytic proteins ATGL, CGI-58 and HSL (12–14) to prevent uncontrolled TG lipolysis. Such regulation matches fatty acid supply to the prevailing energetic requirements of the cell and thereby protects cells from lipotoxic stress (224,229,283). PLIN5 might also be involved in regulating the interactions between LDs and mitochondria, and in doing so, promote efficient transfer of stored lipids for oxidation (225). To date, the understanding of PLIN5 function has been derived from studies in cultured cells or in mice under states of low energy demand (229). Given that intramyocellular TG is a prominent energy source during exercise (64,105,307), the aim of this study was to examine the effects of muscle-specific PLIN5 ablation on substrate metabolism and energy provision during exercise, and in the adaptive response to endurance exercise training.

Muscle-specific *Plin5* knockout (*Plin5^{MKO}*) mice were generated to address our aims, with complete and specific PLIN5 deletion confirmed by immunoblot analysis. *Plin5^{MKO}* mice exhibited normal growth and adiposity compared with lox/lox control mice. The glycogen and TG stores in skeletal muscle and liver, and the concentrations of the major circulating metabolites for energy production including glucose, FFAs, TGs and ß-hydroxybutyrate were indistinguishable from the lox/lox mice. In many respects, these observations in *Plin5^{MKO}* mice reproduce measures of metabolic substrates in whole-body *Plin5$^{-/-}$* mice (224,230,283). The TG content in the heart was significantly reduced in *Plin5^{MKO}* mice compared with lox/lox mice, which is consistent with the finding in the hearts of mice with whole-body *Plin5* deletion due to lack of PLIN5 (224,283).

PLIN5 is clearly important in the regulation of substrate metabolism in sedentary mice (224,230,283), but its involvement in metabolic regulation during exercise was previously unknown. Herein, we provide novel evidence that PLIN5 is dispensable for substrate metabolism during exercise. PLIN5 ablation in muscle did not alter whole-body carbohydrate and fatty acid oxidation rates, as reflected by a similar respiratory exchange ratio, did not affect the degradation of muscle TG, or muscle and liver glycogen, and did not influence the circulating levels of glucose, lactate, FFAs or TGs. Collectively, these findings demonstrate that PLIN5 deletion in

muscle and heart has a negligible impact on substrate metabolism during submaximal exercise in sedentary mice.

Perhaps the most prominent metabolic adaptation to endurance exercise training is a diminished utilization of carbohydrates and a greater reliance on fatty acid oxidation during low to moderate intensity exercise (235). Because PLIN5 is increased in athletes compared with untrained individuals (114), and because athletes store more intramyocellular TG (114,126) and oxidize more TG-derived fatty acids during exercise (305), we hypothesized that PLIN5 is an important protein mediating the adaptation of substrate metabolism to exercise training. The metabolic responses to exercise in *Plin5^{MKO}* mice were almost indistinguishable from the lox/lox mice after endurance exercise training, and thus recapitulated the earlier studies in untrained / sedentary mice. This reinforces the view that PLIN5 is not essential for the regulation of substrate metabolism during exercise and is not important in the metabolic adaptations to endurance exercise training. An exception to this conclusion is the decrease in circulating ß-hydroxybutyrate in *Plin5^{MKO}* mice compared with lox/lox, both at rest and after exercise. This would normally indicate decreased liver fatty acid oxidation, but how *Plin5* deletion signals to impact these processes remains unresolved and will be future line of inquiry.

A notable finding of this study is that *Plin5^{MKO}* mice have normal exercise tolerance in the untrained state, but that these mice demonstrate impaired exercise capacity after prolonged endurance exercise training. Although we did not measured PLIN5 content after exercise training, previous studies unequivocally demonstrate that exercise training increases PLIN5 content in skeletal muscle (114,215,216,228) and ectopic over expression of PLIN5 in rat skeletal muscle increases the expression of several PPARα and PGC1α genes, which would predict enhanced mitochondrial function and improved fatty acid catabolism (227). Consistent with this notion, Koves et al (114) reported a close relationship between PLIN5 expression, intramyocellular TG lipolysis and mitochondrial biogenesis in several experimental models, supporting the premise that lipid signals derived from intracellular TG lipolysis can enhance mitochondrial capacity to facilitate efficient fatty acid catabolism (61,88). Mitochondrial biogenesis and enhanced respiratory capacity are hallmarks of endurance exercise training (308) and we surmised that the impaired exercise capacity in *Plin5^{MKO}* compared with lox/lox mice

after endurance exercise training may have been mediated by an impaired exercise training-induced enhancement in mitochondrial capacity and function. Our results showing similar levels of respiratory chain proteins, mitochondrial DNA, citrate synthase activity and skeletal muscle respiratory function clearly demonstrate that mitochondrial capacity and function were similar between genotypes. We conclude from these results, and those in PLIN5 over expressing (232,284,309) and *Plin5* null (230,283) mice, that increasing PLIN5 confers no beneficial effect on mitochondrial content or function and that PLIN5 is not requisite for the normal increase in mitochondrial biogenesis with endurance exercise training.

Fatty acids derived from intracellular TGs provide a significant component of fatty acid substrate to support cardiac function (249,306) and dysregulated fatty acid oxidation has been linked to cardiomyopathies (310). While our studies focused on skeletal muscle, the MCK promoter used to generate tissue *Plin5* deletion also drives *Cre* activity in cardiac muscle. Hence, dysregulated cardiac performance is one potential explanation for the reduction in exercise capacity after prolonged training. In this context, $Plin5^{-/-}$ mice have reduced cardiac TG content (224,283) and exhibit declines in cardiac function that become apparent at 30-38 weeks (224). $Plin5^{MKO}$ mice exhibited a similar 50% reduction in cardiac TG content, and while we examined mice at 18 weeks, which is well before cardiac dysfunction is evident in $Plin5^{-/-}$ mice, it is possible that an impairment in cardiac performance could limit exercise capacity. However, it is perplexing that exercise capacity was impaired in $Plin5^{MKO}$ mice after, but not before, prolonged exercise training. This questions the likelihood that cardiac dysfunction is associated with impaired work capacity in the $Plin5^{MKO}$ mice and highlights the need for future mechanistic studies of cardiac performance in these mice.

In conclusion, PLIN5 is known to regulate TG metabolism at rest and is postulated to be involved in the adaptive response of skeletal muscle to exercise training. We generated transgenic mice with muscle-specific *Plin5* deletion and show that PLIN5 is dispensable for normal substrate metabolism during exercise and is not required for mitochondrial biogenesis or the normal cellular adaptation to endurance-exercise training. Hence, we postulate that other PLIN proteins may be important in regulating TG metabolism during exercise or that the lipases ATGL and HSL by-pass PLIN5 to mediate lipolysis during exercise.

CHAPTER 5

General discussion

Since the discovery of LD associated proteins 25 years ago (39), researchers have made steady progress in delineating the biological roles of these proteins, especially in understanding the regulation of lipid metabolism. The PLIN protein family (PLIN1-5), which are thought to be involved in LD fusion and/or breakdown of triglycerides have been a major focus of interest (36,173,186). This thesis focused on delineating the role PLIN5 in metabolism because previous studies had shown that it is highly expressed in muscle (10) and very limited studies have been conducted to understand its role in skeletal muscle, particularly at a whole-body level. Previously, the functional evaluation of PLIN5 was confined to overexpression analysis in cell systems, such as CHO and COS-7 cells (10–14), both questionable cell lines when assessing metabolism as these cells are not exposed to the metabolic flucuations of major oxidative tissues *in vivo*. In this thesis, the involvement of PLIN5 in regulating muscle lipid metabolism and insulin action was examined by generating unique *in vivo* and *in vitro* models.

In study 1 (Chapter 2), PLIN5 null mice were generated, which provided a great opportunity to further explore the importance of PLIN5 in the regulation of muscle lipid metabolism *in vivo*. In this mouse model, we found a marked reduction of LDs in skeletal muscle during fasting that was likely caused by excessive lipolysis. This is consistent with previous results reported in cultured cells (12,13) and the heart, which suggested that PLIN5 acts as a barrier on LDs to prevent excessive lipolysis (224). This was further supported by other studies which demonstrated that overexpression of PLIN5 in cardiac muscle resulted in bigger LDs and more triglyceride storage (255,309). Hence, our findings in skeletal muscle indicate that a primary role of PLIN5 is to protect myocytes from uncontrolled TAG lipolysis. As an extension, we did not observe such marked reductions in skeletal muscle TAG content in fed mice, only in fasting mice when plasma fatty acid levels were increased and intramyocellular TAG breakdown was elevated. Thus, it is possible that PLIN5 acts to prevent myocytes from unnecessary intramyocellular lipolysis and to avoid cellular lipotoxicity.

In this thesis, we also determined the effect of PLIN5 deletion on skeletal muscle lipid metabolism *in vitro*. We successfully isolated and cultured myoblasts from the major hind-limb muscles of wild type ($Plin^{+/+}$) and whole-body $Plin5$ null ($Plin^{-/-}$) mice by using an explant culture method (262). This was necessary because examining TAG metabolism *in vivo* is

technically very difficult. As expected, the oxidation of TAG-derived fatty acids was elevated and the TAG level was reduced in *Plin5$^{-/-}$* myotubes, further supporting our interpretation that PLIN5 acts as a regulator in controlling intramyocellular lipolysis. These increases in intramyocellular fatty acid flux then prompted us to investigate the effect of PLIN5 on insulin action. Previous studies have reported that a reduction in intramyocellular TAG turnover can improve insulin action (74,89,90,269), while intramyocellular TAG accumulation is associated with insulin resistance in sedentary individuals (244,245). There are also reports that link the etiology of insulin resistance to the uncoupling of intramyocellular lipolysis from the cellular demand for fatty acids (74,147). The data contained in this thesis suggests that the increase in intramyocellular lipolysis without increased demand for this substrate can cause insulin resistance. In this regard, the reduction in skeletal muscle insulin sensitivity in *Plin5$^{-/-}$* mice and myotubes was associated with the elevation of several lipid metabolites including ceramides and sphingomyelin. The expression of several enzymes involved in ceramide production were also increased in *Plin$^{-/-}$* myotubes, leading to the conclusion that the fatty acids produced by unrestrained TAG lipolysis are channeled towards sphingolipid metabolism and induce insulin resistance in skeletal muscle and enzymes of ceramide production increase the machinery to drive this process.

A reduction in fatty acid oxidation and insulin resistance in skeletal muscle is reported to be closely associated with mitochondrial dysfunction (274). There is also evidence that elevated fatty acid flux from LDs can induce mitochondrial biogenesis and modulate metabolic phenotypes (88,114,267,276). While an increase in fatty acid oxidation from intramyocellular lipid was reported in the *Plin5$^{-/-}$* mice, there were no significant changes in mitochondrial content or function, either in isolated myotubes or intact skeletal muscle. Maximal running capacity was similar between *Plin5$^{-/-}$* mice compared to wild type littermates, further supporting the conclusion that PLIN5 ablation did not affect mitochondrial function. Taken together, the results from Chapter 2 of this thesis demonstrated that PLIN5 acts as a barrier to prevent uncontrolled skeletal muscle lipolysis, does not have a significant impact on mitochondrial capacity and function, and assists the maintenance of insulin sensitivity in skeletal muscle by inhibiting sphingolipid synthesis.

Although the results from Chapter 2 were useful in delineating PLIN5 functions *in vivo*, characterization of metabolism using whole-body knockout mice models are somewhat limited because there is a potential for compensatory tissue crosstalk, which may in turn affect the interpretation of a proteins function. Therefore, in study 2 (Chapter 3) of this thesis, the effects of muscle-specific *Plin5* deletion was examined by producing and performing metabolic phenotyping in mice with muscle-specific *Plin5* ablation. This is a unique *in vivo* model.

We demonstrated that muscle-specific knockout of PLIN5 resulted in increased whole-body fatty acid oxidation and reduced carbohydrate oxidation. This was contrary to the data in $Plin5^{-/-}$ mice, which reported a mild decrease in whole-body fat oxidation. The discrepancy between studies suggests that PLIN5 deletion in other tissues might have the opposing effects to skeletal muscle; that is, PLIN5 deletion in these tissues might decrease fatty acid oxidation. This further highlights the importance of generating tissue-specific knockout mice. Interestingly, there were no changes in fatty acid oxidation *ex vivo* using isolated soleus muscles, hence it is speculated that the increased fatty acid oxidation in $Plin5^{MKO}$ mice might be due to a circulating factor, such as myokines, which is absent when the muscle was isolated for the *ex vivo* experiments. This theory is underpinned by the results of a previous study in mice overexpressing PLIN5 in skeletal muscle, which showed a marked increase in fibroblast growth factor (FGF)-21 expression in skeletal muscle and serum of the PLIN5 transgenic mice compared to their control littermates (284). FGF21 is a myokine that is associated with positive metabolic outcomes including exercise-induced lipolysis, regulation of insulin secretion (311,312), increased substrate utilization by promoting fatty acid oxidation in the liver (313), improved glucose tolerance and reduced serum TGs (314). In the previous study, the increase in FGF21 levels was suggested to prevent insulin resistance from developing in the PLIN5 transgenic mice when they were fed a high-fat diet (284). As PLIN5 muscle-specific overexpression mice were reported to have marked increased in FGF21 (284), it can be suggested that the *Plin5* muscle specific knockout mice might also have altered myokine secretion and this will be the subject of future investigations. Indeed, several myokines other than FGF-21 are involved in the regulation of substrate oxidation, lipid partitioning, insulin sensitivity, inflammation and the pathogenesis of obesity (315).

In chapter 3, mice were challenged with a high-fat diet because high fat feeding is known to cause lipid accumulation and insulin resistance *in vivo* (316). We speculated that the effects of PLIN5 ablation would become particularly pronounced under the challenge of lipid stress. As expected, the increase in whole-body fat oxidation was more pronounced in *Plin5^{MKO}* mice fed with the high-fat diet, but still changes in fatty oxidation were not evident *ex vivo*. The interesting finding here is that *Plin5^{MKO}* mice fed a HFD seemed to be protected from high-fat diet induced glucose intolerance because these mice had increased glucose clearance by peripheral tissues following an oral glucose load. Here, we suggest that the protective effect seen with high-fat feeding is contributed by a factor other than insulin because none of insulin-related parameters were altered in these mice including plasma insulin levels, insulin-stimulated glucose uptake, whole-body insulin action and endogenous glucose production. About two thirds of glucose uptake is reported to be mediated by non-insulin mediated pathways following an oral glucose load (317). Thus, it is speculated that the non-insulin factor that caused improvement in glucose tolerance of these mice might be through activation of AMPK in skeletal muscle. Several studies have been demonstrated that the activation of AMPK can result in increased glucose uptake in muscle (294,318). Therefore, future investigations should focus on confirming the involvement of AMPK in the regulation of glucose uptake in skeletal muscle and its exact mechanism in *Plin5^{MKO}* mice under conditions of high-fat feeding.

As discussed above, it was previously postulated that PLIN5 might be involved in the adaptive response to exercise training. This idea was derived from the observations that PLIN5 protein content was elevated after acute exercise or chronic training (114,228,229,239). PLIN5 was markedly upregulated in endurance-trained athletes when compared to sedentary individuals (114). In study 3 (Chapter 4) of this thesis, we predicted that this adaptive response might be caused by improvement in mitochondrial function and capacity to facilitate β-oxidation in muscle. Although our previous data did not show any impact on skeletal muscle mitochondrial capacity and function with whole-body PLIN5 ablation, we hypothesized that this did not occur because the mice were not metabolically challenged and were only examined in their sedentary state. As exercise training is reported to stimulate mitochondrial adaptation and enhance exercise performance (302), we suspected that the adaptive response may only become apparent with exercise training in *Plin5^{MKO}* mice. Hence, the aims of chapter 4 in this thesis were to investigate

the role of PLIN5 in the regulation of skeletal muscle substrate metabolism during acute exercise and to determine whether PLIN5 is required for the metabolic adaptations and enhancement in exercise tolerance following endurance exercise training.

The novel finding in Chapter 4 was that PLIN5 is not required to regulate substrate metabolism during exercise. These studies showed that the levels of blood metabolites and the rates of glycogen and triglyceride depletion in *Plin5^{MKO}* mice were not different compared to the control littermates. Even though *Plin5^{MKO}* mice exhibited a functional impairment in their response to endurance exercise training (i.e. reduced running capacity after exercise training), this was not accompanied by alterations in carbohydrate and fatty acid metabolism during submaximal exercise. Intriguingly, we also did not find any changes in mitochondrial capacity (mtDNA, respiratory complex proteins, citrate synthase activity) and mitochondrial function (oxygen consumption rate in isolated muscle fiber bundles) in the *Plin5^{MKO}* mice after endurance exercise training. As our *Plin5^{MKO}* mice have almost complete knockdown of PLIN5 in heart and exhibited a reduction in cardiac TG content, it is proposed that the reduction in exercise capacity after prolonged training might be caused by dysregulation of cardiac performance. However, a limitation of this study is that we cannot explain why the exercise capacity impairment only can be seen after the exercise training and not in the sedentary state. Further studies are needed to examine the association between cardiac performance and exercise capacity in *Plin5^{MKO}* mice before and after exercise training.

Cumulatively, the studies completed in this thesis provide novel insights into the role of PLIN5 in skeletal muscle, especially during high-fat feeding and during energetic stress. PLIN5 is undoubtedly necessary in controlling intramyocellular lipolysis, which prevents the production of lipid intermediates in skeletal muscle and potentially improves muscle insulin action. This finding has set the foundation for further exploration of the PLIN proteins as a potential therapeutic target for treating metabolic diseases such as T2D. Currently, there is no convincing evidence showing the involvement of PLIN5 in regulating the components of metabolic disease in humans (169,223,241) and future studies should emphasise the involvement of PLIN5 in pathophysiological states in humans (e.g., its role in obesity, T2D, and hepatosteatosis).

PLIN5 is only one of at least 300 LD associated protein that exists on the surface of lipid droplet (33). Currently, only several PLIN5 binding partners have been identified and include ATGL, CGI-58 and G0S2, while there are probably other possible PLIN5 interacting partners. The discovery of other PLIN5 interacting proteins should be a priority of future research, especially in view of the findings in heart that PLIN5 promotes mitochondria-lipid droplet interactions (225), which would presumably require protein-protein interactions. As other PLIN proteins, such as PLIN2 and PLIN3, are also expressed in skeletal muscle and have been shown to involve in regulation of fatty acid metabolism (192–195,211–213), it will also be important to determine whether or not there are interactions between their role in metabolic control and whether and/or how they interact with PLIN5. Given the prominent role of PLIN2 in metabolism and the likelihood of overlap with PLIN5 functions, generation of PLIN2/5 double knockout mice will be useful for the study of these PLIN proteins in skeletal muscle.

In closing, the work in this thesis has demonstrated that PLIN5 plays an important role in regulating skeletal muscle TAG metabolism, which eventually will influence sphingolipid metabolism, and it is needed for the maintenance of skeletal muscle insulin action. PLIN5 also may impact endocrine signalling, which can alter metabolism in other tissues important in regulating metabolism such as the brain, pancreas, liver and adipose tissue. Future studies are needed to confirm the involvement of PLIN5 in the regulation of endocrine signalling and its role in metabolic diseases such as obesity and T2D.

CHAPTER 6

References

1. Colagiuri S, Lee CMY, Colagiuri R, Magliano D, Shaw JE, Zimmet PZ, et al. The cost of overweight and obesity in Australia. Med J Aust. 2010;192(5):260–4.

2. Must A, Spadano J, Coakley EH, Field AE, Colditz G, Dietz WH. The Disease Burden Associated With. J Am Med Assoc. 1999;282(16):1523–9.

3. Your Weight and Diabetes [Internet]. [cited 2016 Aug 22]. Available from: http://www.obesity.org/content/weight-diabetes

4. Fagot-campagna A, Balkau B, Simon D, Warnet J, Claude J, Eschwege E. High free fatty acid concentration : an independent risk factor for hypertension in the Paris Prospective Study. Int J Epidemiol. 1998;27(5):808–13.

5. Smyth S, Heron A. Diabetes and obesity: the twin epidemics. Nat Med. 2006;12(1):75–80.

6. Hardy OT, Czech MP, Corvera S. What causes the insulin resistance underlying obesity? Curr Opin Endocrinol Diabetes Obes. 2012;19(2):81–7.

7. van Herpen NA, Schrauwen-Hinderling VB. Lipid accumulation in non-adipose tissue and lipotoxicity. Physiol Behav. 2008;94(2):231–41.

8. Golay a, Ybarra J. Link between obesity and type 2 diabetes. Best Pract Res Clin Endocrinol Metab. 2005;19(4):649–63.

9. Wolins NE, Brasaemle DL, Bickel PE. A proposed model of fat packaging by exchangeable lipid droplet proteins. FEBS Lett. 2006;580(23):5484–91.

10. Wolins NE, Quaynor BK, Skinner JR, Tzekov A, Croce MA, Gropler MC, et al. OXPAT/PAT-1 is a PPAR-induced lipid droplet protein that promotes fatty acid utilization. Diabetes. 2006;55(12):3418–28.

11. Dalen KT, Dahl T, Holter E, Arntsen B, Londos C, Sztalryd C, et al. LSDP5 is a PAT protein specifically expressed in fatty acid oxidizing tissues. Biochim Biophys Acta - Mol Cell Biol Lipids. 2007;1771(2):210–27.

12. Wang H, Bell M, Sreenevasan U, Hu H, Liu J, Dalen K, et al. Unique regulation of adipose triglyceride lipase (ATGL) by perilipin 5, a lipid droplet-associated protein. J Biol Chem. 2011;286(18):15707–15.

13. Granneman JG, Moore H-PH, Mottillo EP, Zhu Z, Zhou L. Interactions of perilipin-5 (Plin5) with adipose triglyceride lipase. J Biol Chem. 2011;286(7):5126–35.

14. Wang H, Hu L, Dalen K, Dorward H, Marcinkiewicz A, Russell D, et al. Activation of hormone-sensitive lipase requires two steps, protein phosphorylation and binding to the

PAT-1 domain of lipid droplet coat proteins. J Biol Chem. 2009;284(46):32116–25.

15.   Bartz R, Zehmer JK, Zhu M, Chen Y, Serrero G, Zhao Y, et al. Dynamic activity of lipid droplets: Protein phosphorylation and GTP-mediated protein translocation. J Proteome Res. 2007;6(8):3256–65.

16.   Murphy DJ. The biogenesis and functions of lipid bodies in animals, plants and microorganisms. Prog Lipid Res. 2001;40(5):325–438.

17.   Tauchi-Sato K, Ozeki S, Houjou T, Taguchi R, Fujimoto T. The surface of lipid droplets is a phospholipid monolayer with a unique fatty acid composition. J Biol Chem. 2002;277(46):44507–12.

18.   Lange KHW. Fat metabolism in exercise – with special reference to training and growth hormone administration. Scand J Med Sci Sport. 2004;14(2):74–99.

19.   van Loon LJC, Koopman R, Manders R, van der Weegen W, van Kranenburg GP, Keizer H a. Intramyocellular lipid content in type 2 diabetes patients compared with overweight sedentary men and highly trained endurance athletes. Am J Physiol Endocrinol Metab. 2004;287(3):E558–65.

20.   Wang H, Eckel RH. Lipoprotein lipase: from gene to obesity. Am J Physiol Endocrinol Metab. 2009;297(2):E271–88.

21.   Badin P-M, Loubiere C, Coonen M, Louche K, Tavernier G, Bourlier V, et al. Regulation of skeletal muscle lipolysis and oxidative metabolism by the co-lipase CGI-58. J Lipid Res. 2012;53(5):839–48.

22.   Kerner J, Hoppel C. Fatty acid import into mitochondria. Biochim Biophys Acta. 2000;1486(1):1–17.

23.   Bindesbøll C, Berg O, Arntsen B, Nebb HI, Dalen KT. Fatty acids regulate perilipin5 in muscle by activating PPARδ. J Lipid Res. 2013;54(7):1949–63.

24.   Meex RCR, Schrauwen P, Hesselink MKC. Modulation of myocellular fat stores: lipid droplet dynamics in health and disease. Am J Physiol Regul Integr Comp Physiol. 2009;297(4):R913–24.

25.   Prats C, Donsmark M, Qvortrup K, Londos C, Sztalryd C, Holm C, et al. Decrease in intramuscular lipid droplets and translocation of HSL in response to muscle contraction and epinephrine. J Lipid Res. 2006;47(11):2392–9.

26.   Kim JY, Tillison K, Lee J-H, Rearick D a, Smas CM. The adipose tissue triglyceride

lipase ATGL/PNPLA2 is downregulated by insulin and TNF-alpha in 3T3-L1 adipocytes and is a target for transactivation by PPARgamma. Am J Physiol Endocrinol Metab. 2006;291(1):E115-27.

27. Hickenbottom SJ, Kimmel AR, Londos C, Hurley JH. Structure of a lipid droplet protein: The PAT family member TIP47. Structure. 2004;12(7):1199–207.

28. Walther TC, Farese R V. The life of lipid droplets. Biochim Biophys Acta - Mol Cell Biol Lipids. 2009;1791(6):459–66.

29. Welte MA. Expanding roles for lipid droplets. Curr Biol. 2015;25(11):R470-81.

30. Martin S, Parton RG. Lipid droplets: a unified view of a dynamic organelle. Nat Rev Mol Cell Biol. 2006;7(5):373–8.

31. Shaw CS, Jones DA, Wagenmakers AJM. Network distribution of mitochondria and lipid droplets in human muscle fibres. Histochem Cell Biol. 2008;129(1):65–72.

32. Beller M, Thiel K, Thul PJ, Jackle H. Lipid droplets: A dynamic organelle moves into focus. FEBS Lett. 2010;584(11):2176–82.

33. Zhang H, Wang Y, Li J, Yu J, Pu J, Li L, et al. Proteome of skeletal muscle lipid droplet reveals association with mitochondria and apolipoprotein A-I. J Proteome Res. 2011;10(10):4757–68.

34. Welte MA. Proteins under new management: lipid droplets deliver. Trends Cell Biol. 2007;17(8):363–9.

35. Blanchette-Mackie EJ, Dwyer NK, Barber T, Coxey R a, Takeda T, Rondinone CM, et al. Perilipin is located on the surface layer of intracellular lipid droplets in adipocytes. J Lipid Res. 1995;36(6):1211–26.

36. Londos C, Brasaemle DL, Schultz CJ, Segrest JP, Kimmel a R. Perilipins, ADRP, and other proteins that associate with intracellular neutral lipid droplets in animal cells. Semin Cell Dev Biol. 1999;10(1):51–8.

37. Murphy S, Martin S, Parton RG. Lipid droplet-organelle interactions; sharing the fats. Biochim Biophys Acta - Mol Cell Biol Lipids. 2009;1791(6):441–7.

38. Greenberg AS, Egan JJ, Wek SA, Garty NB, Blanchette-Mackie EJ, Londos C. Perilipin, a major hormonally regulated adipocyte-specific phosphoprotein associated with the periphery of lipid storage droplets. J Biol Chem. 1991;266(17):11341–6.

39. Egan JJ, Greenberg AS, Chang MK, Londos C. Control of endogenous phosphorylation of

the major cAMP-dependent protein kinase substrate in adipocytes by insulin and β-adrenergic stimulation. J Biol Chem. 1990;265(31):18769–75.

40. Egan JJ, Greenberg a S, Chang MK, Wek S a, Moos MC, Londos C. Mechanism of hormone-stimulated lipolysis in adipocytes: translocation of hormone-sensitive lipase to the lipid storage droplet. Proc Natl Acad Sci U S A. 1992;89(18):8537–41.

41. Greenberg AS, Egan JJ, Wek SA, Moos MC, Londos C, Kimmel AR. Isolation of cDNAs for perilipins A and B: sequence and expression of lipid droplet-associated proteins of adipocytes. Proc Natl Acad Sci U S A. 1993;90(24):12035–9.

42. Kimmel AR, Sztalryd C. Perilipin 5, a lipid droplet protein adapted to mitochondrial energy utilization. Curr Opin Lipidol. 2014;25(2):110–7.

43. Farese R V., Walther TC. Lipid Droplets Finally Get a Little R-E-S-P-E-C-T. Cell. 2009;139(5):855–60.

44. Walther TC, Farese R V. The life of lipid droplets. Biochim Biophys Acta - Mol Cell Biol Lipids. 2009;1791(6):459–66.

45. Glatz JFC, Luiken JJFP, Bonen A. Membrane Fatty Acid Transporters as Regulators of Lipid Metabolism: Implications for Metabolic Disease. Physiol Rev. 2010;90(1):367–417.

46. Schwenk RW, Holloway GP, Luiken JJFP, Bonen A, Glatz JFC. Fatty acid transport across the cell membrane: Regulation by fatty acid transporters. Prostaglandins Leukot Essent Fat Acids. 2010;82(4–6):149–54.

47. Stahl a, Gimeno RE, Tartaglia L a, Lodish HF. Fatty acid transport proteins: a current view of a growing family. Trends Endocrinol Metab. 2001;12(6):266–73.

48. García-Martínez C, Marotta M, Moore-Carrasco R, Guitart M, Camps M, Busquets S, et al. Impact on fatty acid metabolism and differential localization of FATP1 and FAT/CD36 proteins delivered in cultured human muscle cells. Am J Physiol Cell Physiol. 2005;288(6):C1264–72.

49. Jeppesen J, Albers P, Luiken JJ, Glatz JFC, Kiens B. Contractions but not AICAR increase FABPpm content in rat muscle sarcolemma. Mol Cell Biochem. 2009;326(1-2) 45–53.

50. Luiken JJ, Miskovic D, Arumugam Y, Glatz JF, Bonen A. Skeletal muscle fatty acid transport and transporters. Int J Sport Nutr Exerc Metab. 2001;11 Suppl:S92-6.

51. Koonen DPY, Glatz JFC, Bonen A, Luiken JJFP. Long-chain fatty acid uptake and

FAT/CD36 translocation in heart and skeletal muscle. Biochim Biophys Acta. 2005;1736(3):163–80.

52. Corpeleijn E, Pelsers MMAL, Soenen S, Mensink M, Bouwman FG, Kooi ME, et al. Insulin acutely upregulates protein expression of the fatty acid transporter CD36 in human skeletal muscle in vivo. J Physiol Pharmacol. 2008;59(1):77–83.

53. Wu Q, Ortegon AM, Tsang B, Doege H, Feingold KR, Stahl A. FATP1 is an insulin-sensitive fatty acid transporter involved in diet-induced obesity. Mol Cell Biol. 2006;26(9):3455–67.

54. Stahl a, Evans JG, Pattel S, Hirsch D, Lodish HF. Insulin causes fatty acid transport protein translocation and enhanced fatty acid uptake in adipocytes. Dev Cell. 2002;2(4):477–88.

55. Chabowski A, Górski J, Luiken JJFP, Glatz JFC, Bonen A. Evidence for concerted action of FAT/CD36 and FABPpm to increase fatty acid transport across the plasma membrane. Prostaglandins Leukot Essent Fat Acids. 2007;77(5–6):345–53.

56. Doege H, Stahl A. Protein-mediated fatty acid uptake: novel insights from in vivo models. Physiology (Bethesda). 2006;21:259–68.

57. Schwenk RW, Luiken JJFP, Bonen A, Glatz JFC. Regulation of sarcolemmal glucose and fatty acid transporters in cardiac disease. Cardiovasc Res. 2008;79(2):249–58.

58. Tarnopolsky M a, Rennie CD, Robertshaw H a, Fedak-Tarnopolsky SN, Devries MC, Hamadeh MJ. Influence of endurance exercise training and sex on intramyocellular lipid and mitochondrial ultrastructure, substrate use, and mitochondrial enzyme activity. Am J Physiol Regul Integr Comp Physiol. 2007;292(3):R1271–8.

59. Coen PM, Dube JJ, Amati F, Stefanovic-racic M, Ferrell RE, Dubé JJ, et al. Insulin resistance is associated with higher intramyocellular triglycerides in type I but not type II myocytes concomitant with higher ceramide content. Diabetes. 2010;59(1):80–8.

60. Kanaley JA, Shadid S, Sheehan MT, Guo Z, Jensen MD. Relationship between plasma free fatty acid, intramyocellular triglycerides and long-chain acylcarnitines in resting humans. J Physiol. 2009;587(Pt 24):5939–50.

61. Meex RCR, Hoy AJ, Mason RR, Martin SD, McGee SL, Bruce CR, et al. ATGL-mediated triglyceride turnover and the regulation of mitochondrial capacity in skeletal muscle. Am J Physiol - Endocrinol Metab. 2015;308(11): E960-70.

62. Sacchetti M, Saltin B, Olsen DB, van Hall G. High triacylglycerol turnover rate in human skeletal muscle. J Physiol. 2004;561(Pt 3):883–91.

63. Zierler K. Fatty acids as substrates for heart and skeletal muscle. Circ Res. 1976;38(6):459–63.

64. Watt MJ, Heigenhauser GJF, Spriet LL. Intramuscular triacylglycerol utilization in human skeletal muscle during exercise: is there a controversy? J Appl Physiol. 2002;93:1185–95.

65. Essén B, Jansson E, Henriksson J, Taylor a W, Saltin B. Metabolic characteristics of fibre types in human skeletal muscle. Acta Physiol Scand. 1975;95(2):153–65.

66. Egan B, Zierath JR. Exercise metabolism and the molecular regulation of skeletal muscle adaptation. Cell Metab. 2013;17(2):162–84.

67. Wang ZQ, Yu Y, Zhang XH, Floyd EZ, Cefalu WT. Human adenovirus 36 decreases fatty acid oxidation and increases de novo lipogenesis in primary cultured human skeletal muscle cells by promoting Cidec/FSP27 expression. Int J Obes (Lond). 2010;34(9):1355–64.

68. Gross DA, Zhan C, Silver DL. Direct binding of triglyceride to fat storage-inducing transmembrane proteins 1 and 2 is important for lipid droplet formation. Proc Natl Acad Sci U S A. 2011;108(49):19581–6.

69. Miranda DA, Koves TR, Gross DA, Chadt A, Al-Hasani H, Cline GW, et al. Re-patterning of skeletal muscle energy metabolism by fat storage-inducing transmembrane protein 2. J Biol Chem. 2011;286(49):42188–99.

70. Papadopoulos C, Orso G, Mancuso G, Herholz M, Gumeni S, Tadepalle N, et al. Spastin binds to lipid droplets and affects lipid metabolism. PLoS Genet. 2015;11(4):e1005149.

71. Gong J, Sun Z, Wu L, Xu W, Schieber N, Xu D, et al. Fsp27 promotes lipid droplet growth by lipid exchange and transfer at lipid droplet contact sites. J Cell Biol. 2011;195(6):953–63.

72. Wu LZ, Zhou LK, Chen C, Gong JY, Xu L, Ye J, et al. Cidea controls lipid droplet fusion and lipid storage in brown and white adipose tissue. Sci China Life Sci. 2014;57(1):107–16.

73. Zimmermann R, Strauss JG, Haemmerle G, Schoiswohl G, Birner-Gruenberger R, Riederer M, et al. Fat mobilization in adipose tissue is promoted by adipose triglyceride lipase. Science. 2004;306(5700):1383–6.

74. Badin PM, Louche K, Mairal A, Liebisch G, Schmitz G, Rustan AC, et al. Altered skeletal muscle lipase expression and activity contribute to insulin resistance in humans. Diabetes. 2011;60(6):1734–42.

75. Sitnick MT, Basantani MK, Cai L, Schoiswohl G, Yazbeck CF, Distefano G, et al. Skeletal muscle triacylglycerol hydrolysis does not influence metabolic complications of obesity. Diabetes. 2013;62(10):3350–61.

76. Haemmerle G, Lass A, Zimmermann R, Gorkiewicz G, Meyer C, Rozman J, et al. Defective lipolysis and altered energy metabolism in mice lacking adipose triglyceride lipase. Science. 2006;312(5774):734–7.

77. Lass A, Zimmermann R, Haemmerle G, Riederer M, Schoiswohl G, Schweiger M, et al. Adipose triglyceride lipase-mediated lipolysis of cellular fat stores is activated by CGI-58 and defective in Chanarin-Dorfman Syndrome. Cell Metab. 2006;3(5):309–19.

78. Yang X, Lu X, Lombes M, Rha GB, Chi YI, Guerin TM, et al. The G0/G1 Switch Gene 2 Regulates Adipose Lipolysis through Association with Adipose Triglyceride Lipase. Cell Metab. 2010;11(3):194–205.

79. Schweiger M, Paar M, Eder C, Brandis J, Moser E, Gorkiewicz G, et al. G0/G1 switch gene-2 regulates human adipocyte lipolysis by affecting activity and localization of adipose triglyceride lipase. J Lipid Res. 2012;53(11):2307–17.

80. Pagnon J, Matzaris M, Stark R, Meex RCR, Macaulay SL, Brown W, et al. Identification and functional characterization of protein kinase A phosphorylation sites in the major lipolytic protein, adipose triglyceride lipase. Endocrinology. 2012;153(9):4278–89.

81. Turnbull PC, Ramos S V, MacPherson REK, Roy BD, S, Peters SJ, et al. Characterization of Lipolytic Inhibitor G(0)/G(1) Switch Gene-2 Protein (G0S2) Expression in Male Sprague-Dawley Rat Skeletal Muscle Compared to Relative Content of Adipose Triglyceride Lipase (ATGL) and Comparitive Gene Identification-58 (CGI-58). PLoS One. 2015;10(3):e0120136.

82. Xie P, Kadegowda AKG, Ma Y, Guo F, Han X, Wang M, et al. Muscle-specific deletion of comparative gene identification-58 (CGI-58) causes muscle steatosis but improves insulin sensitivity in male mice. Endocrinology. 2015;156(5):1648–58.

83. Mason RR, Meex RCR, Russell AP, Canny BJ, Watt MJ. Cellular localization and associations of the major lipolytic proteins in human skeletal muscle at rest and during

exercise. PLoS One. 2014;9(7):e103062.

84. Mason RR, Meex RCR, Lee-Young R, Canny BJ, Watt MJ. Phosphorylation of adipose triglyceride lipase Ser(404) is not related to 5'-AMPK activation during moderate-intensity exercise in humans. AJP Endocrinol Metab. 2012;303(4):E534–41.

85. Kraemer FB, Shen W-J. Hormone-sensitive lipase: control of intracellular tri-(di-)acylglycerol and cholesteryl ester hydrolysis. J Lipid Res. 2002;43(10):1585–94.

86. Haemmerle G, Zimmermann R, Strauss JG, Kratky D, Riederer M, Knipping G, et al. Hormone-sensitive lipase deficiency in mice changes the plasma lipid profile by affecting the tissue-specific expression pattern of lipoprotein lipase in adipose tissue and muscle. J Biol Chem. 2002;277(15):12946–52.

87. Watt MJ, Steinberg GR, Chan S, Garnham A, Kemp BE, Febbraio MA. Beta-adrenergic stimulation of skeletal muscle HSL can be overridden by AMPK signaling. FASEB J. 2004;18(1):1445–6.

88. Haemmerle G, Moustafa T, Woelkart G, Buttner S, Schmidt A, van de Weijer T, et al. ATGL-mediated fat catabolism regulates cardiac mitochondrial function via PPAR-alpha and PGC-1. Nat Med. 2011;17(9):1076–85.

89. Kienesberger PC, Lee D, Pulinilkunnil T, Brenner DS, Cai L, Magnes C, et al. Adipose triglyceride lipase deficiency causes tissue-specific changes in insulin signaling. J Biol Chem. 2009;284(44):30218–29.

90. Huijsman E, van de Par C, Economou C, van der Poel C, Lynch GS, Schoiswohl G, et al. Adipose triacylglycerol lipase deletion alters whole body energy metabolism and impairs exercise performance in mice. Am J Physiol Endocrinol Metab. 2009;297(2):E505–13.

91. Watt M, Holmes A. Regulation of HSL serine phosphorylation in skeletal muscle and adipose tissue. Am J Physiol - Endocrinol Metab. 2006;290:E500–8.

92. Hans Tornqvist PB. Monoacylglycerol Lipase from Rat Adipose Tissue. Methods Enzymol. 1981;71:646–52.

93. Dinh TP, Carpenter D, Leslie FM, Freund TF, Katona I, Sensi SL, et al. Brain monoglyceride lipase participating in endocannabinoid inactivation. Proc Natl Acad Sci U S A. 2002;99(16):10819–24.

94. Makara JK, Mor M, Fegley D, Szabó SI, Kathuria S, Astarita G, et al. Selective inhibition of 2-AG hydrolysis enhances endocannabinoid signaling in hippocampus. Nat Neurosci.

2005;8(9):1139–41.

95.   Taschler U, Radner FPW, Heier C, Schreiber R, Schweiger M, Schoiswohl G, et al. Monoglyceride lipase deficiency in mice impairs lipolysis and attenuates diet-induced insulin resistance. J Biol Chem. 2011;286(20):17467–77.

96.   Zhao S, Mugabo Y, Iglesias J, Xie L, Delghingaro-Augusto V, Lussier R, et al. Alpha/beta-Hydrolase Domain-6-accessible monoacylglycerol controls glucose-stimulated insulin secretion. Cell Metab. 2014;19(6):993–1007.

97.   Lass A, Zimmermann R, Oberer M, Zechner R. Lipolysis - A highly regulated multi-enzyme complex mediates the catabolism of cellular fat stores. Prog Lipid Res. 2011;50(1):14–27.

98.   Watt MJ, Steinberg GR. Regulation and function of triacylglycerol lipases in cellular metabolism. Biochem J. 2008;414(3):313–25.

99.   Donsmark M, Langfort J, Holm C, Ploug T, Galbo H. Contractions activate hormone-sensitive lipase in rat muscle by protein kinase C and mitogen-activated protein kinase. J Physiol. 2003;550(Pt 3):845–54.

100. Macpherson REK, Peters SJ. Piecing together the puzzle of perilipin proteins and skeletal muscle lipolysis. Appl Physiol Nutr Metab. 2015;40(7):641–51.

101. Kiens B, Essen-Gustavsson B, Christensen NJ, Saltin B. Skeletal muscle substrate utilization during submaximal exercise in man: effect of endurance training. J Physiol. 1993;469:459–78.

102. Holloway GP, Bonen A, Spriet LL. Regulation of skeletal muscle mitochondrial fatty acid metabolism in lean and obese individuals 1 – 4. Am J Clin Nutr. 2009;89:455–62.

103. Kiens B. Skeletal Muscle Lipid Metabolism in Exercise and Insulin Resistance. Physiol Rev. 2006;86(1):205–43.

104. Hargreaves M. Skeletal muscle metabolism during exercise in humans. Clin Exp Pharmacol Physiol. 2000;27(3):225–8.

105. Romijn J a, Gastaldelli A, Horowitz JF, Endert E, Wolfe RR. Regulation of endogenous fat and carbohydrate metabolism in relation to exercise intensity and duration. Am J Physiol. 1993;265(3p1):380–91.

106. van Loon LJ, Greenhaff PL. The effects of increasing exercise intensity on muscle fule utilisation in humans. J Physiol. 2001;536(Pt 1):295–304.

107. Klein S, Peters E, Holland O. Effect of short-and long-term beta-adrenergic blockade on lipolysis during fasting in humans. Am J Physiol - Endocrinol Metab. 1989;257(1):E65-73.

108. van Loon LJC, Koopman R, Stegen JHCH, Wagenmakers AJM, Keizer HA, Saris WHM. Intramyocellular lipids form an important substrate source during moderate intensity exercise in endurance-trained males in a fasted state. J Physiol. 2003;553(Pt 2):611–25.

109. van Loon LJ, Thomason-Hughes M, Constantin-Teodosiu D, Koopman R, Greenhaff PL, Hardie DG, et al. Inhibition of adipose tissue lipolysis increases intramuscular lipid and glycogen use in vivo in humans. Am J Physiol - Endocrinol Metab. 2005;289(3):E482–93.

110. Lj VL, Pl G. The effects of increasing exercise intensity on muscle fule utilisation in humans. J Physiol. 2001;536:295–304.

111. Alsted TJ, Ploug T, Prats C, Serup AK, Hoeg L, Schjerling P, et al. Contraction-induced lipolysis is not impaired by inhibition of hormone-sensitive lipase in skeletal muscle. J Physiol. 2013;591(20):5141-55.

112. van Loon LJC. Use of intramuscular triacylglycerol as a substrate source during exercise in humans. J Appl Physiol. 2004;97(4):1170–87.

113. Schenk S, Horowitz JF. Acute exercise increases triglyceride synthesis in skeletal muscle and prevents fatty acid-induced insulin resistance. J Clin Invest. 2007;117(6):1690–8.

114. Koves TR, Sparks LM, Kovalik JP, Mosedale M, Arumugam R, Debalsi KL, et al. PPARγ coactivator-1α contributes to exercise-induced regulation of intramuscular lipid droplet programming in mice and humans. J Lipid Res. 2013;54(2):522–34.

115. Amati F, Dube JJ, Alvarez-Carnero E, Edreira MM, Chomentowski P, Coen PM, et al. Skeletal muscle triglycerides, diacylglycerols, and ceramides in insulin resistance: Another paradox in endurance-trained athletes? Diabetes. 2011;60(10):2588–97.

116. Dubé JJ, Amati F, Stefanovic-Racic M, Toledo FGS, Sauers SE, Goodpaster BH. Exercise-induced alterations in intramyocellular lipids and insulin resistance: the athlete's paradox revisited. Am J Physiol Endocrinol Metab. 2008;294(5):E882–8.

117. Pruchnic R, Katsiaras A, He J, Kelley DE, Winters C, Goodpaster BH. Exercise training increases intramyocellular lipid and oxidative capacity in older adults. Am J Physiol Endocrinol Metab. 2004;287(5):E857-62.

118. Pilegaard H, Saltin B, Neufer PD. Exercise induces transient transcriptional activation of

the PGC-1alpha gene in human skeletal muscle. J Physiol. 2003;546(Pt 3):851–8.

119. Little JP, Safdar a., Cermak N, Tarnopolsky M a., Gibala MJ. Acute endurance exercise increases the nuclear abundance of PGC-1 in trained human skeletal muscle. AJP Regul Integr Comp Physiol. 2010;298(4):R912–7.

120. Rasbach K a., Gupta RK, Ruas JL, Wu J, Naseri E, Estall JL, et al. PGC-1α regulates a HIF2α-dependent switch in skeletal muscle fiber types. PNAS. 2010;107(50):21866–71.

121. Takikita S, Schreiner C, Baum R, Xie T, Ralston E, Plotz PH, et al. Fiber type conversion by PGC-1α activates lysosomal and autophagosomal biogenesis in both unaffected and pompe skeletal muscle. PLoS One. 2010;5(12): e15239.

122. Yamaguchi T, Suzuki T, Arai H, Tanabe S, Atomi Y. Continuous mild heat stress induces differentiation of mammalian myoblasts, shifting fiber type from fast to slow. Am J Physiol Cell Physiol. 2010;298(1):C140–8.

123. Nikolic N, Rhedin M, Rustan AC, Storlien L, Thoresen GH, Stromstedt M. Overexpression of PGC-1 alpha increases fatty acid oxidative capacity of human skeletal muscle cells. Biochem Res Int. 2012;2012:1–12.

124. Nikolić N, Rhedin M, Rustan AC, Storlien L, Thoresen GH, Strömstedt M. Overexpression of PGC-1alpha Increases Fatty Acid Oxidative Capacity of Human Skeletal Muscle Cells. Biochem Res Int. 2012;2012:714074.

125. Little JP, Safdar A, Bishop D, Tarnopolsky M a, Gibala MJ. An acute bout of high-intensity interval training increases the nuclear abundance of PGC-1{alpha} and activates mitochondrial biogenesis in human skeletal muscle. Am J Physiol Regul Integr Comp Physiol. 2011;300(6):R1303-10.

126. Goodpaster BHH, He J, Watkins S, Kelley DEE. Skeletal muscle lipid content and insulin resistance: Evidence for a paradox in endurance-trained athletes. J Clin Endocrinol Metab. 2001;86(12):5755–816.

127. Meex RCR, Schrauwen-Hinderling VB, Moonen-Kornips E, Schaart G, Mensink M, Phielix E, et al. Restoration of muscle mitochondrial function and metabolic flexibility in type 2 diabetes by exercise training is paralleled by increased myocellular fat storage and improved insulin sensitivity. Diabetes. 2010;59(3):572–9.

128. Haus JM, Solomon TPJ, Lu L, Jesberger J a, Barkoukis H, Flask C a, et al. Intramyocellular lipid content and insulin sensitivity are increased following a short-term

low-glycemic index diet and exercise intervention. Am J Physiol Endocrinol Metab. 2011;301(3):E511–6.

129. Bosma M, Kersten S, Hesselink MKC, Schrauwen P. Re-evaluating lipotoxic triggers in skeletal muscle: Relating intramyocellular lipid metabolism to insulin sensitivity. Prog Lipid Res. 2012;51(1):36–49.

130. Moro C, Bajpeyi S, Smith SR. Determinants of intramyocellular triglyceride turnover: implications for insulin sensitivity. Am J Physiol Endocrinol Metab. 2008;294:E203–13.

131. Van Loon LJC, Goodpaster BH. Increased intramuscular lipid storage in the insulin-resistant and endurance-trained state. Pflugers Arch Eur J Physiol. 2006;451(5):606–16.

132. Qatanani M, Mitchell A. Mechanism of Obesity Associated Insulin Resistance: Many Choices on the Menu. Genes Dev. 2007;21(215):1443–55.

133. Winzell MS, Ahrén B. The high-fat diet-fed mouse: a model for studying mechanisms and treatment of impaired glucose tolerance and type 2 diabetes. Diabetes. 2004;53 Suppl 3:S215-9.

134. Surwit RS, Kuhn CM, Cochrane C, McCubbin JA, Feinglos MN. Diet-induced type II diabetes in C57BL/6J mice. Diabetes. 1988;37(9):1163–7.

135. Charbonneau A, Marette A. Inducible nitric oxide synthase induction underlies lipid-induced hepatic insulin resistance in mice: Potential role of tyrosine nitration of insulin signaling proteins. Diabetes. 2010;59(4):861–71.

136. Shi H, Kokoeva M V, Inouye K, Tzameli I, Yin H, Flier JS. TLR4 links innate immunity and fatty acid − induced insulin resistance. J Clin Invest. 2006;116(11):3015–25.

137. Brüning JC, Michael MD, Winnay JN, Hayashi T, Hörsch D, Accili D, et al. A muscle-specific insulin receptor knockout exhibits features of the metabolic syndrome of NIDDM without altering glucose tolerance. Mol Cell. 1998;2(5):559–69.

138. Hofmann SM, Perez-Tilve D, Greer TM, Coburn BA, Grant E, Basford JE, et al. Defective lipid delivery modulates glucose tolerance and metabolic response to diet in apolipoprotein E-deficient mice. Diabetes. 2008;57(1):5–12.

139. Kim JK, Fillmore JJ, Chen Y, Yu C, Moore IK, Pypaert M, et al. Tissue-specific overexpression of lipoprotein lipase causes tissue-specific insulin resistance. Proc Natl Acad Sci U S A. 2001;98(13):7522–7.

140. Turinsky J, O'Sullivan DM, Bayly BP. 1,2-diacylglycerol and ceramide levels in insulin-

resistant tissues of the rat in vivo. J Biol Chem. 1990;265(28):16880–5.

141. Itani SI, Ruderman NB, Schmieder F, Boden G. Lipid-induced insulin resistance in human muscle is associated with changes in diacylglycerol, protein kinase C, and IkappaB-alpha. Diabetes. 2002;51(7):2005–11.

142. Bergman BC, Hunerdosse DM, Kerege A, Playdon MC, Perreault L. Localisation and composition of skeletal muscle diacylglycerol predicts insulin resistance in humans. Diabetologia. 2012;55(4):1140–50.

143. Bergman BC, Perreault L, Hunerdosse DM, Koehler MC, Samek AM, Eckel RH. Increased intramuscular lipid synthesis and low saturation relate to insulin sensitivity in endurance-trained athletes. J Appl Physiol. 2010;108(5):1134–41.

144. Yu C, Chen Y, Cline GW, Zhang D, Zong H, Wang Y, et al. Mechanism by which fatty acids inhibit insulin activation of insulin receptor substrate-1 (IRS-1)-associated phosphatidylinositol 3-kinase activity in muscle. J Biol Chem. 2002;277(52):50230–6.

145. Gual P, Le Marchand-Brustel Y, Tanti J-F. Positive and negative regulation of insulin signaling through IRS-1 phosphorylation. Biochimie. 2005;87(1):99–109.

146. Boura-Halfon S, Zick Y. Phosphorylation of IRS proteins, insulin action, and insulin resistance. Am J Physiol Endocrinol Metab. 2009;296(4):E581–91.

147. Moro C, Galgani JE, Luu L, Pasarica M, Mairal A, Bajpeyi S, et al. Influence of gender, obesity, and muscle lipase activity on intramyocellular lipids in sedentary individuals. J Clin Endocrinol Metab. 2009;94(9):3440–7.

148. Coen PM, Dube JJ, Amati F, Stefanovic-racic M, Ferrell RE. Insulin resistance is associated with higher intramyocellular triglycerides in type I but not type II myocytes concomitant with higher ceramide content. Diabetes. 2010;59(1):80-8.

149. Adams JM, Pratipanawatr T, Berria R, Wang E, DeFronzo RA, Sullards MC, et al. Ceramide Content Is Increased in Skeletal Muscle from Obese Insulin-Resistant Humans. Diabetes. 2004;53(1):25–31.

150. Nordby P, Prats C, Kristensen D, Ekroos K, Forsberg G, Andersen JL, et al. Muscle ceramide content in man is higher in type i than type II fibers and not influenced by glycogen content. Eur J Appl Physiol. 2010;109(5):935–43.

151. Kristensen D, Prats C, Larsen S, Ara I, Dela F, Helge JW. Ceramide content is higher in type i compared to type II fibers in obesity and type 2 diabetes mellitus. Acta Diabetol.

2013;50(5):705–12.

152. Bergman BC, Brozinick JT, Strauss A, Bacon S, Kerege A, Bui HH, et al. Muscle sphingolipids during rest and exercise: a C18:0 signature for insulin resistance in humans. Diabetologia. 2016;59(4):785–98.

153. Petersen KF, Shulman GI. Etiology of insulin resistance. Am J Med. 2006;119(5 suppl 1):S10-6.

154. Petersen KF, Befroy D, Dufour S, Dziura J, Ariyan C, Rothman DL, et al. Mitochondrial dysfunction in the elderly: possible role in insulin resistance. Science. 2003;300(5622):1140–2.

155. Petersen KF, Dufour S, Befroy D, Garcia R, Shulman GI. Impaired mitochondrial activity in the insulin-resistant offspring of patients with type 2 diabetes. N Engl J Med. 2004;350(7):664–71.

156. Wu Z, Puigserver P, Andersson U, Zhang C, Adelmant G, Mootha V, et al. Mechanisms controlling mitochondrial biogenesis and respiration through the thermogenic coactivator PGC-1. Cell. 1999;98(1):115–24.

157. St-Pierre J, Lin J, Krauss S, Tarr PT, Yang R, Newgard CB, et al. Bioenergetic analysis of peroxisome proliferator-activated receptor gamma coactivators 1alpha and 1beta (PGC-1alpha and PGC-1beta) in muscle cells. J Biol Chem. 2003;278(29):26597–603.

158. Lagouge M, Argmann C, Gerhart-Hines Z, Meziane H, Lerin C, Daussin F, et al. Resveratrol Improves Mitochondrial Function and Protects against Metabolic Disease by Activating SIRT1 and PGC-1α. Cell. 2006;127(6):1109–22.

159. Mensink M, Hesselink MKC, Russell a P, Schaart G, Sels J-P, Schrauwen P. Improved skeletal muscle oxidative enzyme activity and restoration of PGC-1 alpha and PPAR beta/delta gene expression upon rosiglitazone treatment in obese patients with type 2 diabetes mellitus. Int J Obes (Lond). 2007;31(8):1302–10.

160. Choi CS, Befroy DE, Codella R, Kim S, Reznick RM, Hwang Y-J, et al. Paradoxical effects of increased expression of PGC-1a on muscle mitochondrial function and insulin-stimulated muscle glucose metabolism. Proc Natl Acad Sci U S A. 2008;105(50):19926–31.

161. Bandyopadhyay GK, Yu JG, Ofrecio J, Olefsky JM. Increased malonyl-CoA levels in muscle from obese and type 2 diabetic subjects lead to decreased fatty acid oxidation and

increased lipogenesis; thiazolidinedione treatment reverses these defects. Diabetes. 2006;55(8):2277–85.

162. Holloway GP, Thrush a B, Heigenhauser GJF, Tandon NN, Dyck DJ, Bonen A, et al. Skeletal muscle mitochondrial FAT/CD36 content and palmitate oxidation are not decreased in obese women. Am J Physiol Endocrinol Metab. 2007;292(6):E1782–9.

163. Trenell MI, Hollingsworth KG, Lim EL, Taylor R. Increased daily walking improves lipid oxidation without changes in mitochondrial function in type 2 diabetes. Diabetes Care. 2008;31(8):1644–9.

164. van Tienen FHJ, Praet SFE, de Feyter HM, van den Broek NM, Lindsey PJ, Schoonderwoerd KGC, et al. Physical activity is the key determinant of skeletal muscle mitochondrial function in type 2 diabetes. J Clin Endocrinol Metab. 2012;97(9):3261–9.

165. Morino K, Petersen KF, Shulman GI. Molecular mechanisms of insulin resistance in humans and their potential links with mitochondrial dysfunction. Diabetes. 2006;55(Suppl. 2)S9-15.

166. Shaw CS, Sherlock M, Stewart PM, Wagenmakers AJM. Adipophilin distribution and colocalisation with lipid droplets in skeletal muscle. Histochem Cell Biol. 2009;131(5):575–81.

167. Kimmel AR, Brasaemle DL, McAndrews-Hill M, Sztalryd C, Londos C. Adoption of PERILIPIN as a unifying nomenclature for the mammalian PAT-family of intracellular lipid storage droplet proteins. J Lipid Res. 2010;51(3):468–71.

168. Londos C, Brasaemle DL, Gruia-Gray J, Servetnick D a, Schultz CJ, Levin DM, et al. Perilipin: unique proteins associated with intracellular neutral lipid droplets in adipocytes and steroidogenic cells. Biochem Soc Trans. 1995;23(3):611–5.

169. Gjelstad IMF, Haugen F, Gulseth HL, Norheim F, Jans A, Bakke SS, et al. Expression of perilipins in human skeletal muscle in vitro and in vivo in relation to diet, exercise and energy balance. Arch Physiol Biochem. 2012;118(1):22–30.

170. Brasaemle DL, Rubin B, Harten IA, Gruia-Gray J, Kimmel AR, Londos C. Perilipin A increases triacylglycerol storage by decreasing the rate of triacylglycerol hydrolysis. J Biol Chem. 2000;275(49):38486–93.

171. Beylot M, Neggazi S, Hamlat N, Langlois D, Forcheron F. Perilipin 1 ablation in mice enhances lipid oxidation during exercise and does not impair exercise performance.

Metabolism. 2012;61(3):415–23.

172. Sztalryd C, Xu G, Dorward H, Tansey JT, Contreras JA, Kimmel AR, et al. Perilipin A is essential for the translocation of hormone-sensitive lipase during lipolytic activation. J Cell Biol. 2003;161(6):1093–103.

173. Brasaemle DL. Thematic review series: adipocyte biology. The perilipin family of structural lipid droplet proteins: stabilization of lipid droplets and control of lipolysis. J Lipid Res. 2007;48(12):2547–59.

174. Brasaemle DL, Levin DM, Adler-Wailes DC, Londos C. The lipolytic stimulation of 3T3-L1 adipocytes promotes the translocation of hormone-sensitive lipase to the surfaces of lipid storage droplets. Biochim Biophys Acta - Mol Cell Biol Lipids. 2000;1483(2):251–62.

175. Su CL, Sztalryd C, Contreras JA, Holm C, Kimmel AR, Londos C. Mutational Analysis of the Hormone-sensitive Lipase Translocation Reaction in Adipocytes. J Biol Chem. 2003;278(44):43615–9.

176. Tansey JT, Sztalryd C, Gruia-Gray J, Roush DL, Zee J V, Gavrilova O, et al. Perilipin ablation results in a lean mouse with aberrant adipocyte lipolysis, enhanced leptin production, and resistance to diet-induced obesity. Proc Natl Acad Sci U S A. 2001;98:6494–9.

177. Martinez-Botas J, Anderson JB, Tessier D, Lapillonne A, Chang BH, Quast MJ, et al. Absence of perilipin results in leanness and reverses obesity in Lepr(db/db) mice. Nat Genet. 2000;26(4):474–9.

178. Granneman JG, Moore HPH, Granneman RL, Greenberg AS, Obin MS, Zhu Z. Analysis of lipolytic protein trafficking and interactions in adipocytes. J Biol Chem. 2007;282(8):5726–35.

179. Miyoshi H, Souza SC, Endo M, Sawada T, Perfield JW, Shimizu C, et al. Perilipin overexpression in mice protects against diet-induced obesity. J Lipid Res. 2010;51(5):975–82.

180. Hamann A, Flier JS, Lowell BB. Decreased brown fat markedly enhances susceptibility to diet-induced obesity, diabetes, and hyperlipidemia. Endocrinology. 1996;137(1):21–9.

181. Mottagui-Tabar S, Ryden M, Lofgren P, Faulds G, Hoffstedt J, Brookes AJ, et al. Evidence for an important role of perilipin in the regulation of human adipocyte lipolysis.

Diabetologia. 2003;46(6):789–97.

182. Wang Y, Sullivan S, Trujillo M, Lee M-J, Schneider SH, Brolin RE, et al. Perilipin expression in human adipose tissues: effects of severe obesity, gender, and depot. Obes Res. 2003;11(8):930–6.

183. Ray H, Pinteur C, Frering V, Beylot M, Large V. Depot-specific differences in perilipin and hormone-sensitive lipase expression in lean and obese. Lipids Health Dis. 2009;8:58.

184. Kern PA, Di Gregorio G, Lu T, Rassouli N, Ranganathan G. Perilipin expression in human adipose tissue is elevated with obesity. J Clin Endocrinol Metab. 2004;89(3):1352–8.

185. Heid HW, Moll R, Schwetlick I, Rackwitz HR, Keenan TW. Adipophilin is a specific marker of lipid accumulation in diverse cell types and diseases. Cell Tissue Res. 1998;294(2):309–21.

186. Bickel PE, Tansey JT, Welte MA. PAT proteins, an ancient family of lipid droplet proteins that regulate cellular lipid stores. Biochim Biophys Acta - Mol Cell Biol Lipids. 2009;1791(6):419–40.

187. Brasaemle DL, Barber T, Wolins NE, Serrero G, Blanchette-Mackie EJ, Londos C. Adipose differentiation-related protein is an ubiquitously expressed lipid storage droplet-associated protein. J Lipid Res. 1997;38(11):2249–63.

188. Wolins NE, Quaynor BK, Skinner JR, Schoenfish MJ, Tzekov A, Bickel PE. S3-12, adipophilin, and TIP47 package lipid in adipocytes. J Biol Chem. 2005;280(19):19146–55.

189. Xu G, Sztalryd C, Lu X, Tansey JT, Gan J, Dorward H, et al. Post-translational regulation of adipose differentiation-related protein by the ubiquitin/proteasome pathway. J Biol Chem. 2005;280(52):42841–7.

190. Masuda Y, Itabe H, Odaki M, Hama K, Fujimoto Y, Mori M, et al. ADRP/adipophilin is degraded through the proteasome-dependent pathway during regression of lipid-storing cells. J Lipid Res. 2006;47(1):87–98.

191. Andersson L, Boström P, Ericson J, Rutberg M, Magnusson B, Marchesan D, et al. PLD1 and ERK2 regulate cytosolic lipid droplet formation. J Cell Sci. 2006;119(Pt 11):2246–57.

192. Gao J, Serrero G. Adipose differentiation related protein (ADRP) expressed in transfected COS-7 cells selectively stimulates long chain fatty acid uptake. J Biol Chem.

1999;274(24):16825–30.

193. Imamura M, Inoguchi T, Ikuyama S, Taniguchi S, Kobayashi K, Nakashima N, et al. ADRP stimulates lipid accumulation and lipid droplet formation in murine fibroblasts. Am J Physiol Endocrinol Metab. 2002;283(4):E775–83.

194. Listenberger LL, Ostermeyer-Fay AG, Goldberg EB, Brown WJ, Brown D a. Adipocyte differentiation-related protein reduces the lipid droplet association of adipose triglyceride lipase and slows triacylglycerol turnover. J Lipid Res. 2007;48(12):2751–61.

195. Fukushima M, Enjoji M, Kohjima M, Sugimoto R, Ohta S, Kotoh K, et al. Adipose differentiation related protein induces lipid accumulation and lipid droplet formation in hepatic stellate cells. In Vitro Cell Dev Biol Anim. 2005;41(10):321–4.

196. Stone SJ, Levin MC, Zhou P, Han J, Walther TC, Farese R V. The endoplasmic reticulum enzyme DGAT2 is found in mitochondria-associated membranes and has a mitochondrial targeting signal that promotes its association with mitochondria. J Biol Chem. 2009;284(8):5352–61.

197. Bell M, Wang H, Chen H, McLenithan JC, Gong D-W, Yang R-Z, et al. Consequences of Lipid Droplet Coat Protein Downregulation in Liver Cells. Diabetes. 2008;57(8):2037–45.

198. Yamaguchi T, Omatsu N, Omukae A, Osumi T. Analysis of interaction partners for perilipin and ADRP on lipid droplets. Mol Cell Biochem. 2006;284(1–2):167–73.

199. Chang BH-J, Li L, Paul A, Taniguchi S, Nannegari V, Heird WC, et al. Protection against fatty liver but normal adipogenesis in mice lacking adipose differentiation-related protein. Mol Cell Biol. 2006;26(3):1063–76.

200. Bell M, Wang H, Chen H, McLenithan JC, Gong DW, Yang RZ, et al. Consequences of lipid droplet coat protein downregulation in liver cells: Abnormal lipid droplet metabolism and induction of insulin resistance. Diabetes. 2008;57(8):2037–45.

201. Bosma M, Hesselink MKC, Sparks LM, Timmers S, Ferraz MJ, Mattijssen F, et al. Perilipin 2 improves insulin sensitivity in skeletal muscle despite elevated intramuscular lipid levels. Diabetes. 2012;61(11):2679–90.

202. Vigelsø A, Prats C, Ploug T, Dela F, Helge JW. Human skeletal muscle perilipin 2 and 3 expression varies with insulin sensitivity. J Biomed Sci Eng. 2013;6(5):65–72.

203. Phillips SA, Choe CC, Ciaraldi TP, Greenberg AS, Kong AP, Baxi SC, et al. Adipocyte differentiation-related protein in human skeletal muscle: relationship to insulin sensitivity.

Obes Res. 2005;13(8):1321–9.

204. Shepherd SO, Cocks M, Tipton KD, Ranasinghe a M, Barker T a, Burniston JG, et al. Preferential utilization of perilipin 2-associated intramuscular triglycerides during 1 h of moderate-intensity endurance-type exercise. Exp Physiol. 2012;97(8):970–80.

205. Aivazian D, Serrano RL, Pfeffer S. TIP47 is a key effector for Rab9 localization. J Cell Biol. 2006;173(6):917–26.

206. Carroll KS, Hanna J, Simon I, Krise J, Barbero P, Pfeffer SR. Role of Rab9 GTPase in facilitating receptor recruitment by TIP47. Science. 2001;292(5520):1373–6.

207. Wolins NE, Rubin B, Brasaemle DL. TIP47 Associates with Lipid Droplets. J Biol Chem. 2001;276(7):5101–8.

208. Miura S, Gan JW, Brzostowski J, Parisi MJ, Schultz CJ, Londos C, et al. Functional conservation for lipid storage droplet association among perilipin, ADRP, and TIP47 (PAT)-related proteins in mammals, Drosophila, and Dictyostelium. J Biol Chem. 2002;277(35):32253–7.

209. Hocsak E, Racz B, Szabo A, Mester L, Rapolti E, Pozsgai E, et al. TIP47 protects mitochondrial membrane integrity and inhibits oxidative-stress-induced cell death. FEBS Lett. 2010;584(13):2953–60.

210. Skinner JR, Shew TM, Schwartz DM, Tzekov A, Lepus CM, Abumrad NA, et al. Diacylglycerol enrichment of endoplasmic reticulum or lipid droplets recruits perilipin 3/TIP47 during lipid storage and mobilization. J Biol Chem. 2009;284(45):30941–8.

211. Buers I, Robenek H, Lorkowski S, Nitschke Y, Severs NJ, Hofnagel O. TIP47, a lipid cargo protein involved in macrophage triglyceride metabolism. Arterioscler Thromb Vasc Biol. 2009;29(5):767–73.

212. Gu J-Q, Wang D-F, Yan X-G, Zhong W-L, Zhang J, Fan B, et al. A Toll-like receptor 9-mediated pathway stimulates perilipin 3 (TIP47) expression and induces lipid accumulation in macrophages. Am J Physiol Endocrinol Metab. 2010;299(4):E593–600.

213. Sztalryd C, Bell M, Lu X, Mertz P, Hickenbottom S, Chang BHJ, et al. Functional compensation for Adipose Differentiation-related Protein (ADFP) by Tip47 in an ADFP null embryonic cell line. J Biol Chem. 2006;281(45):34341–8.

214. Carr RM, Patel RT, Rao V, Dhir R, Graham MJ, Crooke RM, et al. Reduction of TIP47 improves hepatic steatosis and glucose homeostasis in mice. Am J Physiol Regul Integr

Comp Physiol. 2012;302(8):R996-1003.

215. Peters SJ, Samjoo I a., Devries MC, Stevic I, Robertshaw H a., Tarnopolsky M a. Perilipin family (PLIN) proteins in human skeletal muscle: the effect of sex, obesity, and endurance training. Appl Physiol Nutr Metab. 2012;37(4):724–35.

216. Louche K, Badin PM, Montastier E, Laurens C, Bourlier V, De Glisezinski I, et al. Endurance exercise training up-regulates lipolytic proteins and reduces triglyceride content in skeletal muscle of obese subjects. J Clin Endocrinol Metab. 2013;98(12):4863–71.

217. MacPherson REK, Ramos S V, Vandenboom R, Roy BD, Peters SJ. Skeletal muscle PLIN proteins, ATGL and CGI-58, interactions at rest and following stimulated contraction. Am J Physiol Regul Integr Comp Physiol. 2013;304(8):R644-50.

218. Macpherson RE, Vandenboom R, Roy BD, Peters SJ. Skeletal muscle PLIN3 and PLIN5 are serine phosphorylated at rest and following lipolysis during adrenergic or contractile stimulation. Physiol Rep. 2013;1(4):e00084.

219. Scherer PE, Bickel PE, Kotler M, Lodish HF. Cloning of cell-specific secreted and surface proteins by subtractive antibody screening. Nat Biotechnol. 1998;16(6):581–6.

220. Wolins NE, Skinner JR, Schoenfish MJ, Tzekov A, Bensch KG, Bickel PE. Adipocyte protein S3-12 coats nascent lipid droplets. J Biol Chem. 2003;278(39):37713–21.

221. Chen W, Chang B, Wu X, Li L, Sleeman M, Chan L. Inactivation of Plin4 downregulates Plin5 and reduces cardiac lipid accumulation in mice. Am J Physiol Endocrinol Metab. 2013;304(7):E770-9.

222. Yamaguchi T, Matsushita S, Motojima K, Hirose F, Osumi T. MLDP, a novel PAT family protein localized to lipid droplets and enriched in the heart, is regulated by peroxisome proliferator-activated receptor α. J Biol Chem. 2006;281(20):14232–40.

223. Minnaard R, Schrauwen P, Schaart G, Jorgensen JA, Lenaers E, Mensink M, et al. Adipocyte differentiation-related protein and OXPAT in rat and human skeletal muscle: Involvement in lipid accumulation and type 2 diabetes mellitus. J Clin Endocrinol Metab. 2009;94(10):4077–85.

224. Kuramoto K, Okamura T, Yamaguchi T, Nakamura TY, Wakabayashi S, Morinaga H, et al. Perilipin 5, a lipid droplet-binding protein, protects heart from oxidative burden by sequestering fatty acid from excessive oxidation. J Biol Chem. 2012;287(28):23852–63.

225. Wang H, Sreenivasan U, Sreenevasan U, Hu H, Saladino A, Polster BM, et al. Perilipin 5, a lipid droplet-associated protein, provides physical and metabolic linkage to mitochondria. J Lipid Res. 2011;52(12):2159–68.

226. Bosma M, Minnaard R, Sparks LM, Schaart G, Losen M, De Baets MH, et al. The lipid droplet coat protein perilipin 5 also localizes to muscle mitochondria. Histochem Cell Biol. 2012;137(2):205–16.

227. Bosma M, Sparks LM, Hooiveld GJ, Jorgensen JA, Houten SM, Schrauwen P, et al. Overexpression of PLIN5 in skeletal muscle promotes oxidative gene expression and intramyocellular lipid content without compromising insulin sensitivity. Biochim Biophys Acta - Mol Cell Biol Lipids. 2013;1831(4):844–52.

228. Shepherd SO, Cocks M, Tipton KD, Ranasinghe a M, Barker T a, Burniston JG, et al. Sprint interval and traditional endurance training increase net intramuscular triglyceride breakdown and expression of perilipin 2 and 5. J Physiol. 2013;591(Pt 3):657–75.

229. Mason RR, Watt MJ. Unraveling the roles of PLIN5: Linking cell biology to physiology. Trends Endocrinol Metab. 2015;26(3):144–52.

230. Wang C, Zhao Y, Gao X, Li L, Yuan Y, Liu F, et al. Perilipin 5 improves hepatic lipotoxicity by inhibiting lipolysis. Hepatology. 2015; 61(3):870-82.

231. Pollak NM, Schweiger M, Jaeger D, Kolb D, Kumari M, Schreiber R, et al. Cardiac-specific overexpression of perilipin 5 provokes severe cardiac steatosis via the formation of a lipolytic barrier. J Lipid Res. 2013;54(4):1092–102.

232. Wang H. Cardiomyocyte specific perilipin 5 overexpression leads to myocardial steatosis, and modest cardiac dysfunction. J Chem Inf Model. 2013;53(9):1689–99.

233. Trevino MB, Machida Y, Hallinger DR, Garcia E, Christensen A, Dutta S, et al. Perilipin 5 regulates islet lipid metabolism and insulin secretion in a cAMP-dependent manner: implication of its role in the postprandial insulin secretion. Diabetes. 2015;64(4):1299–310.

234. MacPherson REK, Herbst E a. F, Reynolds EJ, Vandenboom R, Roy BD, Peters SJ. Subcellular localization of skeletal muscle lipid droplets and PLIN family proteins OXPAT and ADRP at rest and following contraction in rat soleus muscle. AJP Regul Integr Comp Physiol. 2012;302(25):R29–36.

235. Holloszy JO, Coyle EF. Adaptations of skeletal muscle to endurance exercise and their

metabolic consequences. J Appl Physiol. 1984;56(4):831–8.

236. Holloszy JO. Biochemical adaptations in muscle. Effects of exercise on mitochondrial oxygen uptake and respiratory enzyme activity in skeletal muscle. J Biol Chem. 1967;242(9):2278–82.

237. Ramos S V, MacPherson REK, Turnbull PC, Bott KN, LeBlanc P, Ward WE, et al. Higher PLIN5 but not PLIN3 content in isolated skeletal muscle mitochondria following acute in vivo contraction in rat hindlimb. Physiol Rep. 2014;2(10):1–12.

238. DeFronzo RA, Eldor R, Abdul-Ghani M. Pathophysiologic approach to therapy in patients with newly diagnosed type 2 diabetes. Diabetes Care. 2013;36 Suppl 2:S127-38.

239. Rinnankoski-Tuikka R, Hulmi JJ, Torvinen S, Silvennoinen M, Lehti M, Kivelä R, et al. Lipid droplet-associated proteins in high-fat fed mice with the effects of voluntary running and diet change. Metabolism. 2014;63(8):1031–40.

240. Badin PM, Vila IK, Louche K, Mairal A, Marques MA, Bourlier V, et al. High-fat diet-mediated lipotoxicity and insulin resistance is related to impaired lipase expression in mouse skeletal muscle. Endocrinology. 2013;154(4):1444–53.

241. Boström P, Andersson L, Vind B, Håversen L, Rutberg M, Wickström Y, et al. The SNARE protein SNAP23 and the SNARE-interacting protein Munc18c in human skeletal muscle are implicated in insulin resistance/type 2 diabetes. Diabetes. 2010;59(8):1870–8.

242. Coen PM, Hames KC, Leachman EM, Delany JP, Ritov VB, Menshikova E V., et al. Reduced skeletal muscle oxidative capacity and elevated ceramide but not diacylglycerol content in severe obesity. Obesity. 2013;21(11):2362–71.

243. Kelley D, Mitrakou A, Marsh H, Schwenk F, Benn J, Sonnenberg G, et al. Skeletal muscle glycolysis, oxidation, and storage of an oral glucose load. J Clin Invest. 1988;81(5):1563–71.

244. Krssak M, Falk Petersen K, Dresner A, DiPietro L, Vogel SM, Rothman DL, et al. Intramyocellular lipid concentrations are correlated with insulin sensitivity in humans: A 1H NMR spectroscopy study. Diabetologia. 1999;42(1):113–6.

245. Pan D, Lillioja S, Kriketos D, Milner M, Baur L, Bogardus C, et al. Skeletal muscle triglyceride levels are inversely related to insulin action. Diabetes. 1997;46(6):983–8.

246. Perseghin G, Scifo P, F DC, Pagliato E, Battezzati a, Arcelloni C, et al. Intramyocellular triglyceride content is a determinan of in vivo insulin resistance in humans. Diabetes.

1999;48(8):1600–6.

247. Jacob S, Machann J, Rett K, Brechtel K, Volk A, Renn W, et al. Association of increased intramyocellular lipid content with insulin resistance in lean nondiabetic offspring of type 2 diabetic subjects. Diabetes. 1999;48(5):1113–9.

248. Fujimoto T, Parton RG. Not just fat: The structure and function of the lipid droplet. Cold Spring Harb Perspect Biol. 2011;3(3):1–17.

249. Banke NH, Wende AR, Leone TC, O'Donnell JM, Abel ED, Kelly DP, et al. Preferential oxidation of triacylglyceride-derived fatty acids in heart is augmented by the nuclear receptor PPARα. Circ Res. 2010;107(2):233–41.

250. Watt MJ, Hoy AJ. Lipid metabolism in skeletal muscle: generation of adaptive and maladaptive intracellular signals for cellular function. Am J Physiol - Endocrinol Metab. 2012;302(11):E1315–28.

251. Levin MC, Monetti M, Watt MJ, Sajan MP, Stevens RD, Bain JR, et al. Increased lipid accumulation and insulin resistance in transgenic mice expressing DGAT2 in glycolytic (type II) muscle. Am J Physiol Endocrinol Metab. 2007;293(6):E1772–81.

252. Nagle CA, An J, Shiota M, Torres TP, Cline GW, Liu ZX, et al. Hepatic overexpression of glycerol-sn-3-phosphate acyltransferase 1 in rats causes insulin resistance. J Biol Chem. 2007;282(20):14807–15.

253. McManaman JL, Bales ES, Orlicky DJ, Jackman M, MacLean PS, Cain S, et al. Perilipin-2-null mice are protected against diet-induced obesity, adipose inflammation, and fatty liver disease. J Lipid Res. 2013;54(5):1346–59.

254. Imai Y, Boyle S, Varela GM, Caron E, Yin X, Dhir R, et al. Effects of perilipin 2 antisense oligonucleotide treatment on hepatic lipid metabolism and gene expression. Physiol Genomics. 2012;44(22):1125–31.

255. Wang H, Sreenivasan U, Gong D-W, O'Connell K a, Dabkowski ER, Hecker P a, et al. Cardiomyocyte-specific perilipin 5 overexpression leads to myocardial steatosis and modest cardiac dysfunction. J Lipid Res. 2013;54(4):953–65.

256. Frayn KN. Calculation of substrate oxidation rates in vivo from gaseous exchange. J Appl Physiol. 1983;55(2):628–34.

257. Folch J, Lees M, Sloane Stanley G. A simple method for the isolation and purification of total lipides from animal tissues. J Biol Chem. 1957;226:497–509.

258. Watt MJ, Hevener A, Lancaster GI, Febbraio MA. Ciliary neurotrophic factor prevents acute lipid-induced insulin resistance by attenuating ceramide accumulation and phosphorylation of c-Jun N-terminal kinase in peripheral tissues. Endocrinology. 2006;147(5):2077–85.

259. Borg ML, Andrews ZB, Duh EJ, Zechner R, Meikle PJ, Watt MJ. Pigment epithelium-derived factor regulates lipid metabolism via adipose triglyceride lipase. Diabetes. 2011;60(5):1458–66.

260. Turner N, Kowalski GM, Leslie SJ, Risis S, Yang C, Lee-Young RS, et al. Distinct patterns of tissue-specific lipid accumulation during the induction of insulin resistance in mice by high-fat feeding. Diabetologia. 2013;56(7):1638–48.

261. Crowe S, Turpin SM, Ke F, Kemp BE, Watt MJ. Metabolic remodeling in adipocytes promotes ciliary neurotrophic factor-mediated fat loss in obesity. Endocrinology. 2008;149(5):2546–56.

262. Mokbel N, Ilkovski B, Kreissl M, Memo M, Jeffries CM, Marttila M, et al. K7del is a common TPM2 gene mutation associated with nemaline myopathy and raised myofibre calcium sensitivity. Brain. 2013;136(2):494–507.

263. Peters SJ, Dyck DJ, Bonen A, Spriet LL. Effects of epinephrine on lipid metabolism in resting skeletal muscles. Am J Physiol Physiol. 1998;275(2 Pt 1):E300–9.

264. Rolfe DFS, Brown GC. Cellular Energy Utilization of Standard Metabolic and Molecular Origin Rate in Mammals. Physiol Rev. 1997;77(3):731–58.

265. Watt MJ, Stellingwerff T, Heigenhauser GJF, Spriet LL. Effects of plasma adrenaline on hormone-sensitive lipase at rest and during moderate exercise in human skeletal muscle. J Physiol. 2003;550(Pt 1):325–32.

266. Jocken JWE, Blaak EE. Catecholamine-induced lipolysis in adipose tissue and skeletal muscle in obesity. Physiol Behav. 2008;94(2):219–30.

267. Ahmadian M, Duncan RE, Varady KA, Frasson D, Hellerstein MK, Birkenfeld AL, et al. Adipose overexpression of desnutrin promotes fatty acid use and attenuates diet-induced obesity. Diabetes. 2009;58(4):855–66.

268. Bjørbæk C, El-haschimi K, Frantz D, Flier JS, Bjørbæk C, El-haschimi K, et al. CELL BIOLOGY AND METABOLISM : The Role of SOCS-3 in Leptin Signaling and Leptin Resistance The Role of SOCS-3 in Leptin Signaling and Leptin Resistance *. J Biol

Chem. 1999;274(42):30059–65.

269. Hoy AJ, Bruce CR, Turpin SM, Morris AJ, Febbraio MA, Watt MJ. Adipose triglyceride lipase-null mice are resistant to high-fat diet-induced insulin resistance despite reduced energy expenditure and ectopic lipid accumulation. Endocrinology. 2011;152(1):48–58.

270. Samuel VT, Shulman GI. Mechanisms for insulin resistance: Common threads and missing links. Cell. 2012;148(5):852–71.

271. Greenberg AS, Coleman R a, Kraemer FB, Mcmanaman JL, Obin MS, Puri V, et al. Review series The role of lipid droplets in metabolic disease in rodents and humans. J Clin Invest. 2011;121(6) :2102-10.

272. Bartholomew SR, Bell EH, Summerfield T, Newman LC, Miller EL, Patterson B, et al. Distinct cellular pools of perilipin 5 point to roles in lipid trafficking. Biochim Biophys Acta - Mol Cell Biol Lipids. 2012;1821(2):268–78.

273. Granneman JG, Moore HPH, Krishnamoorthy R, Rathod M. Perilipin controls lipolysis by regulating the interactions of AB-hydrolase containing 5 (Abhd5) and adipose triglyceride lipase (Atgl). J Biol Chem. 2009;284(50):34538–44.

274. Goodpaster BH. Mitochondrial deficiency is associated with insulin resistance. Diabetes. 2013;62(4):1032–5.

275. Hoehn KL, Turner N, Swarbrick MM, Wilks D, Preston E, Phua Y, et al. Acute or Chronic Upregulation of Mitochondrial Fatty Acid Oxidation Has No Net Effect on Whole-Body Energy Expenditure or Adiposity. Cell Metab. 2010;11(1):70–6.

276. Sapiro JM, Mashek MT, Greenberg AS, Mashek DG. Hepatic triacylglycerol hydrolysis regulates peroxisome proliferator-activated receptor alpha activity. J Lipid Res. 2009;50(8):1621–9.

277. Frayn KN, Humphreys SM, Coppack SW. Fuel Selection in White Adipose Tissue. Proc Nutr Soc. 1995;54(1):177–89.

278. Rohner-Jeanrenaud F, Proietto J, Ionescu E, Jeanrenaud B. Mechanism of abnormal oral glucose tolerance of genetically obese fa/fa rats. Diabetes. 1986;35(12):1350–5.

279. Mitrakou a, Mitrakou a, Kelley D, Kelley D, Veneman T, Veneman T, et al. Contribution of Abnormal Muscle and Liver Glucose-Metabolism to Postprandial Hyperglycemia in Niddm. Diabetes. 1990;39(11):1381–90.

280. Best JD, Kahn SE, Ader M, Watanabe RM, Ni TC, Bergman RN. Role of Glucose

Effectiveness in the Determination of Glucose Tolerance. Diabetes Care. 1996;19(9):1018–30.

281. Langhi C, Marquart TJ, Allen RM, Baldan A. Perilipin-5 is regulated by statins and controls triglyceride contents in the hepatocyte. J Hepatol. 2014;61(2):358–65.

282. Li H, Song Y, Zhang LJ, Gu Y, Li FF, Pan SY, et al. LSDP5 enhances triglyceride storage in hepatocytes by influencing lipolysis and fatty acid β-oxidation of lipid droplets. PLoS One. 2012;7(6): e36712.

283. Mason RR, Mokhtar R, Matzaris M, Selathurai A, Kowalski GM, Mokbel N, et al. PLIN5 deletion remodels intracellular lipid composition and causes insulin resistance in muscle. Mol Metab. 2014;3(6):652–63.

284. Harris L-ALS, Skinner JR, Shew TM, Pietka TA, Abumrad NA, Wolins NE. Perilipin 5-Driven Lipid Droplet Accumulation in Skeletal Muscle Stimulates the Expression of Fibroblast Growth Factor 21. Diabetes. 2015;64(8):2757–68.

285. Hua Gu, Jamey D. Marth, Paul C. Orban, Host Mossmann KR. Deletion of a DNA polymerase (beta) gene segment in T cells Using Cell Type-Specific Gene Targeting. Science. 1994;265(5168):103–6.

286. Kowalski GM, Kloehn J, Burch ML, Selathurai A, Hamley S, Bayol SAM, et al. Overexpression of sphingosine kinase 1 in liver reduces triglyceride content in mice fed a low but not high-fat diet. Biochim Biophys Acta. 2015;1851(2):210–9.

287. Trask R V., Billadello JJ. Tissue-specific distribution and developmental regulation of M and B creatine kinase mRNAs. BBA - Gene Struct Expr. 1990;1049(2):182–8.

288. Wijesekara N, Konrad D, Eweida M, Jefferies C, Liadis N, Giacca A, et al. Muscle-Specific Pten Deletion Protects against Insulin Resistance and Diabetes Muscle-Specific Pten Deletion Protects against Insulin Resistance and Diabetes. 2005;25(3):1135–45.

289. Deng C-X. The Use of Cre–loxP Technology and Inducible Systems to Generate Mouse Models of Cancer. In: Green, JE RT, editor. Genetically Engineered Mice for Cancer Research: Design, Analysis, Pathways, Validation and Pre-Clinical Testing. Springer; 2012. p. 17–36.

290. Javed F, He Q, Davidson LE, Thornton JC, Albu J, Boxt L, et al. Brain and high metabolic rate organ mass: Contributions to resting energy expenditure beyond fat-free mass. Am J Clin Nutr. 2010;91(4):907–12.

291. Veatch JR, McMurray MA, Nelson ZW, Gottschling DE. Mitochondrial Dysfunction Leads to Nuclear Genome Instability via an Iron-Sulfur Cluster Defect. Cell. 2009;137(7):1247–58.

292. Lopaschuk GD, Ussher JR, Folmes CDL, Jaswal JS, STANLEY WC. Myocardial Fatty Acid Metabolism in Health and Disease. Physiol Rev. 2010;90(1):207–58.

293. Trevino MB, Mazur-Hart D, Machida Y, King T, Nadler J, Galkina E V, et al. Liver Perilipin5 expression worsens hepatosteatosis but not insulin resistance in high fat fed mice. Mol Endocrinol. 2015;29(10):1414-25.

294. Wiernsperger NF. Is non-insulin dependent glucose uptake a therapeutic alternative ? Part 1 : physiology , mechanisms and role of non insulin-dependent glucose uptake in type 2 diabetes. Diabetes metab. 2005;31(5):415–26.

295. Abu-Elheiga L, Matzuk MM, Abo-Hashema K a, Wakil SJ. Continuous fatty acid oxidation and reduced fat storage in mice lacking acetyl-CoA carboxylase 2. Science. 2001;291(5513):2613–6.

296. Choi CS, Savage DB, Abu-Elheiga L, Liu Z-X, Kim S, Kulkarni A, et al. Continuous fat oxidation in acetyl-CoA carboxylase 2 knockout mice increases total energy expenditure, reduces fat mass, and improves insulin sensitivity. Proc Natl Acad Sci U S A. 2007;104(42):16480–5.

297. Dagenais GR, Tancredi RG, Zierler KL. Free fatty acid oxidation by forearm muscle at rest, and evidence for an intramuscular lipid pool in the human forearm. J Clin Invest. 1976;58(2):421–31.

298. Yang L, Ding Y, Chen Y, Zhang S, Huo C, Wang Y, et al. The proteomics of lipid droplets: structure, dynamics, and functions of the organelle conserved from bacteria to humans. J Lipid Res. 2012;53(7):1245-53.

299. Zechner R, Zimmermann R, Eichmann TO, Kohlwein SD, Haemmerle G, Lass A, et al. FAT SIGNALS - Lipases and lipolysis in lipid metabolism and signaling. Cell Metab. 2012;15(3):279–91.

300. Granneman JG, Moore HPH, Mottillo EP, Zhu Z. Functional interactions between Mldp (LSDP5) and Abhd5 in the control of intracellular lipid accumulation. J Biol Chem. 2009;284(5):3049–57.

301. Murphy RM. Enhanced technique to measure proteins in single segments of human

skeletal muscle fibers: fiber-type dependence of AMPK-alpha1 and -beta1. J Appl Physiol. 2011;110(3):820–5.

302. Hawley JA, Hargreaves M, Joyner MJ, Zierath JR. Integrative biology of exercise. Cell. 2014;159(4):738–49.

303. Schuh RA, Jackson KC, Khairallah RJ, Ward CW, Spangenburg EE. Measuring mitochondrial respiration in intact single muscle fibers. AJP Regul Integr Comp Physiol. 2012;302(6):R712–9.

304. Lowry OH, Passoneau JV. A Flexible System of Enzymatic Analysis. A Flex Syst Enzym Anal. 1972;1:263–82.

305. Horowitz JF, Klein S. Lipid metabolism during endurance exercise. Am J Clin Nutr. 2000;72(2 Suppl):558S–63S.

306. Saddik M, Lopaschuk GD. Myocardial triglyceride turnover and contribution to energy substrate utilization in isolated working rat hearts. J Biol Chem. 1991;266(13):8162–70.

307. Stellingwerff T, Boon H, Jonkers R a M, Senden JM, Spriet LL, Koopman R, et al. Significant intramyocellular lipid use during prolonged cycling in endurance-trained males as assessed by three different methodologies. Am J Physiol Endocrinol Metab. 2007;292(6):E1715–23.

308. Holloszy JO. Biochemical adaptations in muscle. Effects of exercise on mitochondrial oxygen uptake and respiratory enzyme activity in skeletal muscle. J Biol Chem. 1967;242(9):2278–82.

309. Pollak NM. Cardiac-specific overexpression of PLIN5 provokes severe cardiac steatosis via the formation of a lipolytic barrier. J Chem Inf Model. 2013;53(9):1689–99.

310. O'Donnell JM, Fields AD, Sorokina N, Lewandowski ED. The absence of endogenous lipid oxidation in early stage heart failure exposes limits in lipid storage and turnover. J Mol Cell Cardiol. 2008;44(2):315–22.

311. Hojman P, Pedersen M, Nielsen AR, Krogh-Madsen R, Yfanti C, Åkerstrom T, et al. Fibroblast growth factor-21 is induced in human skeletal muscles by hyperinsulinemia. Diabetes. 2009;58(12):2797–801.

312. Kim KH, Kim SH, Min YK, Yang HM, Lee JB, Lee MS. Acute Exercise Induces FGF21 Expression in Mice and in Healthy Humans. PLoS One. 2013;8(5): e63517.

313. Badman MK, Pissios P, Kennedy AR, Koukos G, Flier JS, Maratos-Flier E. Hepatic

Fibroblast Growth Factor 21 Is Regulated by PPARalpha and Is a Key Mediator of Hepatic Lipid Metabolism in Ketotic States. Cell Metab. 2007;5(6):426–37.

314. Kharitonenkov A, Shiyanova TL, Koester A, Ford AM, Micanovic R, Galbreath EJ, et al. FGF-21 as a novel metabolic regulator. J Clin Invest. 2005;115(6):1627–35.

315. Ahima RS, Park HK. Connecting Myokines and Metabolism. Endocrinol Metab (Seoul, Korea). 2015;30(3):235–45.

316. Kraegen EW, Clark PW, Jenkins AB, Daley EA, Chisholm DJ, Storlien LH. Development of muscle insulin resistance after liver insulin resistance in high-fat-fed rats. Diabetes. 1991;40(11):1397–403.

317. Lavelle-Jones M, Scott MH, Kolterman O, Moossa AR, Olefsky JM. Non-insulin-mediated glucose uptake predominates in postabsorptive dogs. Am J Physiol - Endocrinol Metab. 1987;252(5):E660–6.

318. O'Neill HM. AMPK and exercise: Glucose uptake and insulin sensitivity. Diabetes Metab J. 2013;37(1):1–21.